Université d'Ottawa • University of Ottawa

Université d'Ottawa · University of Ottawa

FACULTÉ DE ÉTUDES SUPÉRIEURES ET POSTDOCTORALES

FACULTY OF GRADUATE AND POSTDOCTORAL STUDIES

Abed ZEIBDAWI

AUTEUR DE LA THÈSE - AUTHOR OF THESIS

Ph.D.(Biochemistry)

GRADE - DEGREE

Department of Biochemistry, Microbiology and Immunology

FACULTÉ, ÉCOLE, DÉPARTEMENT - FACULTY, SCHOOL, DEPARTMENT

TITRE DE LA THÈSE - TITLE OF THE THESIS

Function and Structure of Anionic Phospholipid-binding Proteins
I. Factor Va, A Coagulation Cofactor
II. p135, A Novel Protein

E. Pryzdial

DIRECTEUR DE LA THÈSE - THESIS SUPERVISOR

CO-DIRECTEUR DE LA THÈSE - THESIS CO-SUPERVISOR

EXAMINATEURS DE LA THÈSE - THESIS EXAMINERS

J. Baenziger

P. Fay

J. Ngsee

M. Young

J.-M. De Koninck, Ph.D.

LE DOYEN DE LA FACULTÉ DES ÉTUDES SUPÉRIEURES ET POSTDOCTORALES

SIGNATURE

DEAN OF THE FACULTY OF GRADUATE AND POSTDOCTORAL STUDIES

Function and Structure of Anionic Phospholipid-Binding Proteins
I. Factor Va, A Coagulation Cofactor
II. p135, A Novel Protein

Abed R. Zeibdawi

Thesis submitted to the
Faculty of Graduate and Postdoctoral Studies
in partial fulfillment of the requirements
for the Ph.D degree in Biochemistry

Department of Biochemistry, Microbiology & Immunology
Faculty of Medicine
University of Ottawa

Your file Votre référence
ISBN: 0-612-90017-7
Our file Notre référence
ISBN: 0-612-90017-7

ABSTRACT

Coagulation cofactor factor Va (FVa) is an essential component of the prothrombinase complex, and is both produced and inactivated by proteolytic events. The cofactor is a heterodimer noncovalently associated by divalent cations with unknown contact sites. The mechanism of inactivation by the fibrinolytic effector plasmin (Pn) and the Ca^{2+} binding site in the FVa heavy chain (FVaH) was studied. Following Pn inactivation of aPL-bound FVa, a total of 16 fragments were observed. Of these, the 50(L1766), 48(1766), 43(Q1828), 40(Q1828) kDa fragments spanning the C-terminal C1/C2 domains, and 30(L94) kDa fragment, but not the similar 30(M110) kDa fragment, positioned within the N-terminal A1 domain remained associated with anionic phosphilipid (aPL). These data identify the molecular composition of the Pn-cleaved FVa which remains bound to membrane in the presence of Ca^{2+} as largely A1-C1/C2. A speculative model that describes the process of inactivation of FVa by Pn was produced. Chelation by EDTA dissociated the 30(L94) kDa fragment, which then associated with intact FVaL in the presence of Ca^{2+}, indicating that the Leu94-Lys109 region of the A1 domain plays a critical role in the FVaL and FVaH Ca^{2+}-dependent association. To identify the residues involved in the Ca^{2+}-binding, conserved amino acids in a recombinant FV (ΔFV) were replaced with Ala. The following thrombin generating activities were observed: ΔFV (100%), E96A (19%), D111A (30%), D102A (40%), T104A (65%), E108A (70%), D112A (75%), Y100A (84%), D79A (93%), and E119A (100%). D111A resulted in spontaneous dissociation of FVaH and FVaL. Conversely, E96A or D102A had no apparent

effect on Ca^{2+}-dependent subunit interactions, but greatly enhanced chelator-induced dissociation.

In addition to the FVa project, a novel human protein (p135) with two synaptotagmin-like C2-domains (sC2) suggestive of Ca^{2+}-dependent phospholipid binding is described. After cloning, sequencing, expression and monoclonal antibody production a preliminary characterization of p135 was conducted. Strong expression of p135 mRNA was observed in some leukemia and adenocarcinoma cell lines. Northern and Western analysis on sixteen non-pathological human tissues suggested a role of p135 in the immune system. The results indicated that the recombinant protein mediate Ca^{2+}-dependent interactions with phosphatidylserine but not with phosphatidylcholine. Thus, p135 is the first member of the important sC2-family of proteins that appears to be preferentially expressed by blood cells.

ACKNOWLEDGEMENTS

First and foremost, I would like to express my sincere gratitude to my supervisor, Dr. Ed Pryzdial, for his insight, perseverance, patience, guidance and for his support during the last years of research that led to the writing of this thesis. I have learned so much and achieved so much. I'm very grateful to you Ed.

I'm grateful for Dr. Maung Aye for encouraging and supporting me to pursue my graduate work, and I'm very grateful to Dr. Tony Giulivi for his friendship and for allowing me to pursue my doctoral work at the Canadian Blood Services.

I would like to express my sincere gratitude to some of the many people who helped me technically and emotionally during the last few years. I would like to thank my advisory committee members, Dr. Anil Dudani and especially Dr. Peter Anderson, for his interesting questions and support. A special thanks to Dr. Vas Mezl who has, probably without knowing it, given me a lot of momentum, encouragement, and energy to continue researching and writing. You have given me good memories of the department and of the University in general. I acknowledge the great help from my friend Dr. Jean Grundy. I specifically enjoyed all the great discussions that we had about many issues, including factor V and plasmin. I'm also in debt to my friend Erica Peterson for her help with the immunofluorescence microscopy work and for her friendship during difficult times.

A special thanks to my friends and Ph.D. labmates in Ed's lab, by alphabetical order, Mel Derry, and Michael Sutherland. (It was hard to see you both go to Vancouver). Mel, you have helped me so much and kept me updated on deadlines. You even attempted to teach me French! Your nice smile will always be with me. Michael, thanks for caring so much about Noah and Barb, you are very missed in Ottawa. Many thanks to my friend Evan Balaskas who also encouraged me constantly during difficult times.

I cannot fail to acknowledge the enormous debt I owe to my wife Barbara. I'm grateful to you. Your patience, and understanding have helped me pull through right from the beginning and up to the point of writing this last sentence of the thesis; thank you, and thank you for giving us our two-year old Noah, and our two-week old Leah.

TABLE OF CONTENTS

LIST OF ABBREVIATIONS

A549	Lung carcinoma
APL	Anionic Phospholipid
APC	Activated Protein C
AT	Anti-thrombin III
BP	Base Pair
BSA	Bovine Serum Albumin
Ca^{2+}	Calcium
$CaCl_2$	Calcium chloride
cDNA	Complementary deoxyribonucleic acid
CML	Chronic myelogenous leukemia
DAPI	4',6-diamidino-2-phenylindole
DNA	Deoxyribonucleic acid
EC	Endothelial cells
ECL	Enhanced chemiluminescence
EDTA	Ethylenediaminetetraacetic acid
EGTA	Ethylene glycol-bis(beta-aminoethyl ether)-N,N,N',N'-tetraacetic acid
FV	Factor V
FX	Factor X
FVIII	Factor VIII
FII	Prothrombin
FIIa	Thrombin
FITC	Fluorescein isothiocyanate
G361	Melanoma
HEL	Human erythroleukemia
HL-60	Promyelocytic leukemia
HRP	Horse radish peroxidase
HS68	Newborn fibroblasts
HR	Hydrophobic Region
IgG	Immunoglobulin
IMDM	Iscove's modified dulbecco's media
K-562	Chronic myelogenous leukemia
Kd	Dissociation constant
kDa	Kilodalton
LV	Large vesicles
µg	Microgram
µl	Microliter
µM	Micromolar
mM	Millimolar
mAb	Monoclonal antibodies
MOLT-4	Lymphoblastic leukemia
mRNA	Messenger ribonucleic acid
nM	Nanomolar
NMR	Nuclear magnetic resonance

NT	Nuclear targeting region
NTERA-2	Embryonal carcinoma
PAI-1	Plasminogen activator inhibitor-1
PAR	Protease activated receptor
PBL	Peripheral blood leukocytes
PC	Phosphatidylcholine
PCR	Polymerase chain reaction
PR	Pest region
Pgn	Plasminogen
PGI_2	Prostacyclin
PHA	Phytohemagglutinin
PI	Phosphatidylinositol
PS	Phosphatidylserine
PVDF	Polyvinyl difluoride
Raji	Burkitt's lymphoma
RNA	Ribonucleic acid
RT	Room temperature
S3	Hela cells
S2251	H-D-Val-Leu-Lys-p-Nitroaniline dihydrochloride
SC	Stromal cells
$_{s}C2$	Synaptotagmin-like C2 domain
SDS-PAGE	Sodium dodecyl sulfate polyacrylamide gel electrophoresis
SS	Secretory signal
SUV	Small unilamellar vesicles
SW480	Colorectal adenocarcinoma
Taq	Thermus aquaticus
TF	Tissue factor
TFPI	Tissue factor pathway inhibitor
TM	Thrombomodulin
tPA	Tissue plasminogen activator
uPA	Urokinase plasminogen activator
vWF	Von Willebrand Factor

LIST OF FIGURES

CHAPTER 1

CHAPTER 2

CHAPTER 3

CHAPTER 4

LIST OF TABLES

CHAPTER 3

CHAPTER 4

OVERVIEW

Phospholipids play a central role in many important cellular and physiological processes. The research described in this thesis is centered on two phospholipid-binding proteins. The first is factor Va (FVa), a blood clotting cofactor whose function is closely regulated by its Ca^{2+}-independent interaction with anionic phospholipid (aPL) on the surface of cells (1,2,3). The cofactor is both activated and inactivated by plamin (Pn) (4,5). Recently, a new regulatory mechanism has been suggested in our laboratory demonstrating that following Pn inactivation of coagulation FVa, a cofactor complex composed of FVa fragments is generated capable of activating fibrinolysis, the process of clot dissolution, by enhancing Pn generation (6-8). The second protein is a novel protein I discovered that is preferentially expressed by blood cells, named p135 because of its predicted molecular weight. Sequence analysis of the p135 complementary DNA predicted that the protein contains two synaptotagmin-like C2 domains (sC2-domains). sC2 domains, present in a growing number of proteins, have been implicated in the Ca^{2+}-dependent and Ca^{2+}-independent binding of these proteins to phospholipid. While both proteins, FVa and p135, contain homology structures called C2-domains, this nomenclature is unfortunately misleading because they are completely different. In this thesis the different C2 domains will be distinguished as C2 for coagulation-type domains and sC2 for synaptotagmin-type domains. The only similarity that FVa and p135 may have is that both C2 and sC2 are known to bind phospholipids.

To familiarize the reader with the organization of the thesis, the Introduction (chapter 1) starts with a review of blood coagulation. This is followed by a summary of our current understanding of the prothrombinase complex components, and domain assembly, function and regulation with emphasis on FVa. Mechanisms of fibrinolysis, the role Pn plays in regulating fibrinolysis and prothrombinase function, and thrombolytic therapies are described later in the chapter. Chapter 2 describes my research to understand the process of inhibition of FVa by Pn and the fragment composition of the aPL-bound fibrinolytic cofactor. Chapter 3 expands on results from chapter 2 and describes the identification of three residues in the FVa heavy chain (FVaH) that are likely involved in the Ca^{2+}-based contact between the two domains of FVa. A summary of the role of the sC2-domain in protein/phospholipid interaction with emphasis on the role the sC2-domain plays in cellular processes is discussed in the introduction of chapter 4. The remaining part of the chapter describes the identification, localization, and a partial function of the novel p135 protein.

CHAPTER 1

INTRODUCTION

1.1 Haemostasis

The blood haemostatic system has evolved to maintain the integrity of the vascular system. It simultaneously maintains the blood in a fluid state throughout the vasculature and prevents blood leakage by providing solid plugs where vascular injury occurs (9). Mechanical, chemical, or biological damage can initiate vascular disruption to the endothelial cells that line the vessel wall. Haemostatic response to this damage elicits blood coagulation. This event is then followed by fibrinolysis and tissue repair. Balance and cooperation between these two systems maintains proper blood flow in the body (10,11), and ensures that solid plug formation occurs only where vascular damage requires clot formation. These systems are continuously being activated and inactivated without noticeable physiological consequence. In most cases, the response to vascular damage is desirable resulting in the arrest of hemorrhage (coagulation), but in some cases clot formation is undesirable, resulting in an occlusion in the blood vessel supplying oxygen and nutrients to an organ (thrombosis). Hence, the processes of leak-preventing haemostasis and life-threatening thrombosis must be perceived as being separate. The normal haemostatic response to vascular damage depends on closely linked interactions between the blood vessel wall, platelets, and blood coagulation factors (9,10).

1.2 Endothelium

Endothelial cells play a physiological role in modulating vascular permeability and in maintaining blood fluidity (12). The vascular system is composed of a single layer of highly negatively-charged endothelial cells that under ordinary circumstances are primarily anticoagulant in nature (9). The coagulation effector thrombin (FIIa), and a variety of other stimuli, induced by tissue trauma, stimulate endothelial cell synthesis of prostaglandin I2 (PGI2), which has an anti-aggregatory effect towards platelets (9, 13, 14). Furthermore, endothelial cells have various defenses against coagulation that each bind and modify the action of FIIa (12, 15, 16). Vascular heparan sulfate, a glycosaminoglycan present on the surface of the endothelial cells, binds and activates the plasma-derived antithrombin III (AT III), which then inactivates FIIa (17,18). Thrombomodulin (TM), also present on the surface of endothelial cells, binds and inactivates FIIa leading to loss of some coagulant effects. Furthermore, FIIa/TM complex enhances protein C (PC) activation, a plasma-derived protein, which in turn inactivates FVa and therefore inhibits FIIa generation.

Resting endothelial cells are also profibrinolytic in nature, and are capable of secreting plasminogen (Pgn) activators such as tissue plasminogen activator (tPA) and urokinase. These proteolytically stimulate Pgn activation and lead to fibrin clot dissolution (19,20). Thus, loss of the anticoagulant endothelial barrier is an initiating step in coagulation (12).

Underlying the endothelial cells are connective tissue and muscle-like cells not in contact with blood proteins (21). This subendothelial matrix provides procoagulant activity in the form of tissue factor (TF), following the disruption of the endothelium, which in turn provides the activator required to initiate the blood coagulation pathway leading to FIIa formation (22). Simultaneously, the vascular matrix connective tissue components stimulate the adherence and aggregation of blood platelets. (9).

1.3 Platelets

Platelets contribute to the initiation and propagation of haemostatic response to tissue damage. The reactions involved include: adhesion of platelets to the damaged vessel, spreading of the adherent platelets on the exposed subendothelial surface, secretion from platelet's granules, aggregation of platelets, and acceleration of coagulation, resulting in the formation of a fibrin network that stabilizes the otherwise fragile platelet plug (12, 23). Platelet activation leads to the expression of aPL which provide an anchoring surface for the assembly of coagulation complexes that result in FIIa generation and ultimately fibrin, at the site of vascular damage.

The subendothelial connective tissue is a complex array of matrix proteins, including von Willebrand Factor (vWF), and collagen (12,24). Circulating platelets display on their surface passive- and activation-dependent receptors, capable of interacting with agonists such as extracellular matrix

proteins and plasma proteins (9). Receptor-mediated interactions lead to a series of intracellular events. One of the most important events in this series is the interaction of the vWF multimers with glycoprotein Ib-IX complex on platelets. This interaction is associated with platelet adhesion to the damaged site (12,9,25-29). Platelet activation leads to the secretion of effectors, which lead to platelet accumulation, neutralization of heparin (30), and secretion of FV-Va (31) and fibrinogen (32-34). Activated platelets also secrete or absorb from the plasma FV/FVa which then serve as a binding sites for enzyme–cofactor complexes in the presence of Ca^{2+}, thus localizing FIIa formation and fibrin strand generation to the site of injury. Fibrin strands, in turn, stabilize the initial weak platelet plug (35).

2.1 Blood Coagulation

In 1964, Davie and Ratnoff (36) and MacFarlane (37), proposed the waterfall or cascade model for the interaction of clotting factors (Figure 1.1). Each step in the sequence of events was described as an amplification where each clotting factor is an inactive precursor that can be activated by the functional factor immediately preceding it. The literature supports the conclusion that all the steps involved in FIIa generation involve a series of reactions consisting of a vitamin-K dependent serine protease and a cofactor protein that assemble on a membrane surface to express catalytic activity (10, 38, 39, 40). The product of the enzymatic activity of the complex provides the catalysis required for assembly and activity of the following enzyme complex in the

Figure 1.1 **The coagulation cascade.**

A stable fibrin clot is generated from sequential amplification reactions involving zymogens, cofactors, Ca^{2+} and aPL. Factor Va acts as a cofactor for FXa in the activation of FII to FIIa in the presence of Ca^{2+} and aPL.

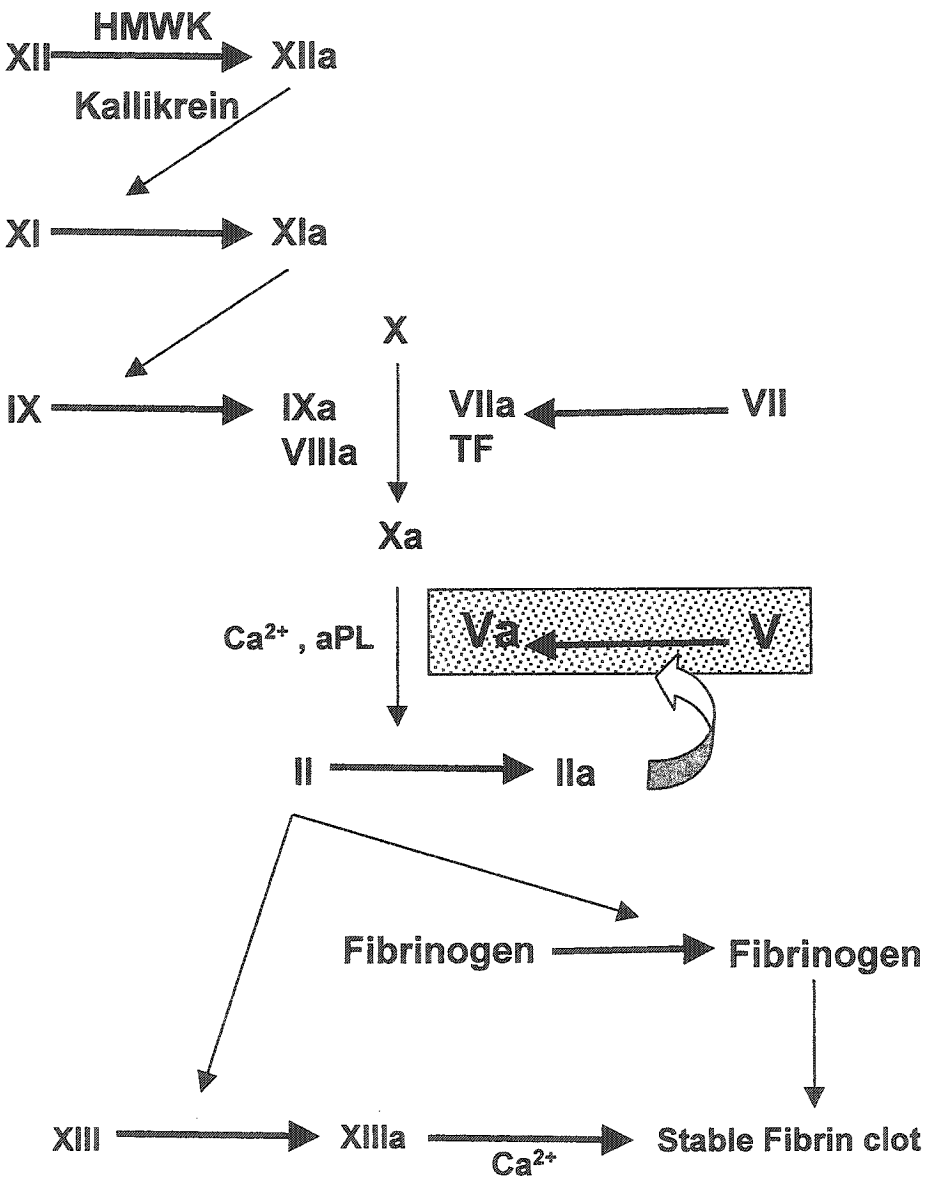
HMWK
XII
XIIa
Kallikrein
XI
XIa
X
IX
IXa
VIIIa
VIIa
TF
VII
Xa
Ca2+ , aPL
Va
V
II
IIa
Fibrinogen
Fibrinogen
XIII
XIIIa
Ca2+
Stable Fibrin clot

cascade (10). This process ultimately leads to the conversion of prothrombin (FII) to FIIa and clot formation (41).

All the components necessary for the initiation of the cascade are found circulating in the plasma except for TF, the triggering mechanism, which, under normal conditions, is confined to the inner leaflet of endothelial cells (12,37). Likewise, under normal circumstances, aPL is confined to the inner leaflet of the plasma membrane. A stimulus, as a result of tissue injury, presents TF and aPL to circulating coagulation factors which results in the initiation of the coagulation cascade (41,42).

Under normal physiological conditions, TF distribution is confined to the interior of the endothelial cells and the subendothelium (10,41), and upon injury and vessel wall rupture, it becomes exposed to the coagulation zymogens present in the circulating plasma (40,41). Three vitamin K-dependent complexes are required for subsequent normal clot formation. The first is the extrinsic tenase (factor VIIa and the membrane bound cofactor TF in the presence of Ca^{2+}) which assembles when TF encounters circulating factor VIIa. This complex then activates a fraction of the circulating zymogens factor IX (FIX) and factor X (FX) to their active forms, factor Xa (FXa) and factor IXa (FIXa) respectively (38,41,43,44,45). Factor Xa produced either directly activates factor V to factor Va, or indirectly activates it by limited FIIa generation (1,3,46,47,48,49). The second complex is the intrinsic tenase complex (FIXa and factor VIIIa (FVIIIa),

and Ca^{2+}). This complex, in turn, produces additional FXa. The third complex, the prothrombinase complex (free FXa and FVa, and Ca^{2+}) converts FII to FIIa. The importance of the extrinsic, and intrinsic tenase is demonstrated by the observation that deficiencies in FVII, FVIII, FIX, and FV are invariably associated with hemorrhagic tendencies (41). Recently, a revised model of blood coagulation was postulated in which there is no distinction between extrinsic and intrinsic pathways (50-52) because of intricate feedback communication and very different roles in initiating and propagating the pathway.

2.1.1 Fibrin Formation

The formation of fibrin represents a second phase in the plug formation, the first being primary platelet aggregation. Thrombin has numerous substrates (9,12,41). In the coagulation reactions, FIIa participates in the feedback activation of FV, FVIII, FXI, FVII. Thrombin substrates also include platelets, factor XIII (FXIII), and protein C (PC) (40). The major substrate of FIIa is fibrinogen, which after initial hydrolysis forms fibrin monomers that undergo spontaneous polymerization to form the fibrin clot (53-56).

2.1.2 The prothrombinase complex

The important task of converting FII to FIIa is mediated by an enzyme complex consisting of the serine protease FXa, the cofactor FVa, negatively charged phospholipid membrane surfaces, and Ca^{2+}. This macromolecular complex is termed the prothrombinase complex since it FII is the only known

substrate (Figure 1.2). Activated platelets, monocytes and endothelial cells present at the site of vascular injury expose aPL on their membrane surface providing a site of assembly for prothrombinase in the presence of Ca^{2+} (57). Although FXa can activate FII directly in the absence of FVa, aPL, and Ca^{2+}, the rate of activation is very slow and does not achieve the immediate physiologic response required to arrest blood loss. However, with prothrombinase, the rate of FII activation is about 300,000 times higher than by FXa alone (58). Thus prothrombinase assembly is essential for health.

2.1.3 Factor X/Xa structure and function

Factor X circulates as an inactive zymogen in plasma at a concentration of 0.17 μM with Mr = 59 kDa, being composed of a heavy chain (Mr = 42 kDa) and a light chain (Mr = 16.5 kDa) covalently associated through a disulfide bond (59). Proteolysis at Arg194 in the heavy chain, catalyzed by the intrinsic tenase (FVIIIa and FIXa), or by the extrinsic tenase (FVIIa and TF), produces the active enzyme FXa (Mr = 48 kDa) by the release of a fragment of Mr = 12 kDa. The resulting FXa is composed of a heavy chain (Mr = 30 kDa) and a light chain (Mr = 18 kDa) covalently associated by a disulfide bond (9, 60).

Factor Xa plays a key role in the coagulation cascade, linking the extrinsic and intrinsic pathways by catalyzing the conversion of FII to FIIa on vascular cell surfaces (10,60). Once generated, FXa forms the Ca^{2+}- and phospholipid-dependent prothrombinase complex with its cofactor FVa on activated platelets,

Figure 1.2 **The components of prothrombinase and plasminogenase.**

The prothrombinase complex constituents FVa, FXa, FII Ca^{2+}, and aPL generate FIIa which converts fibrinogen to fibrin in the process of coagulation. During fibrinolysis, the plasminogenase complex composed of Plasminogen, tPA, a cofactor, and aPL, generate Pn which solubilizes the fibrin clot.

Prothrombinase Plasminogenase

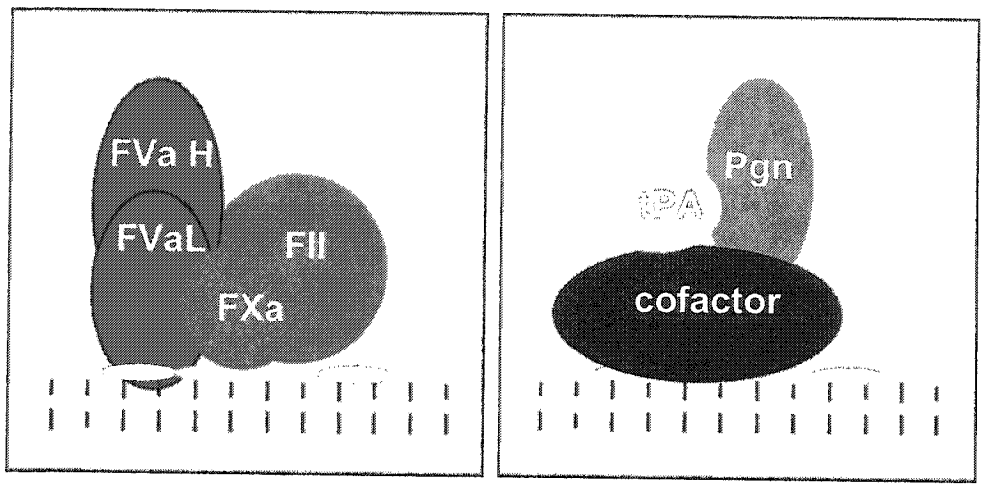

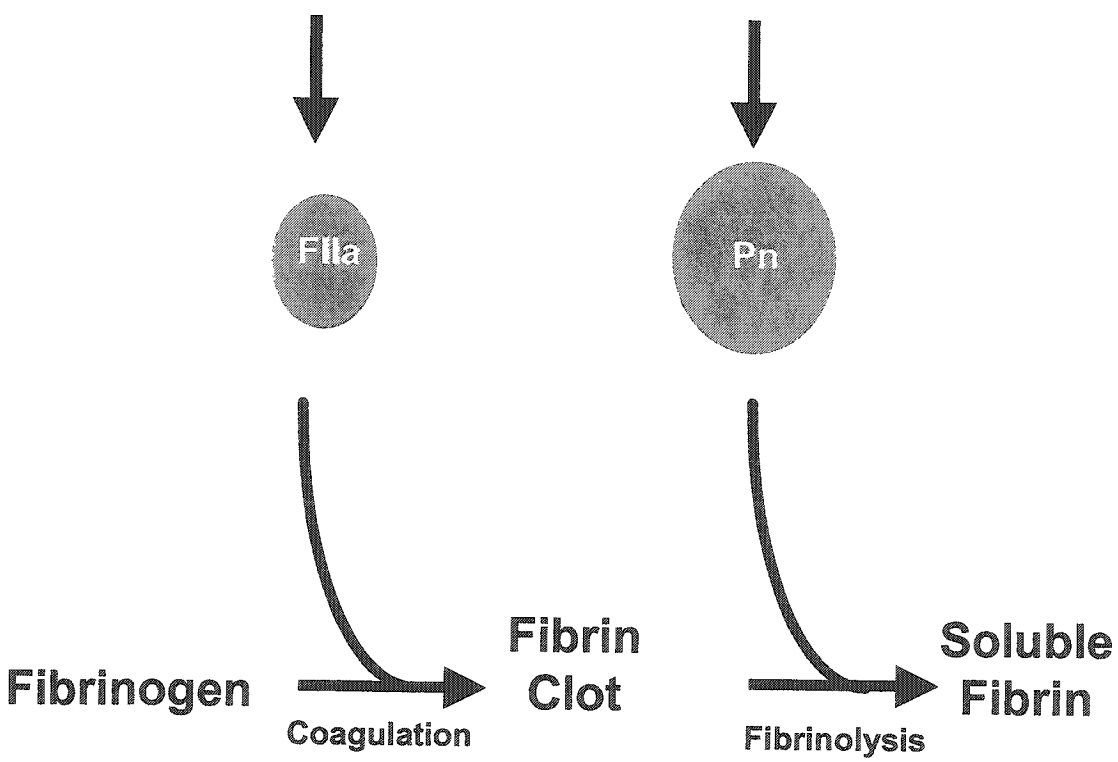

monocytes, or endothelial cells (61,62). Furthermore, FXa has been shown to mediate a variety of other biologic effects mostly through its binding with the membrane receptor the effector cell protease receptor-1 (EPR-1) (63,64,65). These effects include initiation of mitogenesis in endothelial and smooth muscle cells, stimulation of lymphocyte proliferation, and induction of acute inflammatory responses in vivo (66).

2.1.4 Prothrombin/thrombin structure and function

Prothrombin is synthesized as a pre-propeptide, and prior to secretion into the blood, FII is post-translationally modified. Once secreted, FII circulates in the plasma as an inactive zymogen at a concentration of 1.4 μM with Mr = 71.6 kDa (68). Activation of FII occurs by FXa or by the prothrombinase complex (45).

Alpha-thrombin, the principal product of FII activation following tissue injury, is a serine protease heterodimer with Mr = 36.7 kDa, composed of a 6 kDa A chain and a 31 kDa B chain (70-73). Thrombin plays a role through its feedback modulation of haemostasis. This is achieved by its high affinity interaction with a variety of macromolecules. In the presence of thrombomodulin (TM), FIIa can have an anticoagulatory function through the activation of PC, which ultimately switches off the cascade reactions and thereby FIIa production (54,74-76).

2.1.5 Anionic phospholipid

In a resting cell, lipid asymmetry where negatively charged phospholipids (aPL, e.g. phosphatidyl serine (PS), and phosphatidyl inositol (PI)) are largely located in the inner membrane, is regulated by the cellular enzymes that include the enzyme translocase (12). Translocase, first described in red blood cells and later in platelets and endothelial cells, shuttles PS rapidly to the inner leaflet of the membrane on the inside of the cell. In contrast, neutral phospholipids such as phosphatidylcholine (PC) are moved very slowly (37). Activation of platelets, monocytes, and endothelial cells present at the site of injury expose aPL to circulating blood proteins localizing procoagulant (and anticoagulant) complexes to the site of vascular injury where FIIa generation is required. In the case of prothrombinase, aPL provide sites of association for the cofactor FVa and FXa in the presence of Ca^{2+} (54). This is essential to direct coagulation components to the site of vascular injury, and also to enhance the catalytic efficiency of the enzyme as well.

The activity of FII, FVII, FIX, FX, and PC is dependent upon vitamin K, which is responsible for a post-ribosomal carboxylation of a number of N-terminal glutamic acid residues on each of these molecules generating the gamma-carboxyglutamic acid (Gla) residues (45,67). The carboxylation facilitates the binding of Ca^{2+} to the Gla domain required to interact with aPL. In the absence of vitamin K, no carboxylation of Glu occurs, Ca^{2+} is not bound and these factors do not assemble and form complexes on membranes (3,10). Without the

concentration and orientation of these reacting coagulation factors the rate of conversion of substrate is minimal.

At the C-terminus is the serine protease domain, which is largely homologous to that of trypsin and chymotrypsin, with insertions that alter the macromolecular substrate specificity of each enzyme. Between the N- and C-terminal domains is a region that contains either epidermal growth factor (EGF) domains in FVII, FIX, FX, and protein C, or Kringle domains in FII (77) , which have poorly understood functions, but are involved in correctly orienting the protease domain relative to the cell membrane

Without Ca^{2+}, the Gla domain is disordered because of the random positioning of the N-terminal amino acid residues. Calcium ions bind the Gla domain in an almost linear arrangement, and one or more ions interchelate between the double carboxylate groups of the Gla residues. This arrangement leads to a restrained conformational transition (67,78,79) and the correct orientation of the N-terminus (80) allowing for binding to aPL. Additional Ca^{2+} ions could also become sandwiched between the Gla domain and the phospholipid surfaces to bridge their overall negative charge (42).

2.1.6 FACTOR V/Va

Factor V (Figure 1.3) was first discovered from work on a patient with a bleeding disorder that could not be explained by known coagulation factor

Figure 1.3 **Activation of FV.**

The human coagulation FV (A) is activated by proteolysis initially and partially by FXa and then by FIIa at multiple sites which result in the removal of the B domain. The end product is a heterodimer of FVaH and FVaL chains noncovalently associated in the presence of divalent metal ions (B). FVaH is two A domains (A1 and A2) with internal homologies, and FVaL is one A domain (A3) and two C domains (C1 and C2) with internal homologies. The arrows on top and on bottom in A represent activation cleavages by FIIa and FXa respectively. The arrows in B represent the activated protein C (APC) cleavage sites known to inactivate FVa.

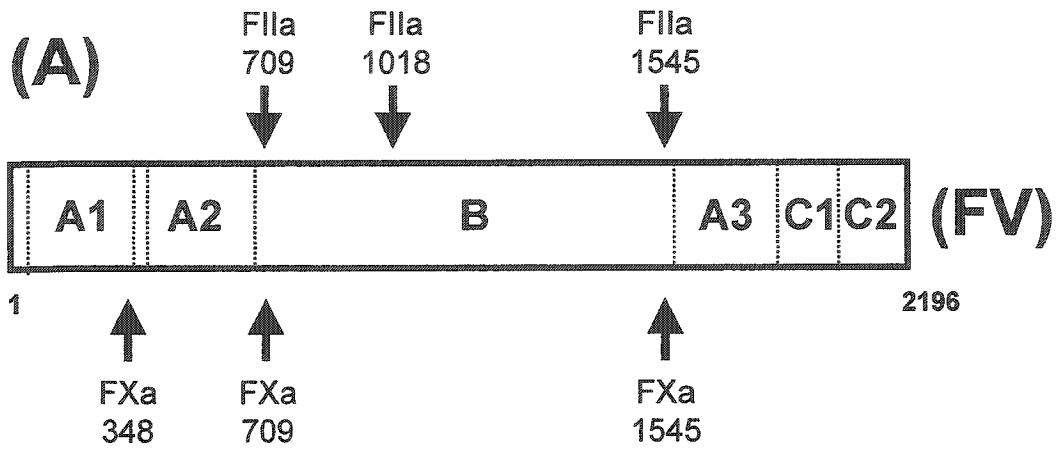
(A)
FIIa
709
FIIa
1018
FIIa
1545
A1
A2
B
A3
C1
C2
(FV)
1
2196
FXa
348
FXa
709
FXa
1545

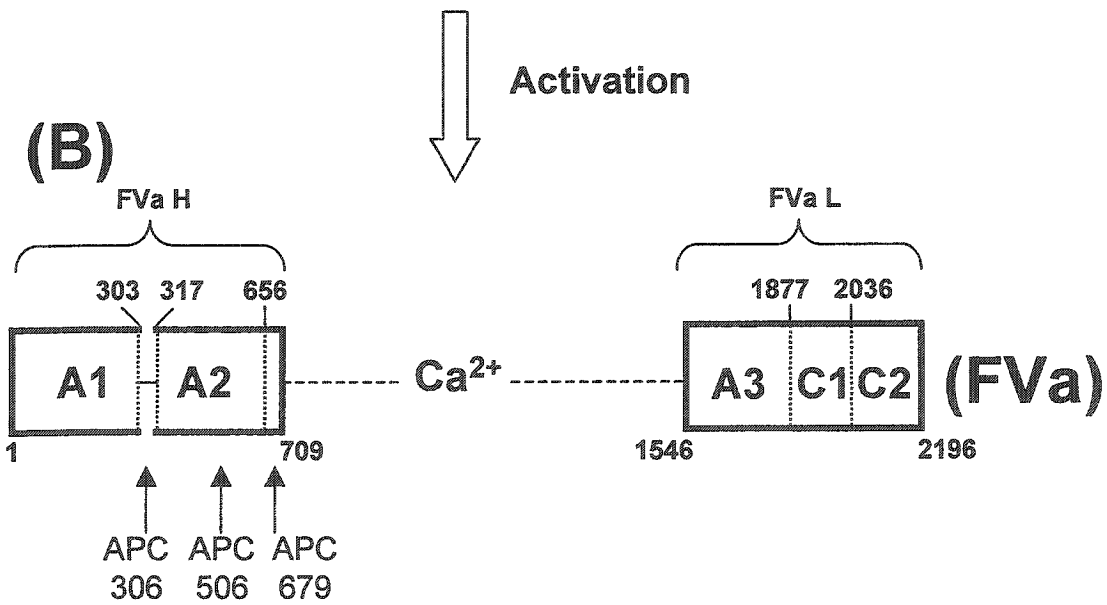
Activation
(B)
FVa H
FVa L
303
317
656
1877
2036
A1
A2
Ca2+
A3
C1
C2
(FVa)
1
709
1546
2196
APC
306
APC
506
APC
679

deficiencies. Paul Owren in 1943 (81), discovered that the disease was due to a deficiency in a factor whose activity must enhance the rate of FIIa generation (49). In replacement assays, this activity was generated upon treatment of normal plasma with FIIa (82,83). Owren named the new component factor V. Seegers (84) later discovered that the missing FV is a plasma protein essential in the conversion of FII to FIIa. Hanahan and Papahadjopoulos (85) in 1965, and Cole and coworkers (86) in 1965 showed that FII activation is a product of two proteins, FXa and FVa, which require phospholipid and Ca^{2+} ions (10, 12,87). Now we know that at the site of vascular injury FV is activated by proteolysis, mainly by FIIa, to yield FVa (Figure 1.3) (10).

2.1.6.1 Domain Structure

The domain structure of FV was elucidated following the isolation of the 6672 base pair complementary DNA (88-90). The human factor V gene is 80 kb in length and has been mapped to chromosome 1q21-25. Factor V is a large single-chain procofactor glycoprotein (2196 amino acids plus a 28 amino acid leader sequence) of Mr=330 kDa. The domain structure is composed of three homologous A-domains and two homologous C-domains, and a unique B-domain arranged in the order NH_2-A1-A2-B-A3-C1-C2-CO_2H (Figure 1.3) (89-91).

The locations of the disulphide bridges in FVa have been determined. In total, the light chain has eight cysteines: two in the A3 domain and three in each C

domain. The heavy chain contains 10 cysteine residues: four in the A1, and six in the A2 domain (92,935). Each A domain contains a 26 residue loop. The A1 and A2 domains, each contain 81 amino acid residue loops (Figure 1.3). The B domain is heavily glycosylated (nearly 50 % carbohydrate by weight) containing 25 of the 37 total Asn-linked glycosylation sites, and one cysteine residue not involved in a disulphide bridge (83). The B domain has no apparent involvement in the cofactor activity of FV (94), but has been shown to serve as a substrate for FXIIIa (95,96), and has been implicated in anticoagulation (94,97).

2.1.6.2 Macromolecular structure

To date structural studies of FV/FVa by X-ray crystallography have been hindered mostly due to its instability, low abundance in plasma and heterogeneous glycosylation (49). Early gel filtration (98,99) and sedimentation equilibrium studies (100,101) indicated that FV has an asymmetric, rod-like structure. Somewhat more recent studies, based on scanning electron microscopy images of human and bovine FV, indicated a globular three-dimensional model of FV structure (102-105). These studies determined that FV is a multi-domain protein, with irregular structure. The protein was found to be composed of three peripheral and one larger central domain of approximately 90 x 70 angstrom each. The three peripheral domains are linked via a thin spacer to the larger domain of approximately 165 x 138 angstrom. Stoylova et al. in 1994 (106), extended previous work and demonstrated that FVa covers an area of

about fifty (50) phospholipid molecules. While a crystal-based structure of FVa has not been solved, two crystal structures of FVa C2 domain has been reported (106a). The C2 domain exhibits a β-barrel motif of eight antiparallel strands arranged in two β-sheets of five and three strands packed together. This creates a scaffold of three protruding loops. The two crystal structures adopt markedly different conformation at one of these loops. The upper part of the barrel structure contains several salt bridges and the lower part contains basic residues.

The X-ray structure of ceruloplasmin (CP), a plasma copper-binding protein, has been reported (107). The A-type domains of FV and FVIII share sequence homology with CP. This enabled a theoretical model for the A domains of FV/FVa (residues 1-656, and 1546-1883) to be constructed (108). In this study, a Ca^{2+} binding pocket was proposed at the A1-A3 interface possibly involving residues E96, D102, E108, D111, and D112. Pellequer et al. (2000) constructed a complete molecular model of the three homologous A-domains and the two homologous C-domains of FVa bound to anionic phospholipids and APC. This was achieved using the X-ray crystal structure derived from ceruloplasmin as a homologous template (109). This model suggested that the subunits of FVa interact exclusively through an elaborate interface between the A-domains of FVa. The model predicts that approximately each half of an A-domain consists of a plastocyanin-like homology repeat, which individually facilitates FVa intersubunit contacts with a cognate A-domain. In this way, the A1

N-terminus and A2 C-terminus would link FVaH to the C- and N-terminus of FVaL-A3, respectively. This study however excluded the absolute requirement for the N-terminal 93 residues of A1 and the N-terminal 216 residues of A3.

2.1.6.3 Activation of FV

Proteolytic activation of FV plays a central role in regulating coagulation. Factor V circulates in the plasma with little or no activity (10,12,58). At the site of vascular injury, FV is activated through a series of cleavages predominantly by FIIa (110) leading to conformational changes in the molecule (111). The sites of FIIa cleavages have been determined and are located at Arg 709, Arg 1018 and Arg 1545, which excise the B-domain to yield FVa (1,101,110,112,113). The cleaved product is a heterodimer comprised of an N-terminal-derived heavy chain (FVaH; A1/A2 domains; Mr = 104 kDa, residues 1-709), and a C-terminal-derived light chain (FVaL; A3/C1/C2 domains; Mr = 74/71 kDa; amino acids 1546-2196) held tightly together in the presence of Ca^{2+} by unknown contact sites (110,112,114-116). The proteolytic sites in human FV are consistent with those for bovine FV although the order of cleavage seems to differ (49,117).

The heavy and light chains are combined in a non-covalent but divalent metal ion-dependent manner to form FVa (115). The metal ion contact sites remain unknown. Factor V is initially activated although at a much slower rate than that of FIIa by the serine protease FXa (111) in an aPL and Ca^{2+}-dependent manner following cleavage at Arg 709 and Arg 1018 and consequently through a

feed back mechanism with FIIa (54,118,119). In addition to FIIa and FXa, other proteases such as the fibrinolytic enzyme Pn cleave FV and generates a transient activated species (4,5). Similarly, Cathepsin G (120), elastase (121), calpain (122), Ca^{2+}-dependent proteinase (123), platelet proteases (124) and homocystein-treated endothelial cells (125) activate factor V by cleaving the protein at various sites generating proteolysed species with different cofactor activity, and unknown physiological significance.

2.1.6.4 Subunit association.

FVaH and FVaL are noncovalently associated by a Ca^{2+} ion (Kd = 6 X 10^{-9} M) (Figure 1.2). Neither FVaH nor FVaL independently bind Ca^{2+} (115), suggesting the Ca^{2+}-binding pocket is conformational or formed by both FVaH and FVaL. Although significant evidence has been obtained for the participation of discrete regions of FVa in the various binding interactions within prothrombinase, both chains of the cofactor are required for biological activity (110,112). The two chains of the cofactor can be dissociated and separated in the presence of chelating agents such as EDTA (110,112,114). The dissociation of the chains results in a reversible loss of cofactor activity, which can be regained by reassociating the isolated subunits in the presence of Ca^{2+}, or other specific divalent metal ions (112,115,126,127). Krishnaswamy et al. (1988) studied FVa subunit reassociation kinetics using fluorescence energy transfer techniques with FVaL modified with 6-acryloyl-2-dimethyaminonaphthalene and FVaH modified with fluorescence 5-maleimide in the presence of 2 mM Ca^{2+} ions or Mn^{2+} ions

(115,128). These experiments have demonstrated that the rate constant of association for Ca^{2+} is second order of 1.58 X 10^5 M^{-1} min^{-1}, three-fold less than that with Mn^{2+}. Furthermore, activity measurements of the Ca^{2+}- or Mn^{2+}-reassociated cofactor were indistinguishable. These studies demonstrated that the subunits reassociate tightly and reversibly with a Kd = 5.9 X 10^{-9} M, and stoichiometry of 1:1.

2.1.6.5 Association with metal ions

To date the site(s) of interaction of metal ions in the heavy and light chains and the physical nature of these interactions remain a complete mystery. Atomic absorption and emission spectroscopy studies with bovine or human FV demonstrated the presence of a single bound copper ion (type II) per mol of protein (129). This copper ion is likely located at the A1-A3 interface in FV (129a). Furthermore, equilibrium binding studies on bovine FV showed the existence of a single extremely high affinity (kd < 10 nM) and two lower affinity (kd 60 μM) Ca^{2+} binding sites (126). In contrast, FVa was found to contain a single Ca^{2+} ion binding site with a kd = 24 μM and several sites of lower affinity (127). Calcium ions are implicated in the expression of biological activity by FV and are required to stabilise the interaction between FVaH and FVaL (130). Following the addition of a chelating agent such as EDTA, the two subunits slowly dissociated and the cofactor activity is abolished. Upon the addition of divalent metal ions such as Ca^{2+}, Mn^{2+}, Cd^{2+}, Co^{2+}, and Sr^{2+}, but not Mg^{2+} or Ba^{2+}, the two subunits reassociate and the activity is restored (112).

Earlier studies using monoclonal antibodies have demonstrated that conformational changes occur following chelation with EDTA, generating one mAb-detectable new epitope (111,131). However spectral studies of FVa in the presence or absence of divalent metal ions, looking for changes in its intrinsic fluorescence, do not seem to support conformational changes in FVa (83).

2.1.6.6 Association with anionic phospholipid

Since clot formation is localized to the site of injury, prothrombinase components (Figure 1.2), including FV/FVa, bind to cells associated with damaged vascular tissue. Due to the inherently difficult nature of analytical binding studies on living cells, defined phospholipid preparations, such as lipid extracts and phospholipid vesicles composed of PS and PC at different ratios, have been utilized to study the bases of the membrane binding of FVa. The majority of these studies demonstrate that FV/FVa interaction is specific for aPL and is mediated through FVaL and is Ca^{2+}- independent (44,132-138). Chelation with EDTA was found to dissociate FVaH, while FVaL remained bound to phospholipid vesicles (115). Using fluorescently labeled FVa and PCPS vesicles (75/25 %), the dissociation constant was found to be ~2.5 nM (132). Furthermore, these studies also reported that FVa binding site is composed of a defined number of properly oriented PS molecules, with each site having the same affinity for FVa. In addition to phospholipid vesicles, prothrombinase assembly was also studied on platelets (31,124,139,140). As with phospholipid vesicles, the binding of FV/FVa to platelets was saturable and reversible

(139,140) with a comparable Kd in the nanomolar range (128). Furthermore, studies with platelets as the phospholipid anchor also demonstrated that FVa binding is mediated by the light chain. Studies using antibodies to human FV have implicated the N-terminal region of the C2 domain in aPL binding (134,135,137,138), while experiments using natural bovine FVa fragments have implicated the A3 (132-134) and the A3/C2 domains (134). Ionic and hydrophobic forces have are suggested to both mediate the interaction between the protein and the membrane surface (136). Using alanine-scanning mutagenesis, Kim et al. (2000) investigated the function of individual amino acids within residues 2037 - 2196 of the C2 domain (137). Charged residues were changed to alanine in clusters of 1-3 mutations per construct. They found that the charged residues K2101, K2103, K2104, K2157, K2159, K2161and K2178 of the C2 domain seem to be involved in the phospholipid interactions. Overall, it seems likely that binding of FVa to membrane occurs in two stages; initially there is a diffusion rate-limited FVa-membrane interaction mediated through the C2 domain, and this is followed by a hydrophobic contribution through the A3 domain (49).

2.1.6.7 Forms

Following activation of the human plasma FV, the light chain is released from the C-terminal region of the pro-cofactor, and appears on SDS-PAGE as a doublet with Mr = 74 (FVa1) and 71 (FVa2) kDa of approximately a 40:60 ratio (141-144). Using chimeric recombinants of FV, it was suggested that the FVa1 and

FVa2 likely differ in the degree of Asn-linked glycosylation in the carboxy-terminus C2 domain, at Asn 2181 (143,144). FVa2 has a much higher affinity for aPL membranes than FVa1 (143). This difference is functionally important, mainly in the presence of limiting conditions of membrane and FXa, with considerably more FVa1 being required to assemble a membrane bound FXa-FVa complex than FVa2 (142). Under several conditions, FVa1 and FVa2 have similar procoagulant activity (143), whereas they considerably differ in their sensitivity for APC (142).

2.1.6.8 Contribution to FXa activity

Factor Xa interacts with FVa and aPL in the presence of Ca^{2+} to form the prothrombinase complex (145,146). In this complex, the two proteins FVa and FXa associate very tightly with a kd ~ 1 nM. In the absence of phospholipid, the kd for the FVa-FXa interaction is weak of kd ~ 0.8 μM and is dependent on Ca^{2+} (147-149). Interaction of the two proteins forms 1:1 complex and involves residues 263-274 of FXa heavy chain and both chains of FVa (150,151).

FVa has known effects on FXa resulting in accelerated FIIa production. Phospholipid-bound FVa increases the affinity of the enzyme to membrane. Without FVa, the duration of retention of FXa on membrane is short-lived with a Kd of approximately 0.1 μM. As a result of FVa retention of FXa to membrane the K_m for FII activation is decreased by two orders of magnitude, while the K_{cat} of the enzymatic reaction is increased by 3 orders of magnitude (49). The combined effects enhance the FXa mediated activation of FII to FIIa by 5-orders of

magnitude (58). It is not clear yet whether this enhancement in K_{cat} is a result of alteration of FXa active site, the substrate FII, or alteration in both FXa and FII manifested by FVa binding (49).

2.1.6.9 FVa inactivation by activated protein C

The regulation of prothrombinase is, in part, achieved by inactivation of FVa by the PC pathway (152-154). The well-studied anticoagulant, activated protein C (APC), is a serine protease derived from the vitamin K-dependent zymogen PC by cleavage in the heavy chain at Arg 12 (38,44). The surface of the endothelium constitutes the main site for PC activation. The cleavage is catalysed by a complex between FIIa and the endothelial cell surface glycoprotein, thrombomodulin (TM) (154). APC catalyses the proteolytic inactivation of two critical blood clotting cofactors, FVa (155) and FVIIIa (156) thereby limiting further FIIa formation (157-161). Of importance to the current work, APC inactivates membrane-bound FVa (155) by cleaving FVa in a sequential fashion at Arg 306, Arg 506 and Arg 679 (164,165) to produce an inactive FVa species.

2.1.6.10 FVa inactivation by plasmin

While the biological role of APC in FVa inactivation is well established, the effect of Pn on FVa inactivation and the specific cleavage sites in FVa remain to be determined. Both FV (5) and FVa (4, 168) have been shown to be susceptible to Pn proteolysis which is specific to the carboxyl-terminus side of lysine and Arg

residues (166,167). FV is sequentially activated then inactivated by Pn resulting in the systemic decrease in the levels of the procofactor (5). The inactivation of FVa by Pn is a complex proteolytic process that is not yet fully understood. It has been shown that plasmin is a potent inactivator of FVa due to proteolysis of both the heavy and the light chain (5,168). One of the main goals of the current project was to determine the Pn cleavage sites in human FVa and the molecular structure (and to a lesser extent function) of the derived product for reasons that will be discussed later in the chapter. While not part of this thesis, Pn further influences coagulation by inactivating FVII (169), FVIII (170), FIX (171,172), FX/Xa (173), FXII (174). Plasmin function is controlled either directly by fast acting inhibitors such as α2-antiplasmin or indirectly by inhibition of plasminogen activators (175).

3.1 Clot lysis

While coagulation generates insoluble fibrin to seal vascular leaks, fibrinolysis solubilizes the clot to restore normal blood flow. Intricate communication mechanisms between these pathways and regulatory mechanisms in each of the pathways exist to insure regulated initiation and to avoid the possibility of thrombosis or haemorrhage. Fibrinolysis, like coagulation, is a normal haemostatic response to vascular injury, and is the last mechanism that limits clot formation and vessel repair. This process resembles the coagulation cascade in that it involves the zymogen activation, feedback activation and inhibition, and inhibition by specific inhibitors (12,50,54).

3.1.1 Activation of the fibrinolytic system

The physiological activators of plasminogen are the serine proteases tissue plasminogen activator (t-PA) and single chain urokinase-type plasminogen activator (scu-PA, or u-PA) (50,176,177). The tPA-mediated pathway is primarily involved in fibrin haemostasis, and the uPA-mediated pathway is primarily involved in processes such as cell migration and tissue remodelling. Consequently, the terminology "fibrinolytic system" has been replaced by "plasminogen system" (12). After vascular repair and during fibrinolysis, the plasminogenase complex, composed of Pg, tPA and a tPA cofactor, generates Pn from its inactive zymogen form plasminogen, yielding two chains which remain covalently associated by a disulfide bond (176-179). Plasmin, a trypsin-like protease, is the sole enzyme responsible for dissolving fibrin. It has a wider range of substrate recognition than FIIa, and may proteolyse a number of proteins relevant to hemostasis (57).

3. 2 Components of fibrinolysis

3.2.1 Plasminogen

The human Pgn protein is organized into several structural domains, composed of a pre-activation domain, five sequential homologous kringle domains numbered K1 to K5, and the serine proteinase domain (180-183). The kringle domains are loop structures of about 80 residues each held together by triple disulphide bonds (182). They contain the high-affinity lysine binding sites crucial for localizing the molecule to fibrinogen, fibrin, and other receptors found on cells. Four of these loops bind lysine residues (183).

Plasminogen is secreted from the liver and upon activation it is converted to Pn by cleavage at a single Arg 561 – Val 562 peptide bond. The N-terminal residue of Pgn is a glutamic acid, and following cleavage of its activation peptide, comprising the seventy-six N-terminal residues, by Pn, a slightly smaller plasminogen with a lysine N-terminal residue is generated. These two molecules are termed Glu-plasminogen and Lys-plasminogen respectively, where the latter binds lysine groups with higher affinity (183,184-188).

3.2.2 Tissue-type plasminogen activator

After vascular repair and during clot dissolution, tPA, tPA cofactor (usually fibrin), Ca^{2+} and aPL, generate Pn by cleavage of Pgn. Tissue plasminogen activator, a highly specific protease, is one of two known physiological proteases that catalyzes the conversion of Pgn to Pn (180, 181,188). Tissue plasminogen activator is synthesized by the vascular endothelium and released into the circulation as a single chain molecule (Mr = 72 kDa) when fibrin clots are formed. The primary sequence contains a finger domain (47 residues), an epidermal growth factor domain, two kringle domains (K1 and K2) with high homology to the five kringles of Pgn, and a serine protease domain that contains the catalytic triad (190-193).

Plasminogen binds to fibrin primarily via specific structures called the "lysine-binding site". Thus one way of regulating fibrinolysis is at the level of Pgn activation

localised at the fibrin surface. The kringle structures contain the lysine-binding sites, which display affinity for C-terminal lysines (186,187). Once Pn is generated on the plug surface, it degrades fibrin and leads to clot dissolution, or fibrinolysis. Although different kinetic constants for the activation of plasminogen by t-PA have been reported, most studies agree that fibrin stimulates plasminogen activation by t-PA by at least two orders of magnitude (194). During fibrin clot lysis, binding of t-PA increases by generation of additional new Pn-generated carboxyl-terminus lysines (186,187).

Tissue plasminogen activator is inactive on its own, but requires conformational changes for full proteolytic activity, brought about by binding to fibrin exposed at the site of injury (195,196). The activity of tPA is greatly enhanced by fibrin, and the assembly of tPA and Pgn on a fibrin surface is of utmost importance for the generation of Pn. It is generally accepted that binding of both Pgn and tPA to fibrin leads to the alignment of the substrate and its enzyme on the fibrin matrix, resulting in efficient formation of Pn (194). In the absence of fibrin, the enzyme has weak affinity for Pgn (Km = 65 x 10^{-6} M), but a much higher affinity in the presence of fibrin (Km between 0.15 and 1.5 x 10^{-6} M).

3.2.3 Urokinase-type plasminogen activator

While not part of the current thesis, the reader should be aware that a second physiological Pgn activator exists. The single chain urokinase-type plasminogen activator (uPA) is composed of an epidermal growth factor domain, a

kringle domain, and a protease domain containing the catalytic triad. Cleavage of uPA at Lys 158 by Pn converts the molecule into a two-chain uPA (tc-uPA) enzyme (Mr = 33 kDa) (196-201). The single-chain uPA exhibits low intrinsic catalytic activity (202,203), and hence does not contribute to the initiation of fibrinolysis. However, sc-uPA can enter the clot through binding of Glu-plasminogen to fibrin. Similarly, by a separate mechanism, sc-uPA enters the clot by binding to a uPA receptor on monocytes (204).

3.2.4 Tissue plasminogen activator cofactors

Apart from Pgn and fibrin, tPA interacts with a number of other cofactors, including: annnexin II (205,206); α-enolase (207); a novel 45 kDa endothelial protein (208,209), osteonectin (210); and complement component C7 (211). Of these annexin II, osteonectin and complement C7 have been shown to accelerate tPA-mediated activation of Pg (210,211,212). Of these, only fibrin is known to localise tPA activity to the site of fibrin formation.

3.3 Plasmin function

Plasmin has a wide range of substrate recognition, hydrolysing both arginine and lysine peptide bonds in target proteins. The primary recognized function of Pn is to degrade fibrin polymers in an orderly, stepwise fashion giving rise to solubilized products that consist primarily of the D and E domains of the fibrinogen molecule (9,183,186). Another important role of Pn is cleavage of its precursor, Pgn, from a C-terminal Glu to Lys form, rendering it more susceptible to

activation by tPA or uPA (12). In addition to its role in haemostasis, Pn plays physiological role in tissue remodeling which involves the activation of matrix metalloproteases that, in turn, degrade the extracellular matrix (213,214). Thus like thrombin, plasmin is pleiotropic.

4.1 Thrombolytic/fibrinolytic therapy

Myocardial infarction and ischemic stroke are the first and third causes of death and disability in Western societies (50,215-217). Thus vascular disease is by far the leading cause of mortality. Thrombolytic therapy is a emerging as a very important treatment for such diseases, consisting of the pharmacological dissolution of the blood clots by activating the plasminogenase system (12,175).

A major advance in treatment of thrombotic disorders was the discovery of tPA (218,219). Tissue plasminogen activator administration (usually sc-tPA or alteplase) reduces the extent of tissue damage by restoring the flow of blood to occluded areas of the blood vessel where lysine residues are presented on the fibrin surface. However, systemic generation of Pn and hemorrhage are usually associated with such treatments. To reduce this risk, a most intensive program of site-directed replacement and deletion strategies in sc-tPA have been undertaken with the aim of generating a "super tPA" by enhancing clot specificity and fibrin binding affinity. While considerable progress has been made, overall these strategies seem not to be ideal suggesting that new strategies need to be considered (183,220).

The presently available non-recombinant thrombolytic agents, streptokinase and urokinase, are also associated with serious, sometimes life-threatening side effects due to the "systemic lytic state" characterized by fibrinogen degradation and α2-antiplasmin depletion in circulating blood (221,222). These thrombolytic drugs have no specific affinity for fibrin, thus activate circulating and fibrin-bound Pgn relatively equally. Consequently, solution-phase Pn is neutralized very rapidly by α2-antiplasmin and residual Pn is lost for thrombolysis, proteolyzing coagulation proteins including FV/FVa and FX/FXa causing serious hemorrhage.

Among the recombinant thrombolytic agents are: a rtPA deletion mutant, consisting of the kringle 2 and protease domain of tPA (retaplase); a rtPA deletion mutant, consisting of the protease domain and both kringle 1 and kringle 2 of tPA (lanoteplase); and a rtPA mutant with amino acid substitutions (223,224). Similarly recombinant sc-uPA (pro-uPA and prourokinase), and recombinant staphylokinase and derivatives have been produced for the purpose of improving upon available therapies (225-228).

The growing need for a better thrombolytic agent has been the driving force behind turning to other plasminogen activators, or molecules, with higher specific activity and different mechanisms of fibrin selectivity. Such molecules include the tPA from saliva of the vampire bat (bat PA) (229,230), and FIIa-specific antibodies (231). The later strategy entails the engineering of bifunctional

molecules that contain both a highly specific antigen binding site that concentrates the molecule at the desired target (the clot) and an effector site that will initiate thrombolysis.

Overall, thrombolytics have been developed exclusively on active enzymes. The most common side-effect is systemic fibrinolysis, since their activity is not exclusively localized to the site of clot formation where aPL are present. Hence, the long term goal of the current research work is to generate a clot-specific FVa-based cofactor, rather than a functional enzyme such as tPA, that will accelerate and localize the activity of tPA.

5.1 Communication between coagulation and fibrinolysis

Coagulation and fibrinolysis are separately regulated by a number of specific mechanisms. Both activation and inhibition of each cascade regulate and maintain a proper balance between fibrin formation at the site of vascular injury and subsequently its dissolution.

Recently a new molecular feedback mechanism between coagulation and fibrinolysis involving a plasma zymogen protein designated TAFI (thrombin-activatable fibrinolysis inhibitor) has been described. Upon activation by FIIa/TM complex, TAFI functions as an inhibitor of fibrinolysis (232,233). Alternatively, APC inactivation of TAFI results in enhanced fibrinolysis (233). TAFI, in vivo, may function as a molecular communicator in a "cross talk" between the

coagulation and the fibrinolytic cascades, such that expression of activity in coagulation down regulates the activity in fibrinolysis. Two other molecular communication mechanisms exist, involving fibrin and FIIa as the molecular communicators. In the first mechanism, clot formation generates a tPA cofactor (fibrin) which up-regulates fibrinolysis by Pgn localization and acceleration of Pn generation (195,196). Similarly, in the second mechanism, FIIa generation by the coagulation cascade induces tPA secretion by the vascular endothelium which leads to up-regulation of fibrinolysis (234-236).

6.1 Discovery of a new function for FVa

Earlier work from our laboratory has shown that prothrombinase components, namely FX (237), FXa (238,239), and FVa (239), when treated with Pn, accelerate tPA activity by as much as 60-fold with Lys-plasminogen and > 150-fold with Glu-plasminogen. Unique among the known tPA cofactors, this activity was highly dependent on Ca^{2+} and aPL. Since molecular feedback mechanisms between coagulation and fibrinolysis maintain blood haemostasis, the observations suggest that during fibrinolysis, and at the vascular damage site where aPL is exposed, Pn-cleaved FVa derivatives enhance Pgn conversion to Pn and may accelerate clot dissolution. While experiments to follow clot dissolution have not yet been conducted, this suggests a novel mechanism linking coagulation and fibrinolysis that involves Pn-cleaved coagulation FVa species present in the clot. Data also suggest that the FVa-derived tPA cofactor contains the FVa aPL-binding domain, which would localize tPA acceleration and

Pn generation to aPL trapped within a clot or other activated vascular cell surface. This characteristic may allow for the development of novel and unique strategies for thrombolytic therapy.

7.1 Thesis objectives

Section 1: The main hypothesis was that Pn and FVa are participants in a new regulatory mechanism to achieve haemostasis. Following Pn inactivation of coagulation components, a cofactor complex of FVa fragments is generated. Some of these fragments then bind and recruit plasminogen to the site of vascular injury and accelerate Pn generation and fibrinolysis. To address this hypothesis, the original objectives were:

(a) Identify the Pn-cleaved FVa fragments remaining associated in the presence of Ca^{2+}.

(b) Identify the aPL-binding fragments of Pn-cleaved FVaL.

(c) Quantify the new FVa-derived cofactor activity.

(d) Generate a recombinant FVa plasminogen cofactor capable of accelerating fibrinolysis in vitro.

However, since interesting structural information was obtained from section (a) implicating a region of 16 amino acids in FVaH in the Ca^{2+}-dependent subunit interaction, the project was redirected somewhat to address the hypothesis that Leu94-Lys109 is involved in FVaH-L interactions. Objectives (c) and (d), were consequently given a lower priority compared to:

(e) Generate recombinant FV proteins with various mutations in the newly identified functional region 96-111.

(f) Determine the cofactor activity of these recombinants in prothrombinase.

(g) Identify the effect of Ca^{2+} and EDTA on the recombinant proteins following FIIa activation.

Section 2: P135 was originally discovered by serendipity during the amplification of the interleukin 11 (IL-11) message from a human erythroleukemia cell line (HEL). Analysis of the unexpected amplicon revealed that the cDNA sequence was novel and had some homology to the sC2-domains. Since we have a general interest in aPL-binding proteins, the following project was undertaken in order to identify the function of p135 and understand the role the p135-sC2-domains play in aPL binding. Hence, the main focus was to identify cells that express the p135 protein and localize the protein in some of these cells. The question of whether C2-domains are functionally active in p135 was also addressed. The objectives were:

(a) Clone and sequence the mRNA for the P135 gene.

(b) Evaluate the P135 mRNA and protein expression in human tissues and in cancer cell lines.

(c) Localize P135 in cells.

(d) Develop a recombinant expression system for P135 that can be used to study P135 function.

(e) Determine whether P135 binds anionic phospholipid in a Ca^{2+}-dependent manner.

CHAPTER 2

Mechanism of FVa inactivation by plasmin: Loss of A2 and A3 from a Ca^{2+}-dependent complex of fragments bound to phospholipid

OVERVIEW

Previous studies had shown that the fibrinolytic effector plasmin (Pn) inactivates the cofactor function of FVa in the prothrombinase complex. The objective of this study was to understand this mechanism of inactivation using FVa bound to aPL-coated microtiter wells or large (1 μm) aPL micelles as affinity matrices. The results suggest that following Pn inactivation of aPL-bound FVa, a total of 16 fragments are generated. These had apparent molecular weights (kDa) and starting residues as follows: 50(L1766)-, 48(L1766)-, 43(Q1828)-, 40(Q1828)-, 30(S1546)-, 12(T1657)-, and 7(S1546) from FVaL; and 65(A1)-, 50(A1)-, 45(A1)-, 34(S349)-, 30(L94)-, 30(M110)-, plus 3 small fragments <5(W457, W457, K365) from FVaH. Of these, 50(L1766), 48(1766), 43(Q1828), 40(Q1828) spanning the C1/C2 domains, and 30(L94), but not the similar 30(M110), positioned within the A1 domain remained associated with aPL. These fragments were also detected antigenically during lysis of fibrin clot formed in plasma. Chelation by EDTA resulted in the dissociation of the 30(L94) fragment, which was observed to associate with intact FVaL upon recalcification. These results strongly indicated that that the Leu94-Lys109 region of the A1 domain plays a critical role in the FVaL and FVaH Ca^{2+}-dependent association. Using domain-specific monoclonal antibodies and an assay that measures α-thrombin generation in the presence of factor Xa (FXa), it was observed that loss of FVa prothrombinase function was coincident with proteolysis at sites in the A2 and A3 domains resulting in their dissociation. These data are consistent with the observation that Pn is an inactivator of FVa function, and specifically identify the

molecular composition of the Pn-cleaved FVa, which remains bound to membrane as largely A1-C1/C2 in the presence of Ca^{2+}. The data also suggest that Pn inhibits FVa by a process analogous to activated protein C, which involves A2 domain dissociation, but for Pn also involves loss of A3.

EXPERIMENTAL PROCEDURES

Chemicals and reagents. N-[2-Hydroxyethyl]piperazine-N'-[2ethanesulfonic acid] (HEPES), ethylenediaminetetracetic acid (EDTA), phosphatidylserine (PS), phosphatidylcholine (PC), bovine serum albumin (BSA), polyethylene glycol (PEG; Av. Mol. Wt.: 8000) (Sigma), aprotinin (Calbiochem), H-D-Phe-Pip-Arg-pNA.2HCl (S-2238, Chromogenix), Tween 20 (Fisher), and a chemiluminescent detection system (ECL, Amersham) were obtained commercially. Small unilamellar vesicles (SUV; average diameter: 50 nm) consisting of 75:25% mixture of PC/PS were prepared (239) and quantified as described (45). Large vesicles (LV; 300-600 nm) were made by extrusion using a Liposofast Basic apparatus (Avestin Inc.). LV consisting of 1-4 mg of 75:25% PC/PS was suspended in 1 ml methanol in glass tubes and dried to a thin film under a steady stream of nitrogen at 4 °C. The phospholipid was resuspended in 0.5 – 1 ml of 20 mM Hepes, 300 mM sucrose, pH 7.4, vortexed for 1 min, and subjected to ten freeze-thaw cycles. The suspension was then extruded through two 1 μm filters (Avestin, Inc.) and collected. The vesicles were then mixed 1:1 with 20 mM Hepes, 150 mM NaCl, pH 7.4 (HBS/Ca^{2+}) and harvested by centrifugation at

13,000 x g at 22 °C for 5-10 min. The pellet was resuspended in HBS, and quantified using an assay for total phosphorous (240)

Proteins. Human FVa, FXa, FII, plasminogen, Pn, monoclonal antibodies (mAb) specific for human FVaH (AHV-#5146), human FVaL (AHV-#5112), bovine FVaL (#5104) bovine FVaH (#5103), and polyclonal sheep anti-human FV (PAHFV-S) were from Haematologic Technologies Inc. TA cloning kit, and GeneClean II kit were from Stratagene, and the TA cloning kit from Invitrogen. Taq DNA polymerase, restriction enzymes, and DH5-α were from GibcoBRL, and the baculovirus expression kit was from Invitrogen. A mAb specific for FVa A3 domain (anti-FVaA3) was produced by Dr. R. Lemieux (Hema-Quebec) for which in-house recombinant FVaL produced using the Baculovirus system and purified by electroelution was used as antigen. PCR-screened R506Q homozygous plasma was a generous gift from Dr. M.C. Poon, U. Calgary, Canada. Rabbit antiserum to human plasminogen (Calbiochem), tissue plasminogen activator (tPA, Genentech), peroxidase-conjugated goat anti-mouse IgG (Jackson ImmunoResearch Inc.), peroxidase-conjugated goat anti-rabbit IgG (Promega), assayed reference plasma (ARP, Helena Laboratories), and thromboplastin (Sigma) were commercially obtained.

Factor Va proteolysis by Pn. FVa (0.1 μM) was incubated with Pn (0.1 μM) in the presence of SUV (250 μM) or LV (600 μM) and Ca^{2+} (2 mM) in HBS/Ca^{2+} at 22 °C. The digests were sampled over time, and heated at 95 °C for 5 min in

sample buffer (2% SDS, 2% 2-mercaptoethanol, 0.325 M Tris base (pH 6.5), 10% glycerol and 0.001% bromphenol blue). The digests were subjected to 10% SDS-PAGE (241), stained with Coomassie Blue, or electrotransferred to polyvinylidene fluoride (PVDF; Immobilon-P, Millipore) (242). The PVDF membrane was blocked at 22 °C for 1 h in milk (5%), and cleavage products of FVa were detected by Western analysis using chemiluminescence (ECL).

FVa was also cleaved by Pn when bound to aPL-coated microtiter wells prepared as previously described (239) except that the wells were blocked with gelatin (5 mg/ml) in HBS/Ca^{2+}, and 0.001% Tween 20 was included in the wash buffer. After equilibration of the FVa with the aPL-coated well in HBS/Ca^{2+}, the wells were washed and Pn (0.1 μM) in HBS/Ca^{2+} was added. At selected time points, four wells were quickly washed and bound protein was eluted with 25 μl SDS-PAGE sample buffer/well and pooled, heated to 95 °C for 10 min, and subjected to 10% SDS-PAGE. To visualize cleavage products, gels were either stained with Coomassie Blue or transferred to PVDF and detected with anti-FVaA3, anti-FVaL, anti-FVaH, or anti-human FV.

Production of human FVaH and FVaL. To generate monoclonal antibodies specific for each of the two FVa subunits, recombinant FVaH and FVaL were produced for our study. Two primers that span the FVaH open reading frame (sense primer: 5'-CGT CGT AAT CCT TAA TCC TCG TTG TTA CCT TTG TCT-3', antisense: 5'-TAC CCA AAG CTT AGC GGG AGC AGG AAA GGA-3'), and

two primers that span the FVaL open reading frame (sense primer: 5'-GCA GCA TTA GGA ATT AGG AGC AAC AAT GGA AAC AGA-3', antisence: 5'-GAC ACT ATA AAT GAT CCG CCG GCG TAT CCA ATT T-3') were used to amplify a FVa plasmid DNA containing the entire FVa cDNA. A volume equivalent to 50 ng of plasmid DNA was added to the amplification reaction (100 mM Tris-HCL pH 8.2, 50 mM KCL, 2.5 mM $MgCl_2$, 200 μM of each of dATP, dCTP, dGTP, dTTP, 20 pmoles of each primer and 2.5 units of Taq polymerase in a 50 μl final volume. The reaction was first heated to 95 °C for 3 minutes to denature the DNA followed by 30 cycles of denaturation at 95 °C for 25 seconds, annealing at 56 °C for 15 seconds and extension at 72 °C for 3 min. Amplification products were analyzed on a 1 % agarose gel in TBE buffer containing 0.5 mg/ml ethidium bromide. The gel was briefly illuminated with UV light, and the 1.8 and 2.2 kb DNA fragments, corresponding to the heavy and light chains of FVa respectively were excised with a scalpel blade. DNA from the gel fragment was purified using the GeneClean II procedure for cloning. This DNA was first ligated to a PCR II vector (3.9 kb) using the TA cloning kit. Positive clones were detected based on their colour; white colonies contain an insert, whereas blue colonies are empty vectors. DNA from positive colonies was purified, cleaved with Bam HI, which was then used to clone into the Bam HI digested pVL1393 cloning vector. PCR was used to detect positive pVL1392 colonies. DNA (500 ng) was extracted from the pVL1392 transfection vector which was then used in the cotransfection procedure. Transfection was performed according to the manufacturer's instructions (Invitrogen). After three rounds of viral amplification in SF9 insect

cells, cells were harvested and nuclear and cytoplasmic cell lysates were prepared. As a negative control pVL1393 vector containing no insert DNA was used to transfect SF9 cells.

FVa proteolysis by Pn in a clot. To determine whether Pn-cleaved FVa fragments observed in a purified system could also be identified in a physiological setting, FVa fragmentation in a lysing clot was studied. In these experiments, pooled plasma (2.5 μl of pooled plasma) was clotted by treatment with thromboplastin (80 μg/μl) after recalcification (10 mM $CaCl_2$). Individual reactions were incubated for various times with Pn (50 nM) or tPA (0.5 nM) at 37°C in a 7.5-μl final volume of HBS. The reactions were stopped by SDS, run on 10% SDS-PAGE, transferred to PVDF, and visualized by Western blotting with anti-FVaL and anti-FVaH antibodies. To better resolve the fragments of interest a concentration of acrylamide was used that in most cases does not allow the single chain FV to enter the gel (10 %).

Amino acid sequencing. N-terminal sequencing of Pn-mediated FVa fragments transferred to PVDF after reducing SDS-PAGE was conducted. To sequence exclusively the FVa-derived fragments remaining bound to aPL in the presence of Ca^{2+} or EDTA, FVa digestions were conducted in the presence of LV and bound fractions were separated by centrifugation prior to electrophoresis. Individual bands were excised for sequence analysis.

Effect of EDTA on dissociation of Pn-cleaved FVa fragments. FVa (0.1 μM) was cleaved with Pn (0.1 μM) for selected time points on aPL-coated wells as described above except that an excess amount of aprotinin (50 Kallikrein-inactivation units/ml; KIU/ml) was added to inhibit residual Pn activity. aPL-bound fragments were incubated at 22 °C for 3 h in HBS/Ca^{2+} or in HBS with EDTA (10 mM: HBS/EDTA) to allow for dissociation of Ca^{2+}-dependent interactions. Protein samples were subjected to 12% SDS-PAGE, transferred to PVDF and visualized with anti-FVaH and anti-FVaL. To determine whether Pn remains associated with the cleaved fragments, antiserum to human Pgn (30 ng/ml) was used on identical membranes.

FVa subunit dissociation kinetics. The 30-kDa fragment and FVaH dissociation with EDTA (10 mM) was monitored electrophoretically. FVa bound to aPL-coated wells was cleaved with Pn (0.1 μM) for 1 h, and Pn proteolytic activity was inhibited with aprotinin (50 KIU/ml). Wells were washed three times and 200 μl of HBS/EDTA (10 mM) was added for selected time points. Dissociation of FVaH due to Ca^{2+} chelation was monitored after SDS-PAGE by Western blotting. In a parallel set of experiments, FVa cofactor activity for FIIa generation was assessed chromogenically (0.5 μM S2238). Following the last wash, factor Xa (0.06 μM), and FII (1.0 μM) in 100 μl HBS/Ca^{2+} were added at 22 °C for 5 min. and the change in absorbence at 405 nm was monitored using a Vmax spectrophotometer (Molecular Devices).

Ca^{2+}-dependent association of the 30-kDa fragment with FVaL. To determine whether the 30-kDa fragment of FVaH can associate with FVaL, we had to initially obtain and concentrate sufficient amounts of the 30-kDa fragment. An aPL-coated plate was coated with FVa (300 ng/well) which was then cleaved with Pn (0.1 μM). Supernatants from all the wells (19 ml) were pooled and the mixture was concentrated by repeated cycles of centrifugation on a Biomax-10 membrane (Millipore) to approximately 2 ml. To determine whether the 30-kDa fragment can associate with intact FVaL, FVaH was separated from aPL-immobilized FVaL with EDTA for 3 h at 22 °C. The 30-kDa fragment was then incubated in HBS/Ca^{2+} or HBS/EDTA with FVaL remaining bound to the aPL-coated well at 22 °C for 2 h, then at 37 °C for 30 min. The wells were washed, and remaining protein was eluted with sample buffer. Association of the 30-kDa fragment was evaluated with anti FVaH by Western blotting.

Ligand blots. To identify FVaH- and FVaL-derived species that interact with plasminogen, ligand blotting experiments were performed. FVa (0.1 μM) was incubated with Pn (0.1 μM) on aPL-coated 96-well microtiter wells. The fragments that remained associated following washing with Ca^{2+} were removed over time with sample buffer (2% SDS, 2% 2-mercaptoethanol, 0.325 M Tris base (pH 6.5), 10% glycerol and 0.001% bromophenol blue) and heated at 95 °C for 5 min. The digests were electrotransferred to PVDF after SDS-PAGE. The PVDF membrane was blocked at 22 °C overnight at 4 °C in bovine serum albumin (10 mg/ml) and then incubated with ^{125}I-plasminogen (0.1 μM) for 1 h at

22°C in the presence of the protease inhibitors, 2-guanidino-ethylmercaptosuccinic acid (50 nM) and aprotonin (Calbiochem, 50 kallikrein-inactivating units/ml). The PVDF membrane was washed with HBS and the location of bound ^{125}I-plasminogen was determined by autoradiography and compared with the electrophoretic patterns made visible by Western blots.

RESULTS

FVa cleavage by Pn. To identify fragments that are generated during inactivation of FVa by Pn in the presence of SUV and Ca^{2+}, SDS-PAGE was conducted on Pn-cleaved FVa, which revealed a sequential cleavage pattern (Figure 2.1). Both the 104-kDa FVaH and the 74/71-kDa doublet of FVaL were rapidly cleaved in a Pn-dependent manner within 10 min. into products of approximately 50-, 48-, 45-, 40-, 34-, 30-, 12-, and 7-kDa, along with several smaller fragments that migrated close to or at the dye-front. To determine whether the digestion profile was aPL-dependent, experiments were performed in the absence of aPL vesicles, but in the presence of Ca^{2+}. It was found that the rate of digestion of the light chain was accelerated in the presence of aPL, whereas the rate of digestion of the heavy chain was not altered (not shown). Aprotinin completely inhibited the cleavage of FVa by Pn. No distinction in the size of fragments generated was observed when the digestion was performed in the absence or presence of aPL, although additional cleavages were observed when the interaction between FVaL and FVaH was inhibited by chelation (not shown).

Figure 2.1 **Time course of Pn cleavage of FVa bound to SUV.**

Purified human FVa (0.1 μM) was incubated with Pn (0.1 μM) in the presence of aPL-containing small unilamellar vesicles (250 μM) in HBS/Ca^{2+} (2 mM) at 22 °C. At selected time intervals aliquots were withdrawn from the mixture, and stopped immediately with SDS-containing sample buffer. Samples were separated on 10% SDS-PAGE and stained with Coomassie blue. Incubation times (min) with Pn are shown above the figure.

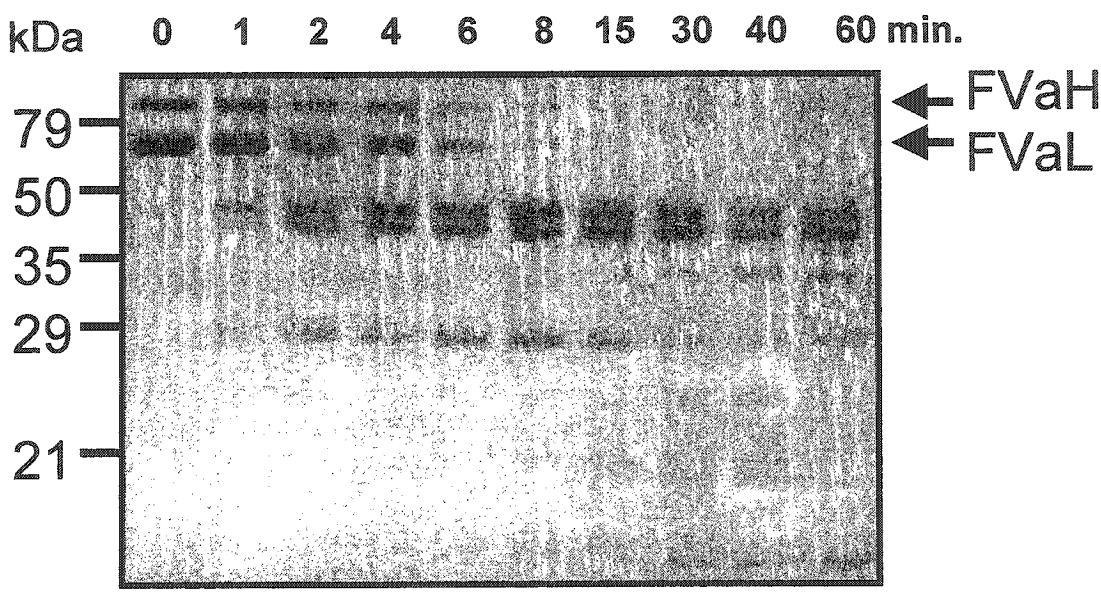
kDa
0
1
2
4
6
8
15
30
40
60 min.
79
50
35
29
21
FVaH
FVaL

Production of monoclonal antibodies. The commercially obtained chain-specific antibodies (FVaH #5146, and FVaL #5112) that were available at the time of this research from Hematologic Technologies were not well characterized. Furthermore, in order to obtain sufficient monoclonal antibodies for the purification of FVa, we generated recombinant FVaH and FVaL using recombinant DNA technologies and the baculovirus expression system (Figure 2.2, and 2.3). Both the FVaH and the FVaL fragments were detected in the insect cell lysate using chain-specific antibodies (Figure 2.3). These were electroeluted from a large SDS-PAGE and injected into several mice (Dr. R. Lemieux, Hema Quebec). Several antibodies were generated and tested for their ability to recognize the FVa chains by Western blotting. Of these, monoclonal antibody anti-FVaA3 additionally recognized a 30-kDa light chain fragment that was not detected with the commercially available anti-FVaL (#5112) antibody and the polyclonal antibody PAHFV-S. For this reason, this antibody was used in fragmentation analysis experiments.

Correlation between Pn-mediated FVa fragments remaining bound to aPL and loss of cofactor activity. To determine phospholipid binding specificity of FVa on 96-well plates, the plates were coated with 300 μg of PC:PS (25:75 %), PC (100 %), or PS (100 %) and FVa was incubated on the plates for 30 min. The fragments that remained bound were analyzed by Western blots. We observed that FVa specifically bound PS and PC/PS (Figure 2.4). Only a small amount of FVa remained bound to PC indicating aPL-specificity by FVa.

Figure 2.2 **Amplification of human FVaL and FVaH by the polymerase chain reaction.**

Recombinant DNA (50 ng) was amplified for 30 cycles as described in materials and methods and a fraction (10 %) of the amplified product was electrophoresed on 1% agarose gel. DNA was then visualized following staining by ethidium bromide and photographed under an ultra violet lamp.

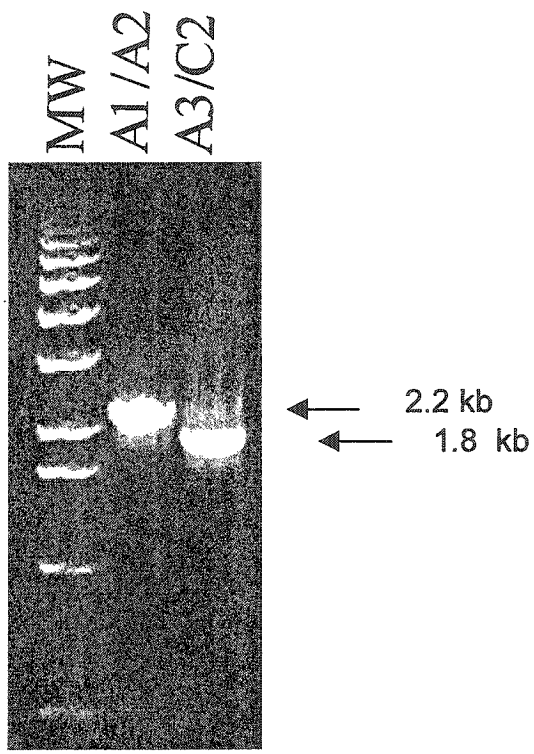
MW
A1 /A2
A3 /C2
2.2 kb
1.8 kb

Figure 2.3 **Expression of recombinant human FVaH and FVaL by the baculovirus expression system.**

Insect SF9 cells were infected with recombinant baculovirus and harvested 3 days after infection. Nuclear (left panels) and Cytoplasmic (right panels) fractions of the cell lysates were electrophoresed on 8% SDS-PAGE. A, proteins were made visible by Coomassie Blue staining. A parallel experiment was performed as in A except that the gels were transferred to PVDF and recombinant protein was detected by Western blotting with mouse anti-FVaH (#5146) (B), or with mouse anti-FVaL (#5112) (C). The arrows indicate the location of the recombinant proteins.

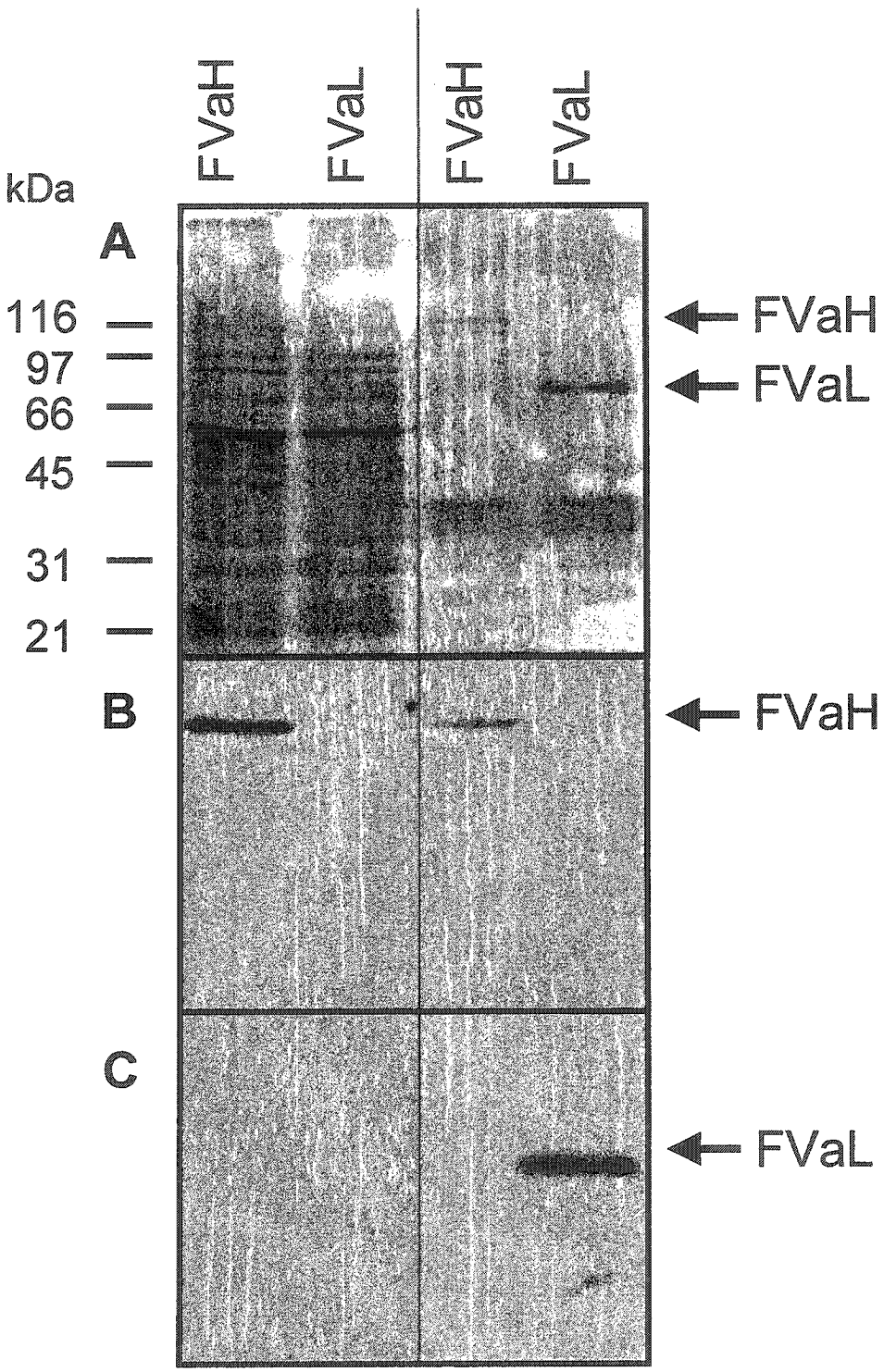
FVaH
FVaL
FVaH
FVaL
kDa
A
116
97
66
45
31
21
B
C
FVaH
FVaL
FVaH
FVaL

Figure 2.4 **Binding of human FVa to aPL-coated wells.**

96-well microtiter wells were coated with 300 μg of PC:PS (75:25 %), PC (100 %), or PS (100 %) and blocked with gelatin (5 mg/ml). The wells were incubated with FVa (0.1 μM) for 30 min, and then incubated in HBS/Ca^{2+} buffer. APL-bound protein was then removed from the wells with sample buffer, and separated on 10 % SDS-PAGE. The protein was transferred to PVDF and detected with anti-FVaL (#5112).

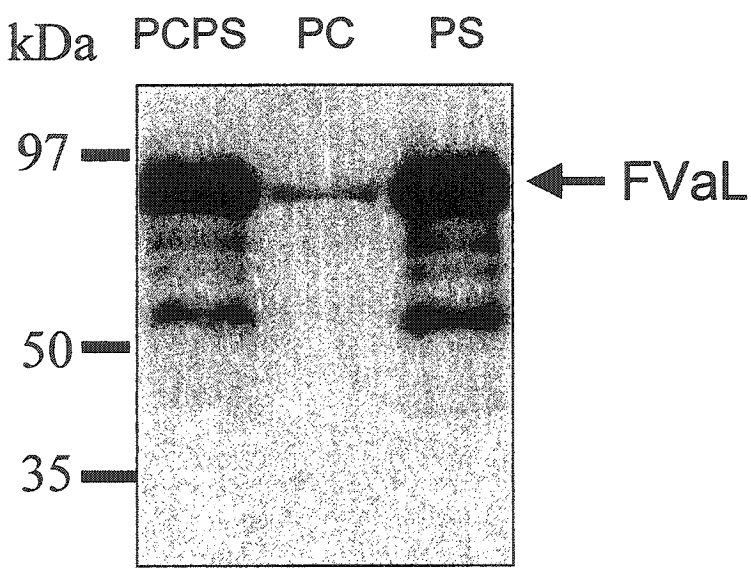
kDa
PCPS
PC
PS
97
50
35
FVaL

To determine which fragments remained non-covalently associated with aPL in the presence of Ca^{2+}, FVa was equilibrated with aPL-coated microtiter wells and fragments that remained bound to the plate after digestion with Pn were washed with buffer containing Ca^{2+}. Remaining fragments were analyzed by Western blots using a FVaH- and two FVaL-specific mAb. These data showed that the fragments of 50-, 48-, 43-, 40-, and 30-kDa were light chain-derived (Figure 2.5A, 2.5B). Since the mAb in panel B recognizes the A3-domain, the completely different fragmentation pattern suggests the commercial mAb used in panel A has specificity for the C-terminal part of FVaL containing C1/C2. As shown, the 50- and 48-kDa FVaL fragments were converted to 43-, and 40-kDa and all remained bound to aPL. Since all aPL binding of FVa is mediated by FVaL, these fragments contain at least part of the Ca^{2+}-independent membrane-binding site(s). Furthermore, we found that the fragments of, 50-, 45-, and 30-kDa were FVaH-derived and remained bound in the presence of Ca^{2+} (Figure 2.5C). The 30-kDa FVaH-derived fragment also remained at least partly bound over the time course of the experiment. A comparable Ca^{2+}-dependent complex of fragments was observed with bovine FVa (not shown). We did not observe a detectable difference in the rate of cleavage or the cleavage pattern, between experiments performed on aPL-coated plates, LV or SUV (not shown). Furthermore, no detectable difference in the cleavage pattern was observed when the samples were electrophoresed under non-reducing conditions, indicating no disulfide-linked fragments were produced (not shown). While all the

Figure 2.5 **Time course of Pn cleavage of FVa subunits bound to aPL-coated wells.**

96-well microtiter wells were coated with aPL (300 μg) and then blocked with gelatin (5 mg/ml). The wells were preincubated with FVa (0.1 μM) for 30 min, and then with Pn (0.1 μM) in HBS/Ca^{2+}. At the selected time points, aPL-bound protein was removed from the wells with sample buffer, and separated on 10% SDS-PAGE. The protein was transferred to PVDF and detected with anti-FVaL (14H12) (A), anti-FVaA3 (3H7) (B), or anti-FVaH (#5146) (C). The arrows indicate the location of the expected protein bands. Panel D, as in panel A except that following incubation with Pn, FXa (0.06 μM), and FII (1.0 μM) were added. Thrombin generation was monitored with S2238. The average of four experiments with standard deviation is shown. Incubation times (min) with Pn are shown.

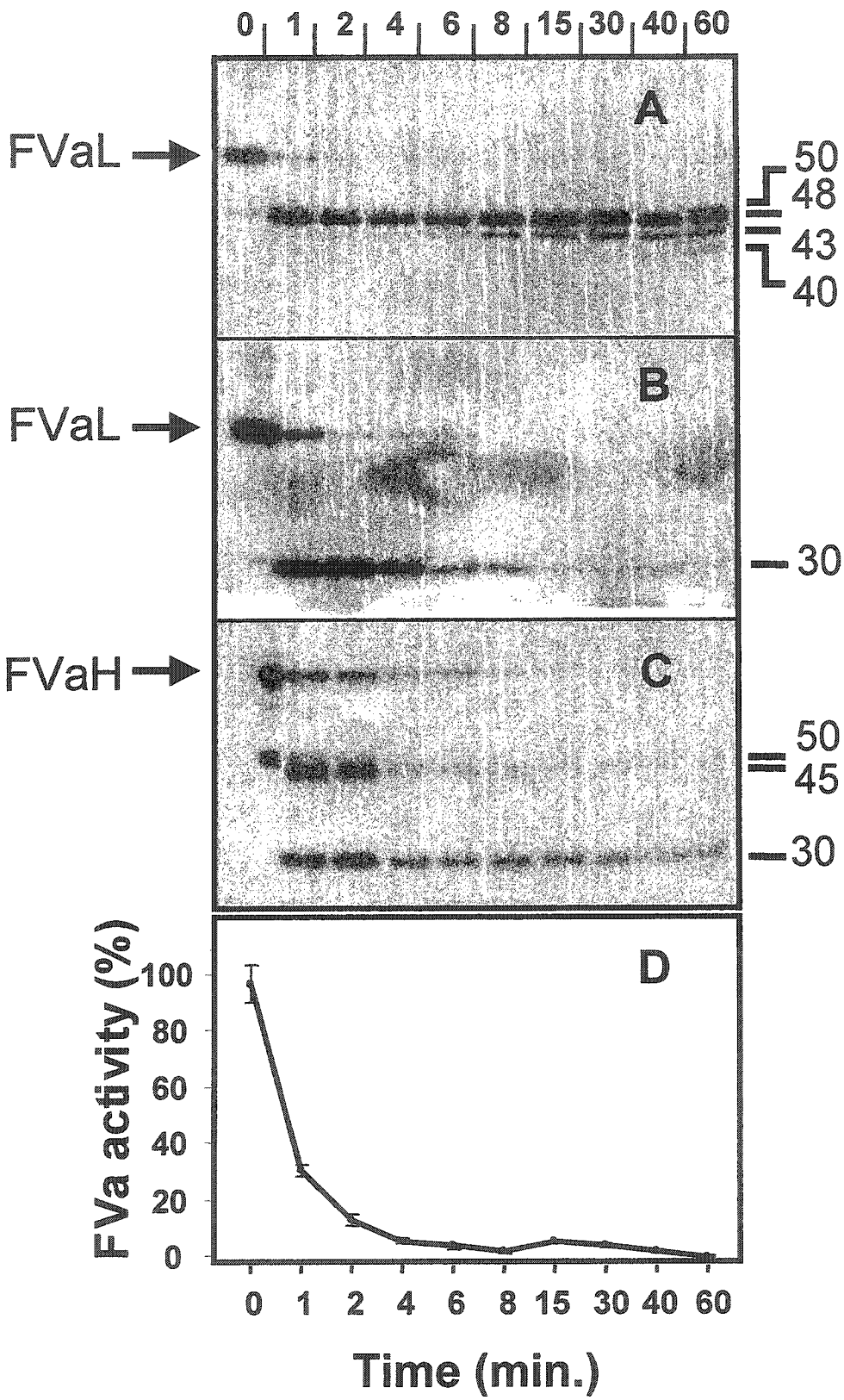
0 1 2 4 6 8 15 30 40 60
A
FVaL
50
48
43
40
B
FVaL
30
C
FVaH
50
45
30
D
FVa activity (%)
100
80
60
40
20
0
0 1 2 4 6 8 15 30 40 60
Time (min.)

aPL-bound bands, visualized by Coomassie blue, silver, and polyclonal staining, were detected with the mAbs (not shown), an additional unbound 34-kDa fragment, released into solution upon cleavage, was observed with Coomassie blue (Figure 2.1).

In order to correlate the appearance of degradation products with observed changes in FVa cofactor activity, fragments remaining bound to aPL were assayed for FVa function. Inactivation of FVa by Pn was rapid over the time course of the experiment (Figure 2.5D). Following an 8 min incubation with Pn, the aPL-bound FVa was completely inactive. The rapid loss of cofactor activity coincided with appearance of the 30-kDa A3, 48- and minor 50-kDa C1/C2-derived fragments and with the 45- and minor 50-kDa heavy chain-derived fragments.

Cleavage of FV and FVa by Pn in a fibrin clot. Having established the fragment composition of purified Pn-inactivated FVa, we determined whether these fragments were also generated under more physiological conditions. Thromboplastin was added to plasma to generate a fibrin clot, and the FV/FVa fragmentation pattern was examined following either Pn- or tPA-induced clot dissolution. Western blots (Figure 2.6) showed that the FVaH- and FVaL-derived fragmentation pattern was identical to those in our purified system regardless of whether Pn or tPA was used to induce clot fibrinolysis. These data support the physiological relevance of the model system.

Figure 2.6 **Pn-cleaved FVa fragments in a lysing clot.**

Microcentrifuge tubes containing recalcified plasma were incubated with thromboplastin (80 μg/μl) in HBS at 37 °C for 3 min. Following clot formation, Pn (50 nM; left panels) or tPA (0.5 nM; right panels) was added to individual reactions for the indicated time points. The reactions were stopped with sample buffer, and the protein was separated on 10% SDS-PAGE, transferred to a PVDF membrane and detected with anti-FVaL (#5112) or anti-FVaH (#5146). Pooled plasma (time 0), incubation times (min) with Pn or tPA are shown above the figures.

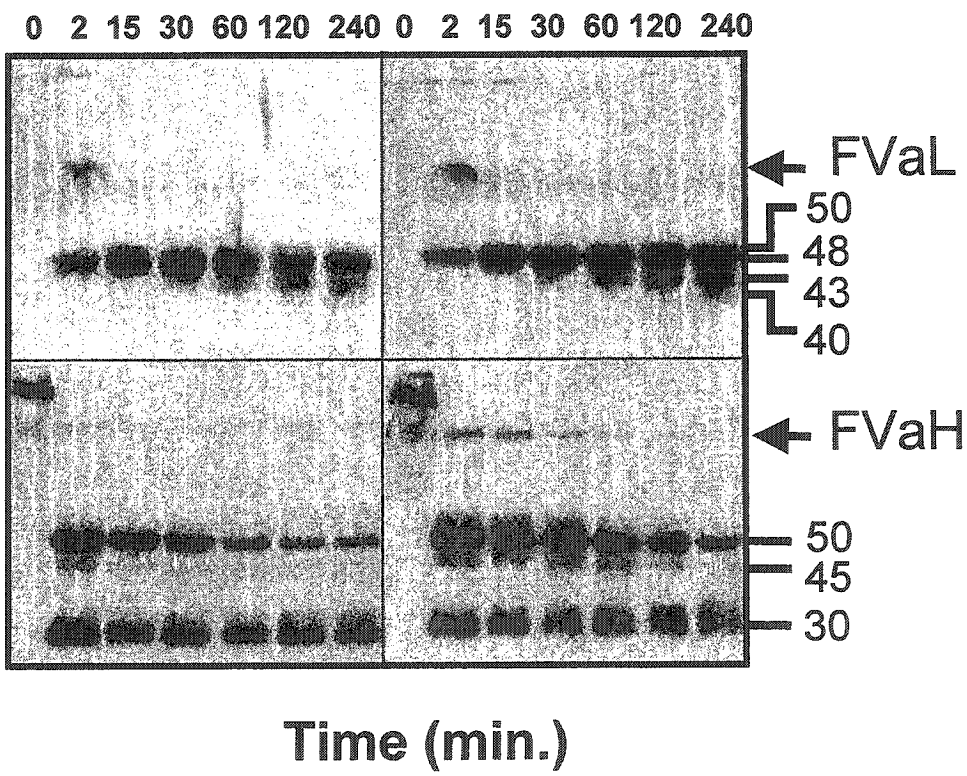
0 2 15 30 60 120 240 0 2 15 30 60 120 240
FVaL
50
48
43
40
FVaH
50
45
30
Time (min.)

Identification of Pn cleavage sites in FVa. To identify the specific sites of Pn-mediated cleavage, amino acid sequence analyses were conducted on all the Coomassie blue-stained fragments derived from purified FVa. Figure 2.7A shows the banding pattern of the fragments subjected to analysis and the sequences are summarized in Figure 2.7B. As expected, because of recognition by a single mAb, the 65-, 50-, 45-, and 30-kDa FVaH fragments overlap and each contains at least a large portion of the A1 domain (starting at Leu94). The 30-kDa FVaH band was found to be two co-migrating species, which differed by 16 amino acids starting at residues Leu94 or Met110, and hence were referred to as 30(L94), and 30(M110). The 34-kDa fragment not detected by the mAbs, corresponded to the C-terminal end of FVaH, and unexpectedly contained a conserved polymorphism at residue 352 (Leu to Thr) (Figure 2.7B). This is the first report to our knowledge of this substitution, which is consistent with the FVa being purified from pooled plasma. Once generated, the 34-kDa fragment was quickly proteolysed into fragments of less than 7-kDa, of which several were sequenced. FVaL is cleaved by Pn to give 50-, 48-, 43-, and 40-kDa fragments that overlap as predicted from their antigenicity and begin toward the C-terminal end of A3. By this method, a 30-kDa FVaL fragment, corresponding to the N-terminal end of the light chain was distinguishable. This fragment was short-lived and was processed into several smaller fragments of which two were sequenced.

Figure 2.7 **Identification of proteolytic cleavages in FVa by Pn.**

FVa (1.5 μM) was preincubated with aPL vesicles (300 μM) in HBS/Ca^{2+} for 15 min prior to cleavage by Pn (0.2 μM) at 22 °C for 1 h. The reaction was then stopped with SDS-containing sample buffer, heated at 95 °C for 5 min, and separated on large (12 x 14 cm) 8% SDS-PAGE. Panel A, protein was transferred to PVDF membrane and stained with Coomassie Blue R250 stain. Panel B, N-terminal sequences of visible FVa fragments shown in panel A.

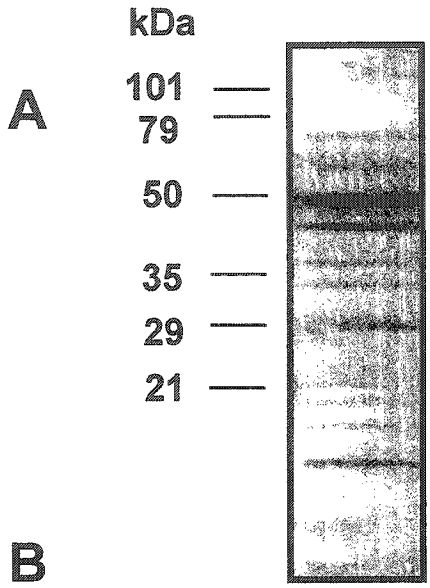

Species	Sequence	Alignment
65-kDa	AQLRQFYV	1-8
50-kDa	AQLRQFYV	1-8
50-kDa	LTSSEMKK	1766-1773
48-kDa	LTSSEMKK	1766-1773
45-kDa	AQLRQFYV	1-8
43-kDa	QHQLGV_P	1828-1835
40-kDa	QHQLGV_P	1828-1835
34-kDa	SQHL(T)DNFSNQ	349-358
30-kDa	LSEGASYLDHTF	94-105
30-kDa	SNNGNRRN	1546-1553
30-kDa	MDDAVAPGRE_T	110-121
12-kDa	TYEDDSPEWF	1657-1666
7-kDa	SNNGNRRNYY	1546-1555
5-kDa	WNILEFDEPT	457-466
<5-kDa	WNILEFDEPT	457-466
<5-kDa	KVMYTQYEDE	365-374

Ca^{2+}-dependent association of Pn-mediated FVa fragments. Since FVaH does not contain the aPL-binding site, and is anchored to aPL through divalent cation-dependent interactions with FVaL, we investigated the effect of EDTA on the FVa fragments remaining bound to aPL. Digestion end-point fragments that remained bound to aPL-coated wells after cleavage of FVa with Pn were subjected to an additional wash containing 10 mM EDTA. Interestingly, the 30-kDa component of FVaH and the 50- and 40-kDa FVaL-derived fragments dissociated from the aPL in the presence of EDTA (Figure 2.8). Conversely, the FVaL 48- and 43-kDa fragments remained associated with aPL following EDTA treatment. Collectively, these data suggest that regions within the 48/43-kDa fragments of FVaL and the 30-kDa fragment of FVaH contribute to the Ca^{2+}-dependent intermolecular association between FVaL and FVaH. It is unknown at present why apparent Ca^{2+}-dependent differences exist between the 48/43-kDa and 50/40-kDa fragments.

To determine if the rate of EDTA-mediated dissociation of the FVaH-derived 30-kDa species from FVaL fragments is representative of dissociation of intact FVaH from intact FVaL, a time course experiment was conducted (Figure 2.9). Release of the 30-kDa (panel A) or FVaH (panel B) from aPL-coated microtiter wells by EDTA was followed by Western blotting. Although the general trend was comparable over the duration of the experiment, intact FVaH has an apparently faster initial phase of dissociation than the 30-kDa fragment. This may be indicative of a role for A2 in FVaL binding. As an additional means of

Figure 2.8 **Effect of EDTA on aPL-associated FVa fragments.**

FVa was treated with Pn (as in Figure 2.5, 60 min), except that after incubating with Pn, Pn activity was inhibited with aprotinin (50 KIU/ml) in HBS/Ca^{2+} for 15 min. Wells were then incubated in HBS/Ca^{2+} (lane 1) or HBS/EDTA (lane 3) at 22 °C for 2 h. In lane 2, Pn was not added to the well prior to the addition of HBS/EDTA. Protein samples were separated on SDS-PAGE and transferred to PVDF. Western blot analysis was performed with a mixture of anti-FVaL (#5112) and anti-FVaH (#5146) (A), or anti-FVaH (#5146))B).

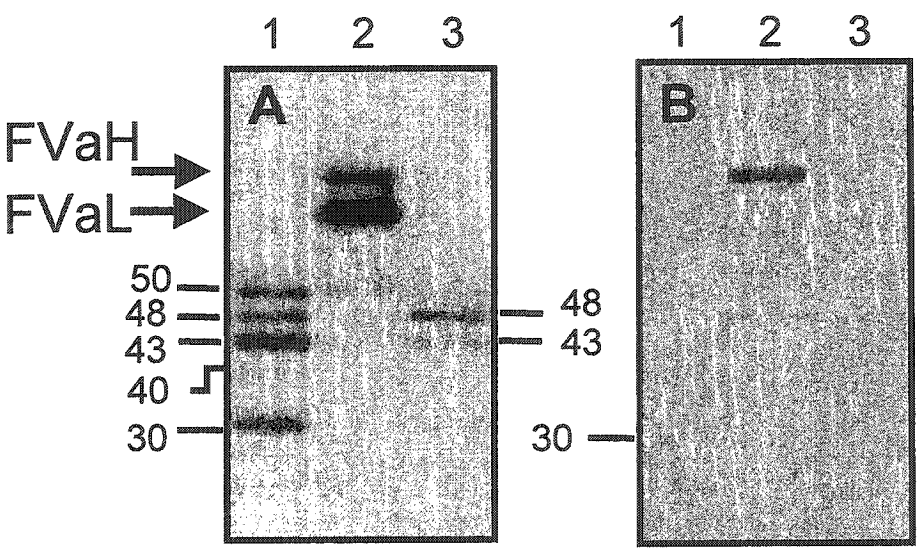
1
2
3
A
FVaH
FVaL
50
48
43
40
30
1
2
3
B
48
43
30

Figure 2.9 **EDTA-induced dissociation of Pn-cleaved FVa and FVa subunits.**

Panel A: FVa was treated with Pn (as in Figure 2.5, 60 min). After a brief wash with HBS/Ca^{2+}, the wells were incubated with HBS/EDTA for the indicated times, and the 30-kDa FVaH fragment remaining bound to the aPL-coated well was detected by Western blotting. Panel B, as in panel A except no Pn was included. Panel C, as in panel B except that following incubation with EDTA, factor Xa (0.06 μM), FII (1.0 μM), and SUV (20 μM) were added. Thrombin generation was monitored with S2238. The average of triplicates with standard deviation is shown.

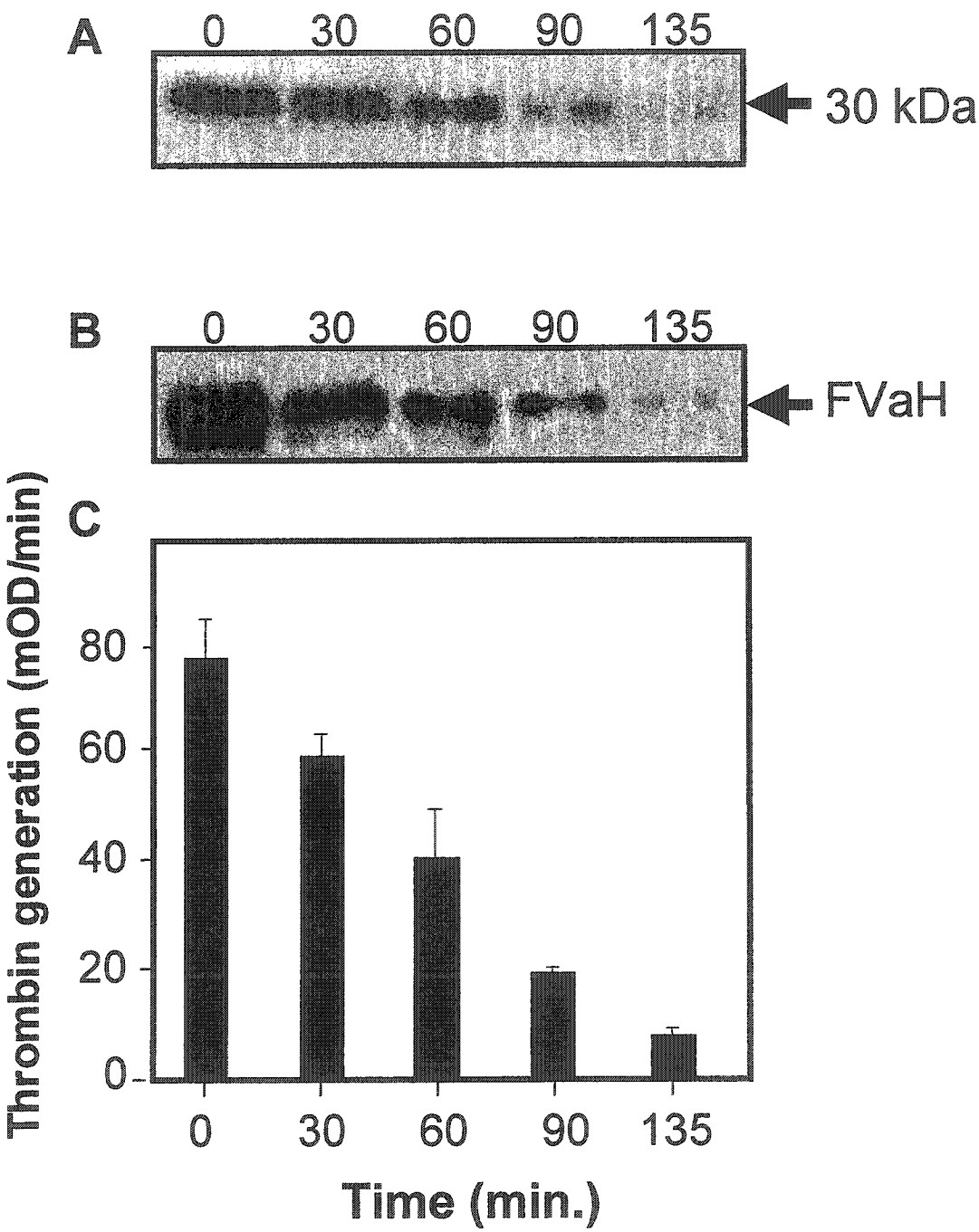
A
0
30
60
90
135
30 kDa
B
0
30
60
90
135
FVaH
C
Thrombin generation (mOD/min)
80
60
40
20
0
0
30
60
90
135
Time (min.)

following FVaL and FVaH dissociation, the effect of EDTA on FVa function was followed by measuring the loss of FIIa generation in a chromogenic assay (Figure 2.9C). As expected, EDTA-mediated inhibition of FVa activity correlated with the dissociation of the 30-kDa fragment or intact FVaH from FVaL and are in agreement with the slow dissociation rates previously reported (8, 12). These results demonstrate that the Ca^{2+}-dependent interactions observed for Pn-cleaved FVa are representative of intact FVa.

The dependence of Ca^{2+} on the association of the 30-kDa FVaH fragment to intact FVaL was studied to further investigate whether the association we observed between Pn-mediated fragments of FVa reflected those within the intact molecule. aPL-coated microtiter wells were saturated with FVa, then treated with EDTA to dissociate FVaH, which was confirmed antigenically. The 30-kDa species of FVaH was then added in the presence of Ca^{2+}, resulting in association specifically with intact FVaL (Figure 2.10). Binding was found to be Ca^{2+}-dependent since no detectable association was observed in the presence of EDTA. Significant Ca^{2+}-dependent binding of the 30-kDa fragment to aPL-coated wells depended on the presence of FVaL (not shown). These data provide additional evidence that the 30-kDa fragment constitutes the FVaH-derived portion of a Ca^{2+}-dependent contact region with FVaL.

Identification of aPL-bound fragments following Pn cleavage of FVa. To identify by sequence analysis the species that remained bound to aPL in the presence or

Figure 2.10 **Effect of EDTA on the association of the 30-kDa fragment with FVaL.**

FVaH was separated from aPL-immobilized FVaL with EDTA. The 30 kDa FVaH fragment was then added to the wells in HBS/Ca^{2+} (lane 1), HBS/EDTA (lane 2) at 22 °C for 2 hr, then at 37 °C for 30 min. The wells were washed with HBS/Ca^{2+} and remaining protein was eluted with SDS-containing sample buffer. Protein was separated on 10% SDS-PAGE, transferred to PVDF membrane and detected with anti-FVaH (#5146) monoclonal antibody.

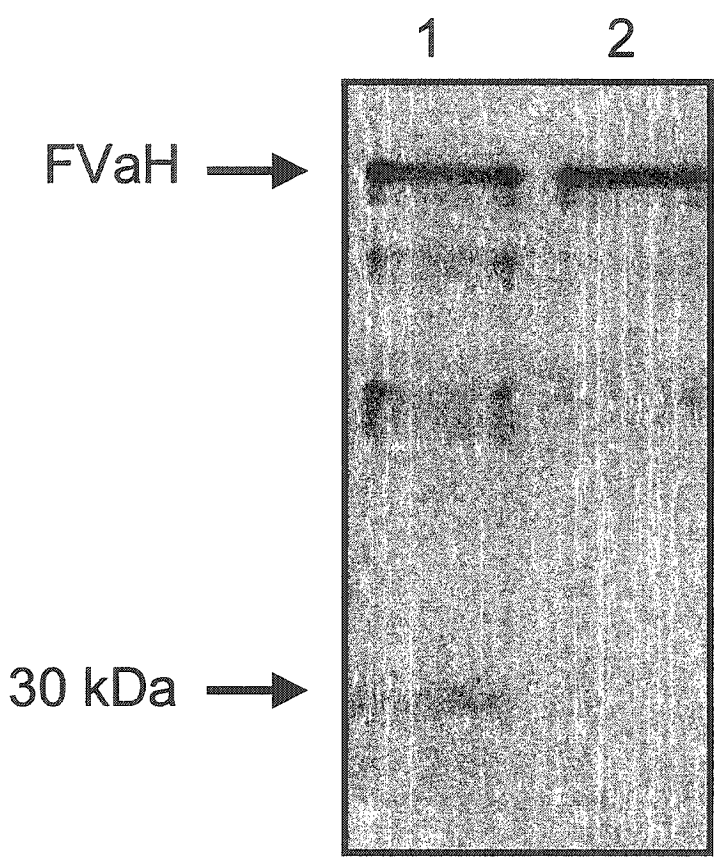
1
2
FVaH
30 kDa

absence of Ca^{2+}, LV were utilized as a preparative affinity matrix. In this experiment, aPL-bound FVa was pelleted by centrifugation after Pn treatment. As before, the 65- and 30-kDa FVaH-derived fragments and the 50-, 48-, 43-, and 40-kDa FVaL fragments were observed to remain bound to aPL in the presence of Ca^{2+}. Of these only the 48-, and 43-kDa fragments remained bound in EDTA (Figure 2.11A). Sequence analyses (Figure 2.11B) confirmed their identification. An unexpected observation was made concerned the co-migrating FVaH-derived 30-kDa fragments we identified in Figure 2.7. After affinity fractionation, sequencing revealed that 30(L94) remained bound to aPL. In contrast, the similar sized fragment starting at Met110 was not observed to remain bound in the presence of Ca^{2+}, suggesting that the 94-110 region is important for the Ca^{2+}-sensitive interchain contact.

Pn-mediated fragments of bovine FVa and their Ca^{2+}-dependent association. By having established the fragmentation pattern and fragment composition of purified Pn-inactivated human FVa, we determined whether a similar fragmentation pattern were also generated following cleavage of bovine FVa by Pn. Commercially available purified bovine FVa was equilibrated with aPL-coated wells and cleaved with Pn. The fragments that remained bound were analyzed. Western blot (Figure 2.12A) showed that a fragmentation pattern is generated that is very similar to the pattern obtained with human FVa (Figure

Figure 2.11 **Identification of the Pn-cleaved FVa fragments that dissociate in the absence of Ca^{2+}.**

Panel A, FVa (1.5 μM) was incubated with LV (600 μM) in HBS/Ca^{2+} and Pn (0.2 μM) as above. Proteolysis was stopped with aprotinin (50 KIU/ml). Following 3 h incubation with EDTA, LV-bound fragments were separated by centrifugation. The pellet fraction (Lane 1) and the supernatant fraction (lane 2) were then run on large (12 x 14 cm) 10% SDS-PAGE, transferred to PVDF and stained with Coomassie blue R250 stain. Panel B, N-terminal sequence of each fragment.

A

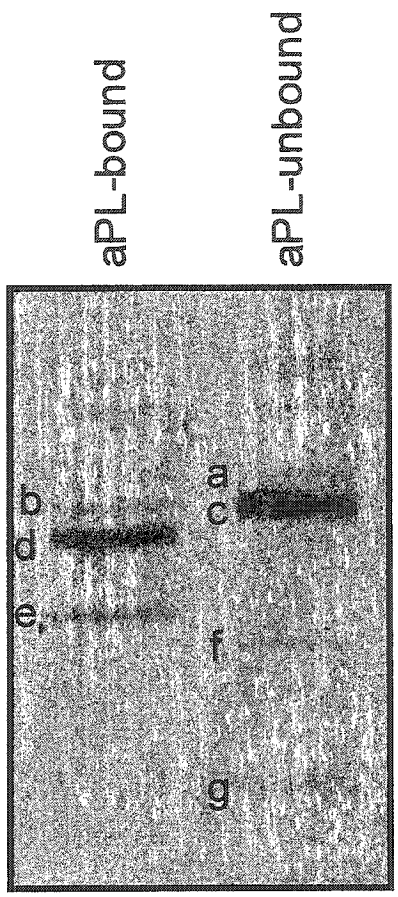

B

Species	Sequence	Alignment
a) 65-kDa	AQLRQ	1-5
b) 50-kDa	no data	
c) 50-kDa	LTSSE	1766-1770
c) 50-kDa	AQLRQ	1-5
d) 48-kDa	LTSSE	1766-1770
e) 43-kDa	_HQLG	1828-1832
f) 40-kDa	no data	
g) 30-kDa	LSEGA	94-98

Figure 2.12 **Time course of Pn cleavage of bovine FVa subunits bound to aPL-coated wells and effect of EDTA on aPL-associated FVa fragments.**

A, 96-well microtiter wells were coated with aPL (0.3 μg) and then blocked with gelatin (5 mg/ml). The wells were preincubated with bovine FVa (0.1 μM) for 30 min, and then with Pn (0.1 μM) in HBS/Ca^{2+}. At the selected time points, aPL-bound protein was removed from the wells with sample buffer, and separated on 10% SDS-PAGE. The protein was transferred to PVDF and detected with a mixture of anti-FVaL (5105) and anti-FVaH (5104). B, bovine FVa was treated with Pn (as in Figure 2.5, 60 min), except that after incubation, Pn activity was inhibited with aprotinin (50 KIU/ml) in HBS/Ca^{2+} for 15 min. Wells were then incubated in HBS/Ca^{2+} (lane 1) or HBS/EDTA (lane 2) at 22 °C for 2 h. Protein samples were separated on SDS-PAGE and transferred to PVDF. Western blot analysis was performed with anti-FVaH (5104).

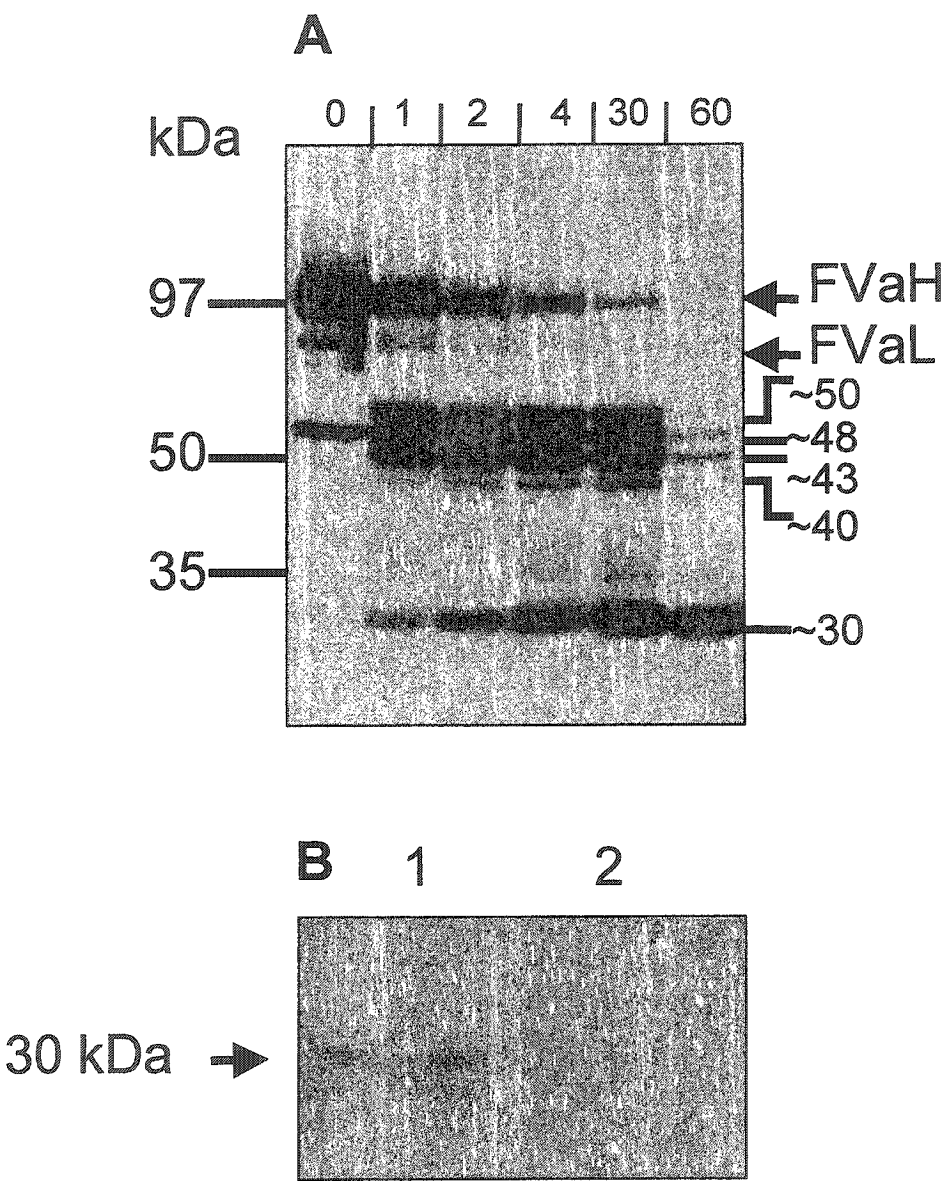
A
kDa
0
1
2
4
30
60
97
50
35
FVaH
FVaL
~50
~48
~43
~40
~30
B
1
2
30 kDa

2.5A, and 2.5C). These data confirm the data from the human FVa experiments and indicates that the mechanism of Pn inactivation of human and bovine FVa is similar. However, these fragments remain to be identified by sequence analysis.

As with the human FVa experiment, we also investigated the effect of EDTA on the bovine FVa fragments remaining bound to aPL-coated wells. The 30-kDa fragment of bovine FVaH chain dissociated from the aPL in the presence of EDTA (Figure 2.12B). These data also confirm the data from the human FVa experiment, and indicates that the two proteins may have a similar Ca^{2+}-dependent contact structure.

Binding of plasminogen to Pn-cleaved FVa fragments. Previous results from our lab have indicated that aPL-bound Pn-cleaved FVa fragment(s) enhances Pn generation (239). To determine whether the fragments that we observed following cleavage of aPL-bound FVa by Pn bind plasminogen, FVa was cleaved with Pn on aPL-coated 96-well microtiter wells, and the fragments that remained associated following washing with Ca^{2+} were transferred to PVDF following SDS-PAGE and incubated with I^{125}-labelled plasminogen overnight. The results from Figure 2.13 indicate that at least two bands bind plasminogen under our experimental conditions. A higher molecular weight band (~ 50 kDa) and a lower molecular weight band (~30 kDa) are observed to interact with plasminogen. Based on their relative mobility, these two fragments may likely have originated from the Pn-FVaL and Pn-FVaH chains respectively (Figure 2.13B).

Figure 2.13 **Binding of plasminogen to Pn-cleaved FVa fragments.**

Purified human FVa (0.1 μM) was incubated with Pn (0.1 μM) on aPL-coated wells in HBS/Ca^{2+} at 22 °C. At selected time intervals aliquots were withdrawn from the mixture, and stopped immediately with SDS-containing sample buffer. Samples were separated on 10% SDS-PAGE, transferred to PVDF membrane and (A) detected with anti-FVaL (#5112) monoclonal antibody, or (B) incubated in the presence of I^{125} labeled plasminogen (B). The reactive bands were visualized by auroradiography.

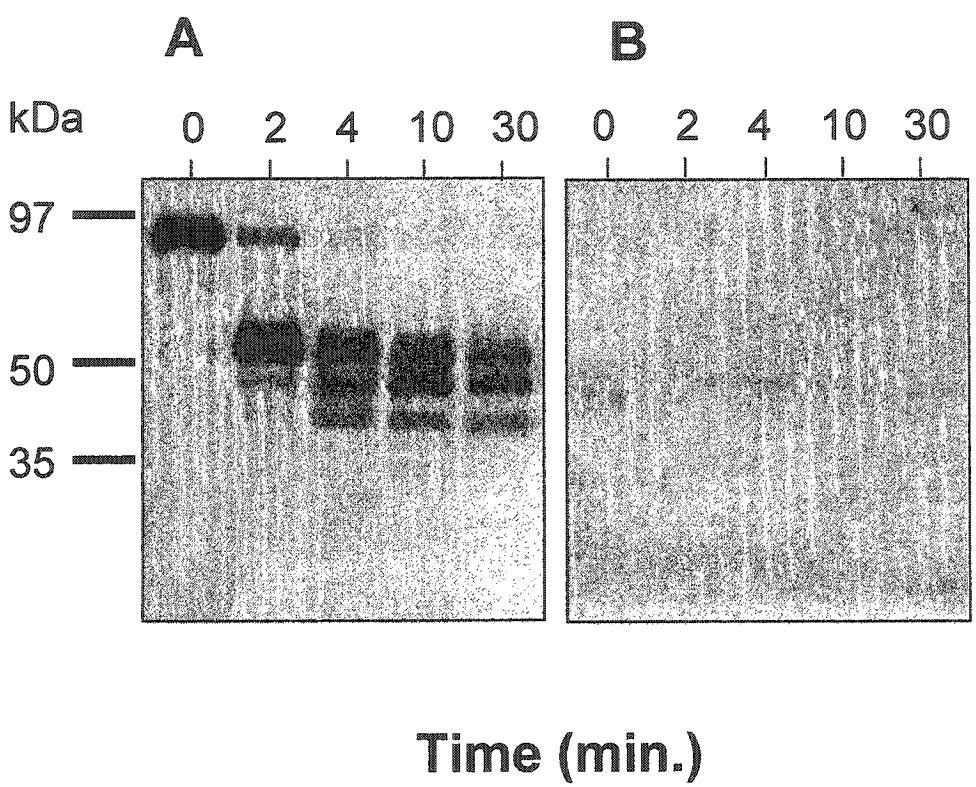
A
B
kDa
0
2
4
10
30
0
2
4
10
30
97
50
35
Time (min.)

DISCUSSION

For over a decade, Pn has been known to induce a complicated cleavage pattern in FVa which causes complete inhibition of coagulation cofactor function. To understand how this functional effect is achieved, we have identified the location of the cleavage sites and present here a fragmentation map (Figure 2.14). This study revealed that the A2 and A3 domains of FVa are proteolysed at several sites resulting in their dissociation, which correlates to inactivation of the molecule. This process is analogous to the A2 dissociation correlated to the inactivation of FVa by APC (243) and for the spontaneous decay of FVIIIa activity (244). However, the loss of A3 from aPL-bound FVa as part of an inhibition mechanism is novel. Since FXa also cleaves FVa at Arg348 and Arg1765 without apparent loss of FVa coagulation cofactor activity (245), our results demonstrate that additional cleavages within these fragments and at Lys1827 ultimately result in the observed complete loss of FVa activity. Cleavage of FVaH by Pn appears to occur by two cleavage pathways (Figure 2.15) that ultimately lead to the loss of the A2 domain and the generation of a 30-kDa doublet. In the major cleavage pathway, the 30-kDa species is generated from a prominent 45-kDa N-terminal fragment. In the minor cleavage pathway, the 30-kDa fragment is generated from a 50-kDa intermediate N-terminal fragment which is produced from a 65-kDa fragment. The C-terminal fragments from both pathways are quickly proteolysed to smaller fragments that migrate close to or at the dye-front (Mr < 7-kDa). In contrast, the 30-kDa fragment was observed to persist throughout the time of the experiment.

Figure 2.14 **Cleavage of FVa by Pn in the presence of Ca^{2+}.**

A Pn-mediated fragmentation map of FVa was constructed to scale based on N-terminal sequence and the apparent molecular weight of fragments which was relativized to the average Mr of an amino acid (110 Da). The estimated fragment number of amino acids in each is complicated by glycosylation not included in the estimate of fragment length. Thin lines indicate disulfide linkages.

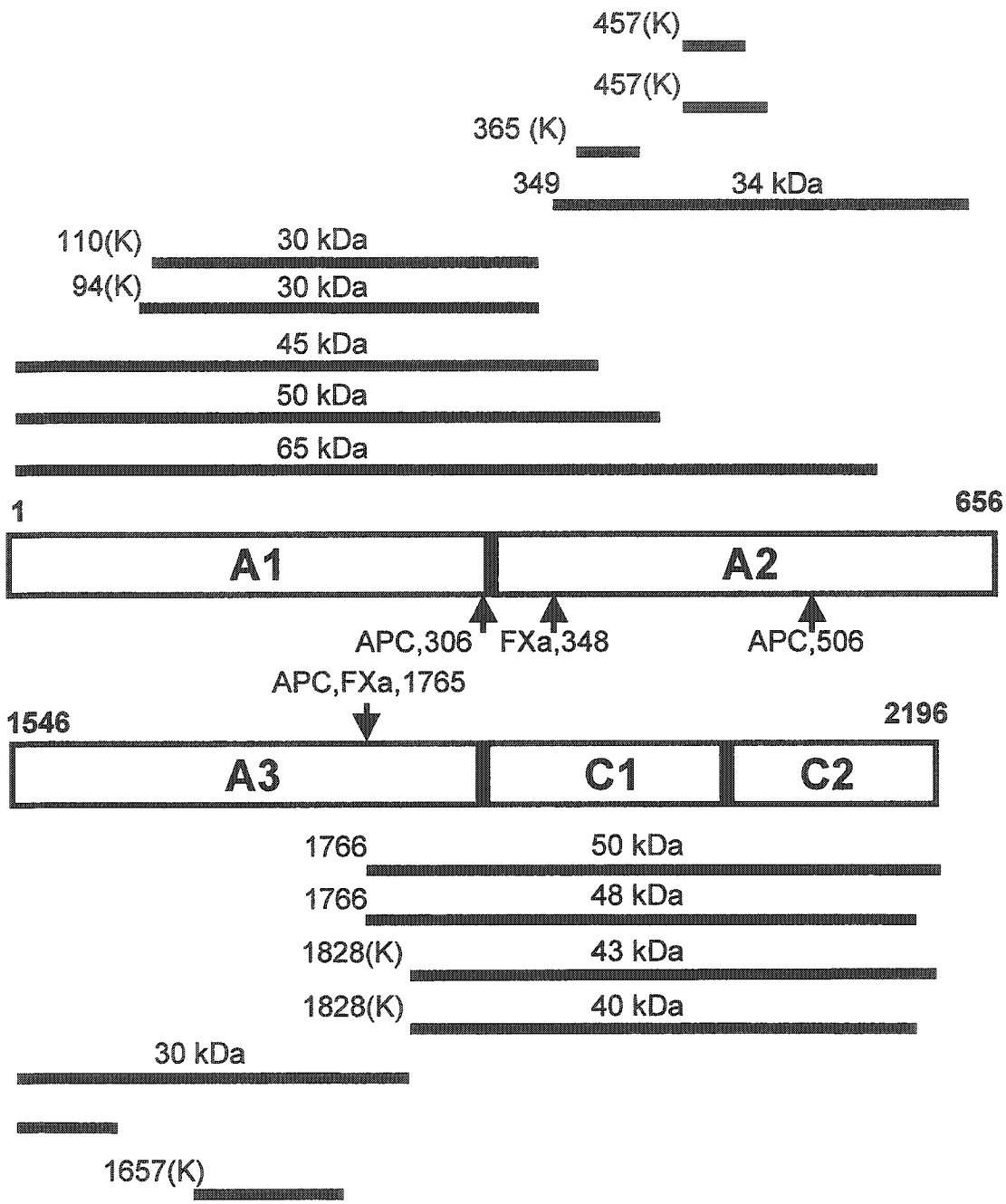
457(K)
457(K)
365 (K)
349
34 kDa
110(K)
30 kDa
94(K)
30 kDa
45 kDa
50 kDa
65 kDa
1
656
A1
A2
APC,306
FXa,348
APC,506
APC,FXa,1765
1546
2196
A3
C1
C2
1766
50 kDa
1766
48 kDa
1828(K)
43 kDa
1828(K)
40 kDa
30 kDa
1657(K)

Figure 2.15 **Predicted order of cleavage of FVa by Pn.**

The probable order of cleavage of FVaH (A) and FVaL (B) is shown. The information was obtained from the fragmentation map presented in Figure 2.14.

A

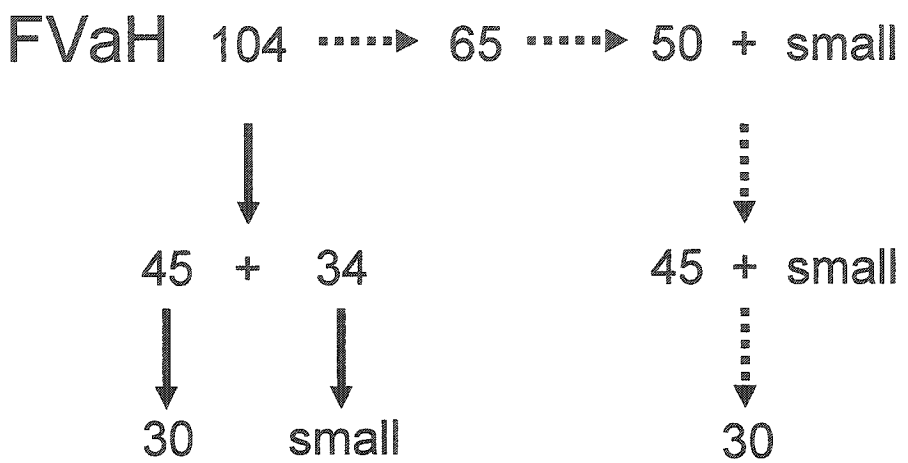
FVaH
104
65
50 + small
45 + 34
45 + small
30
small
30

B

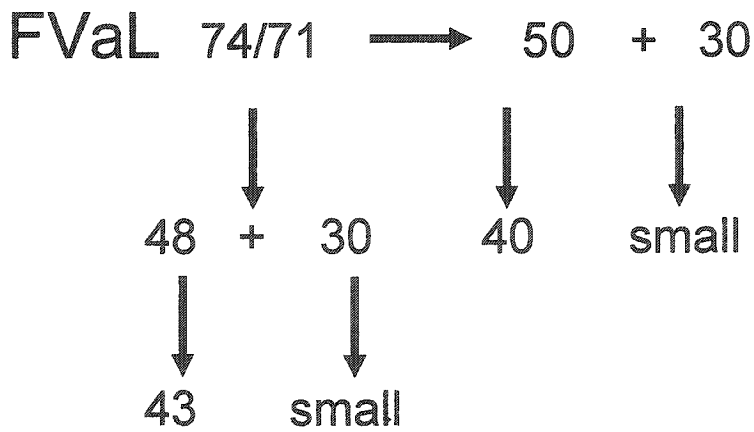
FVaL
74/71
50 + 30
48 + 30
40
small
43
small

Cleavage of FVaL with Pn resulted in the rapid proteolysis of the 30-kDa (A3 domain) N-terminal fragment ultimately leading to dissociation of the A3 domain from the aPL-bound protein and hence the conversion of the 74/71-kDa FVaL into the 40- and 43-kDa C-terminal fragments. We suggest that the 50- and 48-kDa fragments are intermediates of the 40- and 43-kDa fragments, respectively, because of similar Ca^{2+}-dependent aPL-binding properties of the 50/40- and 48/43-kDa species.

To our knowledge, this study is the first to describe the Pn cleavage sites within human FVa, although Kalafatis and Mann presented the N-terminal amino acid sequence of Pn-cleaved fragments from bovine FVa (117,168). They found that Pn cleaves FVa heavy and the light chains generating a total of 6 fragments of Mr 48, 47, 46 42, 40, and 30 kDa from cleavages at K348, K309, K310, and R313 in bovine FVaH and K1664 (K1656 in human FVa), and R1753 (R1765 in human FVa) in bovine FVaL. Complete cleavage of bovine FVaH resulted in the production of two major fragments (Mr 42 and Mr 40 kDa) (168). The identity of some of these species differs from those presented here for human FVa, with cleavages at Arg348, Lys1656, and Arg1765 being in agreement. The most striking difference resulting from the comparison of the bovine fragments with the human ones is that in the bovine studies, no Pn cleavages were detected in the N-terminus of the bovine FVa A1 domain (the 47 and 40 kDa fragments) at K93 and K109. Another major difference is the absence of additional cleavages in the

bovine FVaH A2 domain (Mr 34 kDa in human and Mr 42 kDa in bovine) and bovine FVaL A3 domain (Mr 30 kDa in human and Mr 30 kDa in bovine). Hence, while we report here that the dissociation of the A2 domain is likely due to these additional cleavages at K364, and K456 in the Mr 34 kDa fragment, Kalafatis and Mann reported that the dissociation of the A2 domain occurs following cleavage at R348. These differences in the cofactor cleavage pattern between the two species, especially in the A2 and A3 domains, are likely related to incomplete cleavages in the bovine protein or due to inherent differences in the inactivation process in the two proteins. However, our studies with bovine FVa although preliminary, indicate that, based on visual comparisons of the Coomassie blue stained gels of Pn-cleaved human and bovine FVa, the cleavage pattern of bovine FVa with Pn was identical to that of the human FVa (Figure 2.12A). This observation can be confirmed following sequencing of the bovine fragments. Supporting this observation is the EDTA-induced dissociation of the 30-kDa fragment which was analogous to the dissociation observed with the human 30-kDa FVa fragment.

To determine if the Pn-derived FVa fragments we observed in purified systems can occur in a physiological setting, we tested whether these fragments are generated following either Pn or tPA treatment of plasma-derived clot. The data showed that the 30-kDa fragment of FVaH and the four light chain-derived fragments are generated in clots lysed by either Pn or tPA. Together, these results support the hypothesis that at the site of clot formation, where the local

concentration of the coagulation cofactor is elevated, Pn processing of FVa, may have a physiological function. In further support of physiological relevance, Tracey et al. (246) previously reported the extent of FV proteolysis during thrombolytic therapy with tPA and found that cleavage of FV is primarily Pn-mediated. As an extension of this report, we found no detectable difference between fragments that remain bound to aPL following Pn treatment of FV or FVa (not shown). Independent observations of a FV fragmentation pattern in clots similar to ours have been made (247) where the authors speculated a Pn-dependent origin. We can not, however, omit the possibility that cell-dependent processes may influence the cleavage profile, such as the requirement of cell-surface thrombomodulin for APC function, or cathepsin G or elastase from monocytes (248).

The contribution of aPL to the assembly of prothrombinase components, and to the localization of FIIa production to the site of injury, has been well documented (249-254). Furthermore, it has been shown that FVaL confers all of the aPL-binding function of FVa (114,124,133,255-257) and that this interaction is Ca^{2+}-independent (114,256,258). Several studies suggest that the C2 domain contains the aPL-binding region of FVaL (134,135), while others have implicated the A3 (133) or both the A3 and C2 domains (257). Having identified the cleavages induced by Pn in FVa, we determined which fragments remained bound to aPL. Upon cleavage of FVa by Pn, four FVaL-derived fragments and one FVaH-derived fragment remained bound to aPL in the presence of Ca^{2+}

(Figure 2.16). Amino acid sequencing and antigenicity revealed that the four FVaL-derived species overlap, with the 50/48- and the 43/40-kDa fragments originating from a common cleavage site at R1765 and Lys1827, respectively. Each of these excludes a large portion of the A3 domain, and includes the entire C2 domain, providing support for C2 function in aPL binding.

Of the four FVaL fragments that remained bound to aPL (Figure 2.16B), only the 48- and 43-kDa fragments remained in the presence of EDTA. Since these are encompassed by the 50-kDa fragment and span the 40-kDa fragment, both of which dissociated from aPL due to chelation, an explanation is difficult to provide without further study. One possibility is related to the two forms of FVa that have been identified, designated FVa_1 and FVa_2, which differ in the C-terminus of FVaL (141,142). The difference has been suggested to be due to alternative glycosylation at Asn2181 within the C2 domain (134,143,144) leading to a weaker association between FVa_1 and aPL (141,142,259). Since we found that the 48-kDa fragment associated strongly with aPL, it is possible that the difference in the electrophoretic mobility between the 50- and 48-kDa species is due to derivation from FVa_1 and FVa_2, respectively. At this time, we cannot exclude alternate processing at the C-terminus by Pn resulting in the weaker aPL-binding 40-kDa fragment originating from the heavier 50-kDa species. An additional explanation for the different aPL-binding properties of overlapping fragments may be found in the two forms of the C2 domain recently observed by X-ray crystallography (260). These differ markedly in one of the three protruding

Figure 2.16 **Fragments that remain bound to aPL following cleavage of FVa by Pn in the presence of Ca^{2+}.**

A Pn-mediated fragmentation map of aPL-bound FVaH (A) and FVaL (B) fragments was constructed to scale based on N-terminal sequence and the apparent molecular weight of fragments which was relativized to the average Mr of an amino acid (110 Da), see Figure 2.7. The estimated fragment number of amino acids in each is complicated by glycosylation not included in the estimate of fragment length. The amino acid sequence in the A1 domain starting at 94-115 is shown, and the 94-109 amino acids that are missing from the smaller 30kDa fragment. APC and Pn cleavage sites are shown above and below the sequence. Acidic residues predicted to be involved in Ca^{2+} binding are circled.

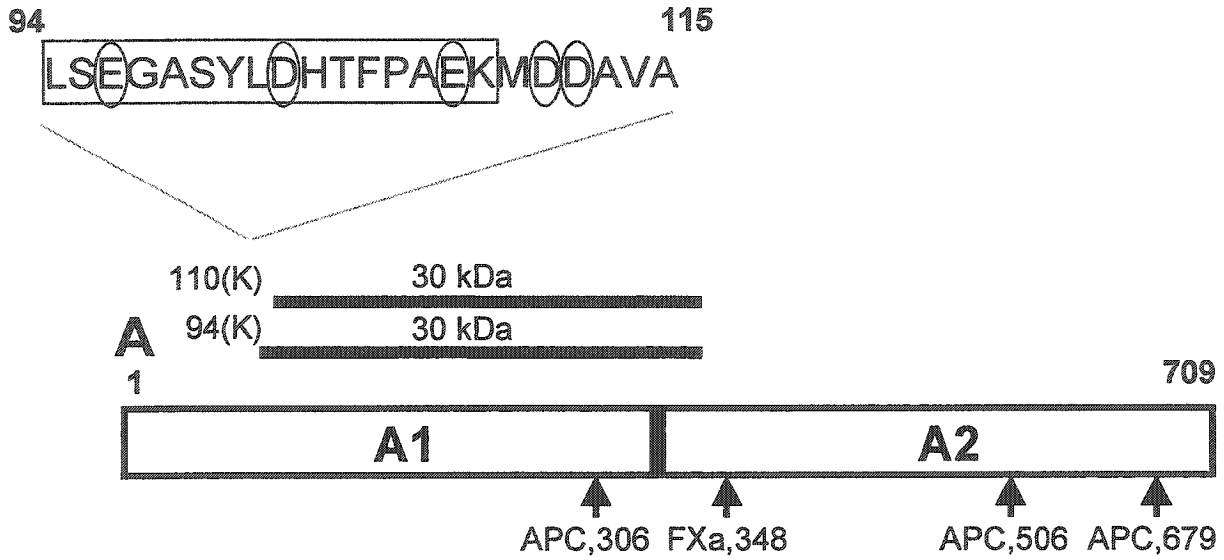
94
115
LSEGASYLDHTFPAEKMDDAVA
110(K)
30 kDa
94(K)
30 kDa
A
1
709
A1
A2
APC,306
FXa,348
APC,506
APC,679

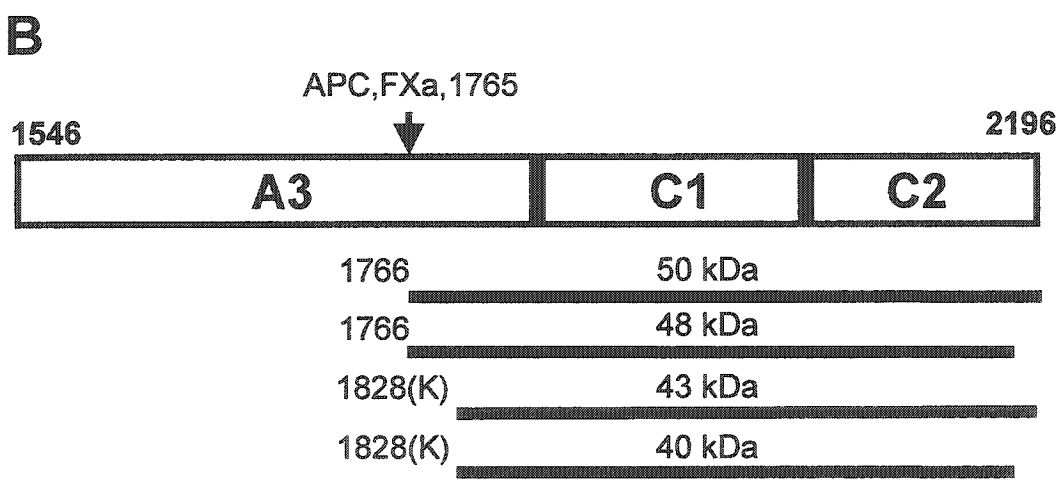
B
APC,FXa,1765
1546
2196
A3
C1
C2
1766
50 kDa
1766
48 kDa
1828(K)
43 kDa
1828(K)
40 kDa

hydrophobic loops implicated in aPL binding. Possibly, the Pn-mediated 50- and 40- kDa fragments originate from the FVaL type suggested by crystallography to have weaker aPL-binding. Notwithstanding, our observations provide further support for a role of the C2 domain in Ca^{2+}-independent aPL-binding.

It is well established that EDTA-dissociated FVaL and FVaH chains can reassociate in the presence of additional Ca^{2+} (Kd = 6 $X10^{-9}$ M) (115). Although Ca^{2+} does not bind to either of the individual FVa chains alone, it has been shown that a single high affinity binding site becomes available when the two chains are bound together (Kd = 24 X 10^{-6} M) (116). The first experimental evidence localizing the Ca^{2+}-sensitive interchain contact comes from our identification of two FVaH fragments with identical electrophoretic mobility. These differ at the N-terminus by only 16 amino acids (Figure 2.16A). Of these, the fragment beginning at Leu94 remained associated with FVaL-derived fragments in a Ca^{2+}-dependent manner, whereas the similar species beginning at Met110 did not interact with FVaL even in the presence of Ca^{2+}. These data suggest that a Ca^{2+} sensitive site may be contained between Leu94 and Lys109. Consistent with this hypothesis, X-ray structure and molecular modeling, using homologous protein templates based on the ceruloplasmin and factor VIII A-type domains, has suggested a putative Ca^{2+} ion-binding site within the A1-A3 interface (97,98). Interestingly, of the five negatively charged residues (Glu96, Asp102, Glu108, Asp111, and Asp112) predicted to be involved in the Ca^{2+} binding pocket in the A1 domain (97), three residues are located between amino

acids Leu94 and Lys109, and the remainder are neighboring (Figure 2.16A). While this molecular modeling supports our finding that a Ca^{2+}-sensitive region between Leu94 and Lys109 may exist, direct studies must be conducted to substantiate this likelihood.

To determine whether the observed Ca^{2+}-dependent association between the fragments of Pn-cleaved FVa is representative of the intact FVaH/FVaL interaction, we demonstrated that the rates of EDTA-induced dissociation of the 30(L94) species from Pn-cleaved FVa and FVaH from intact FVa were comparable. Furthermore, the dissociation rate closely resembled the timing of FVa inactivation by EDTA. To further demonstrate the contribution of the region within FVaH corresponding to the 30-kDa fragment in the FVaL interaction, we followed the 30-kDa fragment association with aPL-bound intact FVaL. Our results demonstrate that the 30(L94) fragment can indeed associate with FVaL. Binding to the microtiter well was dependent on Ca^{2+}, FVaL and aPL. This observation is further evidence that the interaction between FVaH and FVaL is mediated at least in part through Leu94~Lys345 within FVaH and Gln1828~Tyr2196 (C-terminal half; i.e. C1/C2) in FVaL. Since EDTA is a non-selective chelator, we can not exclude the role of other metal ions (88,129) in this process in vivo. However based on previous observations (88) and our data showing that EDTA-mediated dissociation of the 30(L94) fragment from FVaL is restored by recalcification, Ca^{2+} is strongly implicated.

In addition to the inhibitory function Pn has on FVa coagulant activity (4,5), previous data from our laboratory has also suggested that Pn may convert FVa into a tPA accelerator (239). Our results here demonstrated that plasminogen binds at least two of the Pn-derived FVa fragments. A known requirement for plasminogen binding to proteins is a C-terminal lysine (191,187)). Our sequencing data indicated that several Pn-derived FVaH and FVaL fragments may contain a C-terminal lysine (Figure, 2.7, and 2.14). This is predicted based on the N-terminal position of the following fragment. Unequivocal identification of the plasminogen-bound fragments will require isolation and C-terminal sequence analysis.

In order to put the results of this study in perspective we generated a model, based on the model generated from the X-ray crystallographic structures of ceruloplasmin and C2-domain of FV (98,99), representing the fragments that remain bound on membrane following the inactivation of FVa cofactor activity by Pn (Figure 2.17). While this model is not considered to be very accurate, it is merely a starting point for understanding the basis of the molecular interactions between FVa subunits and, in future studies, within FVa and molecules in the prothrombinase complex, i.e., Xa, FII and APC. From this model it is evident that the intersubunit interactions occur mainly between the remaining parts of A1/A2 (amino acids 94 – 348) and the remaining parts of A3 (1766 – 1855). This model also clearly shows that the 94–110 region we identified to be likely involved in the Ca^{2+}-dependent contact between the two FVa chains, is located in a likely A1–

Figure 2.17 **Model representing the fragments that remain on membrane after Pn cleavage.**

The FVa A-domain orientation and structure has been previously predicted by homology modeling to ceruloplasmin. The backbone structure is presented here with color-coded A- and CO_2H-domains. The remainder of the A1- and A2-domain that remains on aPL following Pn cleavage is represented in red and yellow respectively. The remainder of A3- and C1- and C2-domains are shown in blue, the latter is facing the aPL membrane. The region 94-110, which could have an important role in the Ca^{2+}-dependent subunit association is in purple. The green balls represent Ca^{2+} ions and the yellow ball represents a Cu^{2+} ion. The model was generated by Rasmol2 beta version.

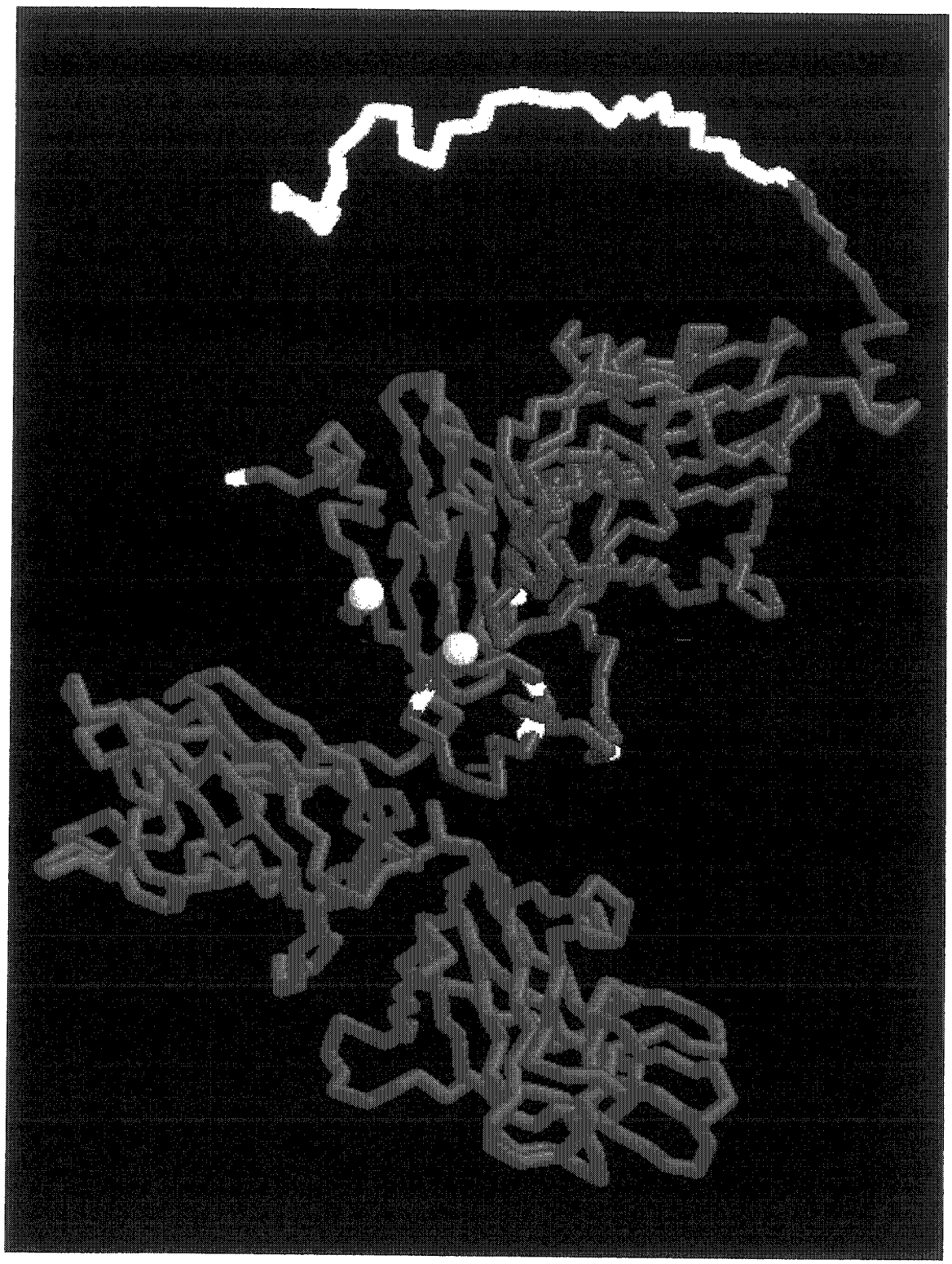

A3 contact zone suggested by the homology model with ceruloplasmin (261). Furthermore, the model shows that the A1–A3 contact zone contains the Ca^{2+} and Cu^{2+} ions proposed to play a binding role at the interface between the two chains.

CHAPTER 3

Coagulation FVa Glu96-Asp111: A chelator-sensitive site involved in function and subunit association

OVERVIEW

Although the noncovalent Ca^{2+}-dependent association between the FVa subunits (FVaH and FVaL) is required for function, little is known about the specific residues involved. The fragmentation studies and homology modeling presented in chapter 2 led us to investigate the contribution of the region L94-D112. Conserved amino acids were replaced with Ala in a recombinant B-domainless FVa precursor, with the following effects on FXa-mediated FIIa generating activity: wild-type (100%), E96A (19%), D111A (30%), D102A (40%), T104A (65%), E108A (70%), D112A (75%), Y100A (84%), D79A (93%), E119A (100%). Mutants targeting the nearest acidic residues outside L94-D112 had activity similar to wild-type, supporting the specific function of select residues. Suggesting a basis for the inhibition, D111A resulted in spontaneous dissociation of FVaH and FVaL. Conversely, E96A or D102A had no apparent effect on divalent cation-dependent subunit interactions, but greatly enhanced chelator-induced dissociation. Observations with multipoint mutants were consistent with D111 and E96-T104 having distinct roles in FVa function. These data identify the participation of E96-D111 in the FVaH-FVaL interaction and for the first time suggest that divalent cations have an effect on FVa function separable from subunit association.

EXPERIMENTAL PROCEDURES

Chemicals and reagents. Polyethylene glycol 8000 (PEG), PMSF (Sigma), hirudin (Calbiochem), H-D-Phe-Pip-Arg-pNA.2HCl (S-2238, Chromogenix), and Tween 20 (Fisher) were obtained commercially. Opti-MEM, DMEM-F12, Geneticin, Fungizone, Gentamycin, trypsin, L-glutamine, and LipofectAMINE 2000 were purchased from GibcoBRL. TA cloning kit and QuickChange XL site-directed mutagenesis kit were from Stratagene, QIAQuick PCR purification kit and maxi-prep kit were from Qiagen. PCR3.1 vector and, INVαF'competent cells were from Invitrogen. The PMT2-V plasmid encoding human FV was from the American Type Culture Collection (ATCC). Bio101 Gene Clean Kit was from Bio-Can. *Pfu* DNA polymerase was from Strategene, and the restriction enzymes were from GibcoBRL and Amersham Pharmacia Biotech. K293 cells were a generous gift from Dr. W.P. Sheffield (Canadian Blood Services, McMaster University, Hamilton, Canada). Primers were synthesized at Queen's University (Kingston, Canada). Small unilamellar vesicles (SUV; average diameter: 50 nm) consisting of 75:25% mixture of PC:PS were prepared and quantified as described (239,45). Large PC:PS 75:25% vesicles (LV; 300-600 nm) were made by extrusion using a Liposofast Basic apparatus (Avestin Inc.) as described (262).

Proteins. Human FVa, FXa, FII, FIIa, monoclonal antibodies (mAb) specific for human FVaH (AHV-#5146) and human FVaL (AHV-#5112), and polyclonal sheep anti-human FV (PAHFV-S) were from Haematologic Technologies Inc.

(Vermont). Rabbit antiserum to human FX was from Diagnostica Stago. mAb specific for FVa A3 domain (anti-FVaA3) was generated by Dr. R. Lemieux (Héma-Québec, Québec City) for which in-house recombinant FVaL produced using a baculovirus expression system and purified by electroelution was the immunogen. Peroxidase-conjugated goat anti-mouse IgG (Jackson ImmunoResearch Inc.) and peroxidase-conjugated goat anti-rabbit IgG (Promega), were used as secondary detection antibodies combined with the chemiluminescent detection system (ECL, Amersham) as substrate.

Production of human B-domainless FV . As shown previously by several groups, recombinant FV engineered to be deficient in the B-domain (ΔFV) retains FXa cofactor activity (263,264). Since the B-domain is a large polypeptide (120kDa) containing numerous potentially complicating post-translational modifications, ΔFV was produced for our studies using oligonucleotide overlap extension (265,266) from human FV encoded on the plasmid PMT2-V (101). The secretory peptide and entire heavy subunit domain within FV were amplified together using the following primers:

(1) 5'-CGT CGT AAT CCT TAA TCC TCG TTG TTA CCT TTG TCT-3'

(2) 5'-TAC CCA AAG CTT AGC GGG AGC AGG AAA GGA-3'

The light subunit of FV was amplified separately using the following primers:

(3) 5'-GCA GCA TTA GGA ATT AGG AGC AAC AAT GGA AAC AGA-3'

(4) 5'-GAC ACT ATA AAT GAT CCG CCG GCG TAT CCA ATT T-3'

In all cases, amplification was performed using native *Pfu* DNA polymerase to minimize errors. Successful PCR was detected by agarose gel electrophoresis. PCR products were cleaned using the QIAQuick PCR purification kit, and then combined with primers (2) and (4), and re-amplified. The amplified hybrid DNA was purified using the Bio101 Gene Clean Kit. The resulting product (4.3 kb) contained a FIIa cleavage site composed of one-half the cleavage site at the end of the A2-domain and one-half the cleavage site at the beginning of the A3-domain, which yielded a recombinant protein with a single novel FIIa cleavage site directly between FVaL and FVaH. The ends of ΔFV DNA were prepared for cloning into the pCR3.1 vector by cleaving outside the FV sequence using *Not* I and *Hind* III. The ligated constructs were transformed into INVαF'-competent cells. Positive clones were selected based on DNA mobility in agarose electrophoresis, PCR amplification using specific primers, and pattern of restriction digestion. DNA was extracted using a maxi-prep kit, and each clone was fully sequenced to confirm the correct sequence and absence of mutations introduced by PCR (University of Ottawa sequencing service, Ottawa, Canada).

Construction of ΔFV mutants. ΔFV mutants were generated using the QuickChange XL site-directed mutagenesis kit. The PCR 3.1 expression vector containing the ΔFV insert was used as a template in the mutagenesis reaction. For each of the mutants, two complementary oligonucleotides with the desired mutation(s) were amplified using the following primers:

($D79_A$), 5'-GTTCACTTTAAAAATAAGGCAGCTAAGCCCTTGAGCATCC-3';

(E96$_A$), 5'-GGTACAGTAAATTATCAGCAGGTGCTTCTTACCTTGACCAC-3';

(Y100$_A$), 5'-ATCAGAAGGTGCTTCTGCCCTTGACCACACATTCCCTGC-3';

(D102$_A$), 5'-AGGTGCTTCTTACCTTGCCCACACATTCCCTGCG-3';

(T104$_A$), 5'-GGTGCTTCTTACCTTGACCACGCATTCCCTGCGGAGAAG-3';

(E108$_A$), 5'-ACACATTCCCTGCGGCGAAGATGGACGACGCTG-3';

(D111$_A$), 5'-TCCCTGCGGAGAAGATGGCCGACGCTGTGGCTCCAG-3';

(D112$_A$), 5'-TGCGGAGAAGATGGACGCCGCTGTGGCTCCAGGC-3';

(E119$_A$), 5'-CTCCATTCATAGGTGTATGCTCGGCCTGGAGCCAC-3'

(E96$_A$/D102$_A$) (referred to as ED),

5'-AGTAAATTATCAGCAGGTGCTTCTTACCTTGCCCACACATTCCC-3';

(E108$_A$/D111$_A$/D112$_A$) (referred to as EDD),

5'-CACACATTCCCTGCGGCGAAGATGGCCGCCGCTGTGGCTCCAGG-3';

(Y100$_A$/T104$_A$) (referred to as YT),

5'-ATCAGAAGGTGCTTCTGCCCTTGACCACGCATTCCCTGCGG-3';

and the insertion mutant (H103-[AAAA]-T104) (referred to as A_4),

5'-CTTCTTACCTTGACCACGCAGCTGCTGCAACATTCCCTGCGGAG-3'.

PCR products were extracted using the maxi-prep kit and the presence of the desired mutations was confirmed by DNA sequencing. To generate the combined mutant E96A/D102A/E108A/D111A/D112A (referred to as ED/EDD), the EDD construct was used as a template in subsequent mutagenesis reactions.

Stable expression of ΔFV and mutants. Transfection was performed using LipofectAMINE 2000 reagent according to the manufacturer's instructions, with

minor modifications. Briefly, purified DNA was linearized with *Sca*I, then heated for 10 min at 55°C to inactivate the enzyme. DNA (25 μg) was suspended in 1.5 ml of Opti-MEM containing 2 mM $CaCl_2$. LipofectAMINE 2000 (75 μl) was suspended in the same volume of Opti-MEM containing 2 mM $CaCl_2$. DNA was combined with LipofectAMINE 2000 for 20 min. at room temperature, and the mixture was used to transfect 80% confluent K293 cells. At 72 h, the media was changed to DMEM/F12 supplemented with 10% FCS, 1% L-Glutamine, 1% gentamycin, and 1mg/ml Geneticin. For stable expression of recombinant protein, cells were removed with trypsin/EDTA (0.25% trypsin, 0.5 mM EDTA, 15 mM NaCl in PBS) and cultured in serum-free medium (OPTI-MEM, supplemented with 1% L-Glutamine, 1% gentamycin, and 1 mg/ml Geneticin). The serum free media was collected 72 h after growth and centrifuged at 15000 RPM (Beckman JA20 rotor) for 20 minutes at 4°C to remove any cell debris. PMSF (Sigma) was added to conditioned media to a final concentration of 200 μM and aliquots were stored at –80°C until use. The amount of ΔFV secreted into media was quantified by Western blot analysis using anti-FVaL as opposed to anti-FVaH, since mutations were exclusively generated in FVaH. Mean pixel intensities from scanned blots were quantified by Northern Eclipse software and compared to pixel intensities generated from a serial dilution of known concentrations of purified natural human FVa. As a negative control, the PCR 3.1 DNA vector containing no ΔFV DNA was used to transfect K293 cells.

Binding of ΔFV and mutants to aPL vesicles. Conditioned media from cells containing ΔFV, mutants (0.5 nM), or mock transfected cell supernatants, was incubated with LV (PC/PS; 75%/25%) in 20 mM HEPES, 150 mM NaCl, pH 7.4 (HBS), 2 mM Ca^{2+}, and 0.1 % w/v PEG at 22 °C for 10 min. The aPL-bound protein was collected by centrifugation and washed. The pellets were heated at 95°C for 5 min in Laemmli sample buffer, subjected to 8% SDS-PAGE, and electrotransferred to PVDF membranes. The PVDF was blocked at 22°C for 1 h in 5% w/v nonfat milk, and cleaved FV products were detected using anti-FVaL mAb.

Proteolysis of ΔFV by FIIa. ΔFV (2 nM) was incubated with FIIa (1U/ml) in the presence of LV (200 μM) and Ca^{2+} (2mM) in HBS at 22°C. The digests were sampled over time and heated at 95°C for 5 min in Laemmli sample buffer. The digests were subjected to 8% SDS-PAGE, stained with Coomassie Blue, or electrotransferred to PVDV. The PVDF membrane was blocked at 22 °C for 1 h in milk (5%), and cleaved products of FV were detected by Western analysis using anti-FVaH or anti-FVaL antibodies.

Cofactor activity of ΔFV and mutants. ΔFV and mutants were tested for their ability to enhance the FIIa generation by prothrombinase at a saturating concentration of phospholipid vesicles (200 μM). Thrombin generation was assessed chromogenically by incubating samples with 70 μl of 0.4 mM S2238 chromogenic substrate. Saturating concentrations of FXa (2 nM), phospholipid

vesicles (200 μM), FII (1.4 μM), and conditioned media containing an equal concentration of either ΔFV or ΔFV mutants in HBS/Ca^{2+} and 0.1% PEG were added at 22°C for 10 min. Thrombin activity was followed spectrophotometrically by monitoring the change in absorbence at 405 nM using a Spectramax kinetic microplate reader (Molecular Devices). In other experiments, conditioned media was activated with FIIa (60 nM) at 22 °C for 10 min, then the minimum amount of hirudin (0.01 units/μl) found to inhibit the activating FIIa was added prior to assaying for new FIIa generation as above.

FVaH-FVaL dissociation. ΔFV and mutants (0.5 nM) were cleaved with FIIa (1 U/ml) for 30 min on LV as described above, except that prior to FIIa treatment the vesicles were briefly centrifuged and the pellet was resuspended in HBS/Ca^{2+} so that only ΔFV bound to LV was assayed. To inhibit residual FIIa activity, the sample was treated with hirudin (0.01 U/μl) prior to sedimentation. The pelleted vesicles were resuspended, and incubated at 22°C for selected times in HBS/Ca^{2+} (2mM), or in HBS with EDTA (10 mM, HBS/EDTA), to allow FVaH dissociation. At each time, the vesicles were centrifuged and washed in HBS/Ca^{2+} and the pellet was subjected to 7% SDS-PAGE, transferred to PVDF, and visualized with anti-FVaH and anti-FVaL.

Binding of FXa and FII to ΔFV and mutants. A gel assay was devised to compare the binding and specificity of binding of FXa and FII to ΔFV and mutants. These experiments capitalized on reports of several order of magnitude

enhancement of FXa and FII binding to aPL in the presence of ΔFV. For these experiments the concentrations were chosen to optimize FVa-dependent binding of FXa or FII to aPL. To determine the specificity of FXa binding, aPL-bound LV (75%:25% PC:PS) and mutants (0.1 nM, 1 nM, 10 nM, and 50 nM) were incubated with FXa (2 nM) in HBS/Ca^{2+}/PEG at 22°C for 10 min. Other experiments were performed in the presence of increasing concentrations of LV (10 μM, 100 μM, and 500 μM), or in the absence of ΔFV. The aPL-bound protein was collected by centrifugation, and washed in HBS/Ca^{2+}/PEG. All reactions were stopped with sample buffer, and the aPL-bound protein was separated on SDS-PAGE, transferred to PVDF, and detected with protein-specific polyclonal Ab.

To determine the specificity of FII binding, aPL-bound ΔFV or mutants (2 nM) were incubated in the absence of FXa (A), or with EGR_{ck}-FXa (2 nM) (B) in HBS/Ca^{2+}/PEG at 22°C for 10 min, in the presence of 0.1 μM, 1.5 μM, and 2 μM FII. Other experiments were performed in the absence of ΔFV or with increasing concentrations of ΔFV (0.1 nM, 2 nM, and 6 nM). FII binding to phospholipids was also assessed using increasing concentrations of FII (0.1 nM, 1 nM, 2 nM, and 6 nM) with either PC (200 μM) or PS (200 μM) vesicles.

RESULTS

Production and mutagenesis of ΔFV. Using plasma-derived human FVa, in chapter 2 we reported that L94-K109 within the A1 domain appears to play a critical part in the FVaL and FVaH Ca^{2+}-dependent association. To investigate the role of acidic residues within this region, I utilised a FV clone containing the heavy subunit up to the FIIa-mediated activation site, and the entire light subunit (ΔFV, Figure 3.1). This construct was generated by Dr. Jean Grundy in our lab. Nine amino acids in ΔFV were individually changed to Ala (Figure 3.2, triangles). Through ceruloplasmin homology modeling, five of the amino acids we selected for mutation, E96, D102, E108, D111 and D112, were previously suggested to have an appropriate orientation to bind Ca^{2+} (97). Y100 and T104 were also mutated because they are highly conserved for unknown reasons in the A1-domains of ceruloplasmin, FVIII and FV from all species of known sequence. As specificity controls, the first acidic amino acid on either side of the implicated 94-112 segment, D79 and E119, were substituted with Ala. The combined functional effects of these single residues were also investigated by producing the five multipoint mutants also depicted in Figure 3.2. These single and multipoint mutations were confirmed by DNA sequencing of individual clones as seen in Figure 3.3. The functional effect of a large disruption in the 94-112 region was evaluated by inserting four alanines (A_4) between H103 and T104 in a final mutant. All mutants secreted into serum-free culture medium were used for all studies. In each case, Western blots revealed a non-reducible protein with estimated molecular mass of ~170 kDa using either commercial

Figure 3.1 **Domain structure of human FV, human FVa, and ΔFV.**

The structure and location of the heavy chain, connecting B domain, and the light chain are indicated. The domains are indicated by the letters in the boxes. The arrows indicate proteolytic cleavage sites at Arg 709, 1018, and 1545 in human FV that yield human FVa. The A1 region (94 to 109) predicted to mediate the Ca^{2+}-dependent association in FVa is shown by the line above the domain. The small segment preceding the A1 domain represents the leader sequence. The deletion mutant (ΔFV) is depicted schematically as a single-chain molecule missing the B domain, and compared with the domain structure of two-chain human FVa.

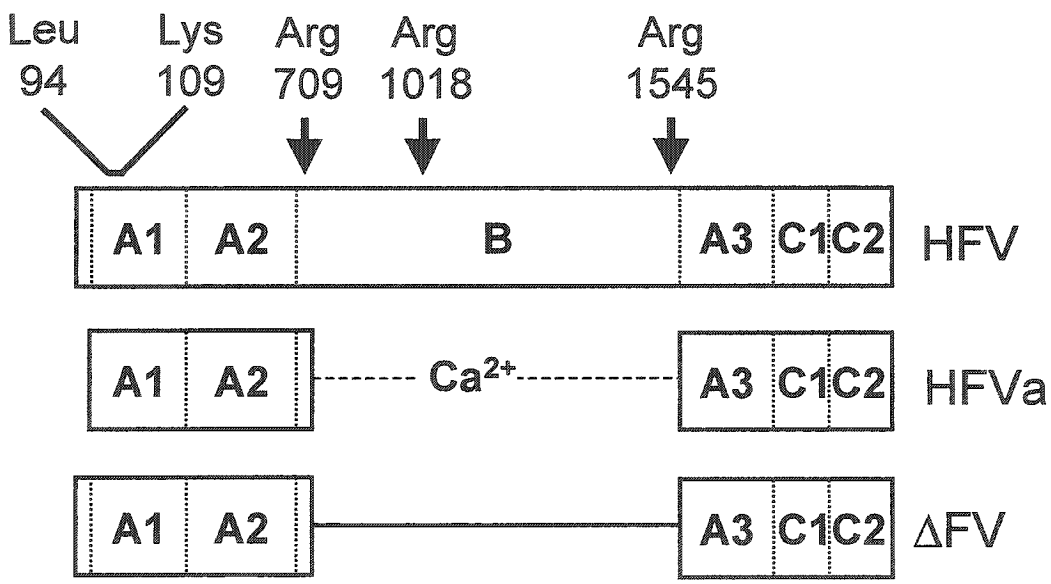
Leu
94
Lys
109
Arg
709
Arg
1018
Arg
1545
A1
A2
B
A3
C1
C2
HFV
A1
A2
Ca2+
A3
C1
C2
HFVa
A1
A2
A3
C1
C2
ΔFV

Figure 3.2 **Human FV residues selected for mutagenesis.**

Amino acids D79 through E119 are shown. Amino acids L94-M109 implicated in the Ca^{2+}-dependent FVaH-FVaL association by previous studies from our laboratory are shown in an open box. Five acidic residues implicated by homology modeling to constitute a potential Ca^{2+}-binding site are individually circled. The residues selected for single point-mutation to Ala (D79, E96, Y100, D102, T104, E108, D111, D112, and E119) are indicated by a filled triangle. ΔFV or mutants containing multiple substitutions of Ala (E96/D102, E108/D111/D112, Y100/T104, E96/D102/E108/D111/D112,) are indicated by the lines above or below the sequence. A final mutant was constructed in which four alanines (A_4) were inserted between H103 and T104 as depicted by the open triangle.

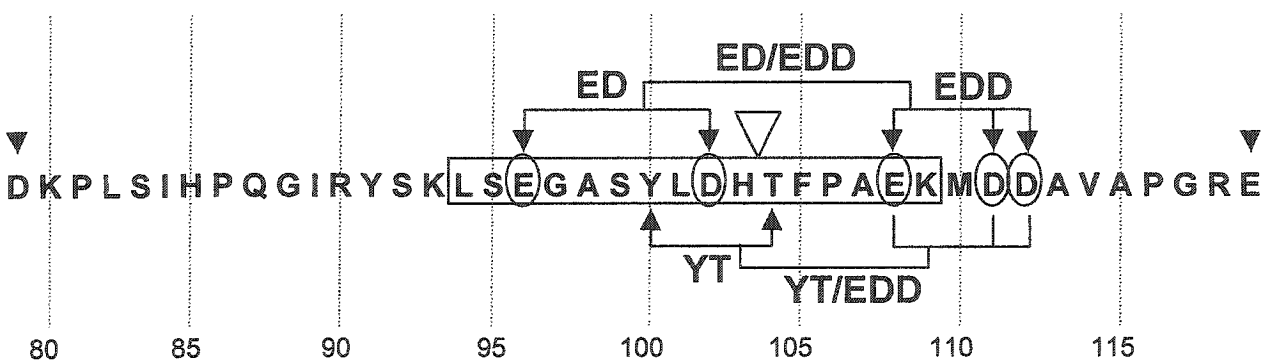
ED
ED/EDD
EDD
DKPLSIHPQGIRYSKLSEGASYLDHTFPAEKMDDAVAPGRE
YT
YT/EDD
80
85
90
95
100
105
110
115

Figure 3.3 **DNA sequencing of vectors containing single-point mutations or multiple substitutions.**

PCR products from recombinant PCR 3.1 expression vectors were sequenced (University of Ottawa) to confirm the presence of the desired nucleotide substitution. The histograms are presented in the large box; adenine is in green, cytosine is in blue, guanine is in black, and thymine is in red. The arrow indicates the site of the nucleotide substitution. The underlined DNA sequence represents the 3-nucleotide codon that was replaced to yield Ala (GCA, GCC, GCG,or GCT). The one-letter amino acid substitution is also indicated.

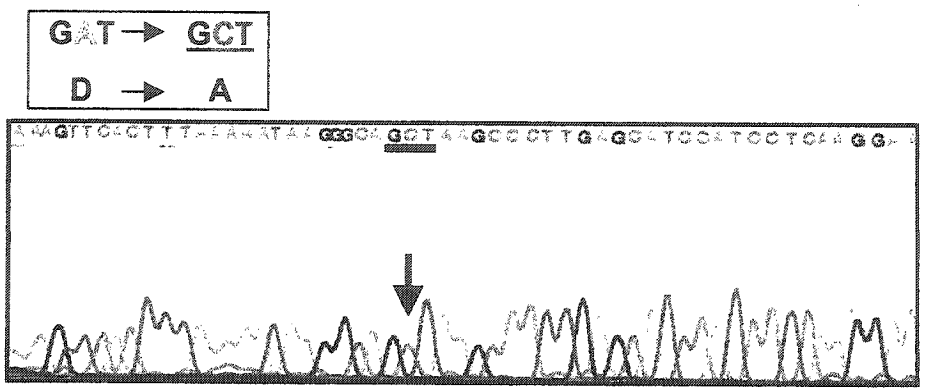

$D79_A$

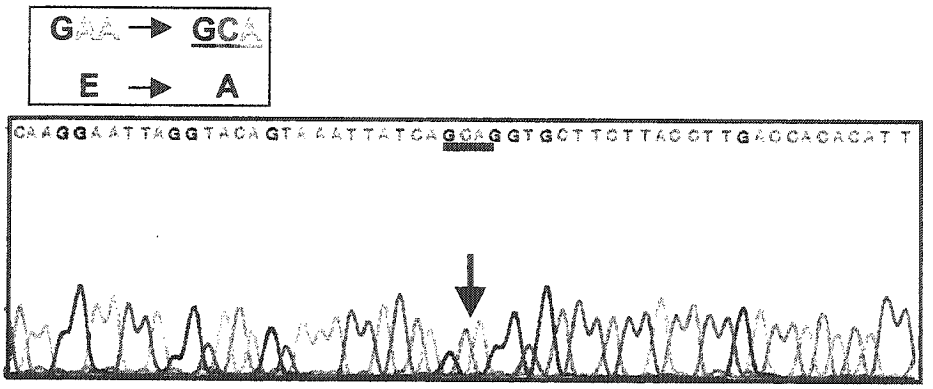

$E96_A$

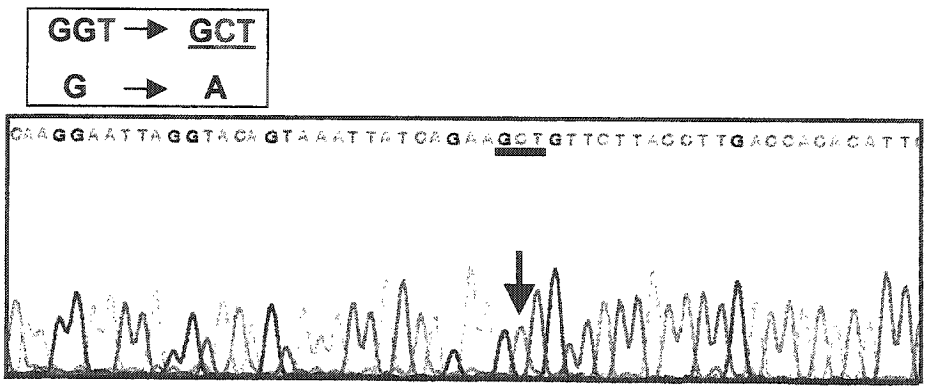

$G97_A$

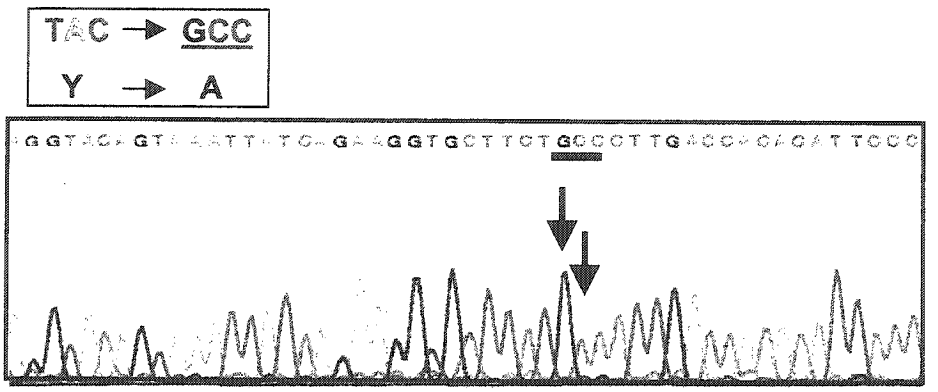

$Y100_A$

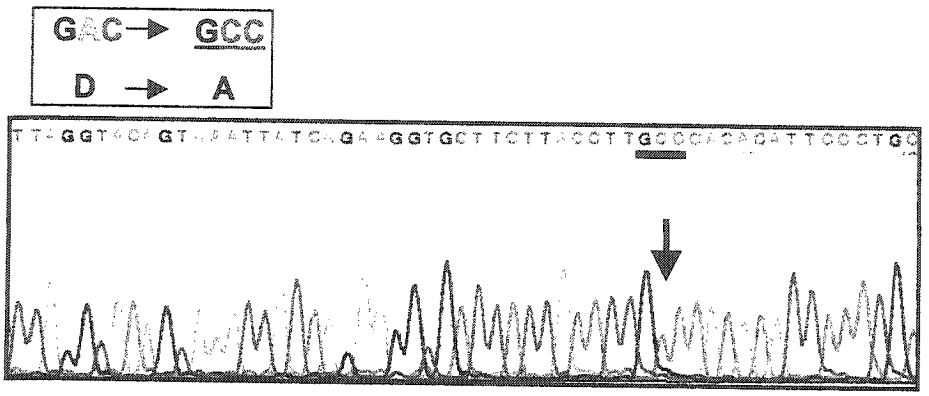

D102A

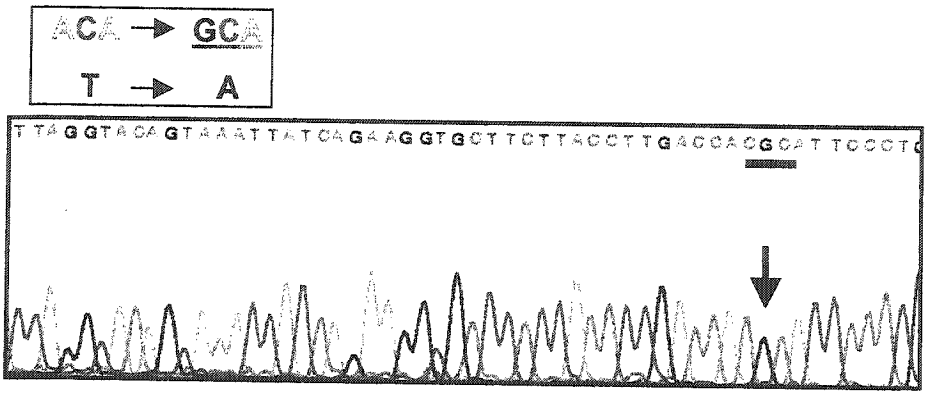

$T104_A$

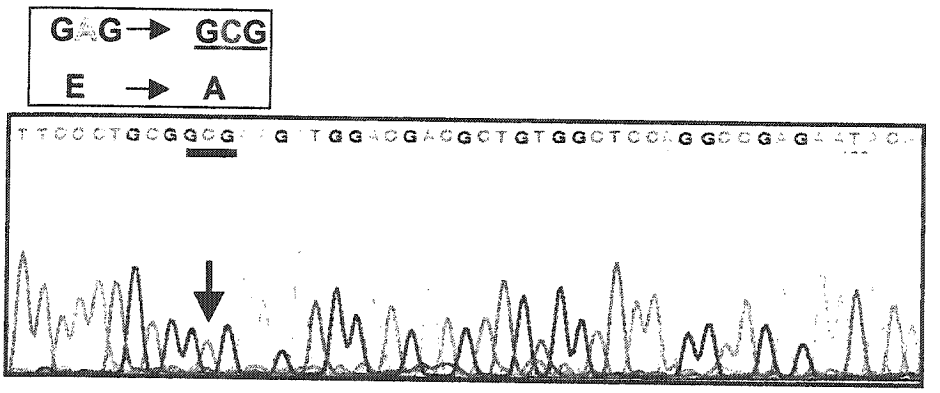

$E108_A$

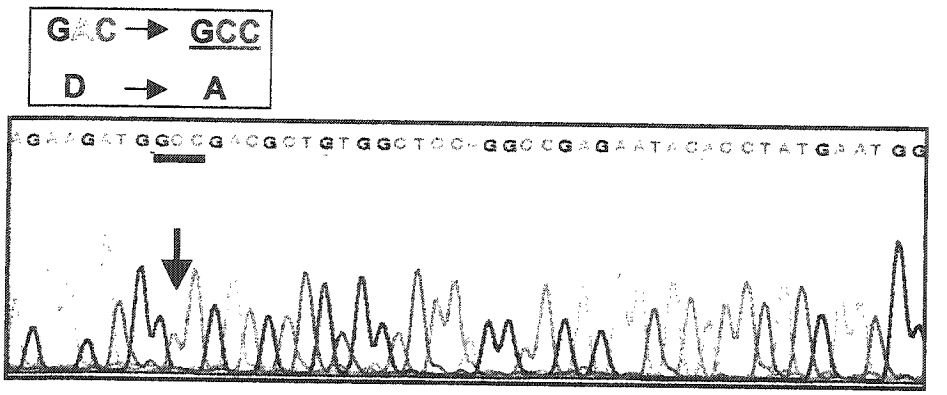

$D111_A$

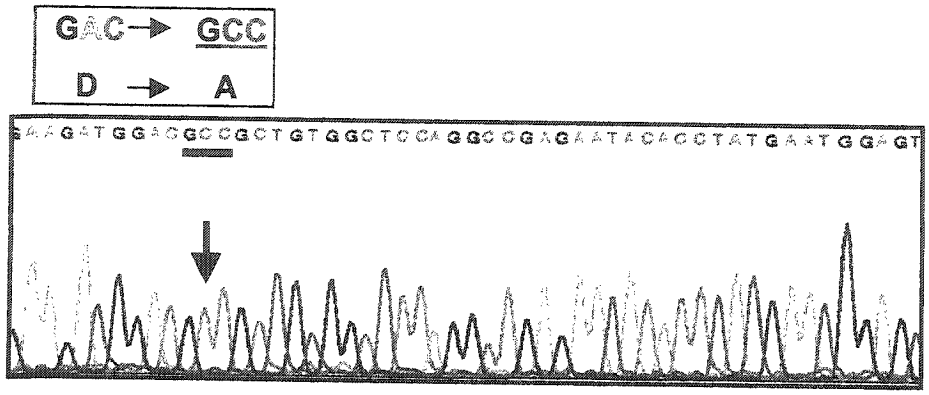
GAC → GCC
D → A
D112A
GAA → GCA
E → A
E119A
GAA → GCA
E → A
GAC → GCC
D → A
E96A/
D102A
GAG → GCG
E → A
GAC,GAC → GCC,GCC
D D → A A
E108A/
D111A/
D112A

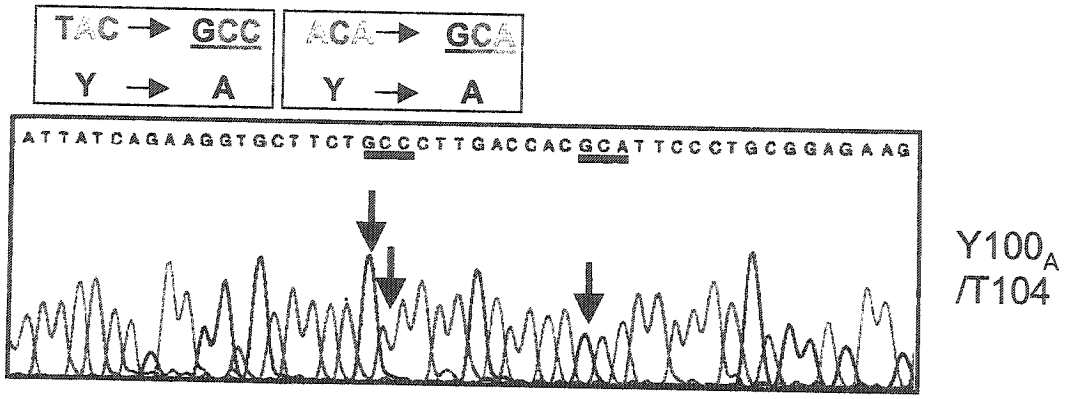
TAC → GCC
Y → A
ACA → GCA
Y → A
ATTATCAGAAGGTGCTTCTGCCCTTGACCACGCATTCCCTGCGGAGAAG
Y100A
/T104

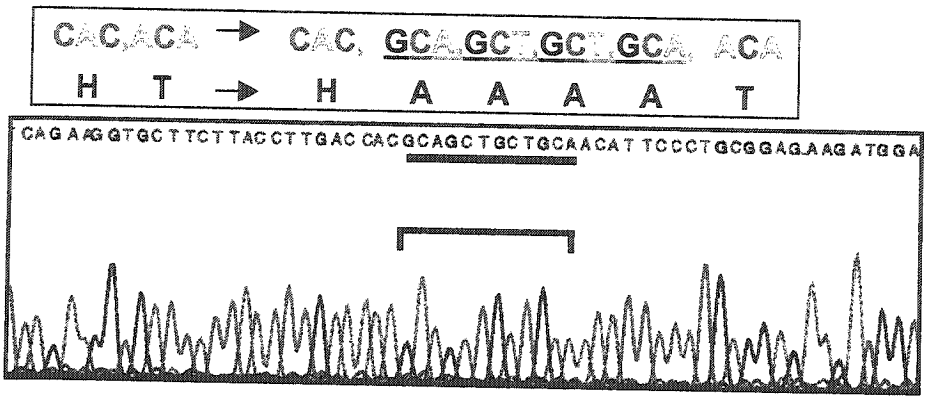
CAC,ACA → CAC, GCA,GCT,GCT,GCA, ACA
H T → H A A A A T
CAGAAGGTGCTTCTTACCTTGACCACGCAGCTGCTGCAACATTCCCTGCGGAGAAGATGGA
A4

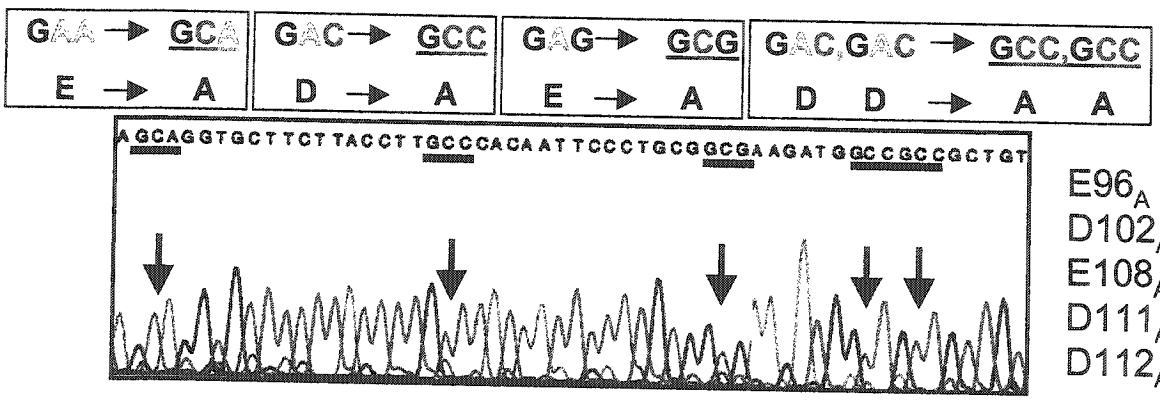
GAA → GCA
E → A
GAC → GCC
D → A
GAG → GCG
E → A
GAC,GAC → GCC,GCC
D D → A A
AGCAGGTGCTTCTTACCTTGCCCACAATTCCCTGCGGCGAAGATGGCCGCCGCTGT
E96A
D102A/
E108A
D111A
D112A

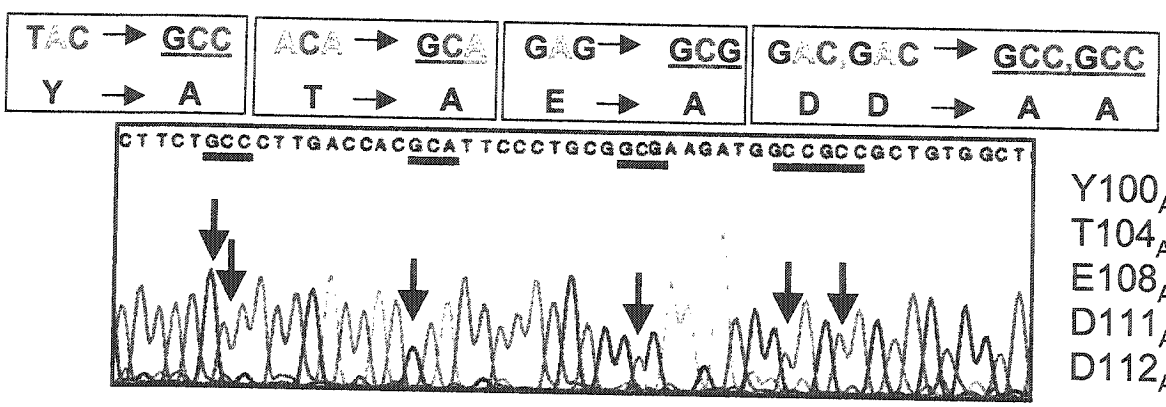
TAC → GCC
Y → A
ACA → GCA
T → A
GAG → GCG
E → A
GAC,GAC → GCC,GCC
D D → A A
CTTCTGCCCTTGACCACGCATTCCCTGCGGCGAAGATGGCCGCCGCTGTGGCT
Y100A
T104A/
E108A
D111A
D112A

monoclonal anti-FV antibodies (Haematologic Technologies, AHFV-#5112 and AHFV-#5146), or a monoclonal antibody produced by our lab against baculovirus-expressed human FV light subunit (14H12). No anti-FV-reactive band was observed in the supernatant of cells transfected with the null expression vector devoid of the ΔFV sequence (mock). The additional control $G97_A$ that lies within the E96 to D112 region was also constructed and sequenced (Figure 3.3) but for an unknown reason did not express any recombinant protein even following several transfection trials.

The concentration of secreted recombinant protein was measured by quantitative Western blots using anti-FVaL mAb. After digitization of the major band at ~170 kDa, the pixel density for each band was determined using Northern Eclipse software (Empix) and compared to a linear standard curve generated using purified natural human FVa. A known amount of purified natural FVa was included on each gel as an internal control for relativizing blot intensity. Using this method, it was found that the secretion levels of ΔFV and the various mutants into media was similar, indicating that mutagenesis had no significant effect on expression levels. The average concentration of the ΔFV mutants, under these conditions, ranged from 2.32 nM to 3.65 nM (Table 3.1), which was similar to the average concentration of 3.11 nM for ΔFV. For each clone, a small variable amount of a lower molecular weight antigen was detectable at ~100 kDa when using the FVaH-specific antibody (Figure 3.4A), which was not included to determine concentration. To confirm the digital quantification of ΔFV and

Table 3.1 **Characterization of ΔFV and FV mutants.**

ΔFV and FV mutants concentration in culture media was determined by quantitative Western blot analysis using anti-FVaL mAb and purified natural FVa for generation of a standard curve. The pixel density for each band was determined using Northern Eclipse software (Empix) and compared to the standard curve. A known amount of purified natural FVa was included on each gel as an internal control for relativizing blot intensity. Activity was determined in a chromogenic assay using purified components of FXa (2 nM), phospholipid vesicles (200 μM), FII (1.4 μM) and conditioned serum-free media of ΔFV or mutant in HBS/Ca^{2+}/PEG at 22 °C. Following a 10 min. incubation, the reaction was stopped with EDTA (15 mM) and FIIa generation was measured chromogenically using S2238 as a substrate. The average of three experiments with standard deviation is shown.

Table 3.1

Designation	Conc. (ng/ml)	Conc. (nM)	FIIa Activity (nM)
$D\ 79_A$	407 +/- 268	2.32	8.68 +/- 1.31
$E\ 96_A$	515 +/- 154	3.02	2.23 +/- 0.34
$Y100_A$	485 +/- 160	2.85	8.65 +/- 1.58
$D102_A$	591 +/- 214	3.48	3.01 +/- 0.23
$T\ 104_A$	619 +/-152	3.64	5.53 +/- 0.71
$E108_A$	620 +/-117	3.65	7.96 +/- 1.27
$D111_A$	620 +/-175	3.65	2.26 +/- 0.24
$D112_A$	532 +/- 179	3.13	9.00 +/- 1.07
$E119_A$	526 +/- 128	3.09	10.09 +/- 1.79
ED	556 +/- 156	3.27	0.66 +/- 0.05
EDD	548 +/-153	3.22	1.32 +/- 0.07
YT	514 +/- 162	3.02	2.24 +/- 0.03
AAAA	559 +/-179	3.29	0.34 +/- 0.04
ED/EDD	589 +/-118	3.47	0.37 +/- 0.04
YT/EDD	567 +/- 95	3.34	0.03 +/- 0.01
ΔFV	529 +/- 165	3.11	10.69 +/- 1.3

Figure 3.4 **Secretion and aPL-binding of ΔFV and mutants.**

A: Media from either mock transfected cells, or cells transfected with ΔFV or mutant were incubated with large vesicles (200 μM) at 22 °C for 10 min in HBS/Ca^{2+} (2 mM). B: as in A, except that following incubation, LV were collected by centrifugation and washed. LV-bound protein was detected following separation on 8% SDS-PAGE, transferred to PVDF membrane, and detected with anti-FVaL mAb.

A
B
D79A
E96A
Y100A
D102A
T104A
E108A
D111A
D112A
ED
EDD
YT
A4
ED/EDD
YT/EDD
ΔFV
Mock

mutants, identical amounts expected from the derived concentrations were compared. As can be seen (Figure 3.4A), the band intensities did not differ appreciably. This was also true when other antibodies directed at FVaH or FVaL were used (not shown), which supported the use of these relative concentrations to compare ΔFV and mutants in functional experiments.

Binding of ΔFV mutants to anionic phospholipid. All binding of FV and FVa to aPL has been previously attributed to the region containing FVaL and involves the C2-domain (134,135,257). We therefore predicted that mutation of ΔFV in the A1-domain would be inconsequential to the interaction with aPL. To confirm that no unforeseen alterations in the recombinant proteins had occurred that would have gross effects on aPL-binding, equal antigenic concentrations of recombinant proteins were incubated with 75:25 PC:PS LV and the protein remaining bound after washing was analyzed by Western blot. These data showed that there was no evident alteration in the capacity of the single or multipoint mutants to bind excess aPL-containing LV compared to ΔFV (Figure 3.4B). Under these conditions, the amount of ΔFV antigen in the supernatant after centrifugation of LV was not detectable (not shown), indicating that each molecule of ΔFV contained a functional aPL-dependent binding domain. Furthermore, the association with LV was Ca^{2+}-independent and required aPL (not shown), consistent with the properties of plasma-derived FV.

Prothrombinase activity of ΔFV and mutants. The substantial prothrombinase cofactor function of ΔFV is demonstrated in Figure 3.5, and contrasted with the negligible FIIa generation that was observed when mock transfected cell supernatant was assayed for FVa cofactor activity. The latter not only demonstrated the dependence of the experiment on added ΔFV, but also that the cells do not endogenously contribute to FII activation. On a molar basis, the observed increase in FIIa generation due to ΔFV was approximately 25% of that mediated by an equal concentration of FVa purified from plasma (not shown), which is similar to or greater than activity reported by other laboratories using recombinant FV (263).

To investigate a potential role for FV residues E96, D102, E108, D111 and D112 in prothrombinase function, the effect of substituting each to Ala was evaluated and compared to ΔFV. The simultaneous substitution of all five acidic residues to Ala (ED/EDD) resulted in nearly complete inhibition (98%) of ΔFV activity, which strongly supported a functional role for this region of FV (Figure 3.5). To minimize conformational changes that may accompany the gross alteration of charge due to the five mutations in ED/EDD and to identify individual residues contributing to function, the respective single point mutants were assayed. When compared to ΔFV, the largest effects on prothrombinase activity occurred when E96 > D111 > D102 were mutated. At 2.2 nM (the concentration where differences appeared to be maximal), substitution to Ala resulted in 81, 70 and 60% inhibition, respectively. Moderate inhibitions were observed for T104

Figure 3.5. **Prothrombinase activity of ΔFV and mutants.**

Thrombin generation catalyzed by prothrombinase was measured in a reaction mixture containing FXa (2 nM), phospholipid vesicles (200 μM), FII (1.4 μM) and conditioned serum-free media containing various concentrations of ΔFV or mutant in HBS/Ca^{2+}/PEG at 22 °C. Following a 15 min. incubation, the reaction was stopped with EDTA (15 mM) and FIIa generation was measured chromogenically using S2238 as a substrate. The average of triplicates with standard deviation is shown.

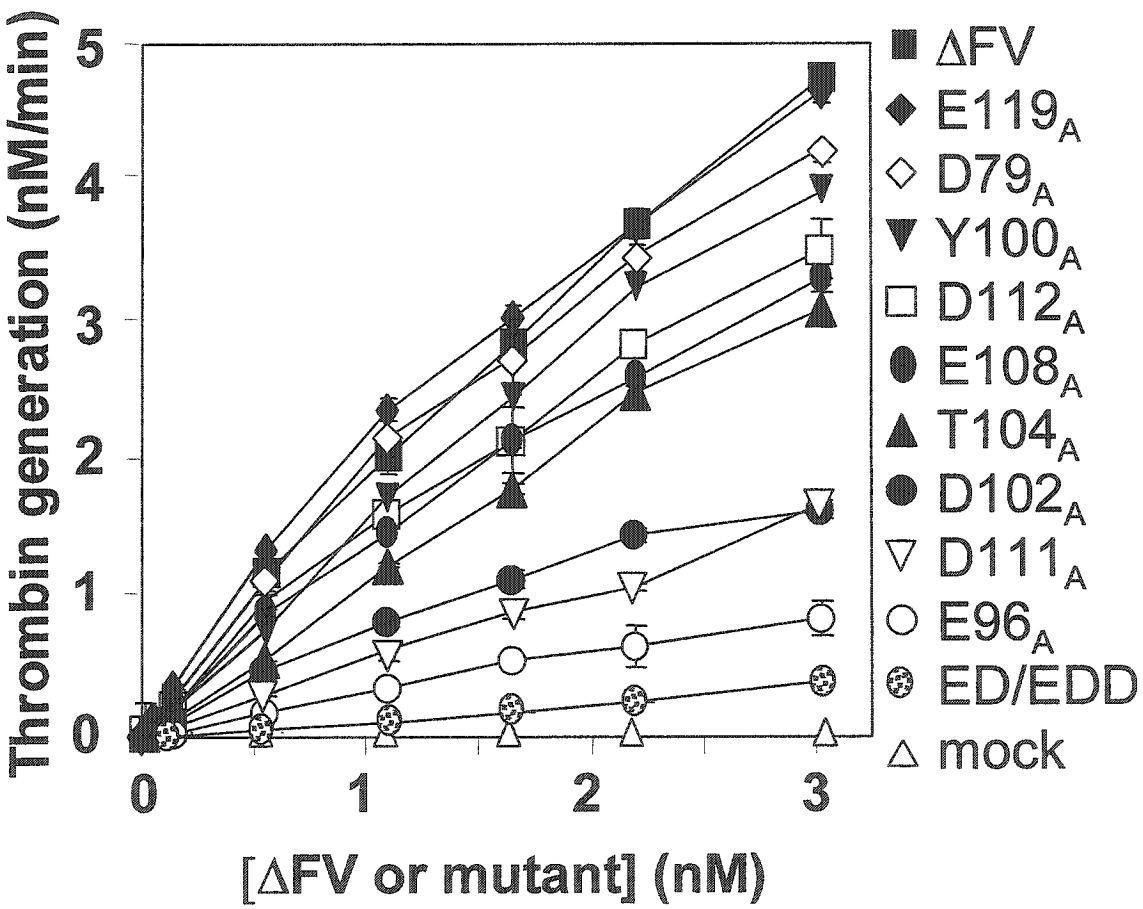
Thrombin generation (nM/min)
0
1
2
3
4
5
0
1
2
3
[ΔFV or mutant] (nM)
ΔFV
E119A
D79A
Y100A
D112A
E108A
T104A
D102A
D111A
E96A
ED/EDD
mock

(35%), E108 (30%), and D112 (25%). In contrast, relatively inconsequential inhibitions were observed for substitution of Y100 (16%), D79 (7%) and E119 (0%) by Ala. The latter two mutations (D79 and E119) are the nearest acidic residues neighboring the predicted Ca^{2+}-sensitive region in the A1 domain (i.e. L94-D112). The finding that these have limited or no involvement in ΔFV function serves as a negative control for mutagenesis and supports the specific contribution of select residues.

Effect of ΔFV mutation on the FVaH-FVaL interaction. Having established that at least E96, D102 and D111 play a significant part in ΔFV function, we next investigated whether the Ca^{2+}-dependent non-covalent interaction between FVaH and FVaL was affected. An experiment was designed to take advantage of the requirement for FVaL to anchor FVaH to aPL (114,124,133,255,256,257). To first establish the conditions needed for complete FIIa-mediated proteolysis and to ascertain that ΔFV had a typical cleavage pattern, a time-course of FIIa-mediated ΔFV cleavage was performed in the presence of aPL-containing vesicles and Ca^{2+} (Figure 3.6). SDS-PAGE showed that the single chain ΔFV was completely converted by 1u/ml FIIa within 20 min into the expected FVaL (~74/71 kDa) and FVaH (~105 kDa) subunits. All ΔFV mutants were comparably proteolysed by 20 min of incubation with the same concentration of FIIa (not shown), which not only demonstrated that mutation had no discernable effects on recognition of ΔFV or the mutants by FIIa, but also established the experimental conditions to ensure complete FVaH and FVaL generation.

Figure 3.6 **Thrombin-mediated conversion of ΔFV to FVa.**

ΔFV (2 nM) was treated with FIIa (1 U/ml) in the presence of LV (200 μM) and Ca^{2+} (2mM) in HBS at 22 °C. At selected time intervals, aliquots were withdrawn from the mixture and the reaction stopped by heating in SDS-containing Laemmli sample buffer. Samples were separated on 8% SDS-PAGE. The protein was transferred to PVDF and detected with anti-FVaL (A), or anti-FVaH (B).

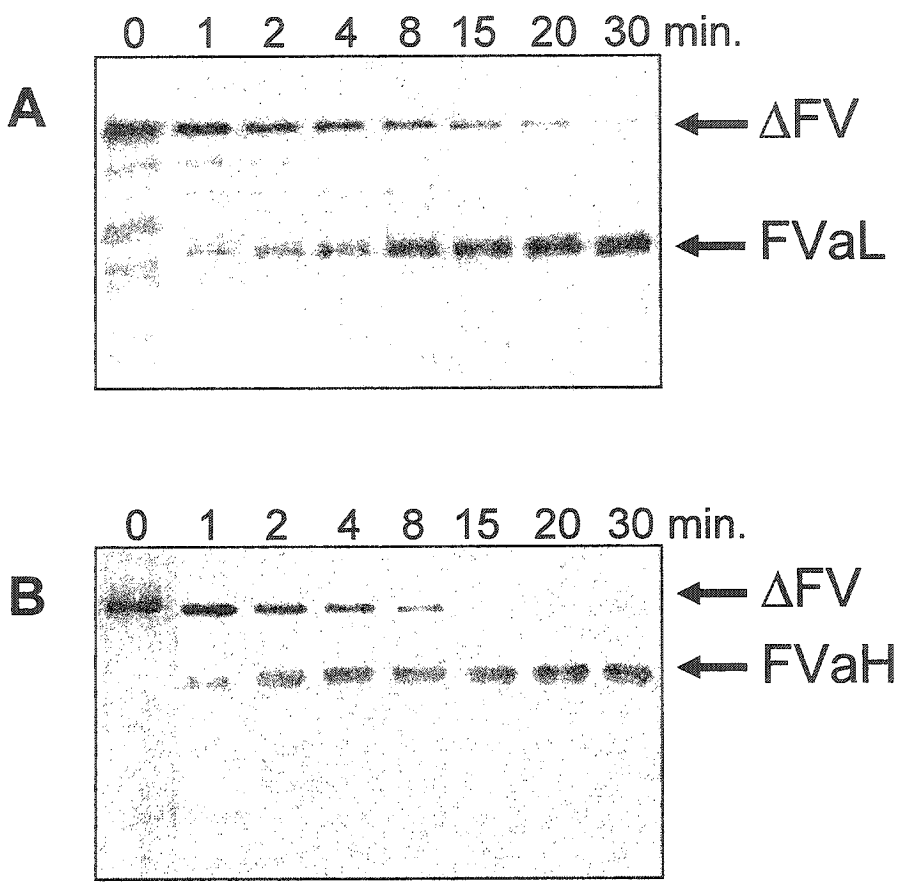
0 1 2 4 8 15 20 30 min.
A
ΔFV
FVaL
0 1 2 4 8 15 20 30 min.
B
ΔFV
FVaH

To follow FVaH-FVaL dissociation, equal antigenic concentrations of the ΔFV mutants were equilibrated with excess aPL-containing LV so that the same amount of each variant was bound to LV at time zero and undetectable amounts remained in buffer, as in Figure 3.4B. Each mixture was treated with FIIa to achieve complete conversion to FVa (as in Figure 3.6) and the amount of each subunit bound to washed LV was probed with either a FVaH- or FVaL-specific antibody at one hour intervals. FVaL has been well established as the exclusive aPL-binding subunit and is expected to remain associated with aPL for the duration of the experiment regardless of the presence of Ca^{2+}. As shown in Figure 3.7, the amount of FVaL generated from each mutant that remained bound to the aPL-containing LV was constant throughout the experiment and was independent of divalent cations. This observation confirmed that approximately the same number of molecules of FVa are generated for each ΔFV mutant and that the efficiency of LV sedimentation does not change over the 3 hour course of the experiment.

In the presence of Ca^{2+}, FVaH derived from ΔFV did not dissociate from its FVaL anchor to aPL, which was expected (132,267). Consistent with observations made with natural FVa purified from human plasma (chapter 2), inclusion of an excess of chelator (EDTA) in the incubation mixture resulted in a relatively slow dissociation of ΔFV FVaH from the aPL-containing LV. In sharp contrast, simultaneous substitution of all five acidic amino acids in the ED/EDD

Figure 3.7 **Effect of ΔFV mutation on FVaH-FVaL association.**

ΔFV and mutants (0.5 nM) bound to aPL in HBS/Ca^{2+}/PEG were incubated with FIIa (1U/ml) for 20 min at 22 °C. Proteolysis was stopped with hirudin (10 U/ml), and Ca^{2+} (2 mM), or EDTA (15 mM) in HBS/PEG was added. The aPL-bound protein was collected by centrifugation at 1, 2 or 3 hours after incubation with Ca^{2+} or EDTA and washed in HBS/Ca^{2+}/PEG. All reactions were stopped by heating in SDS-containing Laemmli sample buffer. Protein remaining bound to aPL was separated on 7% SDS-PAGE, transferred to PVDF, and probed with anti-FVaH (AHV-1546) or anti-FVaA3 mAb by Western analysis.

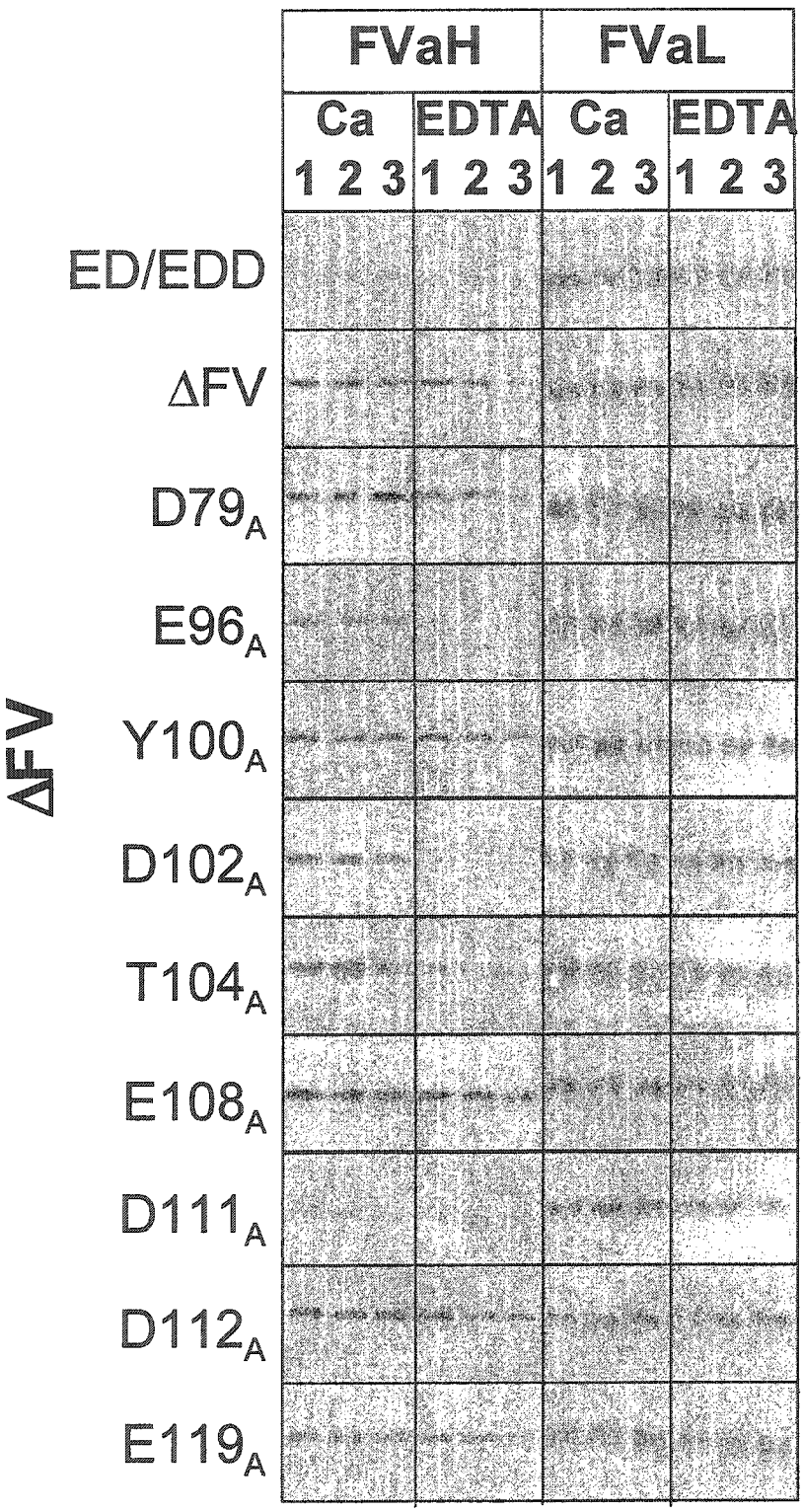
FVaH
FVaL
Ca
EDTA
Ca
EDTA
1 2 3 1 2 3 1 2 3 1 2 3
ED/EDD
ΔFV
D79A
E96A
Y100A
D102A
T104A
E108A
D111A
D112A
E119A
ΔFV

mutant caused complete dissociation of FVaH from FVaL prior to the first sampling at 1 hour, regardless of whether Ca^{2+} was present. Like all of the mutants evaluated, the amount of FVaL bound to aPL did not change, which further confirmed that membrane interactions were not influenced by mutations in the A1-domain. The observed spontaneous and rapid dissociation of FVa subunits provides an explanation for the nearly complete loss of prothrombinase function observed for the ED/EDD mutant (Figure 3.5).

The specific amino acids contributing to the spontaneous dissociation of FVaH from FVaL due to ED/EDD mutation were ascribed using our panel of 9 single point mutants. Figure 3.7 shows the amount of FVaH and FVaL remaining bound to aPL-containing LV after treatment of the respective ΔFV mutant with FIIa. These data revealed that substitution of only D111 by Ala was sufficient to give rise to the phenotype observed for ED/EDD. In the presence of 2mM supplemented Ca^{2+} and the absence of chelator, the FVaH derived from all other single point ΔFV mutants behaved exactly like ΔFV, exhibiting no dissociation from FVaL over the duration of the experiment. This is interesting because at least mutation of E96 and D102 caused significant (i.e. >50%) functional inhibition measured by prothrombinase assays (Figure 3.5), which are conducted at identical divalent cation concentrations. Therefore a property of FVa that is required for FXa activity, other than subunit association, must be affected. A partial explanation for the discrepancy is provided by following subunit dissociation in the presence of chelator. Although FVaH-FVaL association

appeared to be identical to ΔFV in the presence of divalent cations, mutation of E96 or D102 resulted in comparatively rapid FVaH dissociation when EDTA was included in the incubation mixture. FVaH dissociation similar to that of ΔFV in the presence of chelator was observed for Ala substitution of D79, Y100, T104, E108, D112 or E119. Thus, despite being very close in proximity, mutation of D111 or either E96 or D102 causes inhibition of FVa cofactor function by two distinguishable mechanisms.

Effect of FIIa-pretreating ΔFV mutants on prothrombinase activity. The FV-limited prothrombinase assay presented in Figure 3.5 depended on *in situ* activation of ΔFV by FXa and subsequently by the FIIa produced during the experiment. Normally, FIIa preactivation of FV enhances activity in prothrombinase assays. However, mutation of D111 resulted in spontaneous dissociation of FVaH from FVaL in the presence of divalent cations (Figure 3.7). Therefore preactivation with FIIa would be anticipated to cause inhibition of prothrombinase activity in this case, whereas the activity of all other mutants would be enhanced. To test this hypothesis we included a brief FIIa preactivation step in the chromogenic prothrombinase assay. Since FIIa generation is measured as an end point in this experiment, an amount of hirudin sufficient to inhibit only the FIIa used during the preactivation was added. Figure 3.8 shows that FIIa preactivation caused only a moderate increase in FVa-dependent prothrombinase activity except for the D111 mutant as expected. These data provide independent confirmation that mutation of D111 in ΔFV promotes the

Figure 3.8 **Prothrombinase activity of FIIa-pretreated ΔFV and mutants.**

Thrombin generation was measured in a reaction mixture containing FXa (2 nM), phospholipid vesicles (200 μM), FII (1.4 μM) and conditioned media containing B-domainless FV mutants (0.5 nM) (solid bars), or FIIa-activated (1 U/ml) B-domainless FV mutants (0.5 nM) (hatched bars) in HBS/Ca^{2+}/PEG at 22 °C. Following a 10 min. incubation, the reaction was terminated with EDTA (15 mM), and FIIa generation was measured chromogenically using S2238. The average of triplicates with standard deviation is shown.

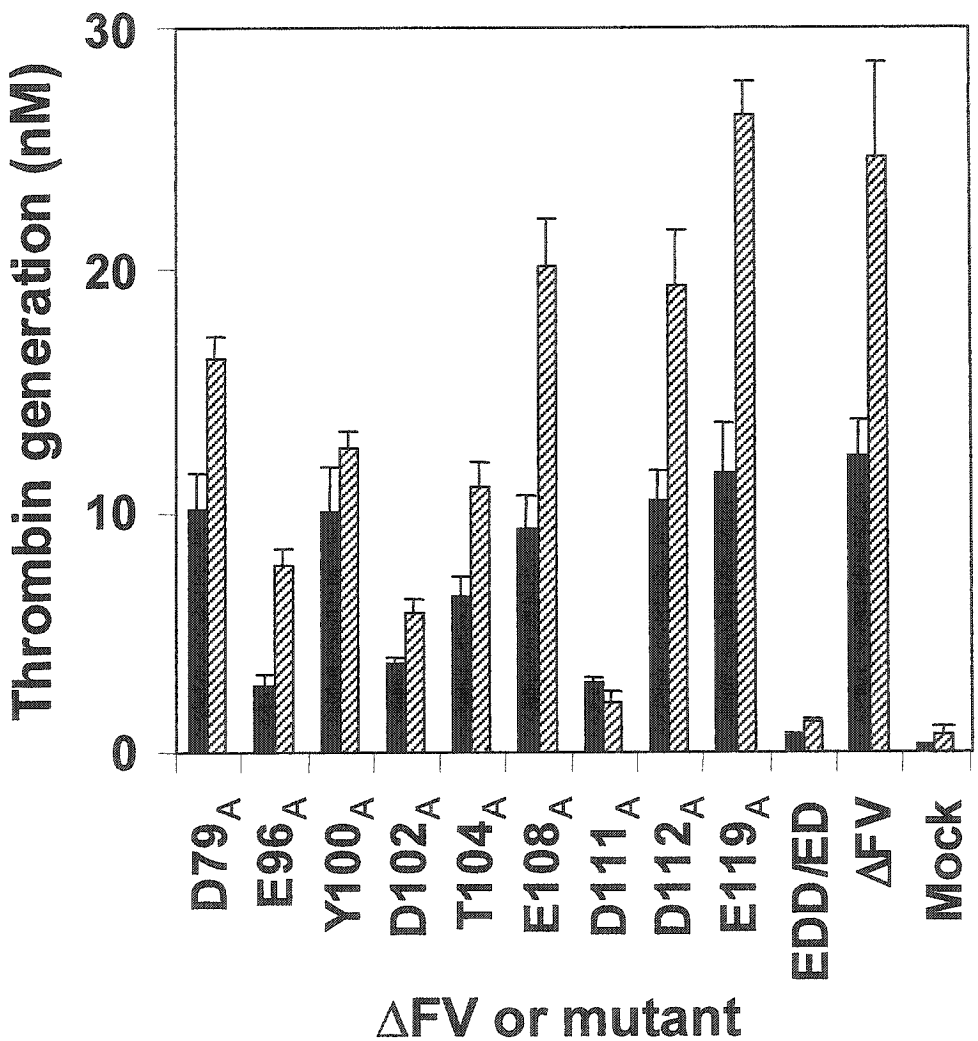
Thrombin generation (nM)
30
20
10
0
D79A
E96A
Y100A
D102A
T104A
E108A
D111A
D112A
E119A
EDD/ED
ΔFV
Mock
ΔFV or mutant

dissociation of FVaH upon conversion to FVa. The prothrombinase activity of all other single point mutants was enhanced upon pretreatment with FIIa, indicating that rapid subunit dissociation does not occur.

Factor V circulates in the plasma as a single-chain glycoprotein with little or no intrinsic procoagulant activity. It is activated by limited proteolysis by FIIa or FXa leading to the loss of the B domain (1,2,3,46) . From the literature, we had expected a more substantial increase in ΔFV cofactor activity following FIIa activation, however our results indicate only a two-fold increase in ΔFV cofactor activity (Figure 3.8). This moderate increase in FIIa activity may have been a result of incomplete FIIa activation or continuing inhibition of FIIa activity by hirudin following FIIa activation and during FIIa generation. A less likely explanation is that the B-domain, which is missing from the mutants, is critical for the expression of full procoagulant activity during the FIIa activation step of FV.

Effect of multipoint mutation on ΔFV. The functional contribution of FV residues spanning 94-112 was further mapped by generating several multipoint mutants, which were evaluated for effects on prothrombinase function and FVa subunit association. Experiments that probed function by single point mutation suggested that the profound inhibition caused by simultaneously mutating all five acidic amino acids, E96, D102, E108, D111 and D112, may be due to two discernible mechanisms. Mutation of D111 appeared to be required to induce the spontaneous dissociation of FVaL and FVaH, whereas mutation of the N-terminal

residues, E96 or D102, resulted in inhibition without subunit dissociation in the presence of Ca^{2+}. We therefore constructed mutants consisting of Ala substitutions at adjacent acidic residues, E108, D111 and D112 (EDD) or E96 and D102 (ED), to ask whether the two functional phenotypes observed for the single point mutants persisted. Figure 3.9 showed that EDD and ED were significantly less active compared to ΔFV by approximately 78 and 85% respectively at an antigenic concentration of 2.2 nM. In comparison, the inhibitory effect of the combined mutant, ED/EDD, was even more profound (98%) which would be expected for an aggregate of distinct effects. The result of EDD or ED mutation on FVa subunit dissociation was similar to the single point mutant findings. Upon conversion of the EDD mutant of ΔFV to FVa by FIIa, a rapid loss of FVaH from FVaL bound to aPL-containing LV was observed in the absence or presence of chelator (Figure 3.10). The same experiment showed that dissociation of FVaH derived from the ED mutant was intermediate between that observed for ΔFV and ED/EDD in the presence of Ca^{2+}. Chelator-mediated dissociation observed for ED was comparable with that of E96A, D102A, D111A or ED/EDD. Like the single point mutants, Figure 3.10 shows that the amount of FVaL remaining bound to the LV was invariant for all multipoint mutants, confirming that the same amount of LV-bound FVa was initially generated and that the sedimentation properties of the LV were not changing during the experiment. These data supported the conclusion drawn from experiments with single point mutants that the L94-D112 region participates in two distinct FVa functions loosely divisible according to C-terminal and N-terminal effects.

Figure 3.9 **Effect of multipoint ΔFV mutation on prothrombinase activity.**

Prothrombinase activity of multipoint ΔFV mutants after treatment with FIIa was performed as described in Figure 3.5 except that multipoint mutants were used in the reaction mixture.

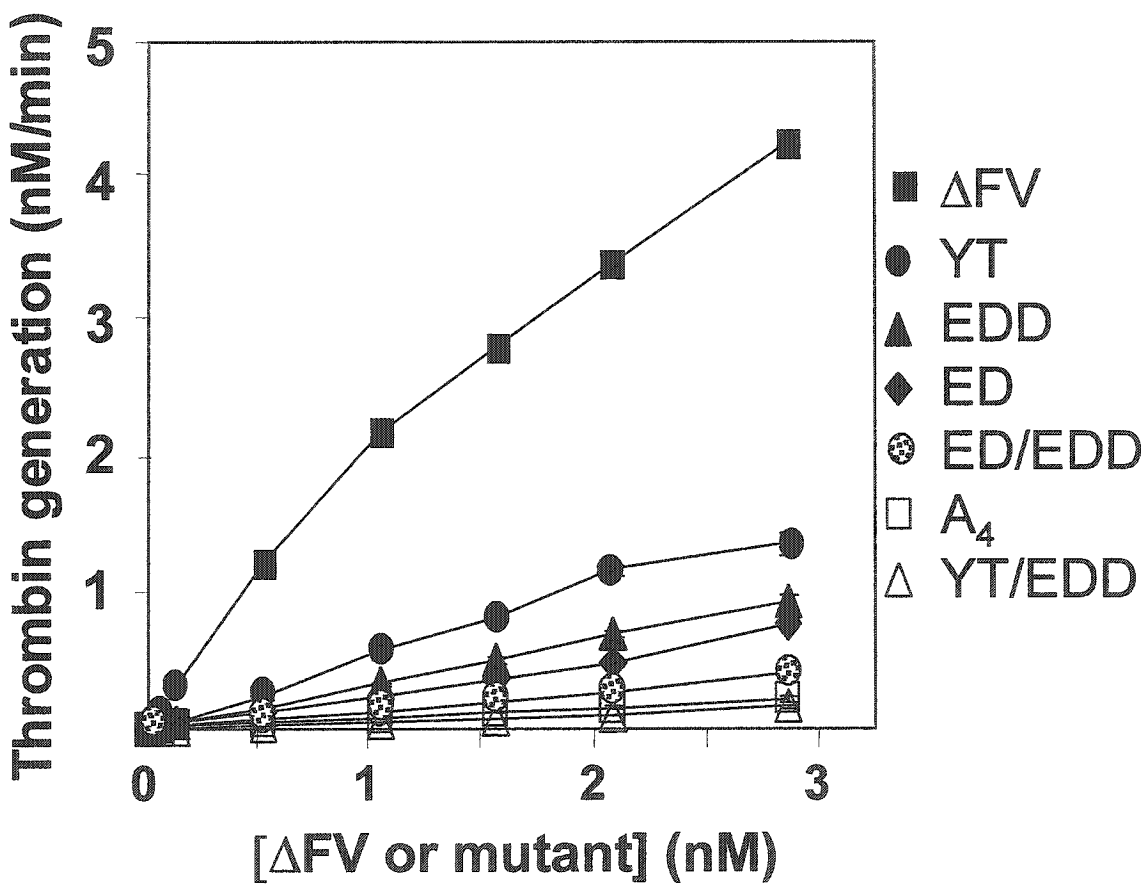
Thrombin generation (nM/min)
0
1
2
3
4
5
[ΔFV or mutant] (nM)
ΔFV
YT
EDD
ED
ED/EDD
A4
YT/EDD

Figure 3.10 **Effect of multipoint ΔFV mutation on FVaH-FVaL association.**

FVaH-FVaL association after treatment with FIIa was performed as described in Figure 3.7.

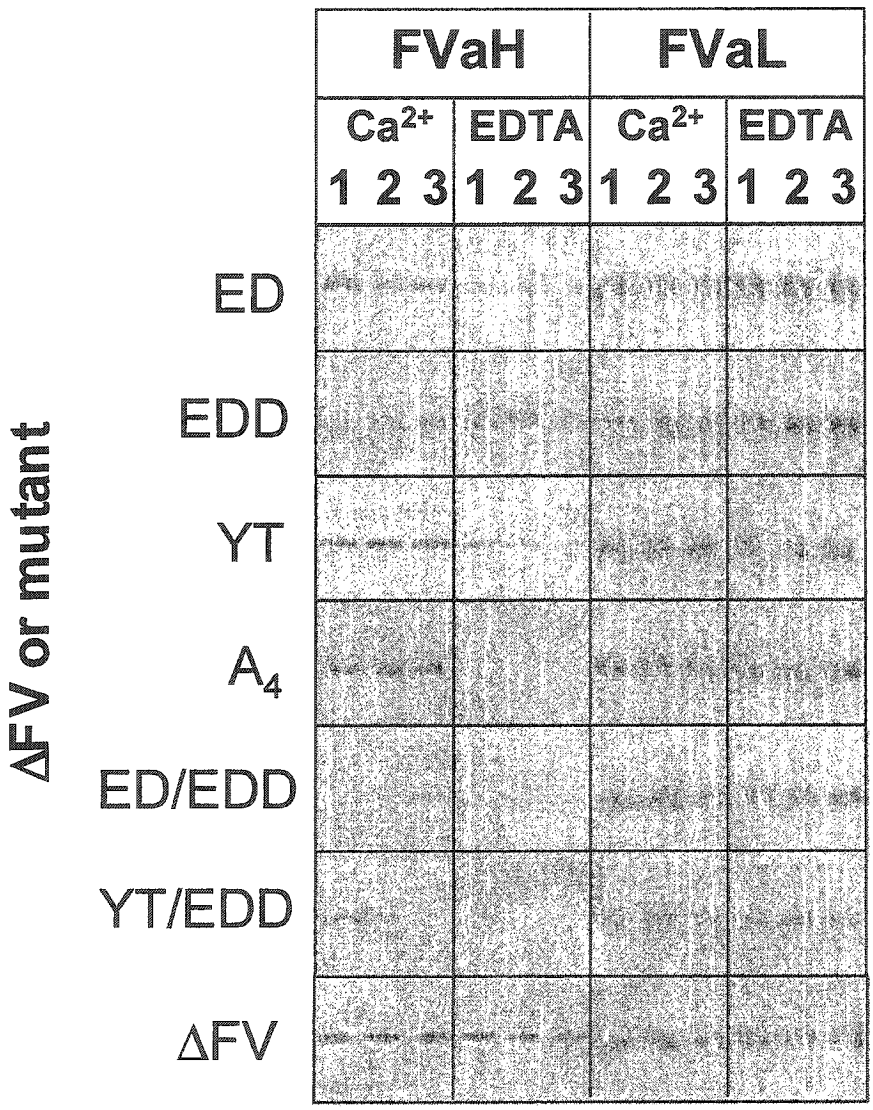
ΔFV or mutant
FVaH
FVaL
Ca2+
EDTA
Ca2+
EDTA
1 2 3 1 2 3 1 2 3 1 2 3
ED
EDD
YT
A4
ED/EDD
YT/EDD
ΔFV

To further explore the functional contribution of the conserved neutral amino acids within L94-D112, a combined mutant consisting of Y100 and T104 was produced (YT). Individual substitution of these residues by Ala was moderately or negligibly inhibitory, respectively (Figure 3.5). However, their simultaneous mutation resulted in 65% inhibition of prothrombinase activity at 2.2 nM (Figure 3.9). Western blot analysis of FVaH and FVaL derived from the YT ΔFV remaining bound to LV after FIIa activation was characteristic of that observed for mutation of E96 or D102 with an arguably slower dissociation of FVaH in the presence of chelator (Figure 3.10). To determine the effect of YT multipoint mutations combined with EDD on prothrombinase activity and subunit dissociation, we generated the construct YT/EDD and found that these combined mutations resulted in a very profound effect comparable to the EDD/ED construct (Figure 3.9). Subunit dissociation after FIIa activation as a result of the YT/EDD substitutions was enhanced especially after longer incubation periods (2 to 3 hrs) in the presence of Ca^{2+} compared to EDD or YT alone (Figure 3.10). However, the enhanced subunit dissociation due to YT/EDD combined multipoint mutations was not as enhanced as in the case of ED/EDD combined mutations, arguably due to the more profound enhancement of subunit dissociation by ED compared to YT (Figure 3.10). However, loss of cofactor activity by YT/EDD was more profound (> 98%) than that of ED/EDD (Figure 3.9) also suggesting two distinct functions. Since single mutation of either Y100 or T104 more closely resembled ΔFV, we investigated whether a general multipoint mutation of the N-

terminal half of L94-D112 was sufficient to confer the rapid chelator-dependent dissociation of FVaH characteristic of a sole mutation at E96 or D102. Four alanines (A_4) were consequently inserted on the N-terminal side of T104. This resulted in 94% inhibition of prothrombinase function (Figure 3.9). Like the single point E96 and D102 mutants, rapid FVaH dissociation from FVaL was observed after conversion to FVa in the presence of chelator, while in the presence of divalent cations the subunit interaction was stable over the three hour duration of the experiment (Figure 3.10). Thus, a substantial insertion causing nearly complete loss of cofactor function was insufficient to mediate spontaneous FVa subunit dissociation. This observation adds further support for a specific contribution of D111 to the association of FVaH and FVaL, and a distinct contribution of at least the region spanning E96-T104 to FVa function.

As with the single mutations, we anticipated that preactivation of the multipoint mutations would cause considerable inhibition of prothrombinase activity in mutants that showed maximum inhibition of prothrombinase activity (Figure 3.9). Following the brief preactivation step with FIIa, we added an amount of hirudin that was sufficient to inhibit the activating FIIa. Figure 3.11 shows that FIIa preactivation caused a moderate increase (about 50%) in FVa-dependent prothrombinase activity in all the multipoint mutants except for EDD which showed a decrease. These results were not anticipated and may suggest that the test may not be as informative at low levels of FIIa activity (1 to 2 nM). This observation is supported by the YT data which shows an enhancement in

Figure 3.11 **Prothrombinase activity of FIIa-pretreated ΔFV and multipoint ΔFV mutants.**

Thrombin generation was measured in a reaction mixture containing FXa (2 nM), phospholipid vesicles (200 μM), FII (1.4 μM) and conditioned media containing B-domainless FV mutants (0.5 nM) (solid bars), or FIIa-activated (1 U/ml) B-domainless FV mutants (0.5 nM) (hatched bars) in HBS/Ca^{2+}/PEG at 22 °C. Following a 10 min. incubation, the reaction was terminated with EDTA (15 mM), and FIIa generation was measured chromogenically using S2238. The average of triplicates with standard deviation is shown. An amount of hirudin was used that was just sufficient enough to terminate the FIIa activity used during the FIIa preactivation step.

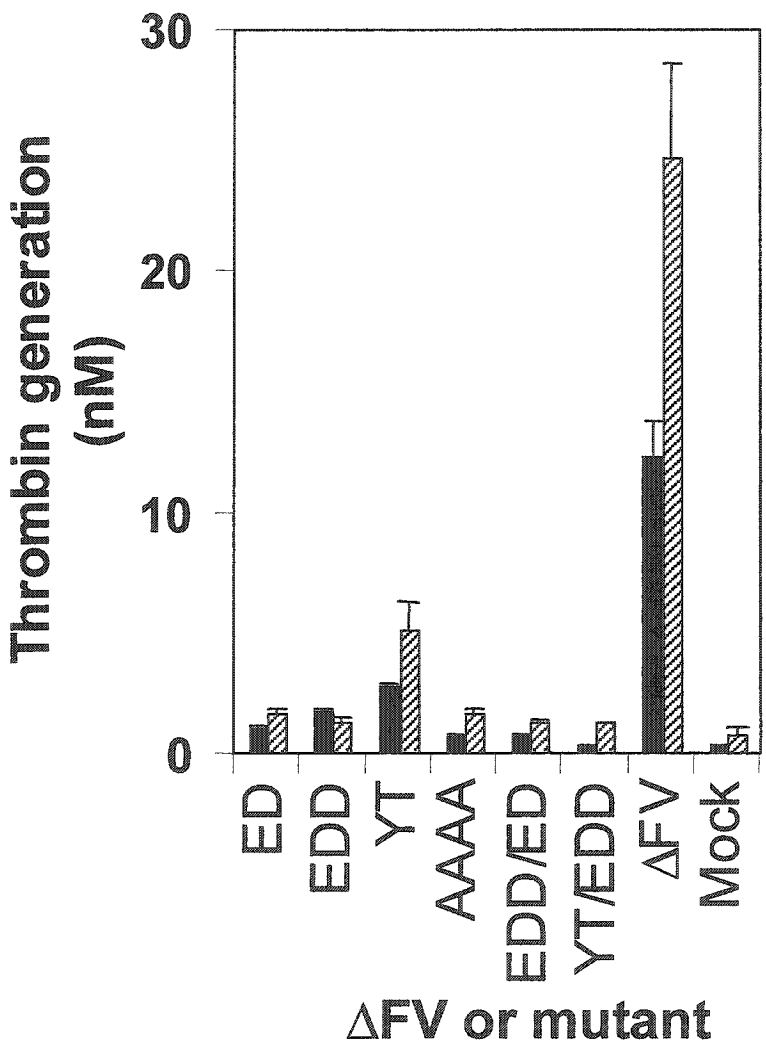
30
20
10
0
Thrombin generation (nM)
ED
EDD
YT
AAAA
EDD/ED
YT/EDD
ΔFV
Mock
ΔFV or mutant

activity following activation when preactivation FIIa activity was higher (Figure 3.11).

Binding of FXa and FII to ΔFV and mutants. APL provides the sites of association for FVa and FXa in the presence of Ca^{2+} (114,124,133,255-257,268). Furthermore, FVa provides a binding site for FXa (269,270) and FII (151,271), and enhances FXa and FII binding to aPL by several order of magnitude. To determine whether the mutations would have an effect on FXa and FII binding that would have a gross effect on our prothrombinase activity assays, FXa or FII was added to LV coated with equal antigenic concentration of recombinant proteins in the presence of Ca^{2+}. The protein remained bound after washing was analyzed by Western blot. These data showed that there was no evident alteration in the capacity of FXa (Figure 3.12) or FII (Figure 3.13 A) to bind to the PC/PS-bound mutants. Furthermore, increasing the concentration of ΔFV resulted in an increase in the binding of FXa and FII (not shown). To determine whether FII binding in the presence of recombinant proteins is effected when FXa is bound, we performed the binding experiment in the presence of the enzymatically inactive EGR_{ck}-FXa (272) in order to eliminate FII activation by otherwise enzymatically active FXa. Under these conditions, no detectable difference was observed in the amount of FII that remained bound in the presence of the recombinant proteins (Figure 3.13B). Furthermore, our data indicate that binding of FII to the LV was ΔFV-dependent, since more binding of FII was observed when ΔFV was present on the LV (Figure 3.14). These data

Figure 3.12 **Binding of FXa to ΔFV and mutants.**

APL-bound recombinant proteins (0.1 nM, 1 nM, and 10 nM) were incubated with FXa (2 nM) in HBS/Ca^{2+}/PEG at 22°C for 10 min. The aPL-bound protein was collected by centrifugation, and washed in HBS/Ca^{2+}/PEG. All reactions were stopped with sample buffer, and the aPL-bound protein was separated on 12% SDS-PAGE, transferred to PVDF, and detected with rabbit anti-human FX polyclonal Ab. The top and bottom arrows indicate the expected location of the heavy and light chains bands of FXa respectively.

D79A
E96A
Y100A
D102A
T104A
E108A
D111A
D112A
E119A
ED
EDD
YT
A4
EDD/ED
ΔFV

Figure 3.13 **Binding of FII to ΔFV and mutants in the presence of EGR_{ck}-FXa.**

APL-bound mutants (2 nM) were incubated with FII (0.1 μM, 1.5 μM, and 2 μM) in the absence of FXa (A), or with EGR_{ck}-FXa (2 nM) (B) in HBS/Ca^{2+}/PEG at 22°C for 10 min. The aPL-bound protein was collected by centrifugation, and washed in HBS/Ca^{2+}/PEG. All reactions were stopped with sample buffer, and the aPL-bound protein was separated on 12% SDS-PAGE, transferred to PVDF, and detected with anti-sera to human FII. The arrow indicates the expected location of the FII band.

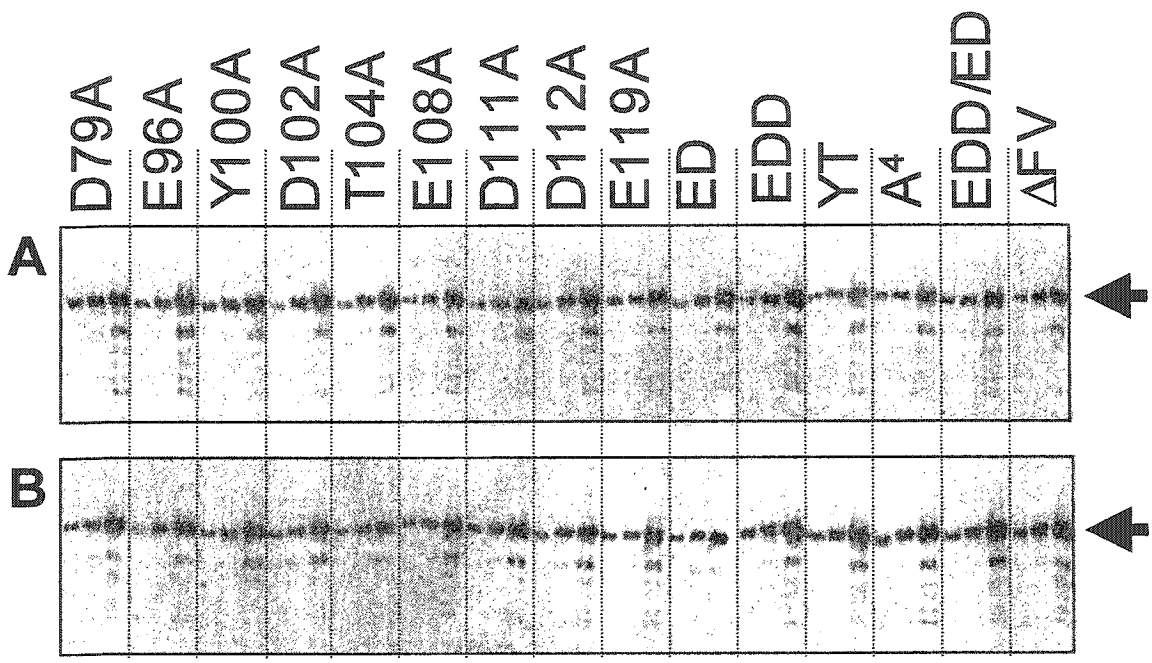
D79A
E96A
Y100A
D102A
T104A
E108A
D111A
D112A
E119A
ED
EDD
YT
A4
EDD/ED
ΔFV
A
B

Figure 3.14 **Binding of FII to aPL vesicles in the presence of ΔFV.**

Increasing concentrations of FII were incubated as in Figure 3.13 except that incubation was either in the presence or absence of ΔFV (2 nM) in HBS/Ca^{2+}/PEG at 22°C for 10 min. The aPL-bound protein was collected by centrifugation, and washed in HBS/Ca^{2+}/PEG. All reactions were stopped with sample buffer, and the aPL-bound protein was separated on 12% SDS-PAGE, transferred to PVDF, and detected with anti-sera to human FII. The arrow indicates the expected location of the FII band.

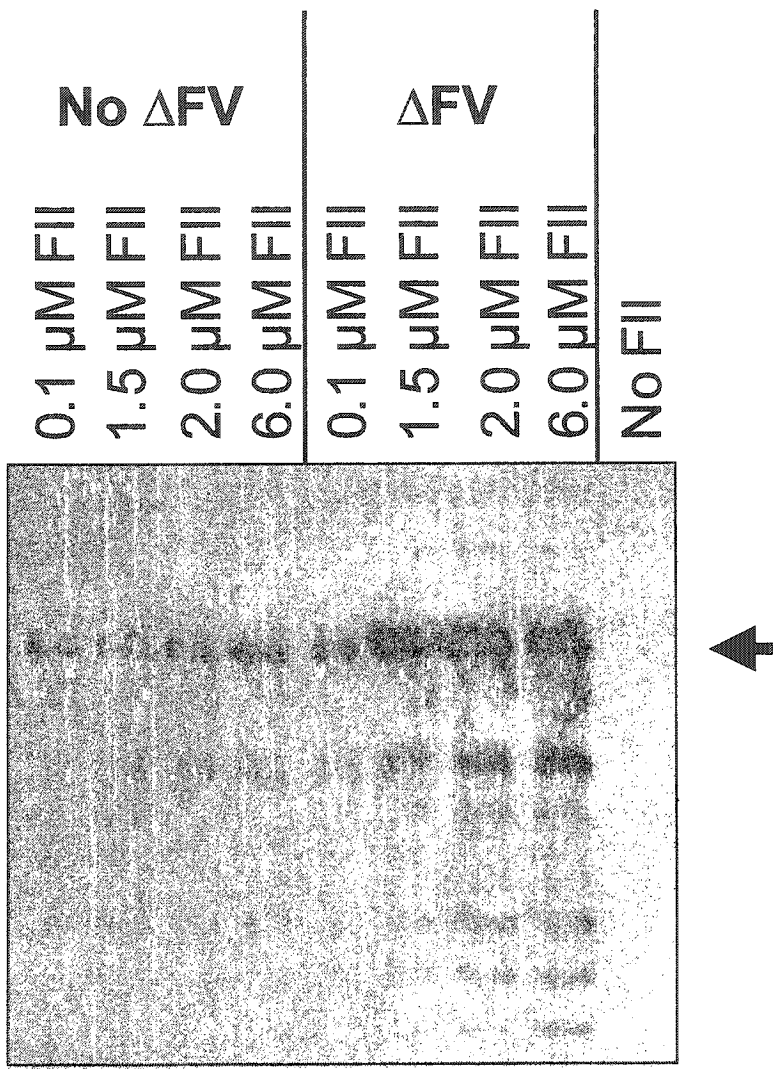
No ΔFV
ΔFV
0.1 μM FII
1.5 μM FII
2.0 μM FII
6.0 μM FII
0.1 μM FII
1.5 μM FII
2.0 μM FII
6.0 μM FII
No FII

also showed that some binding of FII to LV was detected even in the absence of ΔFV. However since the binding was not effected by an increase in the starting FII, this indicated that only residual amounts of FII binds LV (Figure 3.14). This binding was observed to be Ca^{2+}- and PS-dependent since no detectable binding was observed when 5.0 mM EDTA was added or PC vesicles were used in the reaction mixture respectively (not shown).

DISCUSSION

The function of coagulation cofactor FVa is known to be dependent on the association of its subunits FVaL and FVaH (115). The association between these two subunits is mediated through divalent cation binding shown to be reversible (88,115). Despite the importance of the FVaH-FVaL interaction, little is known about the specific residues involved in divalent cation binding or in subunit contact. Their experimental identification has been complicated by the requirement for both subunits in formation of the single Ca^{2+}-binding site (chapter 2).

Results presented in chapter 2 demonstrate that two plasmin-mediated FVaH fragments of similar size (~ 30 kDa) were detected (Figure 2.7). Although these fragments exhibited virtually indistinguishable mobility on SDS-PAGE, they differed greatly in their ability to form Ca^{2+}-dependent complexes with FVaL. One fragment begins at L94, and is capable of forming a complex with FVaL in the presence of Ca^{2+}. The other fragment, which begins only 16 residues away at M110, does not exhibit any interaction with FVaL in the presence of Ca^{2+}. This chance observation identified L94-K109 as a plausible Ca^{2+}-sensitive region involved in FVa subunit association. Interestingly, predictions made earlier from homologous protein modeling that combined the x-ray structure of ceruloplasmin and the sequence identity of FVIII, suggested five acidic amino acids in E96-D112 of FV could be involved in Ca^{2+}-binding. Because of the coincidental overlap of FV functional regions involving Ca^{2+} deduced by data and theory, the

research presented in this chapter addresses the hypothesis that L94-D112 is a divalent cation-sensitive functional region within FV.

Data derived from introducing 9 single point ($D79_A$, $E96_A$, $Y100_A$, $D102_A$, $T104_A$, $E108_A$, $D111_A$, $D112_A$, and $E119_A$) and 6 multipoint mutations ($E96_A$ /$D102_A$ (ED); $Y100_A$ /$T104_A$ (YT); $E108_A$ /$D111_A$ /$D112_A$(EDD); $E96_A$/$D102_A$/$E108_A$/D111/D112 (ED/EDD); $Y100_A$/$T104_A$ /$E108_A$/$D111_A$/$D112_A$ (YT/EDD); and AAAA (A_4) following H102) into ΔFV, strongly support the region spanning L94 to D112 as being vital for FVa function. More specifically, E96-T104 and by a distinct mechanism, D111, are essential for optimal FVa-dependent activation of FII by FXa. Alanine was used as a substitute for the mutated residues, because it is neutral and has the smallest amino acid side chain, except for the amino acid glycine (G), which is not suitable since it has been shown to alter the main chain conformation of the protein (137). This approach, along with amino acid residue deletions (267), and recombinant chimeras (273) has been previously used to identify functionally important amino acid residues within the C2-domain of human FV. The mutations described here did not have a gross effect on the level of expression and secretion (Table 3.1) nor on morphology or replication in the K293 cells (not shown). Furthermore, they did not effect aPL binding because they may not be involved in this process (Figure 3.4). Since interactions between an antibody and antigen are largely dependent on structural complementarity between the antibody and the antigen surface as well as direct contact with the epitope site, we measured phospholipid

binding using antibodies that bind specifically to the light chain of human FV. All the mutants showed no significant decrease in binding to PS (Figure 3.4) under the conditions evaluated. Regardless, an effect of ΔFV mutation on aPL-binding may be effectively ruled-out since all experiments were conducted with excess of large vesicles to minimize the effect of any subtle differences in dissociation constant between recombinant proteins.

In the presence of supplemental Ca^{2+} and potentially other divalent cations that may be contained in culture media, the mutants shared a wide range of inhibition compared to ΔFV, in the order $E96_A$ (81%), $D111_A$ (70%), $D102_A$ (60%), $T104_A$ (35%), $E108_A$ (30%), $D112_A$ (25%), $Y100_A$ (16%), $D79_A$ (7%) and $E119_A$ (0%). The mutations giving rise to insignificant inhibition, D79 and E119, are the nearest acidic amino acids outside the immediate segment of interest. Their lack of functional involvement supports the specificity of effects seen by replacement of the other amino acids. Among those substitutions causing greater than 50% inhibition, the single point mutation of E96 or D102, combined mutation of Y100/T104 or insertion of four alanines between H103 and T104, had no effect on the apparent interaction between FVaH and FVaL in the presence of divalent cations compared to ΔFV. Under the same conditions, simultaneous mutation of E96 and D102 resulted in an intermediate dissociation rate of FVaH. However, when dissociation of FVaH from FVaL was induced by chelation, these mutants demonstrated rapid loss of FVaH from aPL-bound FVaL compared to ΔFV. These data suggest that mutations of E96-T104 effect

prothrombinase activity likely altering an optimal complement of metal ion coordination required for function, which is less important for interchain association. Conversely, the single point mutation of D111 or of a multipoint mutation including D111 (EDD and ED/EDD), resulted in spontaneous dissociation of FVaH from FVaL independent of divalent cation availability. When combined these observations suggest that two key FVa functions may be imparted by this relatively small locus of FV, intersubunit association and a separable cofactor effect on FXa.

At this time, the specific FVa function affected by mutation of residues within E96-T104 is unknown. To optimally accelerate FXa, FVa must simultaneously participate in a number of binary macromolecular interactions. An effect of ΔFV mutation on aPL-binding can be excluded because all experiments were conducted at an excess of aPL-containing vesicles so that subtle dissociation constant differences among the mutants would be negligible. Regardless, it is doubtful that mutation of FVaH affected aPL binding since this function of FV/FVa has been assigned exclusively to FVaL by independent laboratories (114,124,133,256-257). Effects of ΔFV mutation on substrate recognition of FV by FIIa can also be excluded since at least the pre-activation experiment (Figure 3.6) was conducted under conditions that facilitated complete conversion of ΔFV to FVa and maintained subunit association, yet significant inhibition compared to ΔFV was observed when E96 or D102 were changed to Ala.

As far as effects of the ΔFV mutation on the substrate recognition of FV by FXa and FII are concerned, the prothrombinase activity experiments (Figure 3.5, and 3.9) were conducted under conditions where saturating concentrations of FXa (2 nM), phospholipid vesicles (200 μM), and FII (1.4 μM) were added to ensure indistinguishable binding of components to the mutants, hence there would be no detectable gross effect on Ca^{2+}-dependent interchain association and prothrombinase assay. Our data clearly indicate that there was no evident alteration in the capacity of FXa (Figure 3.12) or FII (Figure 3.13A) to bind the aPL–bound mutants (Figure 3.12, 3.13, and 3.14). Also, FII binding to the aPL-bound mutants bound to EGR_{ck}-FXa was indistinguishable (Figure 3.13B). Distinct effects of ΔFV mutations on their recognition by FIIa are unlikely since the preactivation experiment (Figure 3.8, and 3.11), under these experimental conditions, facilitated complete conversion of FV mutants to FVa mutants. The newly generated FVa mutants are suspected to maintain their heterodimer formation since these activation experiments were conducted in the presence of Ca^{2+}. To investigate more fully the effect of E96-T104 on FVa-FXa interactions, however, experiments using purified mutants would need to be performed. Although it seems that mutations of D111 or E96-T104 result in distinguishable FVa functional phenotypes, FVa heterodimer is required if a mechanism(s) governing the inhibition of prothrombinase activity exhibited by mutations of the latter residues is hoped to be elucidated. Direct experiments using purified mutants are required to unambiguously investigate contributions of E96-T104 to

FVa-FXa or FVa-FII interactions, or other direct catalytic effects on FXa activity. Although mutation of D111 or E96-T104 appears to result in distinguishable FVa functional phenotypes, subunit dissociation would preclude detection of the mode of inhibition characteristic of mutating the latter residues. We consequently cannot exclude the possibility that D111 participates in both subunit association and other FVa functions required for prothrombinase activity.

Aside from a requirement for Ca^{2+} to anchor the essential intersubunit complex, the precise role of metal ions in FVa function is unclear. The data presented here show for the first time that subtle changes in metal ion sequestration caused by single point substitution of E96 or D102 in ΔFV are without substantial effects on the FVaH-FVaL association, but correlate to inhibition of prothrombinase function. Therefore metal ions are suggested to confer FVa function in addition to facilitating the noncovalent complex between FVa subunits. This has some similarity to the picture emerging for the homologous procofactor, FVIII, which requires Ca^{2+} to adopt a functional conformation (274). However, in sharp contrast to FVa, Ca^{2+} has little effect on FVIII subunit association (275). It should be noted that this ostensible discrepancy may reflect unknown differences between the metal ion-dependence of the active cofactor compared to the respective procofactor, especially since FV is a single polypeptide, whereas FVIII is a noncovalent heterodimer. While D111 has been demonstrated by our studies to be involved in FVa subunit association, it is unknown whether it constitutes part of the Ca^{2+}-binding site, a fundamental

FVaL contact point or both. On the other hand, the finding that mutations within E96-T104 increase the apparent rate of FVaH-FVaL dissociation only in the presence of a chelator, implies that these residues either directly or indirectly facilitate FVa binding to divalent cations and not subunit interactions.

Amino acids have been implicated in FVIII A-domain association by identifying mutations in hemophilia patients uniquely characterized by a discrepancy in FVIII clotting assays, where pretreatment with FIIa caused reduced rather than enhanced activity (276,277). The FVaH analogue in FVIIIa is composed of two FIIa-mediated polypeptides, corresponding to the A1 and A2 domains. The latter has been observed to undergo dissociation as a normal mode of FVIIIa regulation (278), which was found to be accelerated in patients having the discrepant clotting assays (276,277). A comparable effect was observed in the current study, in which the lower cofactor activity observed after FIIa pretreatment of D111A was attributable to the observed spontaneous FVaH dissociation. Figure 3.15 is the three-dimensional backbone structure predicted for FVa (chapter 2) showing the location of the amino acids having homology to those identified in FVIIIa leading to accelerated A2 subunit dissociation (magenta spacefilling). Also shown in Figure 3.15 are E96, D102 and D111 (white spacefilling), the focus of the current work. All fall at the putative interfaces between A-domains. The finding that the residues in FVIIIa lie close to or at the A2-domain interface is consistent with their discovery being dependent upon A2-domain dissociation. In support of previous plasmin-mediated fragmentation data

Figure 3.15 **Model localizing E96, D102 and D111 to the A1-A3-domain interface.**

The FVa A-domain orientation and structure has been previously predicted by homology modeling to ceruloplasmin. The backbone structure is presented here with color-coded A-domains. Spacefilling depictions of amino acids are shown that are: identified in the current study to have >50% inhibition of FVa activity when replaced by Ala (white); analogous to amino acids giving rise to FVIII 1 stage/2 stage clotting assay discrepancy (magenta); and predicted to bind Cu^{2+} (yellow).

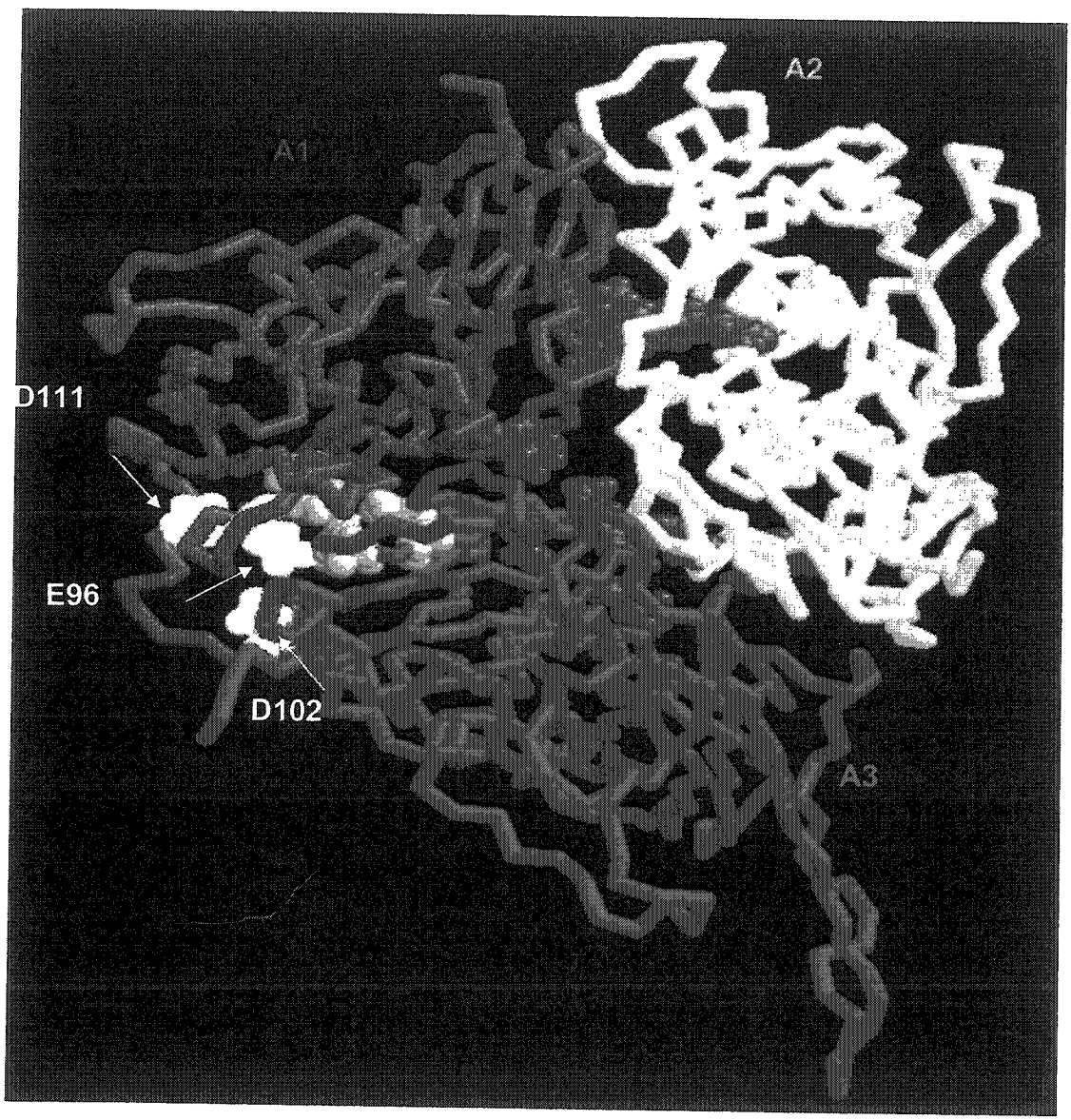
A2
A1
D111
E96
D102
A3

(chapter 2), E96, D102 and D111 are predicted by the model to be at the junction between A1 and A3.

In addition to interactions with Ca^{2+}, both FV (129) and FVIII (279) have been shown to have a single Cu^{2+}-binding site, consistent with homology to ceruloplasmin, the major copper binding protein in plasma (280). Cu^{2+} has been shown to enhance the affinity between FVIII subunits by 2 orders of magnitude (275), while functional studies concerning a role for Cu^{2+} have not been reported for either FV or FVa. Only one of six Cu^{2+} binding sites in ceruloplasmin is identifiable in FV and FVIII by homology modeling (97,98). Interestingly, this corresponds to residues H85 in FVaH, and H1815 and H1817 in FVaL which are depicted in Figure 3.15 (orange spacefilling). Being proximate, it is tempting to speculate that the chelator-sensitive functional site identified in the current work, E96-D111, may also include H85. This could suggest that Ca^{2+} and Cu^{2+} bind adjacent to each other in FVa, making discrete functional effects difficult to experimentally dissect. The added complexity caused by metal ion binding effects may explain why D111 is predicted to be furthest from the putative interface, yet is the only single point mutation we generated that induced FVaH-FVaL dissociation in the presence of divalent cations.

Sequence alignment of the 79 through 119 region, which harbours all of the mutations in this study, of FV, FVIII, and ceruloplasmin from four different species revealed interesting observations (Figure 3.15). Firstly, residues that we

had chosen as controls and had no detectable inhibition of prothrombinase activity or enhanced subunit dissociation, are not conserved among these proteins or, in most cases, even among the species of the same protein. The latter is true specifically for the D79A mutation. Secondly, the 19 residue regions between residues 96 and 114 contains 9 residues (residues E96, G97, A98, Y100, D102, T104, D111, D112, and V114) that are identical among the proteins and the species, clearly indicating that this region is of paramount importance for either function or structure. Thirdly, with the exception of E108, all the acidic residues implicated by homology modeling to constitute a potential Ca^{2+}-binding site (97) are conserved among all the proteins and the species. Curiously, the E108A had only 30% inhibition of prothrombinase activity and no detectable effect on subunit dissociation (Figure 3.5, and 3.7). Fourth, D112A which is conserved (Figure 3.16), showed only 25% inhibition of activity and no detectable effect on subunit association, indicating that residue D112 may perform a crucial function in this region that remains to be identified. This may also indicate that the observed close to complete inhibition of activity and loss of FVa subunit integrity is perhaps partially due to a function of residue D112. Lastly, Y100 and T104 are completely conserved in all the proteins and species, indicating that although these residues are non-acidic and were not considered functionally or structurally crucial, they may perform an essential function in these three proteins. This is reflected by the observation that the YT recombinant FV protein showed considerable inhibition of prothrombinase activity (Figure 3.9) and moderate enhancement of subunit dissociation (Figure 3.10).

Figure 3.16 **Sequence alignment of the 79 through 119 region in FV, FVIII and ceruloplasmin from various species.**

Amino acids D79 through E119 are shown. Amino acids L94-M109 implicated in the Ca^{2+}-dependent FVaH-FVaL association by previous studies from our laboratory are shown with the line below the sequence. The five acidic residues implicated by homology modeling to constitute a potential Ca^{2+}-binding site are in red. Conserved sequences are indicated by the open boxes. Acidic conserved residues are in red, and non-acidic conserved residues are in green. Residues that are not homologous to the conserved sequences are in blue. The residues selected for single point-mutation to Ala (D79, E96, Y100, D102, T104, E108, D111, D112, and E119) are indicated by the arrow.

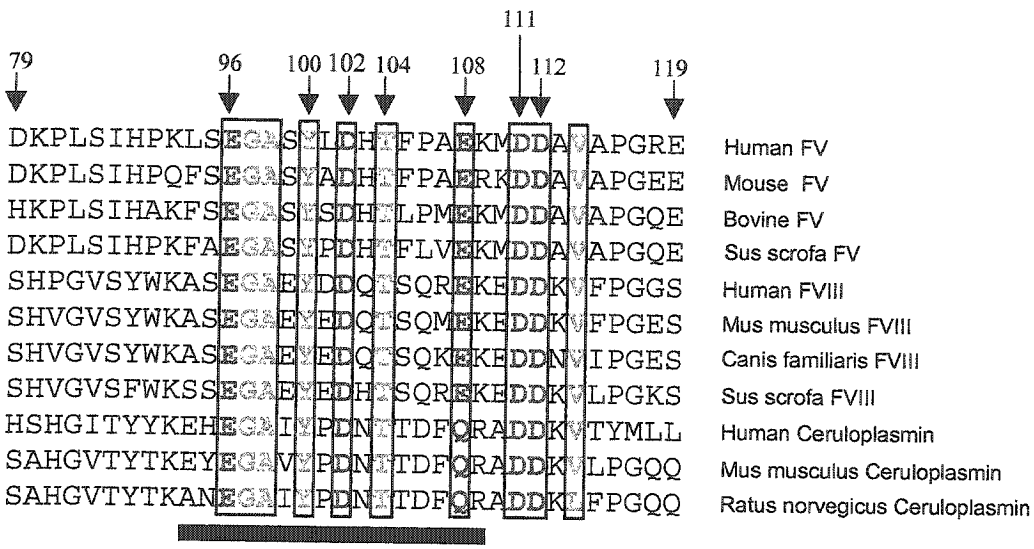
79
96
100
102
104
108
111
112
119
DKPLSIHPKLSEGASYLDHIFPAEKMDDAVAPGRE
DKPLSIHPQFSEGASYADHIFPAERKDDAVAPGEE
HKPLSIHAKFSEGASYSDHILPMEKMDDAVAPGQE
DKPLSIHPKFAEGASYPDHIFLVEKMDDAVAPGQE
SHPGVSYWKASEGAEYDDQTSQREKEDDKVFPGGS
SHVGVSYWKASEGAEYEDQTSQMEKEDDKVFPGES
SHVGVSYWKASEGAEYEDQTSQKEKEDDNVIPGES
SHVGVSFWKSSEGAEYEDHISQREKEDDKVLPGKS
HSHGITYYKEHEGAIYPDNITDFQRADDKVTYMLL
SAHGVTYTKEYEGAVYPDNITDFQRADDKVLPGQQ
SAHGVTYTKANEGAIYPDNITDFQRADDKLFPGQQ
Human FV
Mouse FV
Bovine FV
Sus scrofa FV
Human FVIII
Mus musculus FVIII
Canis familiaris FVIII
Sus scrofa FVIII
Human Ceruloplasmin
Mus musculus Ceruloplasmin
Ratus norvegicus Ceruloplasmin

Figure 3.16 **Sequence alignment of the 79 through 119 region in FV, FVIII and ceruloplasmin from various species.**

Amino acids D79 through E119 are shown. Amino acids L94-M109 implicated in the Ca^{2+}-dependent FVaH-FVaL association by previous studies from our laboratory are shown with the line below the sequence. The five acidic residues implicated by homology modeling to constitute a potential Ca^{2+}-binding site are in red. Conserved sequences are indicated by the open boxes. Acidic conserved residues are in red, and non-acidic conserved residues are in green. Residues that are not homologous to the conserved sequences are in blue. The residues selected for single point-mutation to Ala (D79, E96, Y100, D102, T104, E108, D111, D112, and E119) are indicated by the arrow.

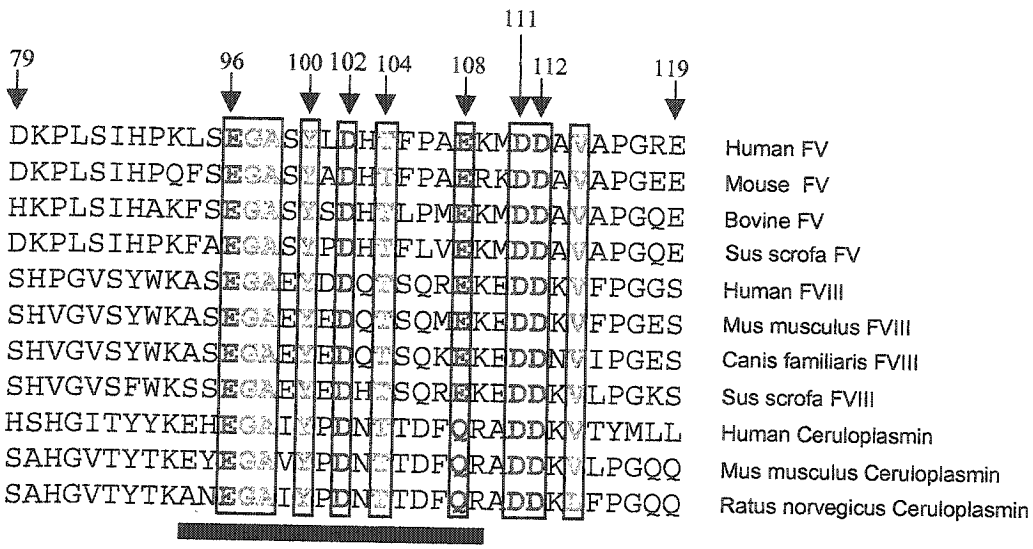
79
96
100
102
104
108
111
112
119
DKPLSIHPKLSEGASYLDHIFPAEKMDDAVAPGRE
DKPLSIHPQFSEGASVADHIFPAERKDDAVAPGEE
HKPLSIHAKFSEGASISDHIYLPMEKMDDAVAPGQE
DKPLSIHPKFAEGASVPDHIFLVEKMDDAVAPGQE
SHPGVSYWKASEGAEYDDQTSQREKEDDKVFPGGS
SHVGVSYWKASEGAEYEDQTSQMEKEDDKVFPGES
SHVGVSYWKASEGAEYEDQTSQKEKEDDNVIPGES
SHVGVSFWKSSEGAEYEDHTSQREKEDDKVLPGKS
HSHGITYYKEHEGAIYPDNITDFQRADDKVTYMLL
SAHGVTYTKEYEGAVYPDNITDFQRADDKVLPGQQ
SAHGVTYTKANEGAIYPDNITDFQRADDKLFPGQQ
Human FV
Mouse FV
Bovine FV
Sus scrofa FV
Human FVIII
Mus musculus FVIII
Canis familiaris FVIII
Sus scrofa FVIII
Human Ceruloplasmin
Mus musculus Ceruloplasmin
Ratus norvegicus Ceruloplasmin

CHAPTER 4

A novel synaptotagmin-like C2-domain-containing protein, P135

OVERVIEW

In this chapter, we describe a novel human protein (p135) with two sC2-domains. The gene was identified in human erythroleukemia cells (HEL). The cDNA predicted a protein of 1232 amino acids (MW 135 kDa) with high sequence homology to the Ca^{2+}-dependent neurotransmitter proteins, synaptotagmin I and Munc-13. The gene was mapped to q25 of human chromosome 17; a locus correlating to various types of cancer. Strong expression of p135 mRNA in promyelocytic and lymphoblastic leukemias (HL-60 and MOLT-4), and adenocarcinoma (SW480) cell lines. We screened sixteen non-pathological human tissues for p135-encoding mRNA and found expression only in peripheral blood leukocytes (PBL), bone marrow, lymph node, thymus and spleen suggesting a role in the immune system. Western blot and flow cytometric analyses using antibodies raised against recombinant protein, purified by gel electroelution, were consistent with the conclusion that p135 is prevalent in white blood cell and platelet lineages. Immunofluorescence microscopy and flow cytometry further revealed that the protein is intracellular, and upon pretreatment of T-cells with phytohemagglutinin (PHA) is upregulated and translocated to the nucleus. Furthermore, in mitotic cells, p135 was predominantly relocalized to the nucleus or nuclear membrane. The recombinant protein showed Ca^{2+}-dependent interactions with phosphatidylserine but not with phosphatidylcholine, and this interaction was reversible in the presence of a chelator such as EDTA.

These data describe the first member of the important sC2 family of proteins that appears to be preferentially expressed by blood cells. Although p135 has significant homology to the recently identified rat Munc 13-4 protein, to our knowledge, it is the first sC2-domain-containing protein known to be predominantly expressed in blood cell lineages. Its localization to T-cells, lymph node and thymus, suggests a function of p135 in the immune system.

The following sections of the Introduction will briefly describe some of the Ca^{2+}-binding motifs, the process of neurotransmitter release in synaptic vesicles, and the role that Ca^{2+} ions play in neurotransmitter release. Since much of our understanding of the structure and function of sC2-domains originate from research work done with the neurotransmitter release protein, synaptotagmin, many of these sections will describe sC2-domains in the context of what we know about synaptotagmin sC2-domains.

INTRODUCTION

1.1 The importance of Ca^{2+} ions in protein function

Calcium metal ions are involved in the regulation of many cellular processes ranging from gene transcription, muscle contraction and cell survival, to neurotransmitter release (281-284). The intracellular concentration of Ca^{2+} is very low in the eukaryotic cell (0.1 μM) whereas the extracellular concentration of Ca^{2+} is roughly 10,000-fold higher (1 mM) (284). Various stimuli, including receptor ligands or changes in membrane polarization can result in the influx of Ca^{2+} ions into the cytosol or the release of stored Ca^{2+} ions from organelles such as the sarcoplasmic reticulum (SR), the endoplasmic reticulum (ER), the mitochondria, and the nucleus.

The increase in free Ca^{2+} ion concentration following stimulation of a cell allows Ca^{2+}-binding proteins to bind Ca^{2+} ions. Of the several hundred Ca^{2+}-binding proteins that have been identified, most of them share a common Ca^{2+}-binding motif, commonly called the EF hand (285,286). This motif comprises about 30 amino acids and consists of a helix-turn-helix where the two helices are arranged similarly to the extended thumb and index finger of a hand. EF-hand proteins typically contain a single Ca^{2+} ion per EF-hand, and have Ca^{2+} sites that are buried. An example of such proteins is calmodulin, the major transducer of Ca^{2+} signals in mammalian cells (287,288), which binds free Ca^{2+} by its multiple cooperative EF hands located at the N- and C-termini of the

protein. Ca^{2+}-binding causes a large conformational change, exposing a hydrophobic region that mediates target recognition (286).

In addition to the EF hand module, other Ca^{2+} modules have characteristic binding properties such as: the annexin fold binds phospholipid (289,290), the src homology-2 domain (SH2) binds phosphotyrosine-containing sequences (291,292), the pleckstrin homology domain (PH) binds phosphatidylinositol phosphates (293,294), the src homology-3 domain (SH3) binds proline-rich sequences (295,296) and the sC2-domain binds Ca^{2+} ions (297,298). The sC2-domains and annexins are unique among all these modules because they also bind phospholipids and this phospholipid binding is usually regulated by Ca^{2+}, hence they are often referred to as Ca^{2+}-dependent lipid-binding domains or CaLB (299,300).

The sC2-domain is the focus of this chapter. Unfortunately, despite the important nature of the sC2-domain, many fewer structural studies have been reported for proteins containing sC2-domains than other families of Ca^{2+}-binding proteins that, for example, contain the EF-hand domain (e.g. calmodulin) (287,288).

2.1 Identification of sC2 Domains

Recent progress in the understanding of the mechanisms that regulate membrane targeting of intracellular peripheral proteins have revealed that the

process is mediated by a limited number of membrane-targeting domains, including the EF hand and the protein kinase C (PKC) conserved 2 domain (C2 domain). The sC2-domain is largely a Ca^{2+}-dependent anionic phospholipid binding module found in many important proteins that function in signal transduction or membrane trafficking (297,298). The functions of many sC2-domains and sC2-domain-containing proteins are not yet known.

The sC2-domain is an important and widespread Ca^{2+}-binding domain of 130 - 140 residues, originally identified as one of four conserved functional domains in the Ca-dependent isoform of protein kinase C (PKC) (301,302,303). It was first identified as a Ca^{2+}-binding module based on the observation that Ca^{2+}-independent PKC isoforms lack the sC2-domain, and was later experimentally shown to bind Ca^{2+} ions in the neurotransmitter protein synaptotagmin I (303). Especially neurotransmitter proteins often contain tandem sC2-domains, referred to as the sC2A- and sC2B-domains (Figure 4.1 and 4.2, 4.3).

In contrast to the annexin family of proteins which consist mainly of the Ca^{2+} and membrane-binding domains, the sC2-domain is a module that is attached to a wide number of enzymatic or protein interaction domains in order to provide Ca^{2+} and/or membrane regulation of functions inherent in the other regions of the protein (303-305) (Figure 4.1).

Figure 4.1 **Comparison of functional domains in proteins containing sC2-domains.**

Schematic domain maps for sC2-domain containing proteins, grouped according to function. sC2-domains are represented by the black boxes. White boxes represent: transmembrane domain (T), Rab-binding domain (Rab-BD), Src homology-2 and –3 domains (SH2 and SH3), pleckstrin homology domain (PH), EF-hand-binding Ca^{2+}-binding domain (EF), GAP-related domain (GRD), conserved sequence of phosphatidylserine decarboxylase (PSD), homology domain of BCR (DBL), homology domain of PKC (HR1), lipase (L), kinase (K). The direction of the arrows indicate the two different topologies of the sC2-domains. Left facing arrows represent topology I sC2-domains, and right facing arrows represent topology II sC2-domains.

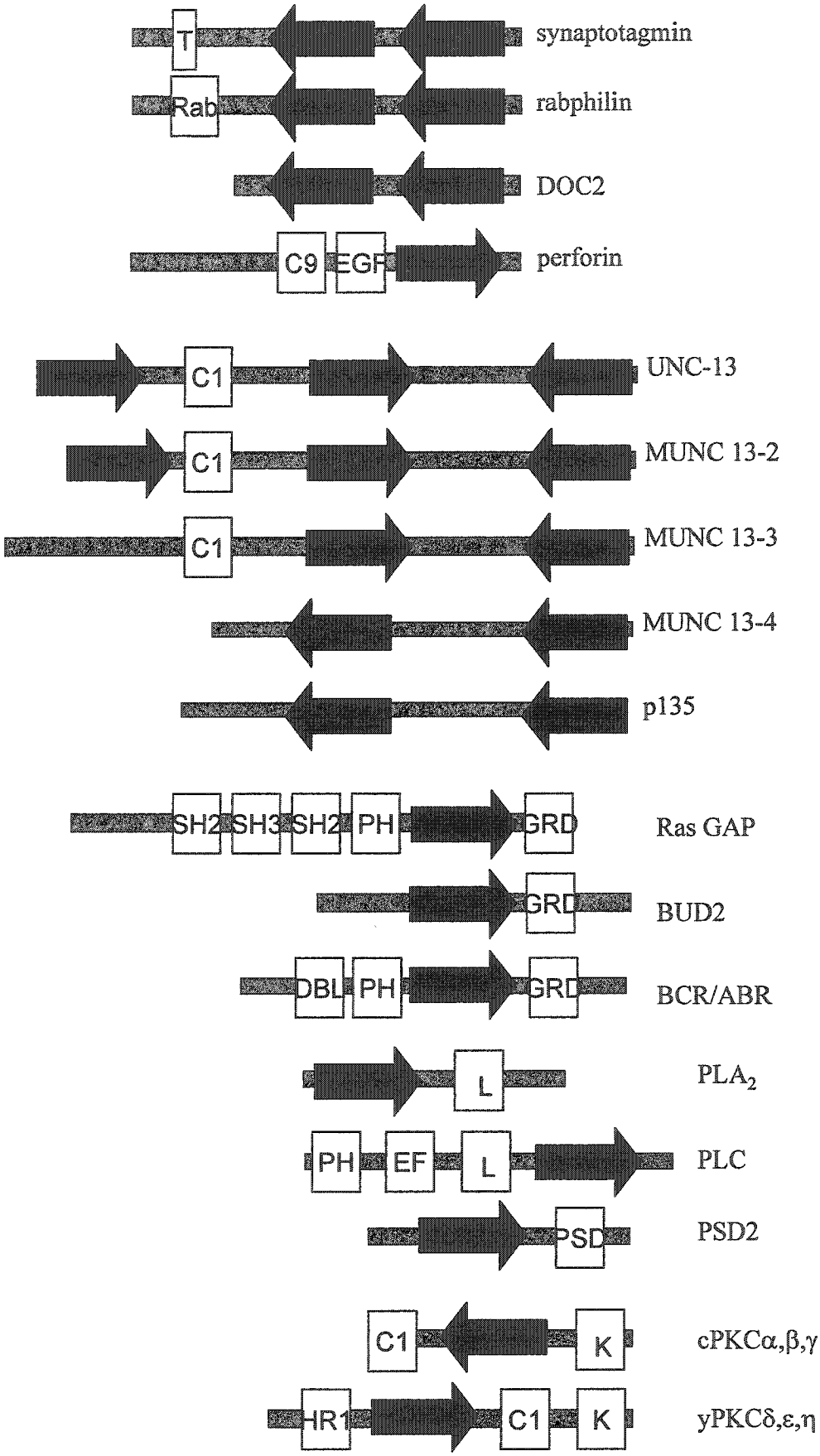
T
synaptotagmin
Rab
rabphilin
DOC2
C9
EGF
perforin
C1
UNC-13
C1
MUNC 13-2
C1
MUNC 13-3
MUNC 13-4
p135
SH2
SH3
SH2
PH
GRD
Ras GAP
GRD
BUD2
DBL
PH
GRD
BCR/ABR
L
PLA2
PH
EF
L
PLC
PSD
PSD2
C1
K
cPKCα,β,γ
HR1
C1
K
yPKCδ,ε,η

Figure 4.2 **Sequence alignment of synaptotagmin sC2A- and sC2B-domains.**

The sequences of the sC2A- and sC2B-domains of rat synaptotagmin I are aligned with each other. Amino acids that bind Ca^{2+} are boxed. The locations of the β strands are shown by the arrows above the sequence. The five Asp residues implicated in Ca^{2+}-binding are shown by the open boxes.

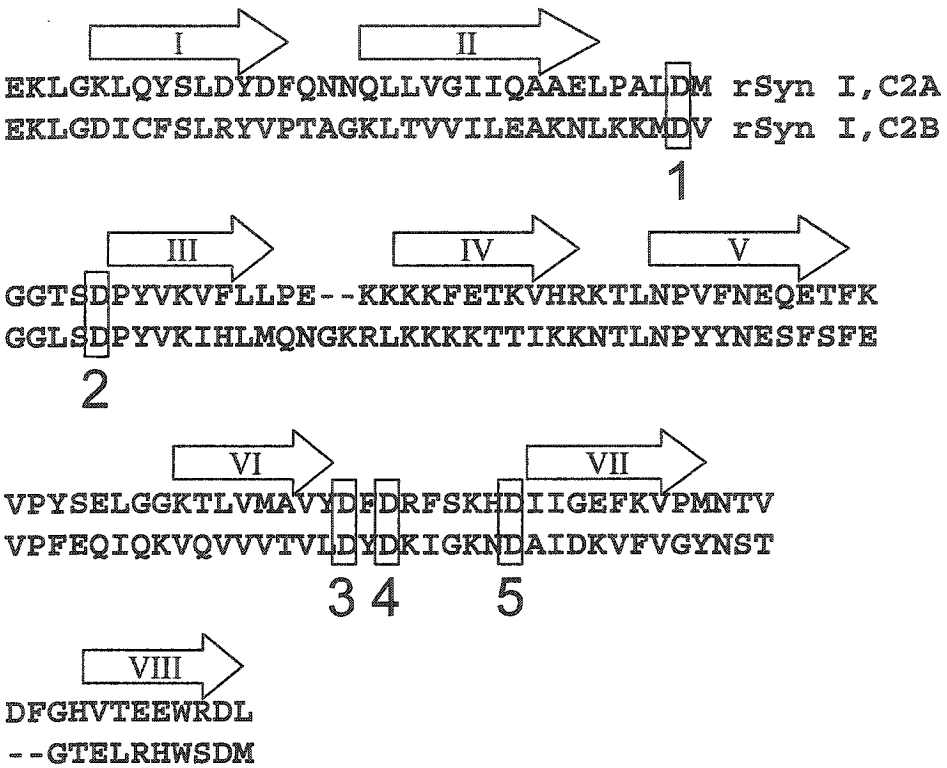
I
II
EKLGKLQYSLDYDFQNNQLLVGIIQAAELPALDM rSyn I,C2A
EKLGDICFSLRYVPTAGKLTVVILEAKNLKKMDV rSyn I,C2B
1
III
IV
V
GGTSDPYVKVFLLPE--KKKKFETKVHRKTLNPVFNEQETFK
GGLSDPYVKIHLMQNGKRLKKKKTTIKKNTLNPYYNESFSFE
2
VI
VII
VPYSELGGKTLVMAVYDFDRFSKHDIIGEFKVPMNTV
VPFEQIQKVQVVVTVLDYDKIGKNDAIDKVFVGYNST
3 4 5
VIII
DFGHVTEEWRDL
--GTELRHWSDM

Figure 4.3 **Sequence alignment of synaptoyagmin sC2-domains from different species**

Shown are the aligned sC2-domain sequences from several species. The five conserved Asp residues, which may be crucial for Ca^{2+} binding are shown by the open boxes.

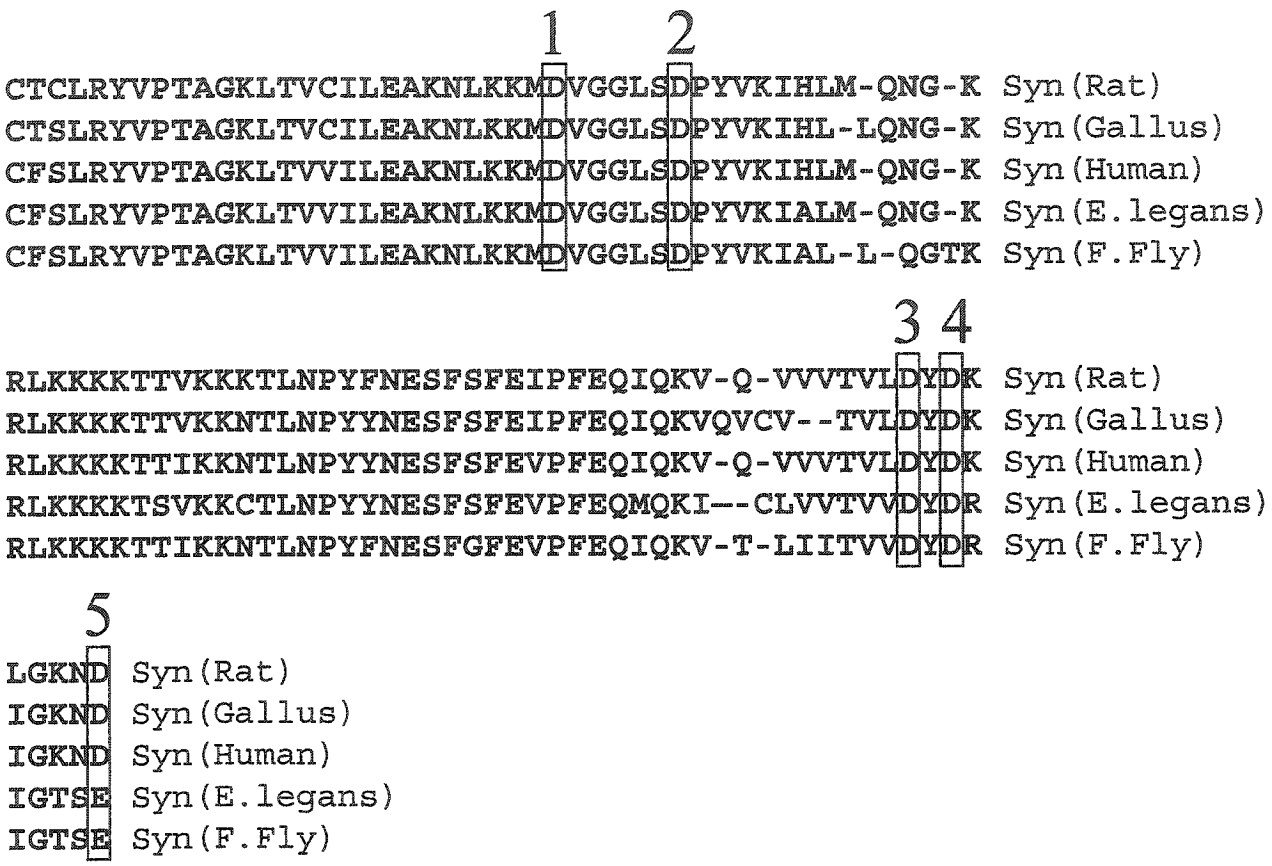
1
2
CTCLRYVPTAGKLTVCILEAKNLKKMDVGGLSDPYVKIHLM-QNG-K Syn(Rat)
CTSLRYVPTAGKLTVCILEAKNLKKMDVGGLSDPYVKIHL-LQNG-K Syn(Gallus)
CFSLRYVPTAGKLTVVILEAKNLKKMDVGGLSDPYVKIHLM-QNG-K Syn(Human)
CFSLRYVPTAGKLTVVILEAKNLKKMDVGGLSDPYVKIALM-QNG-K Syn(E.legans)
CFSLRYVPTAGKLTVVILEAKNLKKMDVGGLSDPYVKIAL-L-QGTK Syn(F.Fly)
3
4
RLKKKKTTVKKKTLNPYFNESFSFEIPFEQIQKV-Q-VVVTVLDYDK Syn(Rat)
RLKKKKTTVKKNTLNPYYNESFSFEIPFEQIQKVQVCV--TVLDYDK Syn(Gallus)
RLKKKKTTIKKNTLNPYYNESFSFEVPFEQIQKV-Q-VVVTVLDYDK Syn(Human)
RLKKKKTSVKKCTLNPYYNESFSFEVPFEQMQKI--CLVVTVVDYDR Syn(E.legans)
RLKKKKTTIKKNTLNPYFNESFGFEVPFEQIQKV-T-LIITVVDYDR Syn(F.Fly)
5
LGKND Syn(Rat)
IGKND Syn(Gallus)
IGKND Syn(Human)
IGTSE Syn(E.legans)
IGTSE Syn(F.Fly)

2.2 Function of sC2-domains

As a group, sC2-domain-containing proteins perform multiple biological functions (some are shown in Figure 4.1). In PKC, and double C2 domain proteins the sC2-domains play a regulatory role by mediating the Ca^{2+}-dependent recruitment of these proteins to phospholipid membranes (297), hence functioning as Ca^{2+}-effector domains. Although the majority of sC2-domains characterized thus far have been shown to bind Ca^{2+} directly, several sC2-domains are believed to act independent of a direct Ca^{2+} interaction, such as some PKC isoforms (PKCδ, -ε, -η and -θ) (303). Some sC2 domains, in addition to binding phospholipids in a Ca^{2+}-dependent manner, facilitate association with other ligands (304-307). Thus in nearly every case, sC2 domains have been implicated as important ligand-binding modules.

2.3 Other proteins with sC2 domains

Over 100 intracellular eukaryotic proteins containing sC2 domains are listed in the current data base, with a wide variety of important intracellular processes. Examples of such proteins are kinases such as PKC, PKC-like kinases, and sCH9; lipid modification enzymes such as phospholipase A2 (PLA_2) phospholipase C (PLC), GTPase-activating proteins such as ras-GAP, GAP1, ubiquitination enzymes, Ca^{2+} sensors in regulated membrane transport such as the synaptotagmins (305), rabphilin 3A (310), double sC2 protein (DOC2) (311), and UNC-13 (302,312,313). Most of these proteins associate specifically with anionic phospholipid (aPL) in a Ca^{2+}-dependent manner.

Much of the current data on the structures and interactions of sC2-domains were derived from studies of PLC1, PKC, and, in particular, synaptotagmin I, hence the next sections will deal mainly with synaptotagmin as a model sC2 domain-conatining protein.

3.1 Synaptotagmins

3.1.1 Function of synaptotagmins at nerve terminus

During neurotransmitter exocytosis, Ca^{2+} floods into the synapse before the propagation of an action potential (315-317). This suggested that there exists a receptor for this Ca^{2+} signal on the presynaptic terminus. Calmodulin, PKC, and the annexins were suggested as possible candidates for the Ca^{+2} trigger of exocytosis (317). More recently, synaptotagmins, the family of synaptic vesicle proteins (in particular synaptotagmin I and II), have been identified as critical proteins of the synaptic machinery. These proteins sense Ca^{2+}-influx and trigger synaptic vesicle fusion and neurotransmitter release (318-321).

3.1.2 Domain structure

Synaptotagmin I contains a single glycosylated amino terminus transmembrane region (TM), a highly charged linker sequence, two C-terminal cytosolic sC2-domains (referred to as the sC2A- and sC2B-domains), and a conserved sequence at the C-terminus (304,305,321). Synaptotagmin I sC2-

domains are stabilized by Ca^{2+}, an ion that is required for phospholipid binding (315,322,323). At present, the sC2-domains of synaptotagmin I, especially its sC2A-domain, are the best-studied sC2-domains.

While most sC2-containing proteins have a single sC2 domain, synaptotagmins, and a small number of other synaptic vesicle proteins such as rabphilin 3A and DOC2, contain two tandem sC2 domains (SC2A and sC2B) (324-327) (Figure 4.1 and 4.3). These proteins contain similar sC2A- and sC2B-domains but are not classified as synaptotagmins because they lack TMRs. Among the many proteins in which two sC2 domains are found is Unc-13, whose mutation causes neurological defects in *C. elegans* (312,313), and in four mammalian homologues of Unc-13, Munc13-1, Munc13-2, Munc13-3, and a recently identified Munc13-4 (Figure 4.1) (302,328-331). The latter was identified in the rat and is highly homologous to the P135 protein at the predicted amino acid sequence level.

3.1.3 The synaptotagmin gene family

A total of thirteen synaptotagmins have been discovered (for review see 305). The sequences of sC2-domains of these synaptotagmins are very similar to those of synaptotagmin I, suggesting that phospholipid binding by most synaptotagmins is functionally important. Many of the synaptotagmins (synaptagmin I, II, III, V, and VII) have sC2-domains that bind phospholipid in a Ca^{2+}-dependent manner. Conversely, the sC2B-domain binds to phospholipids

and polyphosphoinositides in a Ca^{2+}-independent manner (305,315), but not all synaptotagmins bind Ca^{2+} and phospholipids. For example, synaptotagmins IV and XI have an evolutionarily conserved substitution in the Ca^{2+}-binding site of the sC2A-domain that prevents binding of a full complement of Ca^{2+} ions (305). In synaptotagmins VIII, XII, and XIII, the top loops of the sC2A- and the sC2B-domains lack almost all residues involved in Ca^{2+} binding (304,305,315).

4.1 Role of phospholipids and Ca^{2+} in neurotransmitter secretion

The primary mode of communication in the nervous system is associated with the release of neurotransmitter by regulated exocytosis. Neurotransmitters are released from small vesicles that undergo many rounds of fusion and recycling at presynaptic termini (332,333). Prior to neurotransmitter release, these synaptic vesicles fill with transmitter by a process governed by specific transport proteins. Acidic phospholipids and Ca^{2+} ions play a crucial role in the process of neurotransmitter secretion. Increase in the acidic phospholipid (e.g. PS) content of synthetic liposomes increased their fusibility (332,334,335).

4.2 Calcium sensory proteins involved in neurotransmitter release

Calcium is thought to trigger vesicular fusion and neurotransmitter secretion by binding to Ca^{2+}-sensory proteins. Although many Ca^{2+} binding proteins have been identified that could potentially serve as synaptic Ca^{2+} sensors, strong evidence points to the specificity of vesicle fusion being

provided by a complex formation of the synaptic vesicle proteins VAMP (336), syntaxin (337), SNAP-25 (338), and synaptotagmin I; the latter being the protein that directly senses Ca^{2+} influx (332,333). On binding Ca^{2+}, synaptotagmin I binds the other proteins forming a complex referred to as the SNARE (soluble N-ethylmaleimide-sensitive factor attachment protein receptor) complex, and triggers fusion of synaptic vesicles. Ca^{2+}-regulated secretion is also a feature of endocrine and exocrine cells (336).

5.1 Three-dimensional structure of the sC2-domain

The three-dimensional structures of some sC2-domains have been determined (Figure 4.4) (321,339-341). The sC2-domain is a compact region composed of almost identical eight β-strands forming two β-sheets (297,327). Three loops are present on the top of the domain, and four loops are on the bottom. While the β-strands are highly conserved, the loops have a more variable sequence which suggests that they confer sC2-domains binding specificities to target molecules. All sC2B-domains contain a bottom α-helix between the 7th and 8th -strands that is absent from sC2A-domains (297).

5.1.1 Two sC2-domain topologies exist

SC2-domains form two different topological folds, observed from the crystal structures of synaptotagmin I and phosphoinositide-specific phospholipase Cδ1, termed "topology I" and "topology II" respectively (297). The key difference between the two topologies is that the first strand of

Figure 4.4 **Three-dimensional structure of the sC2-domains.**

Two ribbon diagrams of the sC2-domain from synaptotagmin I (A) and phospholipase C-δ1 (B). The diagrams illustrate the type I topology (A) and the type II topology (B) of the sC2-domain. The N and C termini, the Ca^{2+}-binding loops, and the Ca^{2+} ions are also shown.

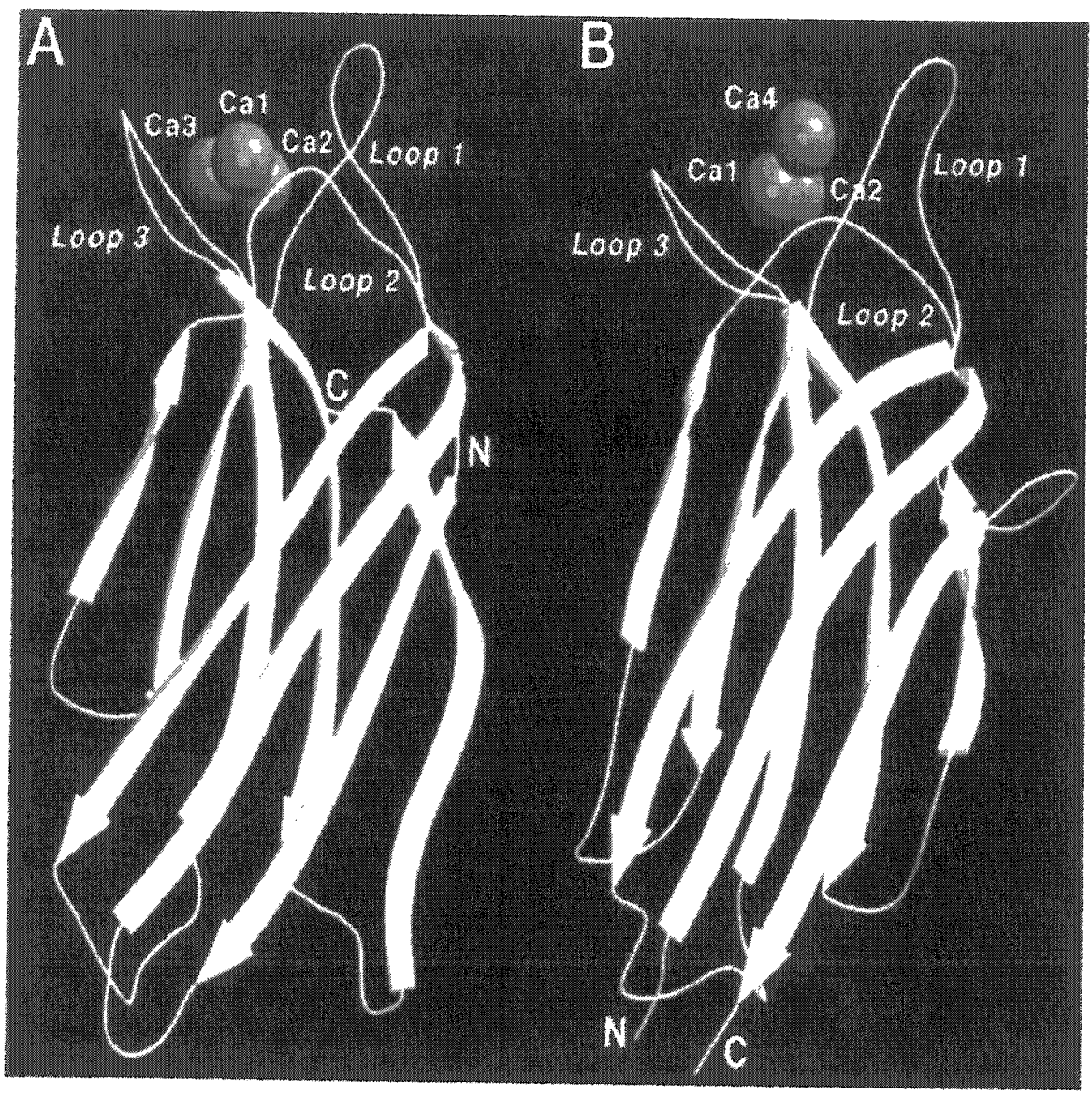

Griffin JH, 2000

topology I occupies the same structural position as the eighth β-strand of topology II, which shifts the order of homologous strands in the primary structure (297). Interestingly, two of the three sC2-domains in Unc-13, the protein with the high homology to P135, are predicted to utilize the type II topology, whereas the third uses the type I topology (297,304). A list of some of the sC2-domain containing proteins with their predicted topologies is shown in Figure 4.1.

6.1 sC2-domains and Ca^{2+}-binding

The Ca^{2+}-binding sites in the sC2-domain are surrounded by a ring of positive charges designed to concentrate multiple Ca^{2+} ions in a small region in the area of the positive charges (297,342). Based on the three-dimensional structure of the synaptotagmin first sC2-domain (Figure 4.4) (339), it has been proposed that the interaction between the domain and its Ca^{2+} ligand occurs via a "SC2 key" (327,343). This key consists of a ~70-residue core (including the CaLB region) that folds into a four-stranded β-sheet, forming a cavity lined with five aspartate (or in some cases aspargine or glutamate) residues, the Ca^{2+}-binding site (Figure 4.4) (304). Five aspartate side chains, a serine side chain, and three carbonyl groups (304) form the Ca^{2+}-binding sites. Among these, the aspartate residues are the most conserved among sC2-domains. Loops 1 and 3 of the sC2A-domain contain all the three Ca^{2+}-binding sites (Ca1, Ca2, and Ca3) (Figure 4.4). Ca^{2+} ions bind to all three sites in order to facilitate phospholipid binding.

6.2 Function

Calcium stabilizes the structure of sC2-domain, but does not mediate a large structural change in the isolated sC2-domains (297). In addition, several studies have shown that the binding energy of the sC2A-domain and Ca^{2+} ions results in a local change in the net electrostatic potential of the domain and only induces a minor conformational change in the top part of the domain. This binding mechanism, referred to as the "electrostatic switch", contributes to target specificity, which includes phospholipid specificity, and does not appear to be mediated by the minor conformation change observed in the sC2B-domain (304).

NMR studies with synaptotagmin sC2-domains indicate that the Ca^{2+}-binding region is flexible in the absence of Ca^{2+} and is stabilized after Ca^{2+} binding. Structural stabilization by Ca^{2+} binding is consistent with the observations that Ca^{2+} causes a large change in denaturation temperature (345,346) and increases the resistance of the synaptotagmin I sC2A-domain against proteolysis. Similar conclusions were made with the PLC1 and PKCs sC2-domains (340,347).

6.3 sC2-domains and Phospholipid-binding

Membrane binding of proteins with sC2-domains exhibits phospholipid specificity, and requires a divalent, rather than monovalent cation. Most sC2-

domains bind to phospholipid as a function of Ca^{2+}. The order of preference is $Ca^{2+}>Sr^{2+}>Ba^{2+}$ (297,348,349). The relative affinities of Mg^{2+}, Na^{+}, and K^{+} has not been determined since these ions failed to promote phospholipid binding (349). Most Ca^{2+}-dependent membrane-binding sC2-domains prefer negatively charged over zwitterionic membranes. PKC sC2- and PLC sC2-domains favor PS membranes, while, some sC2-domains of proteins such as PLA_2 strongly favor PC membranes (297,327).

6.4 Mechanisms of sC2-domain phospholipid-binding

The consensus regarding the synaptotagmin sC2A-domain binding to aPL by Ca^{2+} is that the interaction is primarily electrostatic and is stabilized by hydrophobic interactions (331). As a result, Ca^{2+}-dependent phospholipid-binding proceeds by a multimodal mechanism that mirrors the amphipathic nature of the phospholipid bilayer. Thus, Ca^{2+} likely shields negatively charged residues on the phospholipid binding site and facilitates binding to negatively charged phospholipids (304). This is supported by observations that phospholipid-binding can be completely abolished by moderate increases in NaCl concentration (>0.3 mol/l) (342,350). Also, substitution of one of the positively charged residues surrounding the Ca^{2+}-binding site lowers the apparent Ca^{2+} affinity of the sC2A-domain (320,331). However, fluorescence measurements have revealed that the exposed hydrophobic residues at the tip of the sC2A-domain insert into the phospholipid bilayer, suggesting that they could also contribute to Ca^{2}+-dependent phospholipid binding (351).

7.1 Objectives

P135 was accidentally discovered due to unexpected amplicon homology between interleukin 11 and the C2-domain of synaptotagmin. Since we have a general interest in aPL-binding proteins, the following project was undertaken in order to identify the function of p135 and understand the role the p135-sC2-domains play in aPL binding. Hence, the main focus was to identify cells that express the p135 protein and localize the protein in some of these cells. The question of whether sC2-domains are functionally active in p135 will also be addressed.

The following specific aims will be addressed:

(a) Clone and sequence the mRNA for the P135 gene.

(b) Evaluate the P135 mRNA and protein expression in human tissues and in cancer cell lines.

(c) Localize P135 in cells.

(d) Develop a recombinant expression system for P135 that can be used to study P135 function.

(e) Determine whether the P135 sC2-domains bind phospholipid, and if so, is the binding anionic phospholipid specific and Ca^{2+}-dependent.

EXPERIMENTAL PROCDURES

Chemicals and reagents. HEPES, EDTA, PS (phosphatidylserine), PC phosphatidylcholine, bovine serum albumin, 4',6-Diamidino-2-phenylinodole-dihydrochloride (DAPI), paraformaldehyde (Sigma), Tween 20 (Fisher), and a chemiluminescent detection system (ECL, Amersham Pharmacia Biotech), were obtained commercially. Cy3 and peroxidase conjugated donkey anti-mouse were obtained from Jackson Immunoresearch, and gluteraldehyde were from Merck. Phytohemagglutinin (PHA) was purchased from DIFCO. After immunological staining, the coverslips were mounted on glass slides with mounting media containing 0.1% phenylene diamine in 50% glycerol-PBS (Na_2HPO_4 10.14 mM, KH_2PO_4 1.47 mM, NaCl 136.89 mM, KCl 2.68 mM). Multiple tissue Northern blots were commercially available from Clontech. Murine Moloney leukemia virus (M-MLV) reverse transcriptase was purchased from Gibco-BRL.

Proteins and antibodies. Monoclonal antibodies (mAb) specific for p135, were produced by Dr. R. Lemieux (Hema-Quebec), using as immunogen recombinant p135 produced in the baculovirus system and purified by electroelution. Polyclonal rabbit anti-human p135 was produced at the University of Ottawa by immunizing rabbits with the p135 protein. Peroxidase-conjugated goat anti-mouse IgG (Jackson ImmunoResearch Inc.), peroxidase-conjugated goat anti-rabbit IgG (Promega) were commercially available.

Cells and cell lines. The human Jurkat leukemia and Hut T cell lines were obtained from the American Type Culture Collection (ATCC, Rockville, MD). Daudi, NTERA-2, HS68, RS4:11, HS68, LBRM-33, MEG-01, HFF, HCN-2, NCI-H460, Jurkat, and DU4475 were also from ATCC. Cells were maintained in RPMI 1640 medium (Gibco-BRL) supplemented with 10% (v/v) fetal bovine serum (Sigma), 2 mM L-glutamine (Life Technologies) and 10 μM gentamycin (Life Technologies, Inc). Cells were grown in a humidified incubator containing 5% CO2 at 37 °C. Fresh human resting T cells were obtained from normal healthy peripheral blood buffy coats (collected on site), and were purified by negative selection after passage over nylon wool (Robbins Scientific, Sunnyvale, CA) columns followed by passage over a CD4 negative selection column (R&D Systems, Minneapolis, MN). Activated T cells were prepared by stimulation with PHA (10 μg/ml; Difco) for 2 days. SF9 insect cells were maintained in TNM-FH medium supplemented with 10% (v/v) FBS and 1% penicillin/streptomycin in a humidified incubator at 27 °C.

Reverse transcription-polymerase chain reaction of p135. Cells were washed with ice-cold phosphate buffer saline (PBS) and pelleted. Then cells were lysed, and total RNA was prepared by means of RNeasy kit (Qiagen) and incubated with I unit DNA DNase for 30 minutes at 37 °C to eliminate genomic DNA. Reverse transcription was carried out using 1 μg total RNA, 25 ng of random hexamer plus oligo(dt) primers, and 100 unit M-MLV reverse transcriptase.

Primer pairs, originally designed to amplify IL11, were as follows (numbers refer to the human IL11 cDNA sequence):

p415 (sense primer), 5'-GCTGACAAGGCTGCGAGCGG;

p877 (anti-sense primer), 5'-CCCAGCCCTCACGGAAGGAC.

PCR was performed with 1 unit Taq-polymerase (Perkin-Elmer). Reactions were carried out for 30 cycles consisting of 1 minute denaturing at 94°C, 30 seconds annealing at 62°C, and 2 minutes elongation at 72°C. The products were separated by electrophoresis in 1.5% agarose and visualized with ethidium bromide. The DNA (500 ng) was sequenced in an Applied Biosystems 373 DNA sequencer (ABI 373) by the Dye termination method using the Taq DyeDeoxy Terminator Cycle Sequencing Kit (Applied Biosystems).

cDNA and genomic cloning. Complementary DNA was prepared from 5 μg of poly(A)+ mRNA isolated from human HEL cells and introduced into the Lambda Zap II vector Kit (Stratagene), and packaged using the Gigapack II Packaging Extract Kit (Stratagene). Approximately 5 X 10^4 recombinants were screened using p415/p877 ^{32}p-labelled RT-PCR amplicon. Several positive clones were isolated and the DNA inserts were sequenced as described above. To determine the 5' and 3' termini of p135 cDNA, rapid amplification of cDNA ends (RACE) cloning was performed with the RACE cDNA amplification Kit (Clontech, Palo Alto, CA). Full-length p135 cDNAs were obtained by restriction analysis and sequential ligation of well defined cDNA clones. These inserts were cloned into

the PCR II vector using the TA cloning kit (Invitrogen, Carlsbad, CA), and then subcloned into the Bam H1/Pst1 site in PVL1392 vector (Pharminogen). A genomic high-molecular-weight library was constructed using the bacteriophage P1 cloning system and screened for p135 using p415/p877 primers. Two clones (# 800; 85 Kb, and #801; 75 Kb) were isolated (Genome Systems, Inc.) and partially sequenced at intron/exon junctions. Conditions for PCR amplification of genomic sequences were as described above.

Recombinant protein expression and anti p135 antibody production. The baculovirus expression system (Baculogold kit; Pharmingen) was employed to express the p135 gene. A volume containing 500 ng of the recombinant pVL1393 transfection vector with the complete open reading frame of p135 cDNA was used in the cotransfection step according to protocols provided by the supplier. After three rounds of viral amplification in SF9 insect cells, the insect cells were harvested, and nuclear and cytoplasmic fractions of cell lysate were prepared. N-terminal sequencing of the p135 fragment after reducing SDS-PAGE was conducted as described in chapter 2.

Mouse monoclonal antibodies were raised against the p135 protein. Mouse inoculation was performed with the generous assistance of Dr. Lemieux and his team (Hema Quebec laboratories, Quebec City). Mice were injected intraperitoneally with 100 μg of gel-purified recombinant human p135 protein in complete Freund's adjuvant and were boosted 3 weeks later with a second

injection of 50 μg of protein in complete Freund's adjuvant. One week after the first boost, antibody titers were determined by ELISA analysis of tail bleed samples with a biotinylated goat anti-mouse IgG antibody. The second boost was given 19 days after the first boost, and the spleen was harvested three days later. Colonies generated from fused mouse myeloma and spleen cells positive for the p135 protein were identified by ELISA analysis and subcloned until colonies from a single clone were obtained. Several clones were tested with Western blotting and were found to react specifically with the recombinant protein.

Chromosome mapping. Mapping of the p135 gene was performed by fluorescence in situ hybridization (FISH) to normal human lymphocyte chromosomes counterstained with PI and DAPI at the CGAT Human Genome FISH Mapping Resource Centre (Hospital for Sick Children, Toronto, ONT). In summary, a biotinylated probe (human genomic colony # 800) was detected with avidin-fluorescein isothiocyanate (FITC). Images of metaphase preparations were captured by a thermoelectrically cooled charge-coupled camera (Photometrics, Tucson, AZ).

Northern blot analysis. Total RNA was prepared from blood cells and tissue culture cells using RNAzol B method. RNA samples (5 μg) were electrophoresed in 0.8% agarose formaldehyde gels, transferred to nitrocellulose, and hybridized with a ^{32}P-labeled cDNA probe (amplified by p415/p877 primers). Human

multiple tissue (I and II), cancer cell line, and immune system northern blots were purchased from Clonetech (Palo Alto, CA), and were hybridized with the same probe. RNA products were visualized by autoradiography.

Western blot analysis. Protein samples were heated to 95 °C for 5 min in sample buffer (2% SDS, 2% 2-mercaptoethanol, 0.325 M Tris (pH 6.5), 10% glycerol and 0.001% bromophenol blue), subjected to SDS-PAGE (10% acrylamide), and stained with Coomassie Blue, or electrotransferred to polyvinylidene difluoride (PVDF; Immobilon-P, Millipore) as described in chapter 2. The PVDF membrane was blocked at 22 °C for 1 h in milk (5%), and protein was detected with anti-p135 monoclonal Ab and visualized using enhanced chemiluminescence (Amersham Corp.).

Flow cytometric analysis. PBL, cultured HEL, Jurkat, and SF9 cells were washed in freshly made PBS containing 0.1% BSA (wash solution), collected by centrifugation and resuspended in 4% paraformaldehyde for 10 min at RT. The cells were resuspended in PBS containing 0.2% Triton X-100, and incubated for 5 min, then collected again and blocked with 200 μl freshly made PBS containing 3% BSA and 0.2% Tween 20 for 1 h. Following this incubation, the cells were washed twice and incubated for 1 hour at 25 °C with purified anti-human p135 monoclonal antibody (2ug) in PBS containing 3% BSA and 0.2% Tween 20. The cells were washed three times and then stained with FITC-conjugated goat anti mouse secondary antibody (BD Pharminogen) for 1 hour at 25 °C in PBS

containing 3% BSA and 0.2% Tween 20. Antibodies used in phenotype analysis include PE-conjugated anti-CD4 and anti-CD19, and PE-conjugated anti-CD8; all were purchased from BD Pharminogen. Samples were characterized on a FACS scan flow cytometer and the data were analyzed using Cellquest software (Becton Dickinson).

Immunofluorescense microscopy. To observe the intracellular distribution of p135, Jurkat and HEL cells were adhered to poly-L-lysine coated glass coverslips, and simultaneously fixed and permeabilized using a solution containing 4 % paraformaldehyde, 0.25% gluteraldehyde, and 0.2% TritonX-100 in PBS for 10 minutes at RT. Total p135 was detected in the fixed/permeabilized cells by one of two anti-p135 mAbs (1.07 µg/mL) raised against full-length recombinant human p135 for 1 hour at RT. The p135 antibodies were detected by incubating Cy3 conjugated donkey anti-mouse IgG (1.4 µg/mL, Jackson Immunoresearch) with the cells for 1 hour at RT. Nuclei were detected by staining the DNA with DAPI for 5 minutes at RT.

Assay for the binding of p135 to phospholipd. Phospholipid-coated microtiter wells were prepared as described in chapter 2. Bound protein was eluted with 25 µl of SDS-PAGE sample buffer/well, heated at 95°C for 5 minutes and subjected to 8% SDS-PAGE. Alternatively, PL binding was quantified by liquid scintillation counting. To visualize PL-bound protein, gels were either stained with Coomassie Blue, or electrotransferred to PVDF membrane. The PVDF

membrane was blocked at 22 °C for 1 h in milk (5%), and PL-bound protein was detected by Western analysis using anti-p135 mAb and enhanced chemiluminescence (Amersham Corp.). Alternatively, the gels were air-dried and exposed to film.

RESULTS

Identification of p135 mRNA. A primer-pair p415/p877 designed to amplify a region in IL11 cDNA (462-bp fragment) from mammalian HEL cell lines consistently amplified an unexpected 250-bp fragment (Figure 4.5). Interestingly, amplification of cDNA from PBL, isolated from blood of healthy blood donors, with this set of primers revealed two amplicons that differed by approximately 30 bp. However, the level of mRNA expression in PBL was lower than that of HEL cells. When the same set of primers were used with the cDNA from endothelial cells and stromal cells cDNA, we did not observe any amplified products, indicating that this mRNA is cell specific (Figure 4.5). Sequencing of the 250 bp fragment revealed no homology with any known sequences entered in the databases, indicating that the transcript was novel and interesting since it was selectively expressed in cells.

We also compared the digestion pattern of p135 DNA in 32 healthy blood donors. Genomic DNA was digested with Bam HI or Eco RI and examined by southern blotting with labeled PCR products (Figure 4.6). Under these conditions, the southern blots revealed that there was no difference in the digestion pattern between these donors indicating that, with these restriction endonucleases, there was no major detectable polymorphisms or rearrangements in the p135 gene between these healthy individuals. As can be seen, two distinct bands were detected by southern blotting following the digestion with each of the enzymes (Figure 4.6).

Figure 4.5. **Detection and isolation of p135 mRNA.**

RNA from peripheral blood leukocytes (PBL), stromal cells, human erythroleukemia cells, and endothelial cells was isolated and subjected to RT PCR with IL11 primers. PCR product DNA was electrophoresed on 1% agarose gel and stained with ethidium bromide.

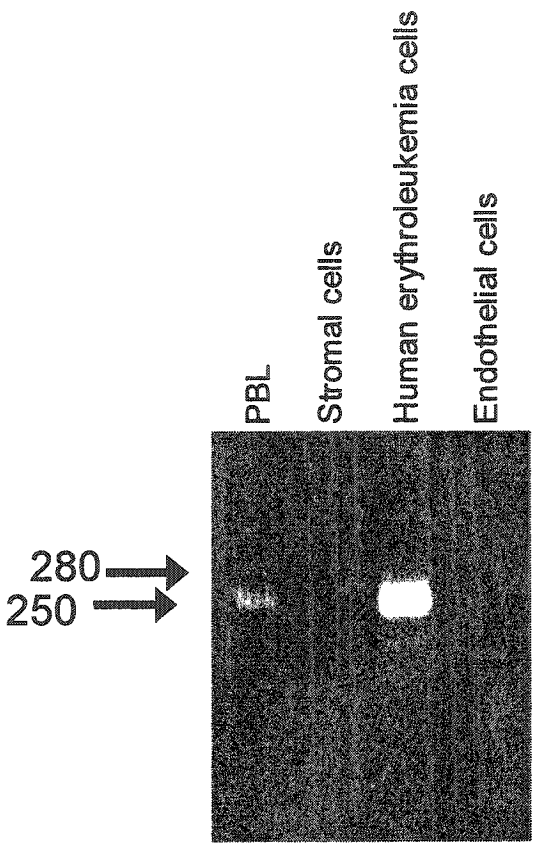
PBL
Stromal cells
Human erythroleukemia cells
Endothelial cells
280
250

Figure 4.6 **Detection of P135 DNA in human genomic DNA.**

Human genomic DNA (5 μg) from leukocytes of 32 healthy blood donors was extracted and digested with Bam HI (A) or Eco RI (B) at 37 °C for 6 hrs. The digested DNA was run on 1% agarose gels and transferred to nylon membranes. The membranes were then hybridized with ^{32}P -labeled p135 DNA and reactive bands were visualized by autoradiography.

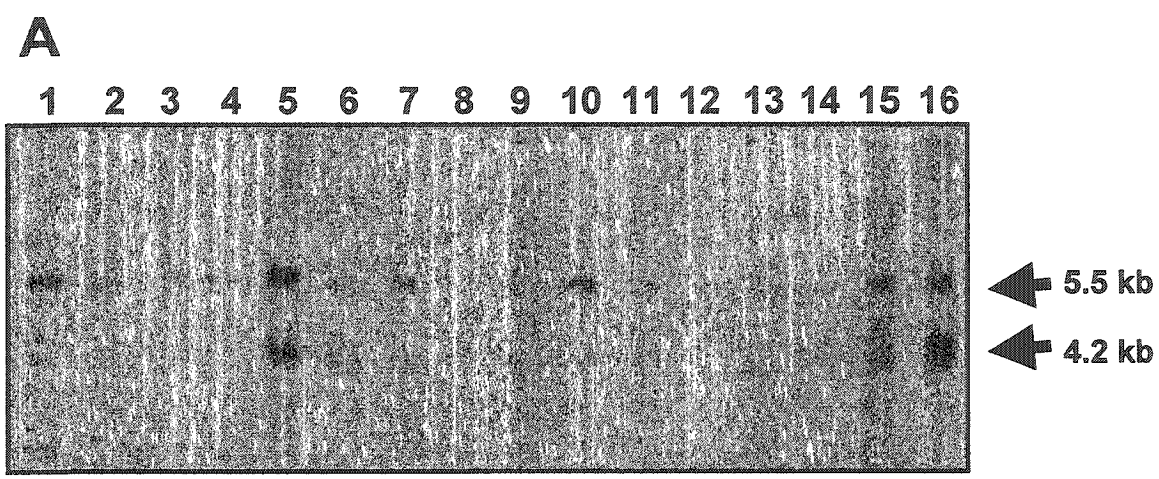
A
1 2 3 4 5 6 7 8 9 10 11 12 13 14 15 16
5.5 kb
4.2 kb

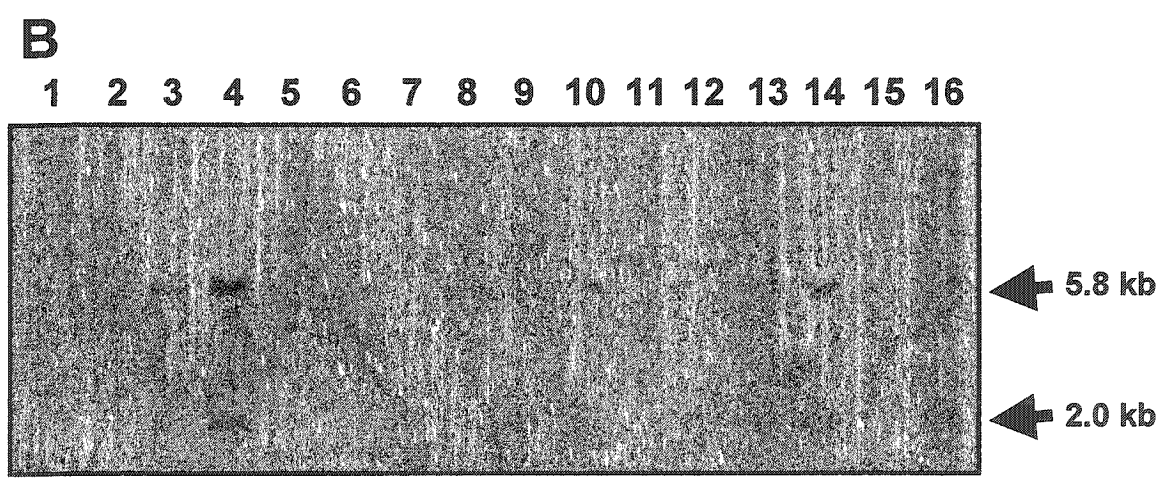
B
1 2 3 4 5 6 7 8 9 10 11 12 13 14 15 16
5.8 kb
2.0 kb

To identify the human chromosome that contains the p135 gene, two approaches were undertaken. The first approach was based on the hybridization of labeled p135 probe to a somatic cell hybrid panel consisting of 24 hybrid lanes representing human chromosomes 1 through 22, X and Y, and two lambda/Hind III marker lanes. This panel mapped the p135 gene to human chromosome 17 (Figure 4.7). As can be seen, three new bands (1.1, 3.2, and 5.5 kb) specific for p135 are detected in lane 11 (chromosome 17). The other bands that can be seen on the gel in Figure 4.7 originate from hamster (lanes 1 to 9, and 12, 13) or mouse (lanes 10, 11, 14, and 15).

In the second approach, mapping of the p135 gene was performed at the CGAT human Genome FISH Mapping Resource Centre (Hospital for Sick Children, Toronto, ONT) by fluorescence in situ hybridization (FISH) to normal human lymphocyte chromosomes counterstained with PI and DAPI. This was performed using biotinylated p135 amplicon obtained from the high molecular weight bacteriophage clone (P1 clone # 800). Figure 4.8 A clearly shows distinct human chromosomes at the metaphase stage. Also, p135-specific staining is seen in two chromosomes that are identical in size and appearance. The assignment of this genomic probe was determined by the analysis of 20 from normal lymphocyte chromosomes at metaphase. Based on their size and banding pattern, the gene was mapped to chromosome number 17 (Hospital for Sick Children, Toronto, ONT). Also, fluorescence can be seen on both

Figure 4.7 **Somatic cell hybrid panel identifies the p135 gene to human chromosome 17.**

Human/rodent hybrid cell line DNA with known individual human chromosomes (Chromosome 1 to 22, and the X and Y chromosomes) has been cleaved with Hind III and transferred to membrane. The membrane was hybridized with P^{32}-labelled P135 DNA and exposed to autoradiographic film for 48 hrs and DNA was visualized. Lanes 1 to 16 contain cell line DNA from chromosomes 7 to 22. Lanes 17 and 18 contain DNA from chromosomes X and Y respectively. The arrows indicate the three p135 Hind III DNA fragments present on chromosome 17.

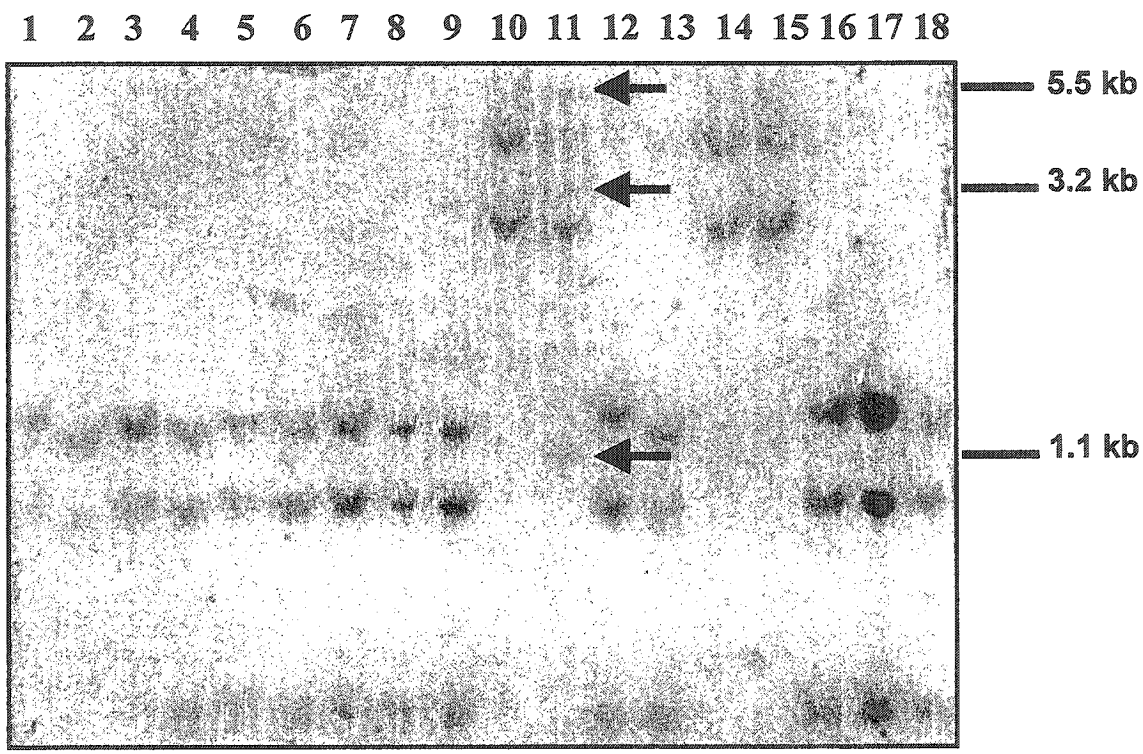
1 2 3 4 5 6 7 8 9 10 11 12 13 14 15 16 17 18
5.5 kb
3.2 kb
1.1 kb

Figure 4.8 **Mapping of p135 gene to human chromosome 17q25.**

(A) The p135 gene was mapped by fluorescence in situ hybridization (FISH) to metaphase preparations of normal human lymphocytes chromosomes counterstained with PI and DAPI using a biotinylated 75 kb p135-specific probe. The probe was detected with avidin-FITC. One stained chromosome is shown in B. (C) The relative positions of previously identified chromosome regions and their numbering is shown. Arrows indicate the location of the stained-chromosome region.

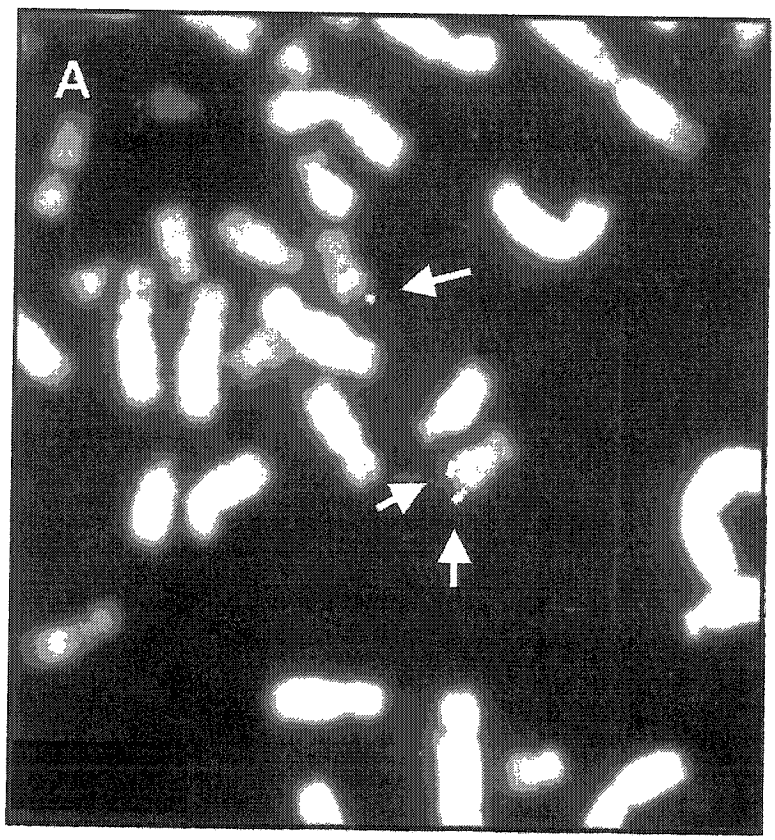
A

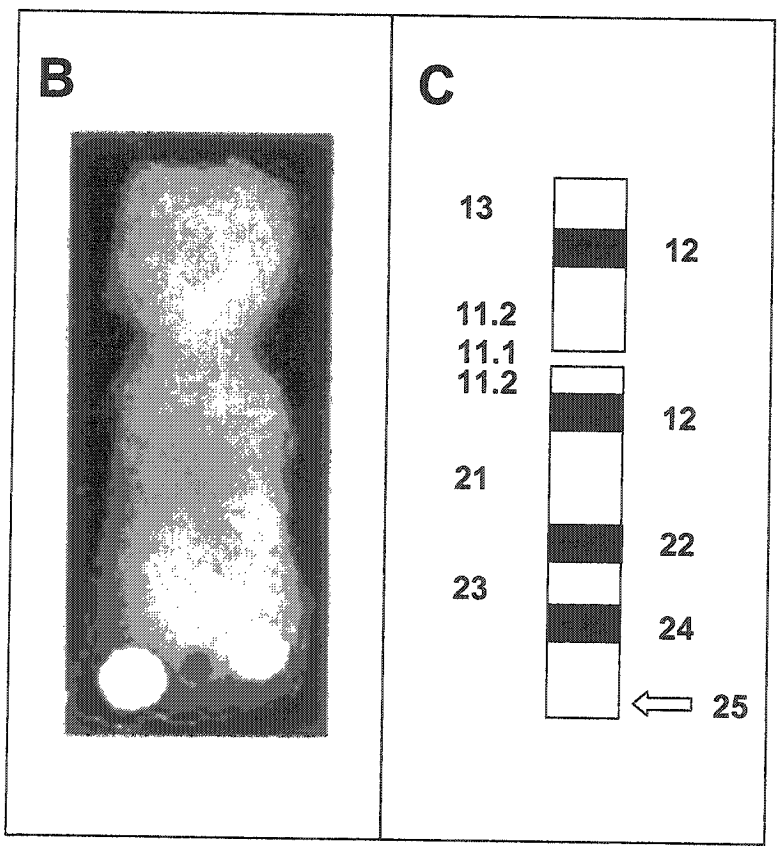
B
C
13
12
11.2
11.1
11.2
12
21
22
23
24
25

chromatids of chromosome 17 representing both p135 gene alleles (Figure 4.8 A and B). As can be seen in Figure 4.8 C, the gene was mapped to the region 17q25 (CGAT FISH Mapping Center). This region is in close proximity to the BCRA1 gene, that has been suggested to correlate to the early onset of breast cancer (352).

Identification of two forms of p135 mRNA. To isolate the entire cDNA, a HEL cDNA library was constructed and screened with a labeled 250-bp PCR probe. A complete cDNA construct was generated by restriction analysis and sequential ligation of well defined cDNA clones. Multiple clones were isolated and analyzed. Amplification of these clones with p415/p877 identified two p135 cDNA isoforms in HEL cells that differ by ~30 bp (Figure 4.9), consistent with PCR results from PBL (Figure 4.5). Approximately one in every five clones was found to be the larger cDNA isoform (Figure 4.9A). The apparent difference in size between the two fragments was confirmed when DNA from clones #2 and #6 were digested with several restriction endonucleases. As seen in Figures 4.9A and 4.9B, Sma I digestion revealed two different digestion patterns confirming that at least two isoforms of the p135 gene exist. Using clone #2, Sma I digestion resulted in 3 bands (6000, 950, and 900 bp in size), whereas clone #6 gave rise to 4 bands (6000, 850, 530, and 420 bp in size).

Two yeast genomic clones (P1 clones) from a human megaYAC screening library were identified and isolated using p135 gene-specific PCR

Figure 4.9 **DNA digestion of plaques with restriction endonucleases.**

A, A cDNA library was constructed from a human erythroleukemia cell line, and individual plaques (lanes 1 – 12) were amplified with IL11 primers. In lane 13, genomic DNA from HEL cell line was subjected to amplification with the same set of primers. B and C, DNA from plaques #2 and #6 respectively (from A) was isolated and 2 μg of each plaque was digested with different restriction enzymes as indicated at 37 °C for 6 hr. DNA was separated on 0.8% agarose and visualized with ethidium bromide. The mobility of the 1 kb molecular weight marker (MW) is also shown.

A

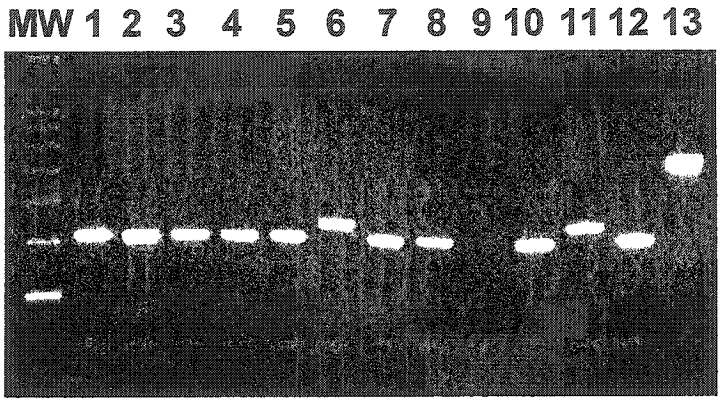
MW 1 2 3 4 5 6 7 8 9 10 11 12 13

B

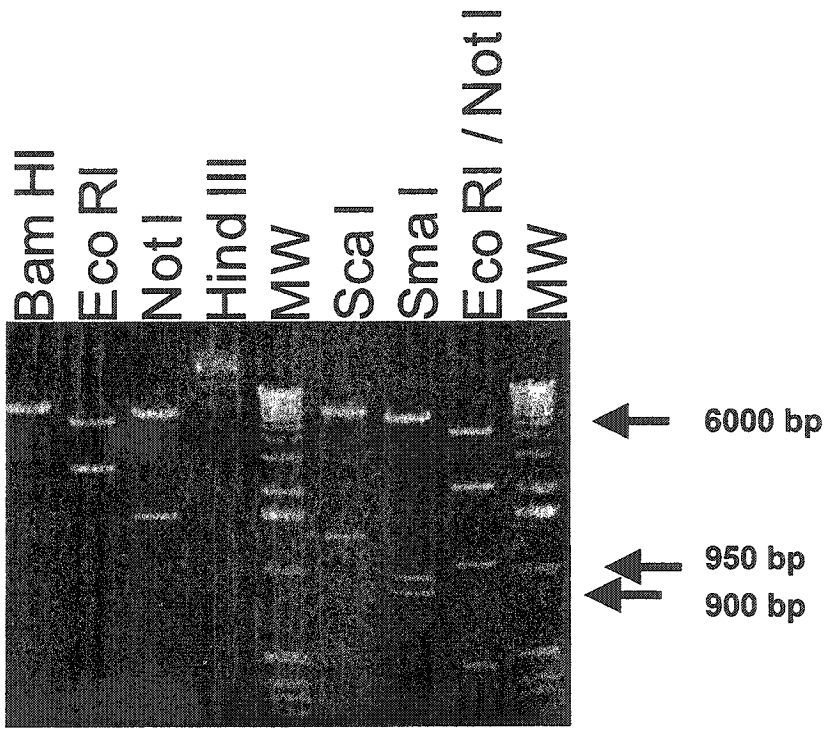
Bam HI
Eco RI
Not I
Hind III
MW
Sca I
Sma I
Eco RI / Not I
MW
6000 bp
950 bp
900 bp

C

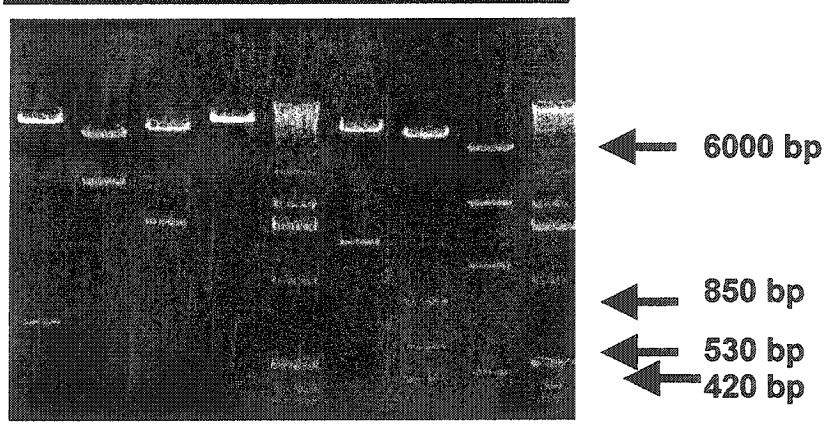
6000 bp
850 bp
530 bp
420 bp

amplicons (Genome Systems, Inc.). Restriction analysis revealed that the average insert size of each of the two clones (named p800 and p801) was 70 to 100 kb (data not shown). PCR amplification and sequencing of specific regions in the high-molecular-weight P1 clones at potential intron/exon junctions identified that the p135 gene encompasses 9 exons and 10 introns as shown in Figure 4.10A. Furthermore, sequencing of the larger cDNA isoform revealed that the entire sequence is identical to p135 except for an insertion sequence located in putative exon 5 which was identified to be 38 bp in length (Figure 4.10 B). Interestingly, this insertion generates a frame shift in the primary sequence leading to a TGA stop codon at amino acid 342 . This predicts a protein of 38 kDa in size (Figure 4.10 B).

Structural analysis of p135 protein. Sequencing of several overlapping cDNA sequences showed that the complete open reading frame is 4130 bp in length, and encodes 1,232 amino acids (Figure 4.11). A protein of 135kDa is suggested from the derived sequence.

Structural analysis of the p135 protein primary sequence using searches of the protein databases with several alignment algorithms including the point accepted mutation and blossom 60 scoring matrices, did not reveal any identical protein. However, it was possible to identify several putative signal and regulatory sequences (Figures 4.11 and 4.12). These include a C-terminal nuclear localization sequence, and a C-terminal hydrophobic sequence. In

Figure 4.10 **Intron/exon structure of the p135 gene.**

The exon content of the p135 gene is based on the consensus intron exon splice sequence and PCR-product DNA sequencing from cDNA and genomic DNA. The relative location of the TGA stop codon mutation is shown in B. The sizes of predicted intact p135 protein (A) and the truncated p135 protein (B) are shown by the black arrows.

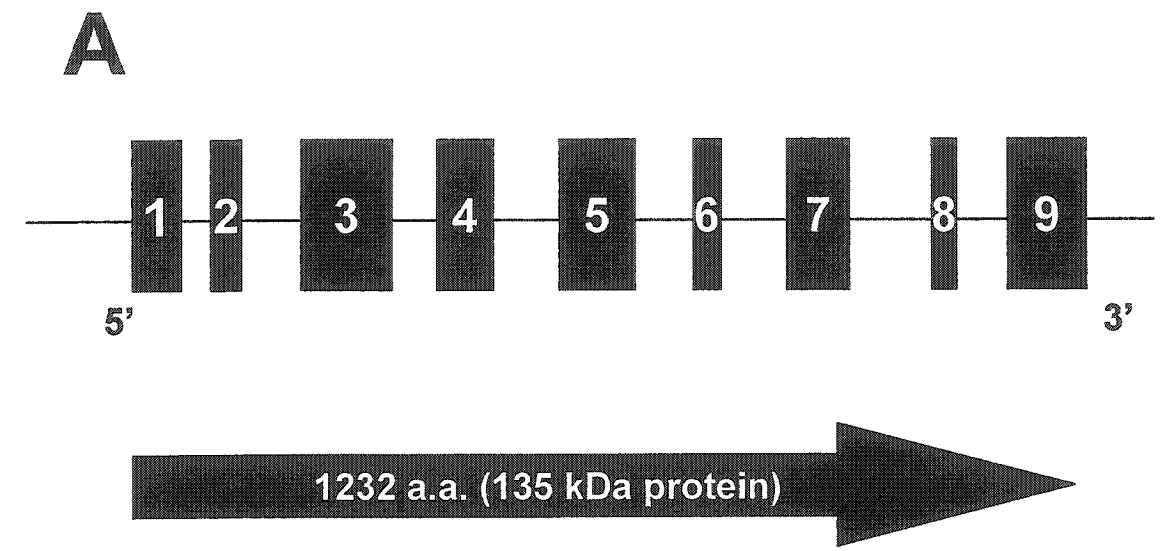
A
1
2
3
4
5
6
7
8
9
5'
3'
1232 a.a. (135 kDa protein)

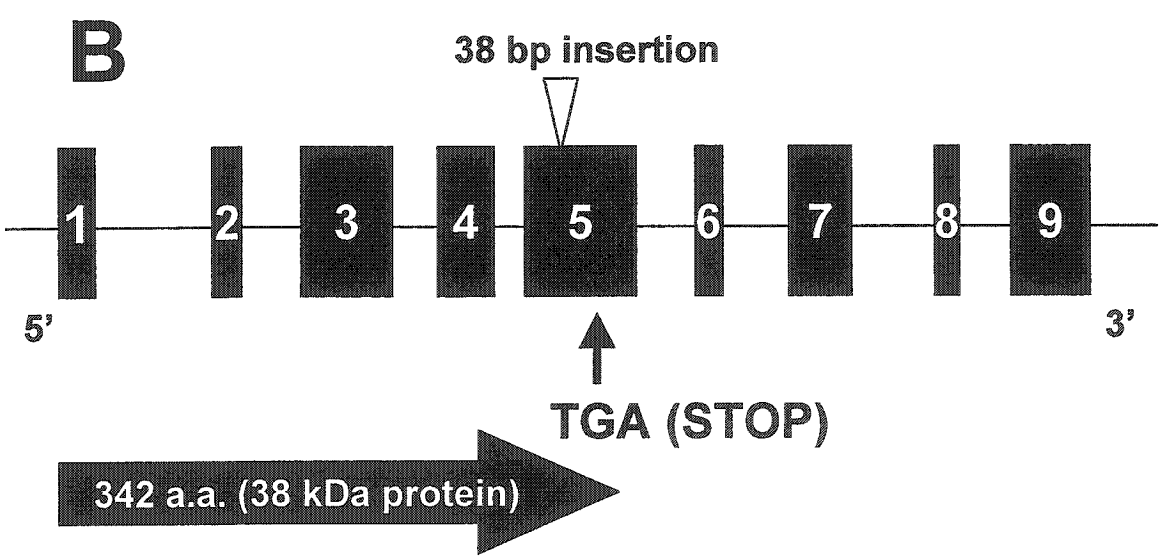
B
38 bp insertion
1
2
3
4
5
6
7
8
9
5'
3'
TGA (STOP)
342 a.a. (38 kDa protein)

Figure 4.11 **Predicted amino acid sequence from the p135 cDNA.**

Conceptual translation of the complete p135 open reading frame based on the nucleotide sequence assembled from several overlapping cDNA clones is presented in the one letter amino acid code. The two sC2 domain sequences are underlined. The nuclear targeting (NT) sequence is boxed with white background, and the hydrophobic region (HR) sequence is boxed with black background. The open arrow indicated the location of the DNA insertion, and the star indicates the location of the TGA stop codon generated due to the insertion.

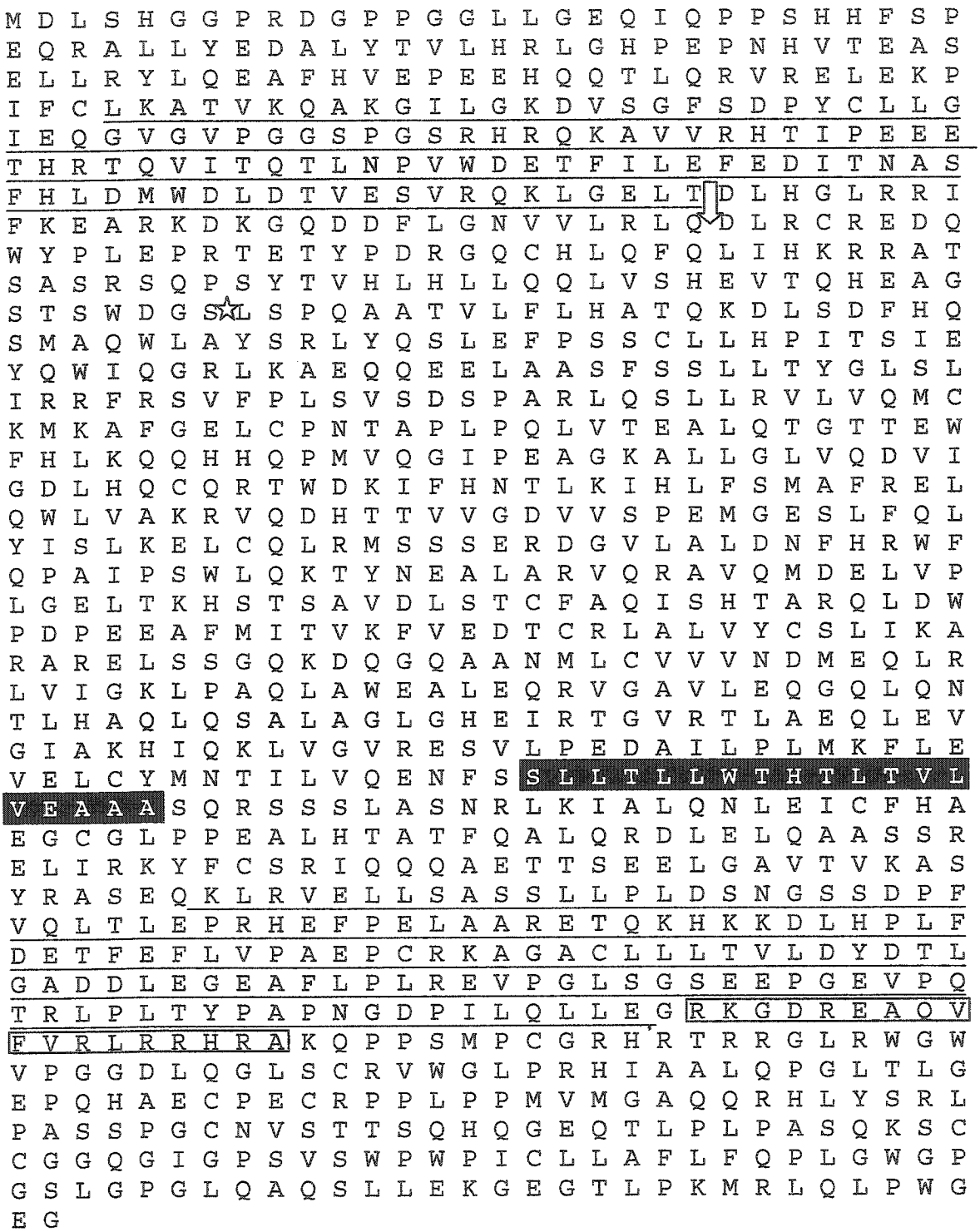
M D L S H G G P R D G P P G G L L G E Q I Q P P S H H F S P
E Q R A L L Y E D A L Y T V L H R L G H P E P N H V T E A S
E L L R Y L Q E A F H V E P E E H Q Q T L Q R V R E L E K P
I F C L K A T V K Q A K G I L G K D V S G F S D P Y C L L G
I E Q G V G V P G G S P G S R H R Q K A V V R H T I P E E E
T H R T Q V I T Q T L N P V W D E T F I L E F E D I T N A S
F H L D M W D L D T V E S V R Q K L G E L T D L H G L R R I
F K E A R K D K G Q D D F L G N V V L R L Q D L R C R E D Q
W Y P L E P R T E T Y P D R G Q C H L Q F Q L I H K R R A T
S A S R S Q P S Y T V H L H L L Q Q L V S H E V T Q H E A G
S T S W D G S L S P Q A A T V L F L H A T Q K D L S D F H Q
S M A Q W L A Y S R L Y Q S L E F P S S C L L H P I T S I E
Y Q W I Q G R L K A E Q Q E E L A A S F S S L L T Y G L S L
I R R F R S V F P L S V S D S P A R L Q S L L R V L V Q M C
K M K A F G E L C P N T A P L P Q L V T E A L Q T G T T E W
F H L K Q Q H H Q P M V Q G I P E A G K A L L G L V Q D V I
G D L H Q C Q R T W D K I F H N T L K I H L F S M A F R E L
Q W L V A K R V Q D H T T V V G D V V S P E M G E S L F Q L
Y I S L K E L C Q L R M S S S E R D G V L A L D N F H R W F
Q P A I P S W L Q K T Y N E A L A R V Q R A V Q M D E L V P
L G E L T K H S T S A V D L S T C F A Q I S H T A R Q L D W
P D P E E A F M I T V K F V E D T C R L A L V Y C S L I K A
R A R E L S S G Q K D Q G Q A A N M L C V V V N D M E Q L R
L V I G K L P A Q L A W E A L E Q R V G A V L E Q G Q L Q N
T L H A Q L Q S A L A G L G H E I R T G V R T L A E Q L E V
G I A K H I Q K L V G V R E S V L P E D A I L P L M K F L E
V E L C Y M N T I L V Q E N F S S L L T L L W T H T L T V L
V E A A A S Q R S S S L A S N R L K I A L Q N L E I C F H A
E G C G L P P E A L H T A T F Q A L Q R D L E L Q A A S S R
E L I R K Y F C S R I Q Q Q A E T T S E E L G A V T V K A S
Y R A S E Q K L R V E L L S A S S L L P L D S N G S S D P F
V Q L T L E P R H E F P E L A A R E T Q K H K K D L H P L F
D E T F E F L V P A E P C R K A G A C L L L T V L D Y D T L
G A D D L E G E A F L P L R E V P G L S G S E E P G E V P Q
T R L P L T Y P A P N G D P I L Q L L E G R K G D R E A Q V
F V R L R R H R A K Q P P S M P C G R H R T R R G L R W G W
V P G G D L Q G L S C R V W G L P R H I A A L Q P G L T L G
E P Q H A E C P E C R P P L P P M V M G A Q Q R H L Y S R L
P A S S P G C N V S T T S Q H Q G E Q T L P L P A S Q K S C
C G G Q G I G P S V S W P W P I C L L A F L F Q P L G W G P
G S L G P G L Q A Q S L L E K G E G T L P K M R L Q L P W G
E G

Figure 4.12 **Domain structure of the two forms of p135 protein.**

The predicted protein domain structure obtained from p135 cDNA sequences from HEL cells are shown. HR, hydrophobic region; NT, nuclear targeting region.

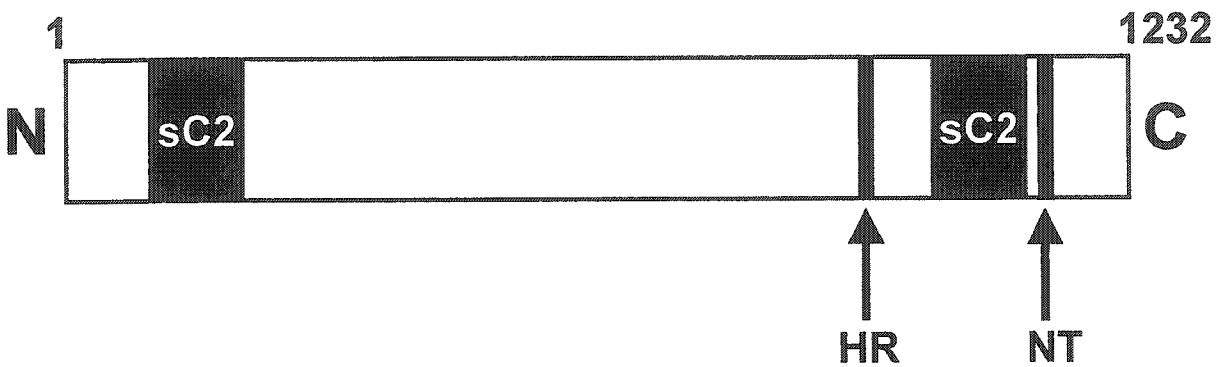
1
1232
N
sC2
sC2
C
HR
NT

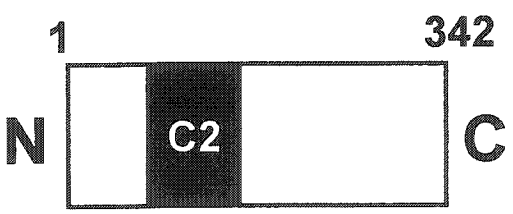
1
342
N
C2
C

addition, two regions were found with significant homology to the consensus sequence of the sC2-regulatory region (297).

Database searches revealed an overall 80% sequence similarity between the P135 cDNA sequence and Munc 13-4, a recently identified rat protein that is ubiquitously expressed, but predominantly in the lung (328). In addition to this sequence, our database searches showed high sequence homology with the sC2-domains in synaptotagmin I and to a lesser extent with that of rabphilin 3A and protein kinase C.

P135 mRNA expression in tissues and cells. To determine the tissue distribution of P135 mRNA in cells and tissues, Northern blot analysis was performed (Figures 4.13, 4.14) using P^{32}-labeled p135 as a probe. This probe recognized a single transcript of about ~4.2 kb. As seen in Figure 4.13, the p135 transcript was highly abundant in PBL, placenta, spleen and thymus, and to a lesser extent in the lung. Furthermore, very low levels of expression were detected in the liver, small intestine, ovary, and colon. Interestingly, in addition to the 4.2 kb transcript, a band of approximately 5.5 kb was detected in the ovary. Furthermore, this larger transcript was present in higher quantities in the ovary. The transcript was not detected in the heart, brain, skeletal muscle, kidney, pancreas, prostate, and testis (Figure 4.13). Since these blots contained equal amounts of mRNA, may suggest that the strongest expression of p135 is in the PBL followed by the thymus. This led us to suspect that the p135 protein might

Figure 4.13 **Expression of p135 mRNA in human tissues analyzed by RNA blotting.**

Membranes containing poly $(A)^+$-enriched RNA (3ug/lane) from the indicated tissues were hybridized with labeled probe from the coding region of p135 and exposed to film for 16 h. A and B are human multiple tissue northern blots I and II respectively. The blots were hybridized with P^{32}-labeled c-DNA probe from the coding region of p135 and exposed to film for 48 h. The arrows show the P135 mRNA.

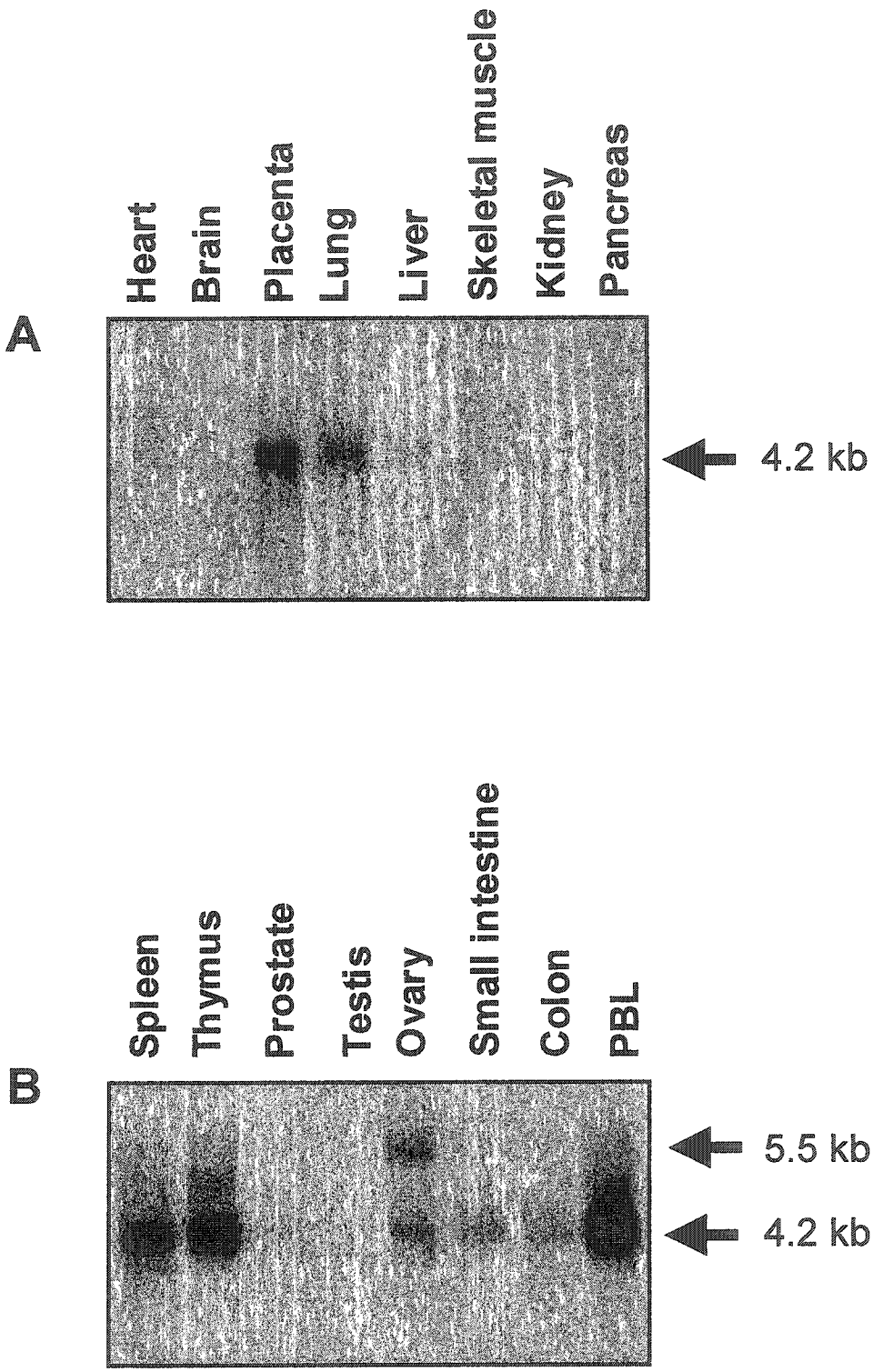
A
Heart
Brain
Placenta
Lung
Liver
Skeletal muscle
Kidney
Pancreas
4.2 kb
B
Spleen
Thymus
Prostate
Testis
Ovary
Small intestine
Colon
PBL
5.5 kb
4.2 kb

Figure 4.14 **Expression of p135 mRNA in tissues and cells analyzed by RNA blotting.**

Membranes containing poly $(A)^+$-enriched RNA (3ug/lane) from; A, human immune tissues; B, cancer cell lines; C, cells were hybridized with labeled probe from the coding region of p135 and exposed to film for 16 hr. The blot was hybridized P135-labeled c-DNA probe from the coding region of p135 and exposed to film for 48 hr. The arrow shows the P135 mRNA. HL-60, promyelocytic leukemia; S3, Hela cells; K-562, chronic myelogenous leukemia; MOLT-4, lymphoblastic leukemia; Raji, Burkitt's lymphoma; SW480, colorectal adenocarcinoma; A549, lung carcinoma; G361, melanoma; EC, endothelial cells; SC, stromal cells.

A
Spleen
Lymph node
Thymus
Appendix
PBL
Bone marrow
Fetal liver
4.2 kb
B
HL-60
S3
K-562
MOLT-4
Raj
SW480
A549
G361
4.2 kb
C
HEL
EC
EC + Thrombin
EC + PHA
B lymphocytes
T lymphocytes
T + PHA
SC
4.2 kb

be expressed in tissues of the immune system. To address this, a multiple tissue blot (Clonetech) that contains mRNAs from tissues from the immune system was probed with the p135 probe. As seen in Figure 4.14A, all the immune system tissues including spleen, lymph node, thymus, appendix, PBL, bone marrow, and liver showed the presence of the 4.2 kb transcript (Figure 4.14). The lowest level of expression was present in the appendix. These results may indicate that p135 functions in the immune system.

Since the gene was mapped to q25 of human chromosome 17; a locus correlating to various types of cancer, I evaluated several cancer cell lines (Figure 4.14B) for the presence of the p135 transcript. The results indicate strong expression of p135 mRNA in promyelocytic, lymphoblastic leukemias (HL-60, and MOLT-4), and adenocarcinoma (SW480) cell lines. Moderate expression was visible in chronic myelogenous leukemia (K-562) , and Burkitt's lymphoma (Raji). No expression of p135 transcript was detected in Hela cells (S3), lung carcinoma (A549), or melanoma (G361).

To determine the subset of cells in the PBL that may express the p135 transcript, T cells, B cells, and stromal cells were examined for p135 expression. The results indicate that p135 transcripts are mainly abundant in T cells and are present to a lesser extent in the B cells (Figure 4.14C). Following stimulation of cells with PHA, enhanced expression was observed in T cells, indicating the

p135 protein function may be altered during cell activation (Figure 4.14C). As seen, no p135 expression was found in stromal cells, cells of the bone marrow matrix, or endothelial cells. Furthermore, PHA and FIIa activation of endothelial cells did not induce p135 expression. HEL cells were also found to express the p135 transcript, supporting the initial identification of p135 transcript by RT-PCR.

Detection of p135 protein in cells. Western blot analysis was performed using antibodies raised against denatured recombinant p135 protein purified by SDS-electroelution. As seen in Figure 4.15A and 4.15B, the recombinant p135 protein was indeed expressed in transfected SF9 insect cells and was absent when the plasmid without the p135 insert was used for transfection (mock lane). The results were consistent with the conclusion that p135 is prevalent in leukocytes since a band (approximately 135 kDa) from PBL lysates reacted very clearly and strongly to mouse monoclonal # 41 (Figure 4.15B and C). In addition, the p135 protein was detected in HEL, and Jurkat hematopoetic cell lines, both being cell lines of the T-cell lineage. HUT, another hematopoetic cell line, also contained the p135 protein (results not shown). Non-hematopoetic cell lines such as the newborn fibroblasts (HS68) and embryonal carcinoma (NTERA-2) did not express the p135 protein (Figure 4.15B). This was not surprising since both cell lines lack markers for T and B cells. Interestingly, a smaller protein of approximately 30 kDa was also detected in PBL, but not in platelets, with monoclonal antibody # 18 (Figure 4.15C). This band may represent the other truncated isoform of p135 that was predicted to exist based on RT-PCR and

Figure 4.15 **Expression of the p135 protein in cells.**

Homogenates from untransfected SF9 cells (Mock), SF9 cells transfected with expression vector encoding full-length p135 (20 μg/lane; lysate), and from the indicated cells (20 μg/lane) were separated on 8% SDS-PAGE. The protein was detected with Coomassie blue staining (A), or transferred to PVDF and detected with mouse anti-p135 monoclonal antibody #41(B), or monoclonal antibody # 18 (C). The arrows indicate the location of the reactive bands. HEL, human erythroleukemia; HS68, newborn fibroblasts; Jurkat, T cells; NTERA-2, embryonal carcinoma; PBL, peripheral blood leukocytes.

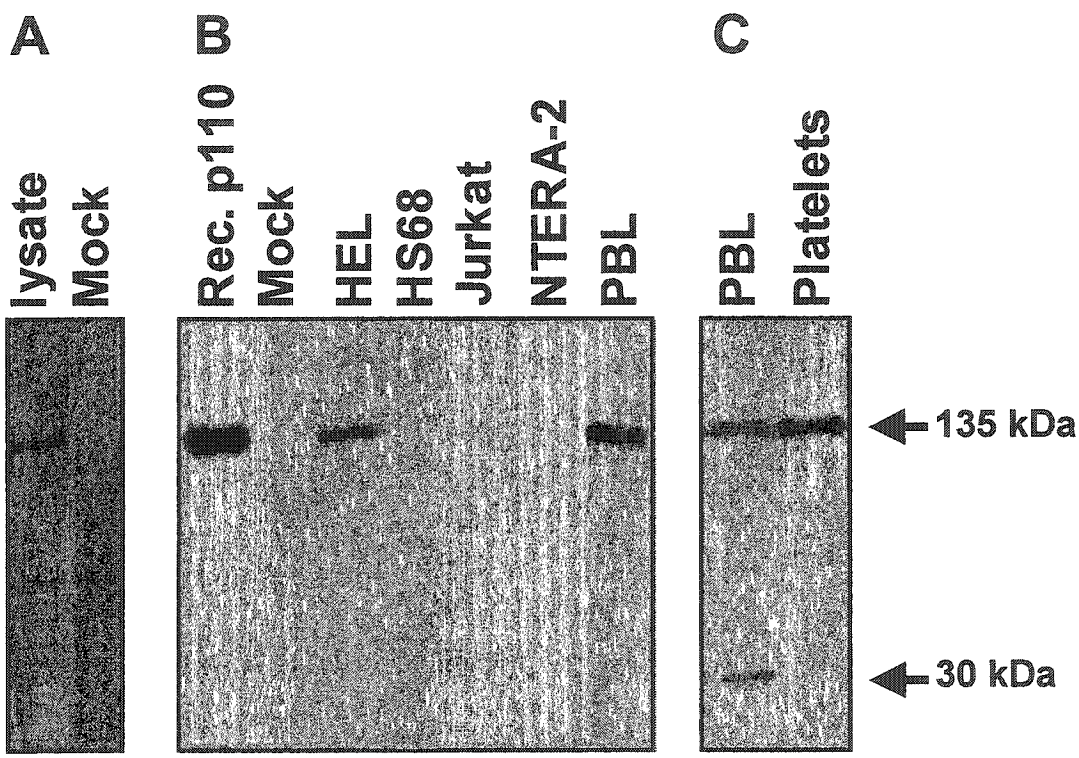
A
B
C
lysate
Mock
Rec. p110
Mock
HEL
HS68
Jurkat
NTERA-2
PBL
PBL
Platelets
135 kDa
30 kDa

sequencing data (Figure 4.5, and 4.10). This 30 kDa band was not detected in PBL with antibody # 41 (Figure 4.15B), indicating its epitope is not present in the full-length isoform.

Identification of p135 protein by flow cytometry. The most reactive antibodies that were positive with Western blots were used to test whether p135 could also be detected by flow cytometry of human cells (Figures 4.16). Cells were fixed and were incubated with FITC-labeled anti-p135 monoclonal antibodies. Among these monoclonal antibodies, as would have been expected, some recognized the p135 protein better than others (results not shown). As seen in Figure 4.16A, an almost two-log shift in the signal intensity was observed with HEL cells. Interestingly, p135 was only detected in a specific cell population of HEL cells (Figure 4.16B). Larger and more granular HEL cells did not result in any detectable shift in the signal intensity, indicating that p135 is not present in these cells (Figure 4.16A versus 4.16B). The T and B cells were also tested for their ability to express p135 protein by flow cytometry. As can be seen in Figure 4.17, the p135 protein is detected in T and B lymphocytes, especially following fixation and permeabilization of the cells (results not shown). No detectable shift in signal intensity was observed with anti-22.4 kDa yeast-specific monoclonal antibody (not shown), or with an IgG isotype control (Figure 4.17B).

Subcellular localization of p135 protein in cells. Immunofluorescence microscopy revealed that the protein is intracellular (Figures 4.18 - 4.20), and may

Figure 4.16 **Detection of the p135 protein in HEL cells by flow cytometry.**

Human erythroleukemia cells were fixed and permeabilized, then incubated with anti-p135 monoclonal antibody # 41. Forward and side scatter as measured by flow cytometry is shown in the figures on the left. Fluorescence was detected by flow cytometry, from goat–anti-mouse FITC-conjugated secondary antibody. Two different populations of HEL cells were gated and tested for p135 expression separately (shown in A and B). Gated cells are represented by the arrows.

A

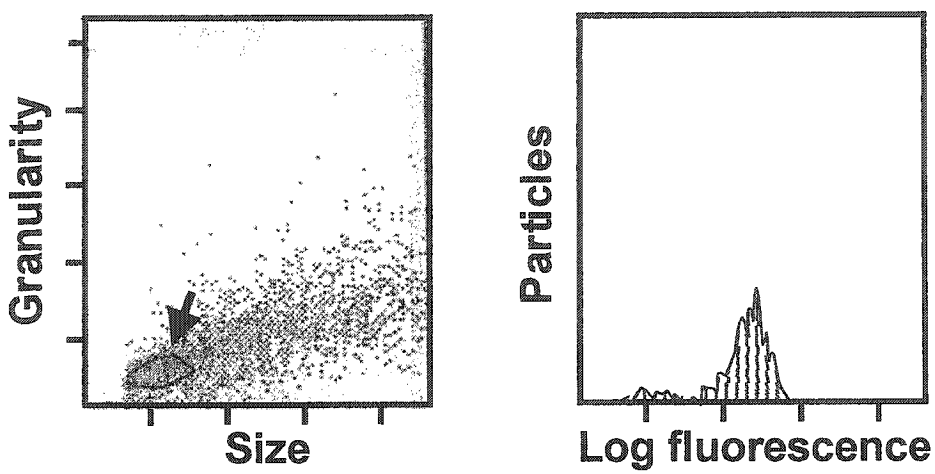
Granularity
Size
Particles
Log fluorescence

B

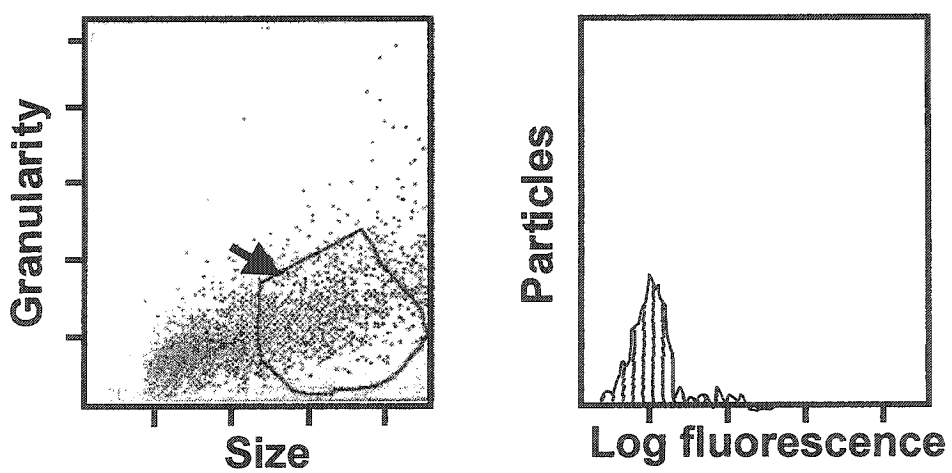
Granularity
Size
Particles
Log fluorescence

Figure 4.17 **Detection of the p135 protein in peripheral blood leukocytes.**

Human peripheral blood leukocytes isolated from human plasma were fixed and permeabilized, then incubated with anti-p135 monoclonal antibody # 41. Forward and side scatter as measured by flow cytometry is shown in A. Fluorescence was detected by flow cytometry from goat–anti-mouse FITC-conjugated secondary antibody. PE-labeled anti-CD3 was used to select T lymphocytes (C), and PE-labeled anti-CD19 was used to select B lymphocytes (D). Isotype control was mouse IgG1 (B).

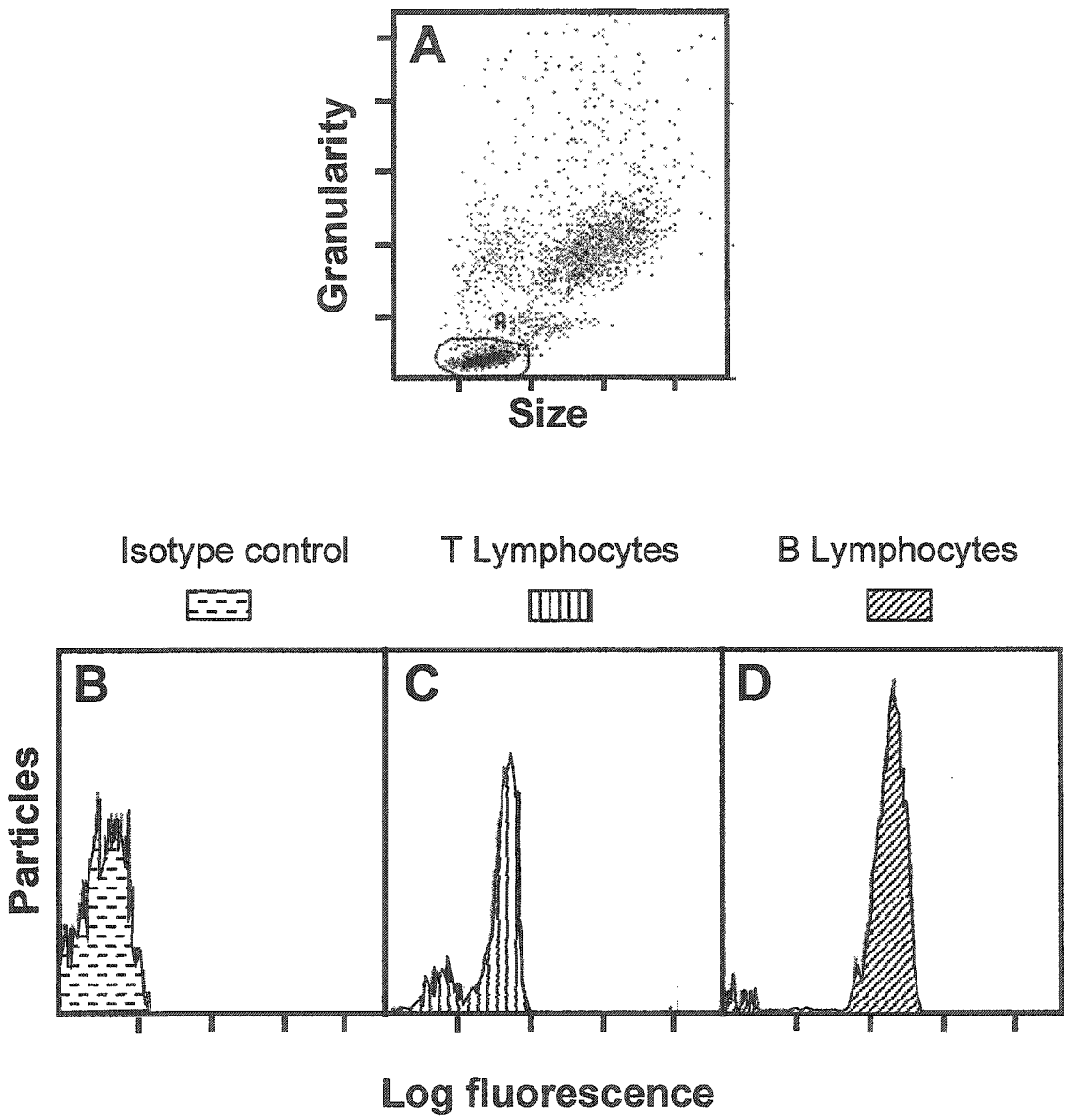
A
Granularity
Size
Isotype control
T Lymphocytes
B Lymphocytes
B
C
D
Particles
Log fluorescence

Figure 4.18 **Immunofluorescence microscopy with anti-p135 antibodies.**

A, Human erythroleukemia cells were adhered to poly-L-lysine coated glass coverslips, and simultaneously fixed and permeabilized with 4% paraformaldehyde, 0.25% gluteraldehyde, and 0.2% TritonX-100. Total P135 was detected with monoclonal antibody # 29 (Left panels), or #41 (right panels). The P135 antibodies were detected with Cy3 conjugated donkey anti-mouse IgG. Nuclei were detected with 4',6-diamidino-2-phenylindole (DAPI). Photographs were taken with a Zeiss Axioplan2 epifluorescent microscope and a Sony 3 CCD color video camera (model DXC-950P). B, as in A except that a mouse IgG1 isotype control (left panels), or an anti-vimentin mouse monoclonal antibody (right panels) was used.

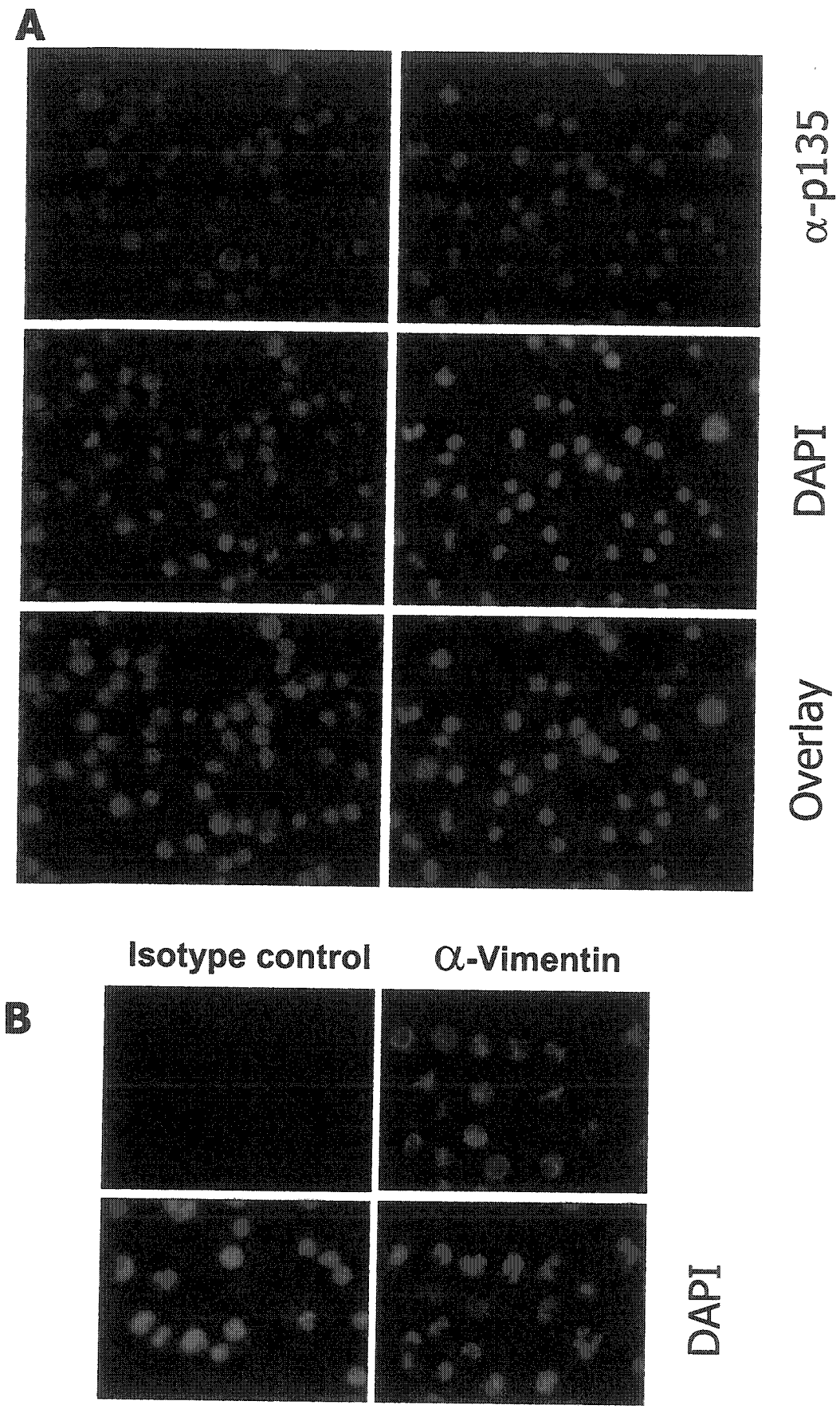
A
α-p135
DAPI
Overlay
Isotype control
α-Vimentin
B
DAPI

Figure 4.19 **Distribution of p135 protein following PHA stimulation.**

A, HEL cells (left panels), or PHA activated (1 mg/ml, for 1 hr) HEL cells (right panels) were adhered to poly-L-lysine coated glass coverslips, and simultaneously fixed and permeabilized with 4% paraformaldehyde, 0.25% gluteraldehyde, and 0.2% TritonX-100. Total P135 was detected with monoclonal antibody # 41. The P135 antibodies were detected with Cy3 conjugated donkey anti-mouse IgG. Nuclei were detected with 4',6-diamidino-2-phenylindole (DAPI). Photographs were taken at a fixed gain setting for the two panels with a Zeiss Axioplan2 epifluorescent microscope and a Sony 3 CCD color video camera (model DXC-950P). B, homogenates from equal number of HEL or PHA activated HEL cells were separated on 8% SDS-PAGE, transferred to PVDF, and probed with mouse anti-p135 monoclonal antibody #18.

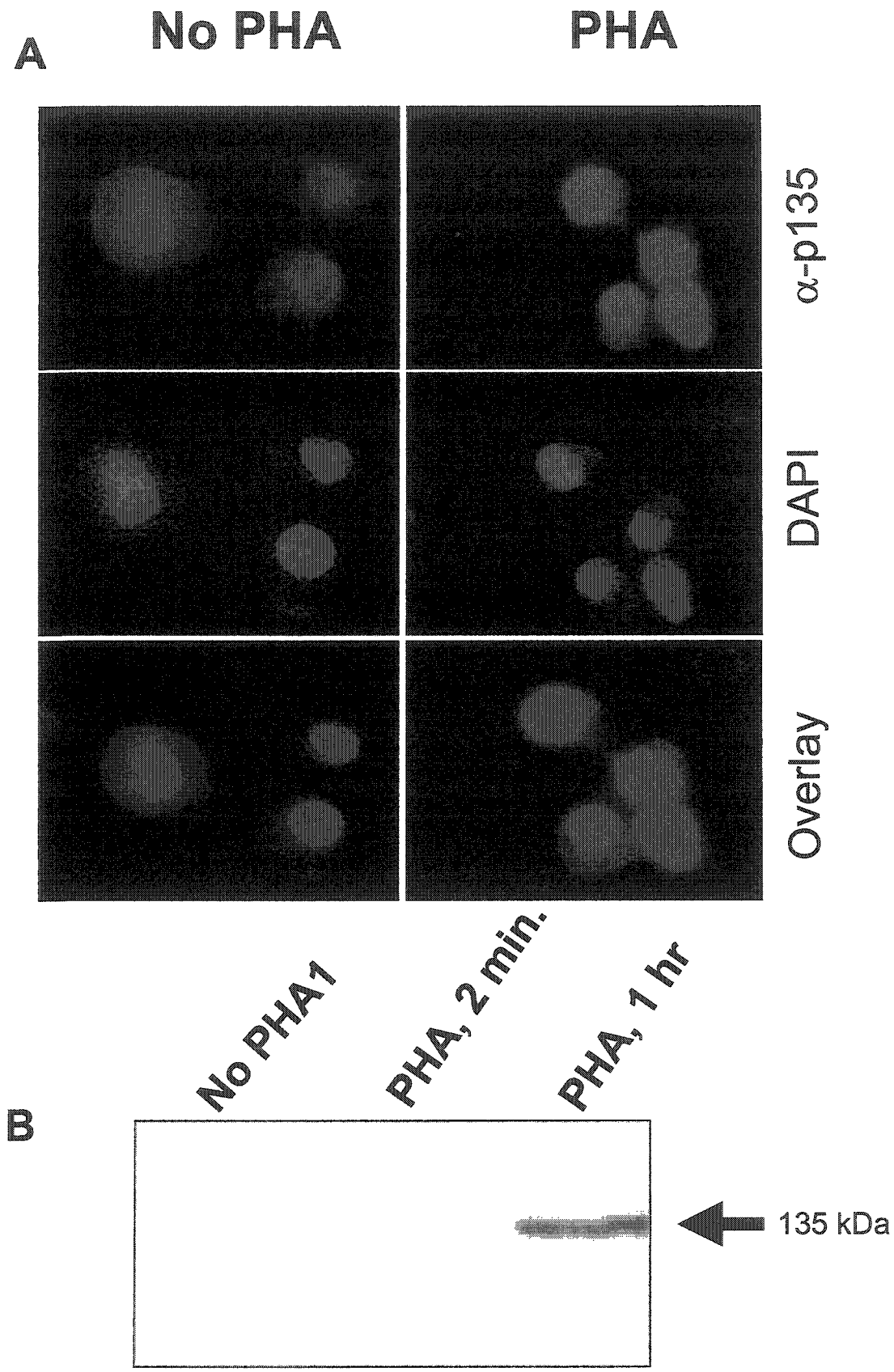
A
No PHA
PHA
α-p135
DAPI
Overlay
B
No PHA1
PHA, 2 min.
PHA, 1 hr
135 kDa

Figure 4.20 **Intracellular distribution of p135 protein in cells.**

A, Human erythroleukemia cells were adhered to poly-L-lysine coated glass coverslips, and simultaneously fixed and permeabilized with 4% paraformaldehyde, 0.25% gluteraldehyde, and 0.2% TritonX-100. Total P135 was detected with monoclonal antibody # 29 (Left panels), or #41 (right panels). The P135 antibodies were detected with Cy3 conjugated donkey anti-mouse IgG. Nuclei were detected with 4',6-diamidino-2-phenylindole (DAPI). Photographs were taken with a Zeiss Axioplan2 epifluorescent microscope and a Sony 3 CCD color video camera (model DXC-950P). B, as in A except that Jurkat cells were used.

A

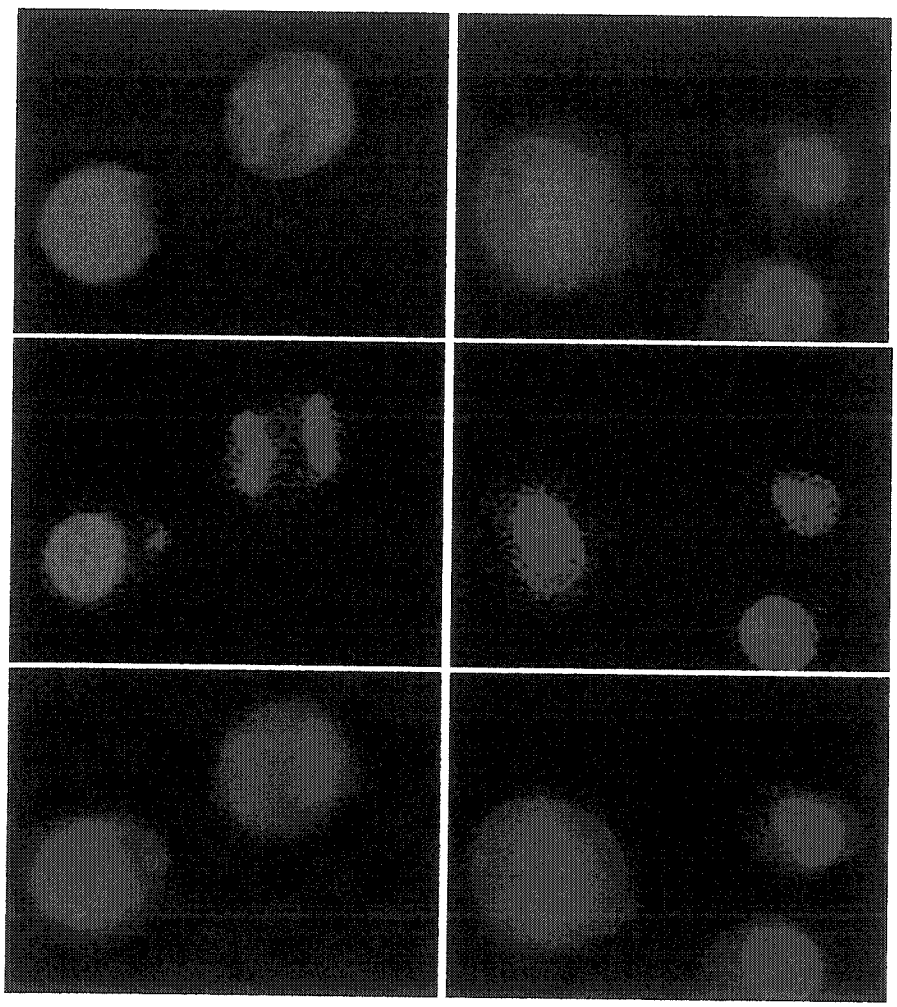

B

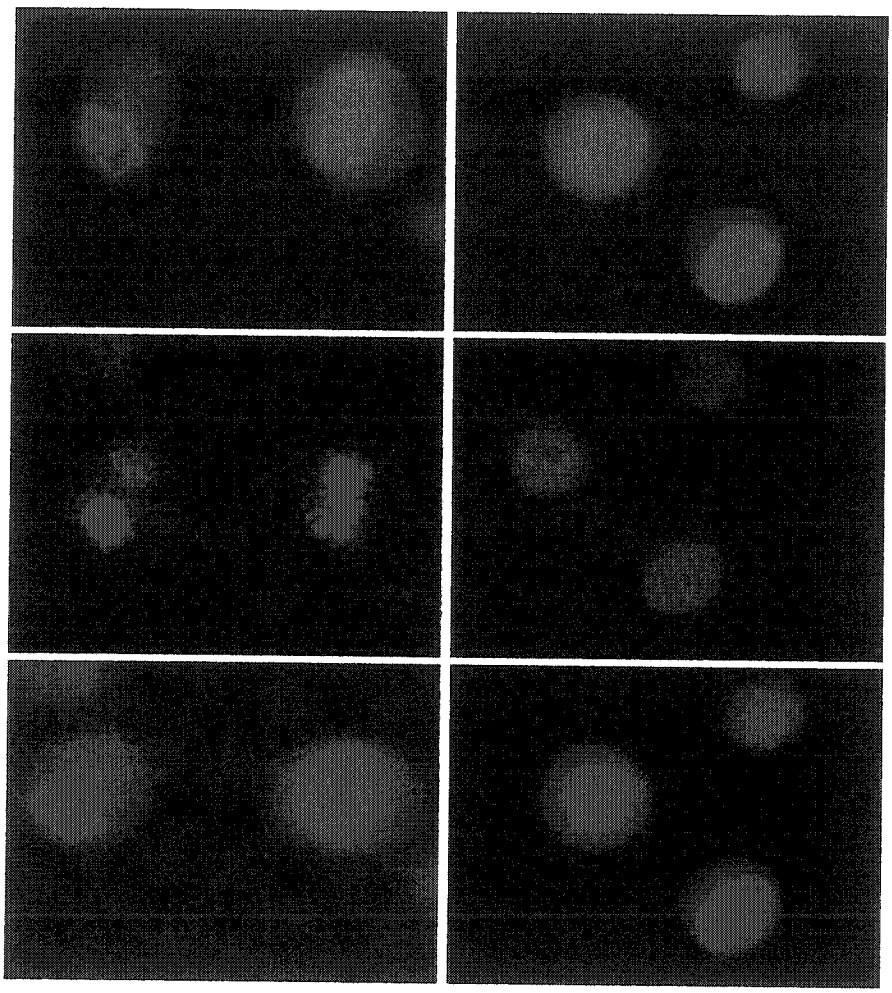

predominantly be expressed in the nucleus or nuclear envelope of HEL cells (Figures 4.19 – 4.20A), and Jurkat cells (Figure 4.20B). Furthermore, upon pretreatment of HEL cells with PHA, the p135 protein expression level was enhanced (Figure 4.19). The increase in the level of p135 expression following PHA treatment was also confirmed by Western blotting (Figure 4.19B). PHA treatment of HEL cells resulted in the translocation of the p135 protein from the cytosol to the nucleus or nuclear envelope of the cell. Nuclear translocation was supported by the observation that the protein likely contains a nuclear translocation signal as observed in the predicted amino acid sequence (Figure 4.11). Interestingly, immunofluorescence microscopy studies on the p135 protein also revealed that, in cells that are in the mitotic stage, the protein is primarily localized to the nucleus (Figures 4.20 left panels).

P135 binds to aPL in a Ca^{2+}-dependent manner. Many proteins contain regions homologous to the sC2 domain, most of which are thought to interact with cellular membranes. To assess whether p135 displays a Ca^{2+}-dependent association with membranes in vivo, we examined the binding of the soluble full-length recombinant p135 protein to 100% PC, 100% PS, or 75/25% PC/PS in the presence or absence of Ca^{2+}. The SF9 cell homogenates and culture media were used in these experiments (Figure 4.21, 4.22). PS was the most effective phospholipid lipid for p135 binding, followed by PC/PS. This interaction was Ca^{2+}-dependent (at 2 mM) since no binding to PS or PC/PS was observed when Ca^{2+} was chelated (Figure 4.21 and 4.22). No significant binding to PC was

Figure 4.21 **Phospholipid binding to recombinant p135.**

A, SF9 cells were infected with either wild type virus or recombinant p135 virus and were labeled with ^{35}S-Met. SF9 cell-lysate or culture media were added to wells that were coated with either phosphatidylcholine (PC), phosphatidylserine (PS), or PC/PS (75/25%). Incubations were performed in the presence of 2 mM Ca^{2+}. EDTA (10 mM) was added to the wells following the incubation period. Solid empty bars, p135 cell-lysate was added to wells; solid black bars, p135 culture media; and bars with diagonal lines, cell lysate from mock-infected SF9 cells. B, protein remaining bound to the plastic wells after three repeated washing steps with HBS/Ca^{2+} were eluted from the plastic wells with SDS and were detected by autoradiography. The ^{35}S-labeled cell lysate is shown in the lane labeled as CL.

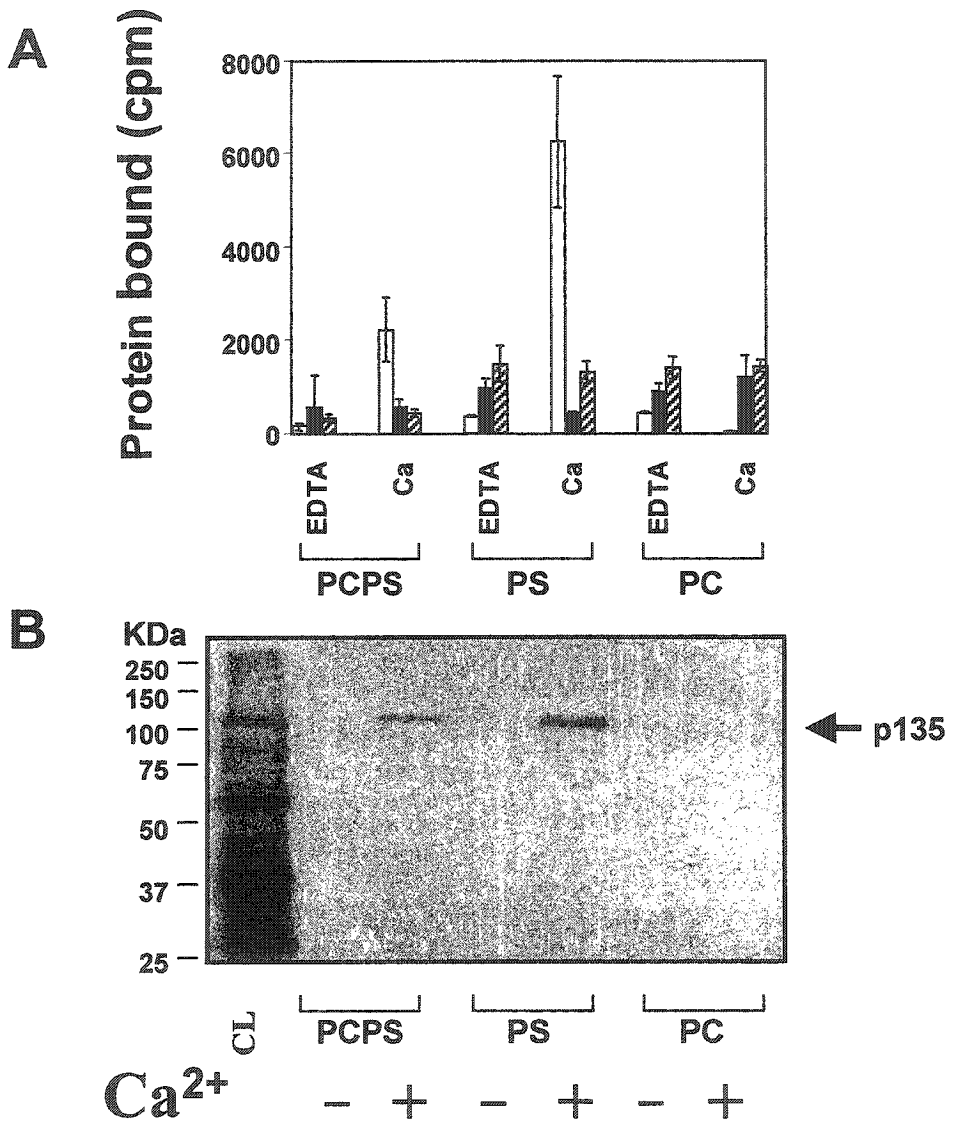
A
Protein bound (cpm)
8000
6000
4000
2000
0
EDTA
Ca
EDTA
Ca
EDTA
Ca
PCPS
PS
PC
B
KDa
250
150
100
75
50
37
25
p135
CL
PCPS
PS
PC
Ca2+
–
+
–
+
–
+

Figure 4.22 **Calcium-dependent phospholipid binding to recombinant p135.**

A, SF9 cells were infected with either wild-type virus or recombinant p135 virus and were labeled with ^{35}S-Met. SF9 cell-lysate (black diamond), or cell lysate from mock-infected SF9 cells (black square) were added to wells that were coated with phosphatidylserine (PS). Incubations were performed in the presence of 0.1 – 6 mM Ca^{2+}. EDTA (10 mM) was added to the wells following incubation with 6 mM Ca^{2+}. B, protein remaining bound in A to the plastic wells from the SF9 cell-lysate (upper panel) or the mock-infected SF9 cell-lysate (lower panel) was eluted from the plastic wells with SDS and detected by autoradiography. The ^{35}S-labeled cell lysate is shown in the lane labeled as CL.

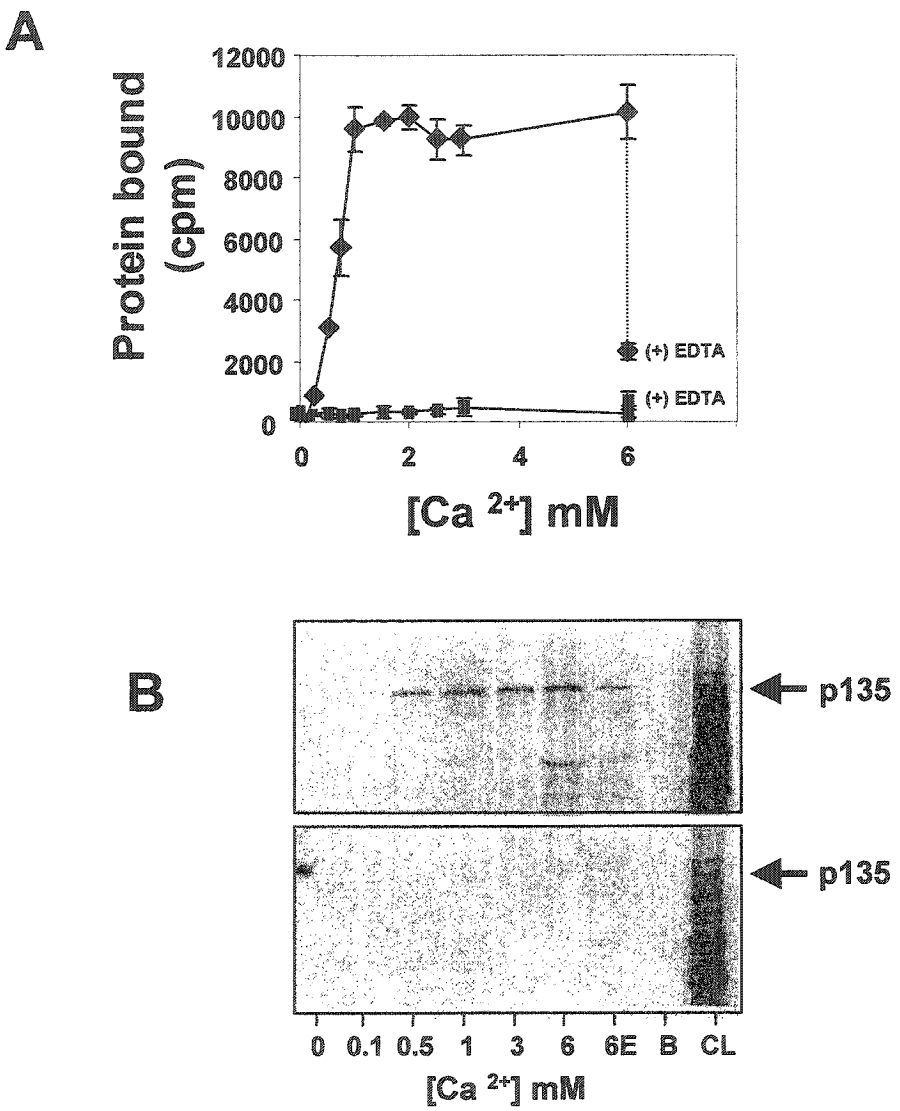
A
Protein bound (cpm)
12000
10000
8000
6000
4000
2000
0
0
2
4
6
[Ca 2+] mM
(+) EDTA
(+) EDTA
B
p135
p135
0 0.1 0.5 1 3 6 6E B CL
[Ca 2+] mM

observed either in the presence or absence of Ca^{2+}, indicating that the binding is PS specific. To determine the relative mobility of the protein(s) that remained bound to the phospholipid coated wells, the bound proteins were eluted from the wells, separated on SDS-PAGE, and visualized by autoradiography. Only one detectable protein species was observed by autoradiography (Figure 4.21B, and 4.22B) and no other bands were detected with longer incubation time (up to 2 weeks exposure). This protein was identified as P135, since its relative mobility was identical to recombinant P135 (~135 kDa), and it was recognized by anti-P135 mAb (results not shown). To determine the effect of Ca^{2+} on p135 binding to PS coated wells, a Ca^{2+} titration was performed and the radioactivity remaining in the wells were measured. Maximal binding was observed at 1 mM Ca^{2+} concentration. Addition of excess EDTA (15 mM) completely reversed the binding of p135 to PS, thereby demonstrating the Ca^{2+} dependency of the interaction. Figure 4.22B shows that the observed activity in the wells was due to the binding of the recombinant p135, and upon the addition of saturating concentration of EDTA, p135 binding to PS diminished to nearly baseline after 1 hour of incubation.

DISCUSSION

The isolation, characterization, and functional analysis of a novel human protein, named p135, is described. The p135 DNA was found in human and mouse erythroleukemia cell lines, and in hamster cells. This seems to indicate that there is a high probability that the gene is conserved among mammalian species. If so, then it is quite probable that p135 plays a fundamental role in eukaryotic cell biology although currently, this function remains unknown.

Genomic analysis of p135 in healthy donors. Genomic DNA from healthy donors was analyzed to try to determine if the p135 gene is a site of chromosomal rearrangement. The DNA was isolated from 32 healthy blood donors and digested with two different restriction enzymes. P135 was present in all individuals tested without any detectable rearrangements (Figure 4.6). This certainly does not exclude the fact that polymorphisms and chromatid rearrangements may still indeed be present but undetected with this method. To completely characterize the variability in this gene, future studies would have to more comprehensively examine loss of heterozygosity (LOH) and transcript variabilities both in healthy subjects, and in cancer patients, as well as in breast and ovarian tumours. This could be accomplished using FISH analysis using one of the p135 cDNA probes to localize the p135 gene to a specific band in the 17q25 locus. FISH analysis could also be used on breast and ovarian tumours to identify loss, duplication, or chromosomal rearrangements. In addition, RT-PCR could be used on RNA from various cancer types to characterize alterations in

the expression of transcripts in p135. Ultimately, transgenic or knock-out mice for p135 could be generated and the mouse phenotype examined.

The truncated form of p135. It is very likely that the 38 nucleotide insertion that was detected at the DNA level in exon 5 (Figure 4.10) contributes to the appearance of the two isoforms of the p135 protein detected both by RT-PCR (Figure 4.5) and Western blotting using monoclonal antibody #18 (Figure 4.15C). Interestingly, we observed that a smaller 38 kDa protein, that we suspect to be the truncated isoform of p135, was present only in PBL. This might be an indication that the truncated form is differentially expressed in specific blood cells that remain to be determined. At this stage, we do not know why other antibodies were not able to detect the smaller form in PBL. Analysis of the truncated form at the protein level, with isoform-specific monoclonal antibodies, would be helpful in clarifying p135's role in PBL. If this role is defined, this could possibly aid in the identification of the function of p135 in blood cells.

P135 homology with synaptotagmins. The P135 protein sequence predicted homology to the sC2 domains of synaptotagmins. This family of secretory proteins has distinct tissue tropism. Where some synaptotagmins (I,II and V) are expressed only in the brain, others are expressed ubiquitously (III, IV, and VI-IX) (305). From the observed tissue distribution of p135, which is predominantly in the spleen, thymus, lymph node, bone marrow, and PBL (data summarized in

Table 4.1) it is unlikely that the protein performs its function in synaptic vesicles during exocytosis. It is more likely that p135 functions specifically in blood cells.

Sequence homology of p135 to Munc 13 proteins. These data describe the first member of the important sC2 family of proteins whose expression is mostly restricted to blood cells and blood cell lineages. Interestingly, p135 showed high homology (~80%) to Munc13-4, which has recently been identified, belongs to a subfamily of Munc13-like molecules. Munc13 constitutes a family of four molecules (Munc13-1, Munc13-2, and Munc13-3 and Munc13-4) and are mammalian homologues of *Caenorhabditis elegans* Unc13, a brain-specific protein that appears to play a role in synaptic transmission (312,313). With the exception of Munc13-2, which is ubiquitously expressed, Munc13-1 and Munc13-3 are specifically expressed in the brain, likely playing a role in synaptic transmission. The transcript for Munc 13-4 has been primarily detected in the lung, testis, and spleen (328), and to a lesser extent in the heart muscle, kidney, liver, brain, and skeletal muscle. In the lung, the protein has been localized specifically to the goblet cells of the bronchial epithelium, and the alveolar type II cells, both of which are cell types with secretory function. Our results indicate that although p135 has high homology to Munc13-4, it is unlikely that p135 is the human form of the rat Munc13-4 protein since the expression pattern differs dramatically. For instance, we were not able to detect the mRNA for p135 in testes, heart, kidney, liver, and skeletal muscle. In addition only a very weak signal was detected in lung, supporting that p135

Table 4.1 **Comparison of p135 RNA and protein expression in tissues.**

RNA expression was determined by Northern blots using p135 cDNA as a probe, and protein expression was determined by Western blots detected with mouse anti-p135 monoclonal antibody #41. Band intensities was estimated and given a value of 4+ for the strongest intensity and 1+ for the weakest. The absence of bands is shown as a minus sign (-). NA indicates that the test has not been performed.

Table 4.1

Tissue	Western	Northern
Heart	NA	+
Brain	-	-
Placenta	-	++
Lung	NA	++
Liver	-	+
Skeletal muscle	NA	+
Kidney	NA	-
Pancreas	NA	+
Prostate	NA	-
Spleen	++	+++
Thymus	NA	+++
Testis	-	-
Ovary	++	++
Small intestine	NA	+
Colon	NA	+
Lymph node	NA	+++
Appendix	NA	++
Bone marrow	NA	+++
Fetal liver	NA	++

is not the human form of the rat Munc 13-4, which is predominantly expressed in the lung (328). However, since our results indicate that p135 and Munc13-4 share the same sC2-domain structure and exhibit significant homology throughout the sequence with each other and to a lesser extent with the other Munc13 proteins, it indicates that p135, Munc13-4 and the three known Munc13 isoforms may be evolutionary descendants of a common ancestor and may have similar functional roles, possibly in secretion.

Topology of p135 sC2-domain. It is widely accepted that there are two distinct topologies for sC2-domains, and that these can be recognized on the basis of the primary sequence. The topologies can be recognized depending upon whether the amino acid sequence of the first β-strand is found before (as in synaptotagmin I; type I) or after (as in phospholipase C; type II) the rest of the sC2-domain sequences. Our data indicate that both domains are topology type I since the first β-strand sequences are present in the N-terminal portion of both sC2-domains. This topology is also common in Synaptotagmins, Rabphilin, Doc 2, and Munc 13-4 proteins (Figure 4.1) indicating perhaps a common ancestor among these proteins. It was surprising to find, however, that Unc 13 and Munc 13 proteins, with the exception of Munc 13-4, contain sC2-domains with different topologies, which argues against the common ancestor theory.

Correlation of p135 to cancer. The p135 gene was mapped to chromosome 17q25, a region characterized by frequent allelic imbalance and losses. This

region has also been proposed to contain a number of tumor suppressor genes (353,354). For instance, a chromosomal region in 17q25 with allelic imbalance was predicted to contain undefined putative breast tumor suppressor genes (355). A large study was designed to correlate this 17q25 region with ovarian, prostate, and breast tumors. The conclusion made from the study was that one or more novel tumor suppressor genes exist on 17q25 within a region of interstitial loss defined in both breast and ovarian tumors. A separate study identified the 17q25-tumor suppressor region to be implicated in the development of all types of epithelial ovarian tumors (356). Similarly, this region has been characterized to contain a number of genes correlated to various types of human cancer. For example, survivin (SVV), a family member of inhibitor of apoptosis proteins (IAPs), has been mapped to 17q25 and is implicated in advanced stages of neuroblastoma (357).

Of the 12 different cancer cell lines that were analyzed by Northern blotting and Western blotting (Table 4.2) high expression of p135 transcript was detected in leukemia cell lines (erythroleukemia, promyelocytic leukemia, and lymphocytic leukemia (HEL, HL60, and MOLT-4), and in adenocarcinoma (SW480)). We did not detect expression in lymphomas, carcinomas and melanomas, with the exception of colorectal adenocarcinoma which showed very high levels of expression of p135 transcript. At this stage of analysis, it would be premature to derive any strong conclusions regarding correlations between the over-expression or the absence of the p135 gene in these specific cancer cell

Table 4.2 **Comparison of p135 RNA and protein expression in cells.**

RNA expression was determined by Northern blots using p135 cDNA as a probe, and protein expression was determined by Western blots detected with mouse anti-p135 monoclonal antibody #41. Band intensities was estimated and given a value of 4+ for the strongest intensity and 1+ for the weakest. The absence of bands is shown as a minus sign (-). NA indicates that the experiment was not attempted.

Table 4.2

Cells	Description	Western	Northern
PBL	Peripheral blood leukocytes	++++	++++
HUT	T cell line	+++	++
Jurkat	T cells	++	NA
Tcells	Enriched T cells from PBL	+++	++
$Tcells_{PHA}$	T cells activated by PHA	NA	++++
B cells	Enriched B cells from PBL	-	+
Monocytes	Enriched monocytes from PBL	NA	++
EC	Endothelial cells	NA	-
HS68	Newborn fibroblast	-	NA
HEL	Human erythroleukemia	+++	+++
HL-60	Promyelocytic leukemia	NA	++++
Molt-4	Lymphoblastic leukemia	NA	+++
RS4;11	Acute leukemia; No T and B	-	NA
MEG-01	Megakaryoblstic leukemia	+	NA
K-562	CML; erythro., gran., mono.	+	++
Raji	Burkitts lymphoma	NA	+
NTERA-2	Embryonal carcinoma	-	NA
SW480	Colorectal adenocarcinoma	NA	+++
S3, Hela	Cervix carcinoma;adenocarcinoma	NA	-
A549	Lung carcinoma	NA	+
G361	Melanoma	NA	_

lines. Hence, although we do not know yet whether p135 is directly involved in cancer, this is a possibility. Extremely interesting and crucial future experiments would include fine analysis of the p135 gene and transcript in these cancers. Furthermore, it would be necessary to look for expression and translation of the truncated form of p135 (30 kDa protein) in these cancers. As well, FISH analysis would need to be performed on the cancer cell lines that showed the expression of p135. Additional experiments could focus on isolating and analyzing the higher molecular weight transcript (~5.5 kb) that was detected primarily in ovarian tissue. Based on the signal intensity generated from the Northern blot (Figure 13B), and the absence of the transcript in the other cells and tissues tested, we have very good reason to believe that this transcript is p135-specific.

The observation that expression of the p135 human gene product was enhanced in HEL cell lines both at the level of mRNA and protein, following stimulation by PHA, may suggest that the protein performs an essential role during cell activation, as in the case of an immune response to a foreign antigen. Hence, this observation, combined with its localization to T-cells, lymph node and thymus, may further suggest a function of p135 in the immune system. Interestingly, PHA stimulation of T cells, but not endothelial cells, also resulted in the increase in the level of p135 mRNA (Figure 4.12). Furthermore, PHA stimulation resulted in the translocation of the p135 protein to the nucleus. Interestingly, the predicted amino acid sequence of p135 suggests the presence of a putative nuclear translocation signal in the C-terminal region of

the protein, nicely supporting the experimental observations made using immunofluorescence microscopy (Figure 4.19).

Our flow cytometry results clearly indicated the presence of p135 in a sub-population of HEL cells (Figure 4.16). This cell line was originally derived from the peripheral blood of a patient with Hodgkin's disease who later developed erythroleukemia (358). P135 was also detected by flow cytometry in the T and B lymphocytes of PBL, also supporting Western and Northern data. Furthermore, identification of p135 in Jurkat, and HUT cells, which are T cell lines, indicates that p135 may be predominantly expressed in cells involved in immune response. Immunofluorescence microscopy results showed that cells that are in the mitotic stage of division show a strong p135 signal in the nuclear membrane. This nuclear membrane translocation may be a function of the two predicted sC2-domains and may indicate that at some stage in the cell cycle p135 may function as a Ca^{2+} sensor protein in the nuclear membrane. Confocal microscopy can be employed in order to more accurately localize the protein in cells at resting-state, at mitosis, as well as during cell division.

Ca^{2+}-dependent binding to PS. Our results indicate that recombinant p135 bind specifically to PS coated wells in a Ca^{2+}-dependent manner, and that binding was reversible following the addition of EDTA (Figure 4.22). Maximum binding was observed at Ca^{2+} concentrations of about 1 mM consistent with observations made with other proteins with sC2-domains (359,360). Because

several isolated sC2-domains have been shown to bind phospholipids, inositolpolyphosphates, or proteins associated with the membrane, the sC2-domain, in general, appears to function as a Ca^{2+}-regulated cellular localization motif that controls the docking of signaling proteins to membranes (323,327). We examined the full-length sequences of human p135 and found a very interesting domain structure that is, along with Munc 13-4, unique among proteins containing sC2-domains. Other than the two sC2-domains, the protein does not share any other domain homologies with other proteins with sC2-domains. The C-terminal sC2-domain was found to be more homologous to the consensus sequences of sC2-domains than the N-terminal sC2-domain . This might indicate that Ca^{2+}-binding is by the second sC2-domain of p135. This is supported by the prediction from sequence that all five acidic residues implicated in Ca^{2+}-binding are identically present in the C-terminal sC2-domain but not in the N-terminal sC2-domain of p135. Furthermore several segments are absent from the N-terminal sC2 domain that might be necessary to maintain the three dimensional structure required for Ca^{2+} and phospholipid binding.

phospholipid binding. Most proteins with sC2-domains are thought to interact with phospholipids, and in many cases has been experimentally proven (297,304,327). Furthermore, the majority of these proteins bind phospholipid in a Ca^{2+}-dependent manner. Experiments were performed which explored the function of the sC2-domains of p135 in phospholipid binding. The results are consistent with a role of sC2-domains in phospholipid binding. A protein from

recombinant insect cell lysate, migrated with the same mobility as recombinant p135 protein, and bound PS and to a lesser extent PS/PC (25%/75%) but not PC. Our results demonstrate that one, or both, sC2-domain(s) is functional and in addition exhibit lipid specificity.

Previous studies have implicated Ca^{2+}-binding sites (specifically Asp residues) 1 , 2, and 3 in the initial binding of protein to membrane surfaces (297,304,327,331). These sites are predicted in the C-terminal sC2-domain of p135 (Figure 4.23 and 4.24). This does not exclude the fact that the Glu residue at Ca^{2+}-binding site 3 in the N-terminal sC2-domain may still function to bind Ca^{2+}, thus allowing for the initial binding. Similar studies identified the binding of another Ca^{2+} to Ca^{2+}-binding sites 1, 3, 4, or 5 (also specifically Asp) induces a conformational change in the molecule which in turn triggers its membrane penetration and activation. Similarly, these residues are identically present in the C-terminal sC2-domain of p135 but not in the N-terminal sC2-domain. Collectively these data may indicate that the observed Ca^{2+}-dependent PS binding by recombinant p135 is by the C-terminal sC2-domain, but this needs to be experimentally confirmed. The ability of the sC2-domain to bind phospholipid vesicles in a Ca^{2+}-dependent manner has been previously demonstrated by functional expression and characterization of recombinant sC2 domains, for example sC2-domains of synaptotagmin and phospholipase A2 (305). Similar phospholipid-binding experiments need to be performed with recombinant N-terminal and C-terminal sC2-domain of p135. These

Figure 4.23 **Sequence alignment of sC2-domains.**

The predicted C-terminal sC2-domain sequence of P135 is aligned with sC2-domains from several different synaptotagmins, rabphilin-3A, UNC-13, and PKC. Sequences are aligned for maximal homology. Similar residues are in blue, and identical residues are in red. Conserved residues are boxed. The five conserved aspartic acid residues, which may be needed for Ca^{2+} binding, are shown by the arrows above the sequence.


1
2
TVKASYRASEQKIRVELTSASSILPLDSNGSSDPFVQLTIEPRHEFP P135.
CTCLRYVPTAGKLTVCILEAKNLKKMDVGGLSDPYVKIHLM-QNG-K Syn.(Rat)
CTSLRYVPTAGKLTVCILEAKNLKKMDVGGLSDPYVKIHL-LQNG-K Syn.(Gallus)
CFSLRYVPTAGKLTVVILEAKNLKKMDVGGLSDPYVKIHLM-QNG-K Syn.(Human)
CFSLRYVPTAGKLTVVILEAKNLKKMDVGGLSDPYVKIALM-QNG-K Syn(C.Elegans)
CFSLRYVPTAGKLTVVILEAKNLKKMDVGGLSDPYVKIAL-L-QGTK Syn.(F.Fly)
3
4
ELAARETQKHKKDLHPLFDETFEFLVPAEPCRKAGACLLLTVLDYDT
RLKKKKTTVKKKTLNPYFNESFSFEIPFEQIQKV-Q-VVVTVLDYDK
RLKKKKTTVKKNTLNPYYNESFSFEIPFEQIQKVQVCV--TVLDYDK
RLKKKKTTIKKNTLNPYYNESFSFEVPFEQIQKV-Q-VVVTVLDYDK
RLKKKKTSVKKCTLNPYYNESFSFEVPFEQMQKI--CLVVTVVDYDR
RLKKKKITTIKKNTINPYYFNESFSFGFEVPFEQIQKV-T-LIITVVDYDR
5
LKADL
LGKNE
IGKND
IGKND
IGTSE
IGTSE

Figure 4.24. **Sequence alignment of the two p135 sC2-domains.**

The predicted N-terminal (top) and C-terminal (bottom) sC2-domain sequences are aligned for maximal homology. Similar residues are in blue, and identical residues are in red. The five conserved aspartic residues, which may be crucial for Ca^{2+} binding, are shown by the arrows above the sequence. The dots represent gaps within the sequence.

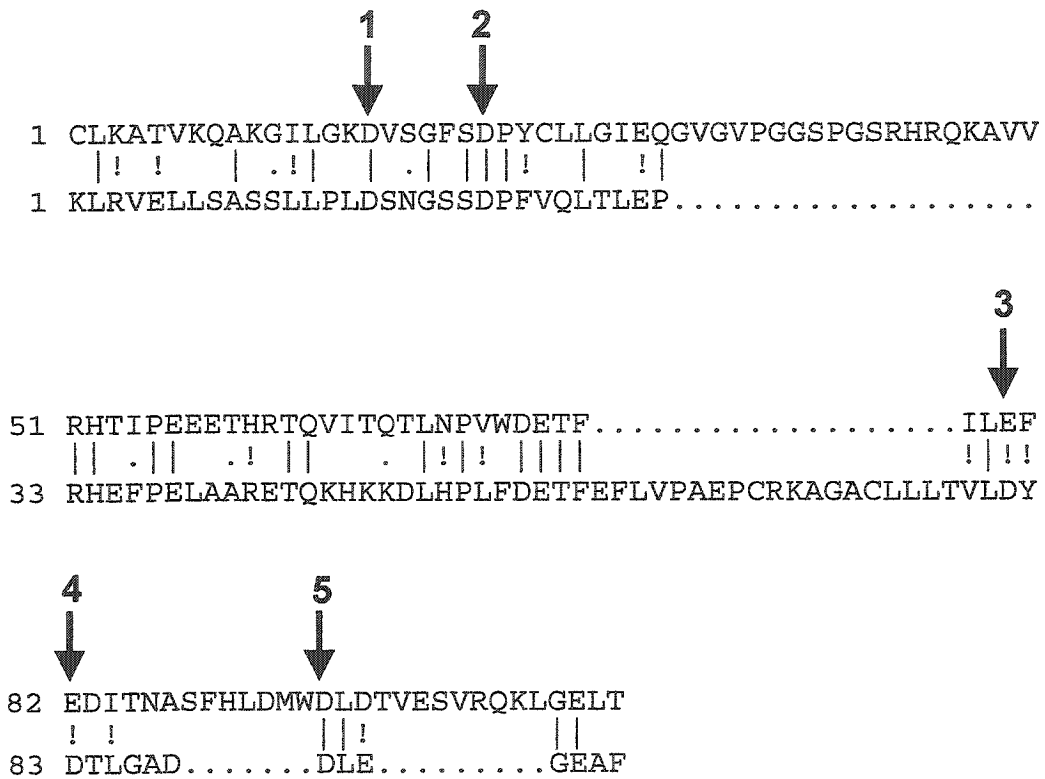
1
2
1 CLKATVKQAKGILGKDVSGFSDPYCLLGIEQGVGVPGGSPGSRHRQKAVV
1 KLRVELLSASSLLPLDSNGSSDPFVQLTLEP.....
3
51 RHTIPEEETHRTQVITQTLNPVWDETF.....ILEF
33 RHEFPELAARETQKHKKDLHPLFDETFEFLVPAEPCRKAGACLLLTVLDY
4
5
82 EDITNASFHLDMWDLDTVESVRQKLGELT
83 DTLGAD.....DLE.....GEAF

experiments will unequivocally attribute the Ca^{2+}-dependent phospholipid-binding to either of the sC2-domains, or both. As well, these experiments will confirm our experimental data with recombinant full-length p135.

Purification. Although our studies with recombinant p135 clearly indicate that the protein specifically binds aPL in a Ca^{2+}-dependent manner, it is desirable to be able to confirm this activity using purified protein. Repeated attempts were made to purify the protein by immunoprecipitation, using the monoclonals that recognized p135 in immunofluorescence and flow cytometry. Unfortunately, these attempts failed to precipitate the protein, even from the highly-expressing cell such as insect SF9 cells (results not shown). Future work might, however, focus on utilizing the functional role of p135 in aPL binding. Affinity techniques might prove to be successful in obtaining a high enough yield of p135 to perform functional analysis. Our data demonstrate that p135, in the presence of Ca^{2+}, remains bound to aPL coated on microtiter wells. Furthermore, this bound p135 was the predominant protein to remain bound considering that the initial material was labeled cell lysate. Hence these experiments seem to indicate that affinity techniques might be useful in obtaining purified recombinant p135. At this stage, we do not know whether similar experiments using cell lysates from non-recombinant cell lines, such as HEL, or PBL would also yield purified p135. Calcium-dependent, membrane-binding proteins have been isolated by affinity techniques for a number of proteins. Sometimes,

these techniques unfortunately yield, in addition to the desired protein, a number of other proteins including annexins. Interestingly, non-recombinant protein kinase C, and phospholipase C have been purified in small amounts using their Ca^{2+}-dependent membrane-binding properties.

Predicted function. Many of the proteins that are known to contain sC2-domains have been found to play a role in Ca^{2+}-dependent membrane targeting and trafficking. Well documented examples of such proteins include synaptotagmin, rabphilin, and Munc 13, all of which have two or three sC2-domains (Figure 4.1). Other proteins that contain sC2-domains perform enzymatic functions in many cell signaling processes, including phosphorylation by PKC, release of diacylglycerol and inositol triphosphate by phospholipase C, release of arachidonic acid by cytosolic phospholipase A2, and ubiquitination of proteins targeted for destruction (305,331). These proteins, in contrast to membrane trafficking proteins, usually contain a single sC2-domain in their sequence. Our identification of p135 as a Ca^{2+}-dependent membrane-associated protein is based on the presence of two sC2-domains in the primary amino acid sequence. In addition, the observed sequence homology with synaptotagmin and Munc 13-4 suggests that p135 may also be involved in membrane trafficking. Such a role would be consistent with a need for distinct cell-specific membrane targeting proteins that function in distinct pathways. In the case of p135, the protein may have a functional role in membrane targeting, perhaps specifically in cells of the immune system.

Future studies. To fully understand the role(s) p135 plays in cell biology, it would be important to identify other proteins that may interact with p135. This future work can be achieved by performing experiments using the yeast two hybrid systems with recombinant p135 as the bait protein, or by immunoprecipitating p135 from cells, then isolating and identifying proteins that may remain bound to p135.

Clearly, a greater understanding of the cellular distribution and its specific function in target cells is necessary to determine the role p135 may play in blood cells. Although in this study we show that recombinant p135 binds vesicles in a Ca^{2+}-dependent manner, and may also be involved in a membrane trafficking pathway, this does not exclude other functions of the protein. Furthermore, the function of the truncated (~38 kDa) p135 isoform needs to be addressed in future experiments. This isoform was predicted based on the detection of a 38 bp insertion in exon 5 that may generate a stop codon downstream of the molecule. Indeed, a protein of about 30 kDa was detected in PBL, but not in the other cells tested, using one of the monoclonal antibodies that was generated. It is logical to assume that this truncated form plays a regulatory role in the overall function of p135 in blood cells. This is especially true since 1 in every 5 cDNA clones tested by RT-PCR contained the 38 bp insertion. Furthermore, the amino acid sequence of the 38 kDa p135 protein predicts a single sC2-domain. It is

necessary then to identify whether this truncated form is also capable of binding membrane and whether the binding is Ca^{2+}-dependent.

Apart from attempting to pursue structural analysis and cellular localization of p135 protein, an important objective of the present study was to gain insight into the overall functional role of the protein in expressing cells, or at least specific functions predicted from its primary amino acid sequence. Unfortunately, the function of Munc13 proteins, proteins with the highest observed homology to p135, is either completely unknown, as in the case of Munc 13-4 which is present in secretory cells of the lung, or has only been linked to secretory processes, as in this case to neurotransmitter release. Once more information is gained regarding these p135-homologous proteins, it is then conceivable that we will then have a better understanding of p135 function in cells and in blood. At present, a number of important tools have been generated to facilitate further functional studies including, cDNA, recombinant protein and monoclonal antibodies.

REFERENCES

1. Suzuki, K., Dahlbach, B., and J. Stenflow. 1982. Thrombin-catalyzed activation of human coagulation factor V. J. Biol. Chem. 257: 6556-6564.

2. Foster, W. B., Nesheim M. E., and G. M. Kennet. 1983. The Factor Xa-catalyzed Activation of Factor V. J. Biol. Chem. 258: 13970-13977.

3. Mann, K.G., Jenny, R.J., and S. Krishnaswamy. 1988. Cofactor proteins in the assembly and expression of blood clotting enzyme complexes. Annu. Rev. Biochem 57: 915-956.

4. Omar, M.N., and K.G. Mann. 1987. Inactivation of factor Va by plasmin. J. Biol. Chem. 262: 97509755.

5. Lee, C.D., and K.G. Mann. 1989. Activation/inactivation of human factor V by plasmin. Blood. 73:185-190.

6. Bajzar, L., Manuel, R., and M.E. Nesheim. 1995. Purification and characterization of TAFI, a thrombin-activable fibrinolysis inhibitor. J. Biol. Chem. 270: 14477-14484.

7. Nesheim, M.E., Wang, W., Boffa, M., Nagashima, M., Morser, J., and L. Bajzar. 1997. Thrombin, thrombomodulin and TAFI in the molecular link between coagulation and fibrinolysis. Thromb. Haemostasis. 78: 386-391

8. Pryzdial, E.L.G., Barrette, N., Dupuis, N., and G.E. Kessler. 1999. Plasmin converts factor X from coagulation zymogen to fibrinolysis cofactor. J. Biol. Chem. 274: 8500-8505.

9. Mann, K.G. 1997. Thrombosis: theoretical considerations. Am J. Clin Nutr. 65(suppl): 1657S-1664S.

10. Mann, K.G. 1992. Surface-dependent hemostasis. Seminars in Hematology. 29: 213-216.

11. Hensyl W.R. 1982. Stedman's illustrated medical dictionary. Baltimore, Williams and Wilkins.

12. Colman R.W., Marder V.J., Salzman E.W., and J. Hirsh. 1985. Overview of Hemostasis. In Hemostasis and Thrombosis: Basic Principles and Clinical Practice.2nd ed. J.B. Lippincott Co., Philadelphia, PA. pp. 3-16.

13. Marcus A.J., Weksler B.B., and E.A Jaffe. 1978. Enzymatic conversion of prostaglandin endoperoxide H_2 and arachidonic acid to prostacyclin by cultured human endothelial cells. J. Biol. Chem. 253: 7138-7174.

14. Weiss H.J., and V.T. Turitto. 1979. Prostacyclin (prostaglandin I2, PGI2) inhibits platelet adhesion and thrombus formation and subendothelium. Blood. 53: 244-250.

15. Esmon C.T., and W.G. Owen.1981. Identification of endothelial cell cofactors for thrombin catalyzed activation of protein C. Proc. Natl. Acad. Sci. USA. 78: 249.

16. Lollar P., and W.G. Owen. 1980. Clearance of thrombin from circulation in rabbits by high affinity binding sites on endothelium: possible role in the inactivation of thrombin by antithrombin III. J. Clin. Invest. 66: 1222-1230.

17. Hatton M.W.C., Berry L.R., and E. Regoeczi. 1978. Inhibition of thrombin by antithrombin III in the presence of certain glycosaminoglycans found in mammalian aorta. Thromb. Res. 13: 655-670.

18. Busch C., and W.G. Owen. 1982. Identification in vitro of endothelial cell surface co-factor for antithrombin III. J. Clin. Invest. 69: 726-729.

19. Levin E.G. 1983. Latent tissue plasminogen activator produced by human endothelial cells in culture: evidence for an enzyme-inhibitor complex. Proc. Natl. Acad. Sci. USA. 80: 6804-6808.

20. Esmon N.L., Owen W.G., and C.T. Esmon. 1982. Isolation of a mambrane-bound cofactor for thrombin-catalyzed activation of protein C. J. Biol. Chem. 257: 859-864.

21. Vatner S.F., and D.A. Cox. 1992. Structural features of the heart and their impact on function. In Kelly W.N., ed, Textbook of internal medicine. 2nd ed. Philadelphia: Lipincott. pp.96-104.

22. Jesty J., and Y. Nemerson. 1995. The pathways of blood coagulation. In Beutler E., and J.T. Kipps, eds. Williams hematology. 5th ed. New York. McGrow-Hill. pp.1227-1238.

23. Shattil, S.J., and J.S. Bennett. 1981. Platelets and their mrembranes in hemostasis: physiology and pathophysiology. Ann. Intern. Med. 94: 108-118.

24. Weiss, H.J., Turitto, V.T., and H.R. Baumgartner. 1978. Effect of shear rate on paltelet interaction with subendothelium in citrated and native blood. J. Lab. Clin. Med. 92: 750-764.

25. Mason, R.G., Mohammad S.F., Chaung, H.Y., and P.D. Richardson. 1976. The adhesion of platelets to subendothelium, collagen and artificial surfaces. Semin. Thromb. Hemost. 3: 98-116.

26. Sakariassen, K.S., Bolhuis, P.A., and J.J. Sixma. 1979. Human blood platelet adhesion to artery subendothelium is mediated by factorVIII-von Willebrand factor bound to the subendothelium. Nature. 279: 636-638.

27. White, J.G. 1999. Current concepts of platelet structure. Am. J. Clin. Pathol. 71: 363-378.

28. Lyons, R.M., Stanford, N., and P.W. Majerus. 1975. Thrombin-induced protein phosphorylation in human platelets. J. Clin. Invest. 56: 924-936.

29. Feinstein, M.B. 1991. The role of calcium in blood platelet function. In Weiss GB, ed. Calcium in drug action. New York, Plenum. pp.197-239.

30. Niewiarowski, S. 1991. Secreted platelets proteins. In Bloom Al.ed. Hemostasis and thrombosis. 3rd 3d. New York, Churchill Livingstone. pp.167-181.

31. Tracy, P.B., Eide, L.L., Bowie E.J.W., and K.G. Mann. 1982. Radioimmunoassay of FV in human plasma and platelets. Blood. 60: 59-63.

32. Savage, B., and Z.M. Ruggeri. 1991. Selective recognition af adhesive sites in surface-bound fibrinogen by glycoprotein lib-IIIa on nonactivated platelets. J. Biol. Chem. 266: 11227-11233.

33. Deuel, T.F., Haung, J.S., Proffitt, R.T., Baenziger, J.U., Chang, D., and B.B. Kennedy. 1981. Human platelet-derived growth factor, purification and resolution into two active protein fractions. J. Bil. Chem. 256: 8896-8899.

34. Swords, N.A.,Tracy, P.B., and K.G. Mann. 1993. Intact platelet membrabes, not platelet-released microvesicles, support the procoagulant activity of adherent platelets. Arterioscler. Thromb. 13: 1613-22.

35. Mann, K.G. 1984. Membrane-bound enzyme complexes in blood coagulation. Prog. Hemost. Thromn. 7: 1-23.

36. Davie, E.W., and O.D. Ratnoff. 1964. Waterfall sequence of intrinsic blood clotting. Science. 145:1310-1312.

37. MacFarlane, R.G. 1964. An enzyme cascade in the blood clotting mechanism, and its function as a biochemical amplifier. Nature. 202: 498-499.

38. Mann, K.G., Nesheim, M.E., Church, W.R., and S. Krishnaswamy. 1990. Surface-dependent reactions of the vitamin K-dependent enzyme complexes. Blood. 76: 1-16.

39. Mann, K.G., Jenny, R.J., and S. Krishnaswamy. 1988. Cofactor proteins in the assembly and expression of blood clotting enzyme complexes. Annu. Rev. Biochem. 57: 915-956.

40. Mann, K.G., and L. Lorand. 1993. Blood Coagulation. Methods In Enzymology. 222: 1-15.

41. Kalafatis, M., Egan, J.O., van't Veer, C., Cawthern, K.M., and K.G. Mann. 1997. The Regulation of Clotting Factors. Critical Reviews in Eukaryotic Gene Expression. 7: 241-280.

42. Stubbs, M.T., and B. Wolfram. 1995. The clot thickens: clues provided by thrombin structure. TIBS. 20: 23-28.

43. Mann. K.G. 1992. The Coagulation Explosion. Annals New York Academy of Science. 265-269.

44. Kalafatis, M., Swords, N.A., Rand, M.D., and K.G. Mann. 1994. Membrane-dependent reactionns in blood coagulation: role of the vitamin K-dependent enzyme complexes. Biochemica et Biophysica Acta. 1227: 113-129.

45. Krishnaswamy, S., Nesheim, M.E., Pryzdial, E.L.G., and K.G. Mann. 1994. Assembly of the prothrombinase complex. Meth. Enz. 222: 260-280.

46. Rosing, J. and G. Tans. 1997. Coagulation factor V: an old star shines again Thromb. Haemost. 78: 427-433.

47. Kalafatis, M., Krishnaswamy, S., Rand, M.D., and K.G. Mann. 1993. Factor V. Methods in Enzymology. 222: 224-236.

48. Stoylova, S., Mann, K.G., and A. Brisson. 1994. Structure of membrane-bound human factor Va. FEBS Letters. 351: 330-334.

49. Mann, K.G., and M. Kalafatis. 2003. Factor V: a combination of Dr. Jekyll and Mr. Hyde. Blood. 101: 20-30.

50. Bouma, B.N., and J.C.M. Meijers. 1999. Fibrinolysis and the contact system: a role for Factor XI in the down-regulation of fibrinolysis. Thrombosis and Haemostasis. 82: 243-250.

51. Bouma, B.N., von dem Borne, P.A.K., and J.C.M. Meijers. 1998. Factor XI and protection of the fibrin clot against lysis-a role of the intrinsic pathway of coagulationn in fibrinolysis. Thrombosis and Haemostasis. 80: 24-27.

52. Broze, J.G. 1992. The role of tissue factor pathway inhibitor in a revised coagulation cascade. Semin. Hematol. 29: 159-169.

53. von dem Borne, P.A.K., Meijers, J.C.M., and B.N. Bouma. 1995. Feedback activation of Factor XI by thrombin results in additional formation of thrombin and protects fibrin clots from fibrinolysis. Blood. 86: 3035-3042.

54. Lai, T.S. 1994. Carboxyl-terminal truncation of recombinant FXIII A-chains. Characterization of minimum structural requirement for transglutaminase activity. J. Biol. Chem. 269: 24596.

55. Rocco, M. 1987. Models of fibronectin. EMBO J. 6: 2343-2349.

56. Mosher, D.F., and R.B., Johnson. 1983. Specificity of fibronectin-fibrin cross-linking. Ann NY Acad. Sci. 408: 583-594.

57. Furie, B., and B.C. Furie. 1995. Molecular basis of blood coagulation. Hematology:Basic principles and practice 2nd ed. Ronald, H., and J. Edward eds. New York, Churchill Livingstone.

58. Nesheim, M.E., Taswell, J.B., and K.G. Mann, 1979. The contribution of bovine Factor V and Factor Va to the activity of prothrombinase. J. Biol. Chem. 254: 10952-10962.

59. Ahmad, S.S., Rawala-Sheikh, R., and P.N. Walsh. 1992. Components and assembly of the factor X activating complex. Semin Thromb Hemost. 8: 311-323.

60. Davie, E.W., Fujikawa, K., and W. Kisiel. 1991. The coagulation cascade: initiation, maintenance, and regulation. Biochemistry 30: 10363-10370.

61. Furie, B., and B. C. Furie. 1988. The molecular basis of blood coagulation. Cell 53: 505-518.

62. Altieri, D. C.. 1995. Inflammatory cell participation in coagulation. Semin. Cell. Biol. 6: 269-274.

63. Nicholson, A. C., Nachman, R.L., Altieri, D.C., Summers, B.D., Ruf, W., Edgington, T.S., and D. P. Hajjar. 1996. Effector cell protease receptor-1 is a vascular receptor for coagulation factor Xa. J. Biol. Chem. 45:28407-28413.

64. Altieri, D. C., and T. S. Edgington. 1990. Identification of effector cell protease receptor-1: a leukocyte-distributed receptor for the serine protease factor Xa. J. Immunol. 145: 246-253.

65. Altieri, D. C. 1994. Molecular cloning of effector cell protease receptor-1, a novel cell surface receptor for the protease factor Xa. J. Biol. Chem. 269: 3139-3142.

66. Cirino, G., Cicala, C., Bucci, M., Sorrentino, L., Ambrosini, G., DeDominicis, G., and D. C. Altieri. 1997. Factor Xa as an interface between coagulation and inflammation: molecular mimicry of factor Xa association with effector cell protease receptor-1 induces acute inflammation in vivo. J. Clin. Invest. 99: 2446-2451.

67. Kalafatis, M., Egan, J.O., van't Veer, C., and K.G. Mann. 1996. Regulation and regulatory role of gamma-carboxyglutamic acid containing clotting factors. Critical Reviews in Eukaryotic Gene Expression. 61(1): 87-101.

68. Vogel, C.N., Butkowski R.J., Mann K.G., and R.L Lundblad. 1976. Effect of polylysine on the activation of prothrombin. Polylysine substitutes for calcium

ions and factor V in the factor Xa catalyzed activation of prothrombin. Biochemistry. 15: 3265-9.

69. Heldebrant CM, and K.G. Mann. 1973. The activation of prothrombin. I. Isolation and preliminary characterization of intermediates. J Biol Chem. 248: 3642-3652.

70. Westcott, R.J., Cheetham, P.S.J., and A.J. Barraclough. 1994. Phytochemistry. 35: 135-138.

71. Baglin T.P., Carrell R.W., Church F.C., Esmon C.T., and J.A. Huntington. 2002. Crystal structures of native and thrombin-complexed heparin cofactor II reveal a multistep allosteric mechanism. Proc Natl Acad Sci U S A. 99: 11079-84.

72. Platt, E. 1993. The comparison of an interim tertiary predicted model of bovine thrombin and the x-ray structure of human thrombin. Adv Exp Med Biol. 340:79-81.

73. Riley, K.A., and D.H. Kleyn. 1989. Food Technol. 43: 64-77.

74. Wu K.K., and N. Matijevic-Aleksic. 2000. Thrombomodulin: a linker of coagulation and fibrinolysis and predictor of risk of arterial thrombosis. Ann Med. 1: 73-7.

75. Ohlin A.K., Norlund L., and R.A. Marlar. 1997. Thrombomodulin gene variations and thromboembolic disease. Thromb Haemost. 78: 396-400.

76. Qingyu, W., Tsiang, M., Lentz, S.R., and J.E. Sadler. 1992. Ligand specificity of human thrombomodulin. J. Biol. Chem. 267: 7083-7088.

77. Davie E.W., and K. Fujikawa. 1975. Basic mechanisms in blood coagulation. Annu Rev Biochem. 44: 799-829.

78. Seshadri, T.P., Tulinski, A., Skrzypczak-Junkun, E., and C.H. Park. 1991. Structure of bovine prothrombin fragment 1 refined at 2.25 A resolution. J. Mol. Biol. 220: 481-494.

79. Soriano-Gracia, M., Padmanabhan, K., deVos, A.M., and A. Tulinski. 1992. The Ca2+ ion and membrane binding structure of the Gla domain of Ca-prothrombin fragment 1. Biochemistry. Biochemistry. 31: 2554-2566.

80. Park, C.H., and A. Tulinski. 1986. Three dimentional structure of the Kringle sequence: structure of prothrombin fragment I. Biochemistry. 25: 3977-3982.

81. Owren PA. 1947. Parahaemophila: haemorrhagic diathesis due to absence of a previously unknown clotting factor. Lancet. 1993: 446-448.

82. Owren PA, T. Cooper. 1955. Parahemophilia. Arch Intern Med. 95: 194-201.

83. Jenny, R.J., and K.G. Mann. 1989. Factor V: a prototype pro-cofactor for vitamin K-dependent enzyme complexes in blood clotting. Clinical Haematology. 4: 919-943.

84. Seegers W.H., Marciniak E., and D. Heene. 1965. Enzyme basis of prothrombin activation (blood clotting) with an analysis of hemophilia B. Tex Rep Biol Med. 23: 675-704.

85. Hanahan D.J., and D. Papahadjopoulos. 1965. Interactions of phospholipids with coagulation factors. Thromb Diath Haemorrh Suppl. 17: 71-84.

86. Cole E.R., Koppel J.L., and J.H. Olwin. 1965. Phospholipid-protein interactions in the formation of prothrombin activator. Thromb Diath Haemorrh. 14: 431-44.

87. Mann, K.G., Nesheim, M.E., and P.B. Tracy. 1986. Nonenzymatic cofactors: Factor V. In Blood Coagulation. Zwaal, R.F.A., and H.C. Hemker, eds. p.p. 15-34.

88. Kane, W.H., and E.W. Davie. 1986. Cloning of a cDNA coding for human factor V, a blood coagulation factor homologous to factor VIII and ceruloplasmin. Proc. Natl. Acad. Sci. USA. 83: 6800-6804.

89. Jenny, R.J., Pittman D.D., Toole J.J., Kriz. R.W., Aldape R.A., Hewick R.M., Kaufman R.J., and K.G. Mann. 1987. Complete cDNA and derived amino acid sequence of human factor V. Proc. Natl. Acad. Sci. U.S.A. 84: 4846-4850.

90. Kane W.H., Ichinose A., Hagen F.S., Davie E.W. 1987. Cloning of cDNAs coding for the heavy chain region and connecting region of human factor V, a blood coagulation factor with four types of internal repeats. Biochemistry. 26: 6508-6514.

91. Kane W.H., Ichinose A., Hagen F.S., and E.W. Davie. 1987. Cloning of cDNAs coding for the heavy chain region and connecting region of human Factor V, a blood coagulation factor with four types of internal repeats. Biochemistry. 26: 6508-6514.

92. Xue J., Kalafatis M., and K.G. Mann. 1993. Determination of the disulfide bridges in factor Va light chain. Biochemistry. 32: 5917-5923.

93. Xue J., Kalafatis M., Silveira J.R., Kung C., and K.G. Mann. 1994. Determination of the disulfide bridges in factor Va heavy chain. Biochemistry. 33: 13109-13116.

94. Thorelli, T., 1999. Mechanisms that regulate the anticoagulant function of coagulation FV. Scand J. Clin. Lab Invest. 59: 19-26.

95. Francis R.T., McDonagh J., and K.G. Mann. 1986. Factor V is a substrate for the transamidase factor XIIIa. J. Biol. Chem. 261: 9787-92.

96. Huh MM, Schick BP, Schick PK, Colman RW. 1988. Covalent crosslinking of human coagulation factor V by activated factor XIII from guinea pig megakaryocytes and human plasma. Blood. 71: 1693-702.

97. Thorelli E., Kaufman R.J., and B. Dahlback. 1998. The C-terminal region of the factor V B-domain is crucial for the anticoagulant activity of factor V. J Biol Chem. 273:16140-16145.

98. Esmon C.T. 1979. The subunit structure of thrombin-activated factor V. Isolation of activated factor V, separation of subunits, and reconstitution of biological activity. J. Biol. Chem. 254: 964-973.

99. Mann K.G., Nesheim M.E., Hibbard L.S., and P.B. Tracy. 1981. The role of factor V in the assembly of the prothrombinase complex. Ann. NY. Acad. Sci. 370: 378-88.

100. Nesheim, M.E., Myrmel K.H., Hibbard, L., and K.G. Mann. 1979. Isolation and characterization of single chain bovine factor V. J. Biol. Chem. 254: 508-517.

101. Mann, K.G., Nesheim, M.E., and P.B. Tracy. 1981. Molecular weight of undegraded plasma factor v. Biochemistry. 20: 28-33.

102. Dahlback, B., 1985. Ultrastructure of human coagulation factor V. J. Biol. Chem. 260: 1347-1349

103. Mosesson, M.W., Nesheim, M.E., DiOrio, J., Hainfeld, J.F., Wall, J.S., and K.G. Mann. 1985. Studies on the structure of bovine factor V by scanning transmission electron microscopy. Blood. 65: 1158-1162.

104. Dahlback, B., 1986. Bovine coagulation factor V visualized with electron microscopy. J. Biol. Chem. 261: 9495-9501.

105. Mosesson M.W., Church W.R., DiOrio J.P., Krishnaswamy S., Mann K.G., Hainfeld J.F., and J.S. Wal. 1990. Structural model of factors V and Va based on scanning transmission electron microscope images and mass analysis. J Biol Chem. 265:8863-8688.

106. Stoylova S., Mann K.G., and A. Brisson. 1994. Structure of membrane-bound human factor Va. FEBS Lett. 351: 330-334.

107. Villoutreix, B.O., and B. Dahlbach. 1998. Structural investigation of the A domains of human blood coagulation factor V by molecular modeling. Protein Science. 7: 1317-1325.

108. Pellequer, J., Gale, A.J., Getzoff, E.D., and J.H. Griffin. 1999. Three-dimantional homology model of the complete coagulation factor Va molecule in complex with activated protein C. Thrombosis & Haemostasis (supplement) 8: 34

109. Pellequer, J.L., Gale, A. J., Getzoff, E. D. and J.H. Griffin. 2000. Three-dimensional model of coagulation factor Va bound to activated protein C. Thromb. Haemostasis 84: 849-857.

110. Nesheim M.E., and K.G. Mann. 1979. Thrombin-catalyzed activation of single chain bovine factor V. J Biol Chem. 254:1326-1334.

111. Foster W.B., Tucker M.M., Katzmann J.A., and K.G. Mann. 1983. Monoclonal antibodies selective for activated Factor V. Immunochemical probes for structural transitions occurring during the thrombin-catalyzed activation of the procofactor. J Biol Chem. 258: 5608-13.

112. Esmon, C. T. 1979 The subunit structure of thrombin-activated factor V. Isolation of activated factor V, separation of subunits, and reconstitution of biological activity. J. Biol. Chem. 254: 964-973.

113. Nesheim M.E., Foster W.B., Hewick R., and K.G. Mann. 1984. Characterization of factor V activation intermediates. J Biol Chem. 259: 3187-3196.

114. Higgins, D. L., and K. G. Mann. 1983. The Interaction of Bovine Factor V and Factor V-derived Peptides with Phospholipid Vesicles. J. Biol. Chem. 258: 6503-6508.

115. Krishnaswamy, S., Russell. G.D., and K.G. Mann. 1989. The reassociation of factor Va from its isolated subunits. J. Biol. Chem. 264: 3160-3168.

116. Guinto E.R., and C.T. Esmon. 1982. Formation of a calcium-binding site on bovine activated factor V following recombination of the isolated subunits. J. Biol. Chem. 257: 10038-10043.

117. Kalafatis, M., and K.G. Mann. 1997. Proteolytic alterations of membrane-bound factor Va during inactivation by plasmin. Thrombosis and Haemostasis (supplement). PS-2503.

118. Hockin M.F., Jones K.C., Everse S.J., and K.G. Mann. 2002. A model for the stoichiometric regulation of blood coagulation. J Biol Chem. 277:18322-18333.

119. Brummel K.E., Paradis S.G., Butenas S., and K.G. Mann. 2002. Thrombin functions during tissue factor-induced blood coagulation. Blood. 100:148-152.

120. Camire R.M., Kalafatis M., and P.B. Tracy. 1998. Proteolysis of factor V by cathepsin G and elastase indicates that cleavage at Arg1545 optimizes cofactor function by facilitating factor Xa binding. Biochemistry. 37: 11896-906.

121. Allen D.H., and Tracy P.B. 1995. Human coagulation factor V is activated to the functional cofactor by elastase and cathepsin G expressed at the monocyte surface. J. Biol. Chem. 270: 1408-15.

122. Bradford H.N., Annamalai A., Doshi K., and R.W. Colman. 1988. Factor V is activated and cleaved by platelet calpain: comparison with thrombin proteolysis. Blood. 71: 388-394.

123. Rodgers G.M., Cong J.Y., Goll D.E., and W.H. Kane. 1987. Activation of coagulation factor V by calcium-dependent proteinase. Biochim Biophys Acta. 929: 263-270.

124. Tracy, P.B, and K.G. Mann. 1983. Prothrombinase complex assembly on the platelet surface is mediated through the 74,000-dalton component of factor Va. Proc. Natl. Acad. sCi. U.S.A. 80: 2380-2384.

125. Rodgers, G.M., and W.H. Kane. 1986. Activation of endogenous factor V by a homocysteine-induced vascular endothelial cell activator. Journal of Clinical Investigation. 77:1909-1916.

126. Hibbard L.S., and K.G. Mann. 1980. The calcium-binding properties of bovine factor V. J. Biol. Chem. 255: 638-645.

127. Guinto, E. R. and Esmon, C. T. 1982. Formation of a calcium-binding site on bovine activated factor V following recombination of the isolated subunits. J. Biol. Chem. 257: 10038-10043.

128. Krishnaswamy S., Jones K.C., and K.G. Mann. 1988. Prothrombinase complex assembly. Kinetic mechanism of enzyme assembly on phospholipid vesicles. J Biol Chem. 263: 3823-3834.

129. Mann, K. G., Lawler, C. M., Vehar, G. A. and W.R. Church. 1984. Coagulation Factor V contains copper ion. J. Biol. Chem. 259: 12949-12951.

129a. Villoutreix, B. O. and B. Dahlback. 1998. Structural investigation of the A domains of human blood coagulation factor V by molecular modeling. Prot. Sci. 7: 1317-1325.

130. Day W.C., and P.G. Barton. 1971. Studies on the stability of bovine plasma factor V. Biochim Biophys Acta. 261: 457-468.

131. Foster W.B., Tucker M.M., Katzmann J.A., Miller R.S., Nesheim M.E., and K.G. Mann. 1983. Monoclonal antibodies to human coagulation factor V and factor Va. Blood. 61:1060-1067.

132. Krishnaswamy, S., and K.G. Mann. 1988. The binding of factor Va to phospholipid vesicles. J. Biol. Chem. 263: 5714-5723.

133. Kalafatis M., Jenny R.J., and K.G. Mann. 1990. Identification and characterization of a phospholipid-binding site of bovine factor Va. J Biol Chem. 265: 21580-21589.

134. Ortel T.L., Quin-Allen M.A., Keller F.G., Peterson J.A., Larocca D., and W.H. Kane. 1994. Localization of functionally important epitopes within the second C-type domain of coagulation factor V using recombinant chimeras. J Biol Chem. 269: 15898-15905.

135. Ortel T.L., Quinn-Allen M.A., Charles L.A., Devore-Carter D., and W.H. Kane. 1992. Characterization of an acquired inhibitor to coagulation factor V: antibody binding to the second C-type domain of factor V inhibits the binding of factor V to phosphatidylserine and neutralizes procoagulant activity. J Clin Invest. 90: 2340-2347.

136. Lecompte M.F., Bouix G., and K.G. Mann. 1994. Electrostatic and hydrophobic interactions are involved in factor Va binding to membranes containing acidic phospholipid. J Biol Chem. 269: 1905-1910.

137. Kim S.W., Quin-Allen M.A., and J.T. Camp. 2000. Identification of functionally important amino acid residues within the C2-domain of human factor V using alanine-scanning mutagenesis. Biochemistry. 39: 1951-1958.

138. Izumi T., Kim S.W., and A. Greist. 2001. Fine mapping of inhibitory anti-factor V antibodies using factor V C2 domain mutants: identification of two antigenic epitopes involved in phospholipid binding. Thromb Haemost. 85: 1048-1054.

139. Tracy PB, Peterson JM, Nesheim ME, McDuffie FC, Mann KG. Interaction of coagulation factor V and factor Va with platelets. J Biol Chem. 1979 Oct 25;254(20):10354-61

140. Tracy P.B., Nesheim M.E., and K.G. Mann. 1981. Coordinate binding of factor Va and factor Xa to the unstimulated platelet. J Biol Chem. 256: 743-751

141. Rosing, J., Bakker, H.M., Christella, M., Thomassen, L.G.D., Hemker, H.C., and G. Tans. 1993. Characterization of two forms of human factor Va with different cofactor activities. J. Biol. Chem. 268: 2113021136.

142. Hoekema, L., Nicolaes, G.A.F., Hemker, H.C., Tans, G., and J. Rosing.1997. Human factor Va1 and factor Va2: Properties in the procoagulant and anticoagulant pathways. Biochem. 36: 3331-3335.

143. Kim, S.W., Ortel, T.L., Quinn-Allen, M., Yoo, L., Worfolk, L., Zhai, X., Lentz, B.R., and W.H. Kane. 1999. Prtial glycosylation at Aspargine-2181 of the second C-type Domain of human factor V modulates assembly of the prothrombinase complex. Biochem. 38: 11448-11454.

144. Nicolaes, G.A., Villoutreix, B.O., and B. Dahlbach. 1999. Partial glycosylation of Asn2181 in human factor V as a cause of molecular and functional heterogeneity. Modulation of glycosylation efficiency by mutagenesis of the consensus sequence for N-linked glycosylation. *Biochemistry* 38: 13584-13591.

145. Krishnaswamy, S., Nesheim, M. E., Pryzdial, E. L.G. and K.G. Mann. 1993. Assembly of prothrombinase complex. Meth. Enzymol. 222: 260-280.

146. Pryzdial, E. L. G. and K.G. Mann. 1991. The association of coagulation factor-Xa and factor-Va. J. Biol. Chem. 266: 8969-8977.

147. Krishnaswamy S., Mann K.G., and M.E. Nesheim. 1986. The prothrombinase-catalyzed activation of prothrombin proceeds through the intermediate meizothrombin in an ordered, sequential reaction. J. Biol. Chem. 261: 8977-8984.

148. Krishnaswamy S. 1990. Prothrombinase complex assembly: contributions of protein-protein and protein-membrane interactions toward complex formation. J. Biol. Chem. 1990. 265: 3708-3718.

149. Krishnaswamy, S., and R.K. Walker. 1997. Contribution of the prothrombin fragment 2 domain to the function of factor Va in the prothrombinase complex. Biochemistry. 36: 3319-3330.

150. Rosing, J., Tans, G., Govers-Riemslag, J. W., Zwaal, R. F., and H.C. Hemker. 1980. The role of phospholipids and factor Va in the prothrombinase complex. J. Biol. Chem. 255: 274-283.

151. Blostein M.D., Rigby A.C., Jacobs M., Furie B., and B.C. Furie. 2000. The Gla domain of human prothrombin has a binding site for factor Va. J Biol Chem. 275: 38120-6.

152. Nesheim, M.E., Canfield, W.M., Kisiel, W., and K.G., Mann. 1982. Stusdies of the capacity of Fxa to protect Factor Va from inactivation by activated protein C. J. Biol. Chem. 257: 1443-1447.

153. Suzuki, K., Stenflo, J., Dahlback, B., and B. Teodorsson. 1983. Inactivation of human coagulation factor V by activated protein C. J. Biol. Chem. 258: 1914-1920.

154. Esmon, C.T., 1989. The roles of protein C and thrombomodulin in the regulation of blood coagulation. J. Biol. Chem. 264: 4743-4746.

155. Egan J.O., Kalafatis M., Mann K.G. 1997. The effect of Arg306-->Ala and Arg506-->Gln substitutions in the inactivation of recombinant human factor Va by activated protein C and protein S. Protein Sci. 6: 2016-2027.

156. Regan L.M., Lamphear B.J., Huggins C.F., Walker F.J., and P.F. Fay. 1994. Factor IXa protects factor VIIIa from activated protein C. Factor IXa inhibits activated protein C-catalyzed cleavage of factor VIIIa at Arg562. J. Biol. Chem. 269: 9445-9452.

157. Rezaie A.R., Cooper S.T., Church F.C., and C.T. Esmon. 1995. Protein C inhibitor is a potent inhibitor of the thrombin-thrombomodulin complex. J. Biol. Chem. 270: 25336-25339.

158. Bourin M.C., and U. Lindahl. 1993. Glycosaminoglycans and the regulation of blood coagulation. Biochem J. 289: 313-330.

159. Stearns-Kurosawa D.J., Kurosawa S., Mollica J.S., Ferrell G.L., and C.T. Esmon. 1996. The endothelial cell protein C receptor augments protein C activation by the thrombin-thrombomodulin complex. Proc Natl Acad Sci U S A. 93: 10212-10216.

160. Xu J., Esmon N.L., and C.T. Esmon. 1999. Reconstitution of the human endothelial cell protein C receptor with thrombomodulin in phosphatidylcholine vesicles enhances protein C activation. J. Biol. Chem. 274: 6704-6710.

161. Hanson S.R., Griffin J.H., Harker L.A., Kelly A.B., Esmon C.T., and A. Gruber. 1993. Antithrombotic effects of thrombin-induced activation of endogenous protein C in primates. J. Clin. Invest. 92: 2003-2012.

162. Heeb M.J., and J.H. Griffin. 1988. Physiologic inhibition of human activated protein C by alpha 1-antitrypsin. J. Biol. Chem. 263:11613-11616.

163. Scully M.F., Toh C.H., Hoogendoorn H., Manuel R.P., Nesheim M.E., Solymoss S., and A.R. Giles. 1993. Activation of protein C and its distribution between its inhibitors, protein C inhibitor, alpha 1-antitrypsin and alpha 2-macroglobulin, in patients with disseminated intravascular coagulation. Thromb Haemost. 69: 448-453.

164. Walker F.J., 1980. Regulation of activated protein C by a new protein. A possible function for bovine protein S. J. Biol. Chem. 255: 5521-5524.

165. Rosing J., Hoekema L., Nicolaes G.A., Thomassen M.C., Hemker H.C., Varadi K., Schwarz H.P., and G. Tans. 1995. Effects of protein S and factor Xa on peptide bond cleavages during inactivation of factor Va and factor aR506Q by activated protein C. J. Biol. Chem. 270: 27852-27858.

166. Sun Z., Chen Y.H., Wang P., Zhang J., Gurewich V., Zhang P., Liu J.N. 2002. The blockage of the high-affinity lysine binding sites of plasminogen by EACA significantly inhibits prourokinase-induced plasminogen activation. Biochim Biophys Acta. 1596: 182-192.

167. Bok R.A., and W.F. Mangel. 1985. Quantitative characterization of the binding of plasminogen to intact fibrin clots, lysine-sepharose, and fibrin cleaved by plasmin. Biochemistry. 24: 3279-3286.

168. Kalafatis M., and K.G. Mann. 2001. The role of the membrane in the inactivation of factor Va by plasmin: amino acid region 307-348 of factor V plays a critical role for factor Va cofactor function. J. Biol. Chem. 276: 18614-18623.

169. Laake, K., and B. Osterud. 1974. Activation of purified plasma factor VII by human plasmin, plasma kallikrein, and activated components of the human intrinsic blood coagulation system. Thromb. Res. 5: 759-772.

170. Rick, M.E., and D.M. krizek. 1986. Platelets modulate the proteolysis of factor VIII:C protein by plasmin. Blood 67: 1649-1654.

171. Osterud, B., Laake K., and H. Prydz. 1975. The activation of human factor IX. Thromb. Diath. Haemorrh. 33: 553-563.

172. Samis, J.A., Ramsey G.D., Walker J.B., Nesheim M.E., and A.R. Giles. 2000. Proteolytic processing of human coagulation factor IX by plasmin. Blood 95: 943-951.

173. Pryzdial, E.L.G., and G.E. Kessler. 1996. Autoproteolysis or plasmin-mediated cleavage of factor Xa exposes a plasminogen binding site and inhibits coagulation. J. Biol. Chem. 271: 16614-16620.

174. Ewald, G.A., and P.R. Eisenberg. 1995. Plasmin-mediated activation of the contact system in response to pharmacological thrombosis. Circulation. 91: 28-36.

175. Hekman C.M., and D.J. Loskutoff. 1987. Fibrinolytic pathways and the endothelium. Semi. Thromb. Hemost. 13: 514-527.

176. Fisher R., Waller E.K., Grossi G., Thompson D., Tizard R., and W.D. Schleuning. 1985. Isolation and characterization of the human tissue-type plasminogen activator structural gene including its 5' flanking region. J. Biol. Chem. 260: 11223-11230.

177. Fisher R., Waller E.K., Grossi G., Thompson D., Tizard R., Schleuning W.D., van Zonneveld A.J., Eerman H., MacDonald M.E., van Mourik J.A., and H. Pannekoek.1986. Structure and function of human tissue-type plasminogen activator (t-PA). J. Cell Biochem. 32: 169-178.

178. Lamba D., Bauer M., Huber R., Fischer S., Rudolph R., Kohnert U., and W. Bode. 1996. The 2.3 A crystal structure of the catalytic domain of recombinant two-chain human tissue-type plasminogen activator. J. Mol. Biol. 258: 117-135.

179. Stubbs M.T., Renatus M., and W. Bode. 1998. An active zymogen: unravelling the mystery of tissue-type plasminogen activator. J. Biol Chem. 379: 95-103

180. Ranby M. 1982. Studies on the kinetics of plasminogen activation by tissue plasminogen activator. Biochim Biophys Acta. 704: 461-469.

181. MacDonald M.E., van Zonneveld A.J., and H. Pannekoek. 1986. Functional analysis of the human tissue-type plasminogen activator protein: the light chain. Gene. 42: 59-67.

182. Teuten A.J., Smith R.A., and C.M. Dobson. 1991. Domain interactions in human plasminogen studied by proton NMR. FEBS Lett. 278: 17-22

183. Collen, D. 1999. The plasminogen (fibrinolytic) system. Thrombosis and haemostasis. 82: 259-270.

184. Miles L.A., Castellino F.J., and Y. Gong. 2003. Critical role for conversion of glu-plasminogen to lys-plasminogen for ptimal stimulation of plasminogen activation on cell surfaces. Trends Cardiovasc Med. 13: 21-30.

185. Gong Y., Kim S.O., Felez J., Grella D.K., Castellino F.J., and L.A. Miles. 2001. Conversion of Glu-plasminogen to Lys-plasminogen is necessary for optimal stimulation of plasminogen activation on the endothelial cell surface. J. Biol. Chem. 276: 19078-19083.

186. Christensen U. 1984. The AH-site of plasminogen and two C-terminal fragments. A weak lysine-binding site referring ligands not carrying a free carboxylate function. Biochem J. 223: 413-421.

187. Christensen U. 1985. C-terminal lysine residues of fibrinogen fragments essential for binding to plasminogen. FEBS Lett. 182: 43-46.

188. Laffan M., 1998. Tuddenham E Science, medicine, and the future: assessing thrombotic risk. BMJ. 317: 520-523.

189. Collen, D. 1980. On the regulation and control of fibrinolysis. Edward Kowalski Memorial Lecture. Thromb Haemost. 43: 77-89.

190. Edlund T., Ny T., Ranby M., Heden L.O., Palm G., Holmgren E., and S. Josephson. 1983. Isolation of cDNA equences coding for a part of human tissue plasminogen activator. Proc. Natl. Acad. Sci. USA. 80: 349-352.

191. Ny T., Elgh F., and B. Lund. 1984. The structure of the human tissue-type plasminogen activator gene: correlation of intron and exon structures to functional and structural domains. Proc. Natl. Acad. Sci. USA. 81: 5355-5359.

192. Madison E.L., Kobe A., Gething M.J., Sambrook J.F., and E.J Goldsmith. 1993. Converting tissue plasminogen activator to a zymogen: a regulatory triad of Asp-His-Ser. Science. 262: 419-421.

193. Gerard R.D., and R.S. Meidell. 1989. Regulation of tissue plasminogen activator expression. Annu Rev Physiol. 51: 245-262.

194. van Zonneveld A.J., Veerman H., MacDonald M.E., van Mourik J.A., and H. Pannekoek. 1986. Structure and function of human tissue-type plasminogen activator (t-PA). J. Cell. Biochem. 32: 169-178.

195. Harpel P.C., Chang T.S., and E. Verderber. 1985. Tissue plasminogen activator and urokinase mediate the binding of Glu-plasminogen to plasma fibrin I. Evidence for new binding sites in plasmin-degraded fibrin I. J. Biol. Chem. 260: 4432-4440.

196. Woodhouse K.A., Weitz J.I., and J.L. Brash. 1996. Lysis of surface-localized fibrin clots by adsorbed plasminogen in the presence of tissue plasminogen activator. Biomaterials. 17: 75-77.

197. Collen D. 1986. Tissue-type plasminogen activator (t-PA) and single chain urokinase-type plasminogen activator (scu-PA): potential for fibrin-specific thrombolytic therapy. Prog Hemost Thromb. 8 :1-18.

198. Blasi F., Vassalli J.D., and K. Dano. 1987. Urokinase-type plasminogen activator: proenzyme, receptor, and inhibitors. J. Cell. Biol. 104: 801-804.

199. Lijnen H.R., Stump D.C., and D.C. Collen. 1987. Single-chain urokinase-type plasminogen activator: mechanism of action and thrombolytic properties. Semin Thromb Hemost. 13:152-159.

200. Diefenbach C., Erbel R., Pop T., Mathey D., Schofer J., Hamm C., Ostermann H., Schmitz-Hubner U., Bleifeld W., and J. Meyer. 1988. Recombinant single-chain urokinase-type plasminogen activator during acute myocardial infarction. Am. J. Cardiol. 61: 966-970.

201. Dear A.E., and R.L. Medcalf. 1998. The urokinase-type-plasminogen-activator receptor (CD87) is a pleiotropic molecule. Eur J Biochem. 252: 185-193.

202. Wolf B.B., and M.D. Brown. 1995. Epidermal growth factor-binding protein activates soluble and receptor-bound single chain urokinase-type plasminogen activator. FEBS Lett. 376: 177-180.

203. Schenk-Braat E.A., Morser J., and D.C. Rijken. 2001. Identification of the epidermal growth factor-like domains of thrombomodulin essential for the acceleration of thrombin-mediated inactivation of single-chain urokinase-type plasminogen activator. Eur J Biochem. 268: 5562-5569.

204. Ellis V., Scully M.F., and V.V Kakkar. 1989. Plasminogen activation initiated by single-chain urokinase-type plasminogen activator. Potentiation by U937 monocytes. J Biol Chem. 264: 2185-21888.

205. Hajjar, D.A., and J.C. Jacovina. 1994. An endothelial cell receptor for plasminogen/tissue plasminogen activator: identity with annexin II. J. Biol. Chem. 269: 21191-21198.

206. Kassam G., Choi K.S., Ghuman J., Kang H.M., Fitzpatrick S.L., Zackson T., Zackson S., Toba M., Shinomiya A., and D.M. Waisman. 1998. The role of annexin II tetramer in the activation of plasminogen. J Biol Chem. 273: 4790-4799.

207. Miles L.A., Dahlberg C.M., Plescia J., Felez J., Kato K., and E.F. Plow. 1991. Role of cell-surface lysines in plasminogen binding to cells: identification of alpha-enolase as a candidate plasminogen receptor. Biochemistry. 30: 1682-1691.

208. Dudani A.K., Cummings C., Hashemi S., and P.R. Ganz. 1993. Isolation of a novel 45 kDa plasminogen receptor from human endothelial cells. Thromb Res. 69: 185-196.

209. Dudani A.K., Pluskota A., and P.R. Ganz. 1994. Interaction of tissue plasminogen activator with a human endothelial cell 45-kilodalton plasminogen receptor. Biochem Cell Biol. 72: 126-131.

210. Kelm R.J., Swords N.A., Orfeo T., and K.G. Mann. 1994. Osteonectin in matrix remodeling. A plasminogen-osteonectin-collagen complex. J Biol Chem. 269: 30147-30153.

211. Reinartz J., Hansch G.M., and M.D. Kramer. 1995. Complement component C7 is a plasminogen-binding protein. J Immunol. 154: 844-850.

212. Cesarman G.M., Guevara C.A., and K.A. Hajjar. 1994. An endothelial cell receptor for plasminogen/tissue plasminogen activator (t-PA). II. Annexin II-mediated enhancement of t-PA-dependent plasminogen activation. J Biol Chem. 269: 21198-21203.

213. Collen D., and H.R. Lijnen. 1991. Basic and clinical aspects of fibrinolysis and thrombolysis. Blood. 78: 3114-3124.

214. Birkedal-Hansen H. 1995. Proteolytic remodeling of extracellular matrix. Curr Opin Cell Biol. 7:728-735.

215. Lee DH, K.D., Kim H.G., Choi S.J., Jung S.M., Ryu D.S., and M.S. Park. 2002. Local intraarterial urokinase thrombolysis of acute ischemic stroke with or without intravenous abciximab: a pilot study. J Vasc Interv Radiol. 13: 769-774.

216. Collen, D. 1996. Fibrin-selective thrombolytic therapy for acute myocardial infarction. Circulation. 93: 857-865.

217. Collen, D., and M. Verstraete. 1983. Systemic thrombolytic therapy of acute myocardial infarction. Circulation. 68:462-465

218. Callif, R.M. 1997. The Gusto trial and open artery theory. Eur. Heart J. 18(supplement):F2

219. Moser, M., Kohler, B.,Schmittner, M.,and C. Bode. 1998. Recombinant plasminogen activators – A comparative review of the clinical pharmacology and therapeutic use of alteplase and reteplase. Biodrugs. 9: 455-458.

220. Horrevoets A.J.G., Pannekoek H., M.E. Nesheim. 1996. A Steady-state Template Model That Describes the Kinetics of Fibrin-stimulated J Biol Chem. 272: 2183-2191.

221. Bell, W.R. 1997. Evaluation of thrombolytic agents. Drugs 54 (supplement 3):11

222. Smalling, R.W. 1997. Pharmacological and clinical impact of the unique molecular structure of a new plasminogen activator. Eur. Heart J. 18 (supplement F): F11

223. Al-Shwafi K.A., de Meester A., Pirenne B., and J.J. Col. 2003. Comparative fibrinolytic activity of front-loaded alteplase and the single-bolus mutants tenecteplase and lanoteplase during treatment of acute myocardial infarction. Am Heart J. 145: 217-225.

224. Collen, D., 1991. Towards better thrombolytic therapy. Prog. Cardiovasc. Dis. 34: 101-112.

225. Collen D., Vanderschueren S., and F. Van de Werf. 1996. Fibrin-selective thrombolytic therapy with recombinant staphylokinase. Haemostasis. 26 Suppl 4: 294-300.

226. Vanderschueren S., Collen D., and F. van de Werf. 1996. A pilot study on bolus administration of recombinant staphylokinase for coronary artery thrombolysis. Thromb Haemost. 76: 541-544.

227. Tait J.F., Engelhardt S., Smith C., and K. Fujikawa. 1995. Prourokinase-annexin V chimeras. Construction, expression, and characterization of recombinant proteins. J Biol Chem. 270: 21594-21599.

228. Tanaka K., Einaga K., Tsuchiyama H., Tait J.F., and K. Fujikawa. 1996. Preparation and characterization of a disulfide-linked bioconjugate of annexin V with the B-chain of urokinase: an improved fibrinolytic agent targeted to phospholipid-containing thrombi. Biochemistry. 35: 922-929.

229. Montoney M., Gardell S.J., and V.J. Marder. 1995. Comparison of the bleeding potential of vampire bat salivary plasminogen activator versus tissue plasminogen activator in an experimental rabbit model. Circulation. 91:1540-1544.

230. Gardell S.J., Hare T.R., Bergum P.W., Cuca G.C., O'Neill-Palladino L., and S.M. Zavodny. 1990. Vampire bat salivary plasminogen activator is quiescent in human plasma in the absence of fibrin unlike human tissue plasminogen activator. Blood. 76: 2560-2564.

231. Collen, D., and E. Haber. 1998. The fibrinolytic system and thrombolytic therapy. In. Chien K.R. ed. Molecular Basis of Cardiovascular Disease. Saunders, W.B., Philadelphia. p.p.537-565.

232. Bajzar L., Manuel R., and M.E. Nesheim. 1995. Purification and characterization of TAFI, a thrombin-activable fibrinolysis inhibitor. J Biol Chem. 270: 14477-14484.

233. Bajzar L., Morser J., and M. Nesheim. 1996. TAFI, or plasma procarboxypeptidase B, couples the coagulation and fibrinolytic cascades through the thrombin-thrombomodulin complex. J Biol Chem. 271: 16603-16608.

234. Fukushima M., Nakashima Y., and K. Sueishi. 1989. Thrombin enhances release of tissue plasminogen activator from bovine corneal endothelial cells. Invest Ophthalmol Vis Sci. 30: 1576-1583.

235. Dichek D., and T. Quertermous. 1989. Thrombin regulation of mRNA levels of tissue plasminogen activator and plasminogen activator inhibitor-1 in cultured human umbilical vein endothelial cells. Blood. 74: 222-228.

236. Grulich-Henn J., and G. Muller-Berghaus. 1990. Regulation of endothelial tissue plasminogen activator and plasminogen activator inhibitor type 1 synthesis by diacylglycerol, phorbol ester, and thrombin. Blut. 61: 38-44.

237. Pryzdial E.L., Lavigne N., Dupuis N., and G.E. Kessler. 1999. Plasmin converts factor X from coagulation zymogen to fibrinolysis cofactor. J Biol Chem. 274:8500-8505.

238. Pryzdial E.L., and G.E. Kessler. 1996. Autoproteolysis or plasmin-mediated cleavage of factor Xaalpha exposes a plasminogen binding site and inhibits coagulation. J Biol Chem. 271: 16614-16620.

239. Pryzdial E.L., Bajzar L., and M.E. Nesheim. 1995. Prothrombinase components can accelerate tissue plasminogen activator-catalyzed plasminogen activation. J Biol Chem. 270: 17871-17877.

240. Gomori G: J.Lab.Clin.Med. 27:955, 1942

241. Laemmli, U.K. 1970. Cleavage of structural proteins during the assembly of the head of bacteriophage T4. Nature. 227: 680-685.

242. Towbin, H., Staehelin, T., and J. Gordon. 1979. Electrophoretic transfer of proteins from polyacrylamide gels to nitrocellulose sheets: Procedure and some applications. Proc. Natl. Acad. sCi. U.S.A. 76: 4350-4354.

243. Mann, K.G., Hockin, M.F., Begin, K.J., and M. Kalafatis. 1997. Activated protein C cleavage of factor Va leads to dissociation of the A2 domain. J. Biol. Chem. 272: 20678-20683.

244. Lollar, P., Parker, E.T., and P.J. Fay. 1992. Coagulant properties of hybrid human/porcine factor VIII molecules. J. Biol. Chem. 267: 23652-23657.

245. Odegaard, B., and K.G. Mann. 1987. Proteolysis of factor Va by factor Xa and activated protein C. J. Biol. Chem. 262: 11233-11238.

246. Tracy, R.P., Rubin, D.Z., Mann, K.G., Bovill, E.G., Rand, M., Geffken, D., and Tracy, P.B. (1997) Journal of the American Colloege of Cardiology 30: 716-724.

247. Bajzar, L., Kalafatis, M., Simioni, P., and P.B. Tracy, P.B. 1996. An antifibrinolytic mechanism describing the prothrombotic effect associated with factor Vleiden. J. Biol. Chem. 271: 22949-22952.

248. Camire, R.M., Kalafatis, M., and P.B. Tracy. 1998. Proteolysis of factor V by cathepsin G and elastase indicates that cleavage at Arg1545 optimizes cofactor function by facilitating factor Xa binding. Biochemistry 37: 11896-11906.

249. Tracy, P.B., Nesheim, M.E., and K.G. Mann. 1992. Platelet factor Xa receptor. Meth. Enz. 215: 329-360.

250. Bevers, E.M., Comfurius, P., and R.F.A. Zwaal. 1982. The nature of the binding for prothrombinase at the platelet surface as revealed by lipolytic enzymes. Eur. J. Biochem. 122: 81-85.

251. Bevers, E.M., Comfurius, P., and R.F.A. Zwaal. 1983. Changes in membrane phospholipid distribution during platelet activation. Biochem. Biophys. Acta 736: 57-66.

252. Packham, M.A., and J.F. Mustard. 1984. Blood Platelet Function and Medical Chemistry. p. 61-128. Elsevier Biomedical. New York.

253. Zwaal, R.F.A., Comfurius, P., and E.M. Bevers. 1993. Mechanism and function of changes in membrane-phospholipid asymmetry in platelets and erythrocytes. Biochem. Soc. Trans. 21: 248-253.

254. Mann, K.G., Tracey, P.B., Krishnaswamy, S., Jenny, R.J., Odsegaard, B.H., and M.E. Nesheim. 1987. Thrombosis and Haemostasis. P. 505-523. Leuven, University Press, Leuven.

255. Van de Waart, p., Burls, H., Hemker, C., and T. Lindhout. 1983. Interaction of bovine blood clotting FVa and its subunits with phospholipid vesicles. Biochemistry. 22: 2427-2432.

256. Krishnaswamy, S. and K.G. Mann, K. G. 1988. The binding of factor Va to phospholipid vesicles. J. Biol. Chem. 263: 5714-5723.

257. Kalafatis, M., Rand, M.D., and K.G. Mann. 1994. Factor Va-membrane interaction is mediated by two regions located on the light chain of the cofactor. Biochemistry. 33: 486-493.

258. Bloom, J.W., Nesheim, M.E., and K.G. Mann. 1979. Phospholipid-binding properties of bovine factor V and factor Va. Biochem. 18: 4419-4425.

259. Koppaka, V., Talbot, W.F., Zhai, X., and B.R. Lentz. 1997. Roles of factor Va heavy and light chains in protein and lipid rearrangements associated with the formation of a bovine factor Va-membrane complex. Biophys. J. 73: 2638-2652.

260. Macedo-Ribeiro, S., Bode, W., Huber, R., Quinn-Allen, M.A., Kim, S.W., Ortel, T.L., Bourenkov, G.P., Bartunik, H.D., Stubbs, M.T., Kane, W.H., and P. Fuentes-Prior. 1999. Crystal structures of the membrane-binding C2 domain of human coagulation factor V. Nature. 402: 434-439.

261. Villoutreix, B. O. and B. Dahlback. 1998. Structural investigation of the A domains of human blood coagulation factor V by molecular modeling. Prot. Sci. 7: 1317-1325.

262. Grundy J.E., Lavigne N., Hirama T., MacKenzie C.R., and Pryzdial E.L. 2001. Binding of plasminogen and tissue plasminogen activator to plasmin-modulated factor X and factor Xa. Biochemistry. 40: 6293-6302.

263. Kane, W. H., Devore-Carter, D. and T.L. Ortel. 1990. Expression and characterization of recombinant human factor V and a mutant lacking a major portion of the connecting region. Biochem. 29: 6762-6768.

264. Pittman, D. D., Marquette, K. A. and R.J. Kaufman. 1994. Role of the B-domain for factor-VIII and factor-V expression and function. Blood 84: 4214-4225.

265. Ho, S. N., Hunt, H. D., Horton, R. M., Pullen, J. K. and L.R. Pease. 1989. Site-directed mutagenesis by overlap extension using the polymerase chain reaction. Gene 77: 51-59.

266. Horton, R. M., Hunt, H. D., Ho, S. N., Pullen, J. K. and L.R. Pease. 1989. Engineering hybrid genes without the use of restriction enzymes: gene splicing by overlap extension. Gene 77: 61-68.

267. Ortel T.L., Devor C.D., Quin A.M., and W.H. Kane. 1992. Deletion analysis of recombinant human factor V. Evidence for a phosphatidylserine binding site in the second C-type domain, J. Biol. Chem. 267: 4189-4198.

268. Banerjee M, Drummond D.C., Srivastava A., Daleke D., and B.R. Lentz. 2002. Specificity of soluble phospholipid binding sites on human factor Xa. Biochemistry. 41:7751-7762.

269. Kalafatis M., and D.O. Beck. 2002. Identification of a binding site for blood coagulation factor Xa on the heavy chain of factor Va. Amino acid residues 323-331 of factor V represent an interactive site for activated factor X. Biochemistry. 41: 12715-12728.

270. Steen M., Villoutreix B,O., Norstrom E,A., Yamazaki T, and B. Dahlback. 2002. Defining the factor Xa-binding site on factor Va by site-directed glycosylation. J Biol Chem. 277: 50022-50029.

271. Yegneswaran S., Fernandez J.A., Griffin J.H., and P.E. Dawson. 2002. Factor Va increases the affinity of factor Xa for prothrombin: a binding study using a novel photoactivable thiol-specific fluorescent probe. Chem Biol. 9: 485-494.

272. Nesheim M.E., Kettner C., Shaw E., and K.G. Mann. 1981. Cofactor dependence of factor Xa incorporation into the prothrombinase complex. J Biol Chem. 256: 6537-6540.

273. Kim S.W., Ortel T.L., Quinn-Allen M.A., Yoo L., Worfolk L., Zhai X., Lentz B.R., and W.H. Kane. Partial glycosylation at asparagine-2181 of the second C-type domain of human factor V modulates assembly of the prothrombinase complex. Biochemistry. 38: 11448-11454.

274. Wakabayashi H., Schmidt K.M., and P.J. Fay. 2002. Ca(2+) binding to both the heavy and light chains of factor VIII is required for cofactor activity. Biochemistry. 41: 8485-8492.

275. Wakabayashi H., Koszelak M.E., Mastri M., and P.J. Fay. 2001. Metal ion-independent association of factor VIII subunits and the roles of calcium and copper ions for cofactor activity and inter-subunit affinity.Biochemistry. 40: 10293-10300.

276. Pipe S.W., Saenko E.L., Eickhorst A.N., Kemball-Cook G., and R.J. Kaufman. 2001. Hemophilia A mutations associated with 1-stage/2-stage activity discrepancy disrupt protein-protein interactions within the triplicated A domains of thrombin-activated factor VIIIa. Blood. 97: 685-691.

277. Pipe S.W., Eickhorst A.N., McKinley S.H., Saenko E.L., and R.J. 1999. Kaufman RJ. Mild hemophilia A caused by increased rate of factor VIII A2 subunit dissociation: evidence for nonproteolytic inactivation of factor VIIIa in vivo. Blood. 93: 176-183.

278. Lollar P., and E.T. Parker. 1991. Structural basis for the decreased procoagulant activity of human factor VIII compared to the porcine homolog. J Biol Chem. 266: 12481-12486.

279. Bihoreau N., Pin S., de Kersabiec A.M., Vidot F., and M.P. Fontaine-Aupart. 1994. Copper-atom identification in the active and inactive forms of plasma-derived FVIII and recombinant FVIII-delta II. Eur J Biochem. 222: 41-48.

280. Zaitseva, I., Zaitsev, V., Card, G., Moshkov, K., Bax, B., Ralph, A. and P. Lindley. 1996. The x-ray structure of human serum ceruloplasmin at 3.1 Å: Nature of the copper centres. J. Biol. Chem. 1: 15-23.

281. Putney J.W. 2001. Cell biology. Channelling calcium. Nature. 410: 648-649.

282. Perez-Reyes E, and T. Schneider. 1995. Molecular biology of calcium channels. Kidney Int. 48:1111-1124.

283. Berridge M.J. 1994. The biology and medicine of calcium signalling. Mol Cell Endocrinol. 98: 119-124.

284. Nishiki T.I., and G.J. Augustine. 2001. Calcium-dependent neurotransmitter release: synaptotagmin to the rescue. J Comp Neurol. 436:1-3.

285. Lewit-Bentley A, and S. Rety. 2000. EF-hand calcium-binding proteins. Curr Opin Struct Biol. 10: 637-643.

286. Ikura M. 1996. Calcium binding and conformational response in EF-hand proteins. Trends Biochem Sci. 21: 14-17.

287. Chin D., and A.R. Means. 2000. Calmodulin: a prototypical calcium sensor. Trends Cell Biol. 10: 322-328.

288. Levitan I.B. 1999. It is calmodulin after all! Mediator of the calcium modulation of multiple ion channels. Neuron. 22: 645-648.

289. Gerke V., and S.E. Moss. 2002. Annexins: from structure to function.Physiol Rev. 82: 331-371.

290. Hawkins T.E., Merrifield C.J., and S.E. Moss. 2000. Calcium signaling and annexins. Cell Biochem Biophys. 33: 275-296.

291. Zhou Y., and R. Abagyan. 1998. How and why phosphotyrosine-containing peptides bind to the SH2 and PTB domains. Fold Des. 3: 513-522.

292. Ogura K., Tsuchiya S., Terasawa H., Yuzawa S., Hatanaka H., Mandiyan V., Schlessinger J., and F. Inagaki. 1999. Solution structure of the SH2 domain of Grb2 complexed with the Shc-derived phosphotyrosine-containing peptide. J Mol Biol. 289: 439-445.

293. Rebecchi M.J., and S. Scarlata. 1998. Pleckstrin homology domains: a common fold with diverse functions. Annu Rev Biophys Biomol Struct. 27: 503-28.

294. Lemmon M.A., and K.M. Ferguson. 1998. Pleckstrin homology domains. Curr Top Microbiol Immunol. 228: 39-74.

295. Musacchio A. 2002. How SH3 domains recognize proline. Adv Protein Chem. 61: 211-68.

296. Macias M.J., Wiesner S., and M. Sudol. 2002. WW and SH3 domains, two different scaffolds to recognize proline-rich ligands. FEBS Lett. 513: 30-7.

297. Nalefski E.A., and J.J. Falke. 1996. The C2 domain calcium-binding motif: structural and functional diversity. Protein Sci. 5: 2375-90.

298. Ubach J., Zhang X., Shao X., Sudhof T.C., and J. Rizo. 1998. Ca2+ binding to synaptotagmin: how many Ca2+ ions bind to the tip of a C2-domain? EMBO J. 17: 3921-3930.

299. Davis A.J., Chow A.H., and D.J. Gawler. 1998. Protein-protein and protein-lipid interactions of the CaLB domain. Biochem Soc Trans. 26: S119.

300. Zhang H., Wendel B., van Wyk V., and S. Nigam. 1996. Identification and molecular characterization of the CalB domain of the cytosolic phospholipase A2 (cPLA2) in human neutrophils. Adv Exp Med Biol. 416: 305-308.

301. Tanaka C., and Y. Nishizuka. 1994. The protein kinase C family for neuronal signaling. Annu Rev Neurosci. 17: 551-567.

302. Brose N., Hofmann K., Hata Y., and T.C. Sudhof. 1995. Mammalian homologues of Caenorhabditis elegans unc-13 gene define novel family of C2-domain proteins. J Biol Chem. 270: 25273-25280.

303. Li C., Ullrich B., Zhang J.Z., Anderson R.G., Brose N., and T.C. Sudhof. 1995. Ca(2+)-dependent and -independent activities of neural and non-neural synaptotagmins. Nature. 375: 594-599.

304. Sudhof T.C., and J. Rizo. 1996. Synaptotagmins: C2-domain proteins that regulate membrane traffic. Neuron. 17: 379-388.

305. Sudhof T.C. 2002. Synaptotagmins: why so many? J Biol Chem. 277: 7629-7632.

306. Zhang J.Z., Davletov B.A., Sudhof T.C., and R.G. Anderson. 1994. Synaptotagmin I is a high affinity receptor for clathrin AP-2: implications for membrane recycling. Cell. 78: 751-760.

307. Fukuda M., Aruga J., Niinobe M., Aimoto S., and K. Mikoshiba. 1994. Inositol-1,3,4,5-tetrakisphosphate binding to C2B domain of IP4BP/synaptotagmin II. J Biol Chem. 269: 29206-29211.

308. Schiavo G., Gmachl M.J., Stenbeck G., Sollner T.H., and J.E. Rothman. 1995. A possible docking and fusion particle for synaptic transmission. Nature. 378: 733-736.

309. Sheng Z.H., Yokoyama C.T., and W.A. Catterall. 1997. Interaction of the synprint site of N-type Ca2+ channels with the C2B domain of synaptotagmin I. Proc Natl Acad Sci U S A. 94: 5405-5410.

310. Oishi H., Sasaki T., and Y. Takai. 1996. Interaction of both the C2A and C2B domains of rabphilin3 with Ca^{2+} and phospholipid. Biochem Biophys Res Commun. 229: 498-503.

311. Orita S., Sasaki T., Naito A., Komuro R., Ohtsuka T., Maeda M., Suzuki H., Igarashi H., and Y. Takai. 1995. Doc2: a novel brain protein having two repeated C2-like domains. Biochem Biophys Res Commun. 206: 439-48.

312. Brose N., Rosenmund C., and J. Rettig. 2000. Regulation of transmitter release by Unc-13 and its homologues. Curr Opin Neurobiol. 10: 303-311.

313. Betz A., Telemenakis I., Hofmann K., and N. Brose. 1996. Mammalian Unc-13 homologues as possible regulators of neurotransmitter release. Biochem Soc Trans. 24: 661-6.

314. Matthew W.D., Tsavaler L., and L.F. Reichardt. 1981. Identification of a synaptic vesicle-specific membrane protein with a wide distribution in neuronal and neurosecretory tissue. J Cell Biol. 91: 257-69.

315. Kidokoro Y. 2003. Roles of SNARE proteins and synaptotagmin I in synaptic transmission: studies at the Drosophila neuromuscular synapse. Neurosignals. 12: 13-30.

316. Katz B., and R. Miledi. 1967. The timing of calcium action during neuromuscular transmission. J Physiol. 189: 535-544.

317. Pollard H.B., Pazoles C.J., Creutz C.E., and O. Zinder. 1980. Role of intracellular proteins in the regulation of calcium action and transmitter release during exocytosis. Monogr Neural Sci. 7: 106-116.

318. Geppert M, Goda Y, Hammer RE, Li C, Rosahl TW, Stevens CF, Sudhof TC. Synaptotagmin I: a major Ca2+ sensor for transmitter release at a central synapse. Cell. 1994 Nov 18;79(4):717-27.

319. Ullrich B., Li C., Zhang J.Z., McMahon H., Anderson R.G., Geppert M., and T.C. Sudhof. 1994. Functional properties of multiple synaptotagmins in brain. Neuron. 13: 1281-1291.

320. Fernandez-Chacon R., Konigstorfer A., Gerber S.H., Garcia J., Matos M.F., Stevens C.F., Brose N., Rizo J., Rosenmund C., and T.C. Sudhof. 2001. Synaptotagmin I functions as a calcium regulator of release probability. Nature. 410: 41-49.

321. Sutton R.B., Ernst J.A., and A.T. Brunger. 1999. Crystal structure of the cytosolic C2A-C2B domains of synaptotagmin III. Implications for Ca(+2)-independent snare complex interaction. J. Cell Biol. 147: 589-598.

322. Chapman E.R., and R. Jahn. 1994. Calcium-dependent interaction of the cytoplasmic region of synaptotagmin with membranes. Autonomous function of a single C2-homologous domain. J. Biol. Chem. 269: 5735-5741.

323. Cho W., Bittova L., and R.V. Stahelin. 2001. Membrane binding assays for peripheral proteins. Anal Biochem. 296: 153-61.

324. Damer C.K., and C.E. Creutz. 1998. Calcium-dependent self-association of synaptotagmin I. Journal of Neurochemistry. 67: 1661-1668.

325. Orita S., Sasaki T., Naito A., Komuro R., Ohtsuka T., Maeda M., Suzuki H., Igarashi H. and Y. Takai. 1995. Doc2: A Novel Brain Protein Having Two Repeated C_2-like Domains. *Biochem. Biophys. Res. Commun.* 206, 439-448.

326. Duncan R.R., Shipston M.J., and R.H. Chow. 2000. Double C2 protein. A review. Biochimie. 82: 421-426.

327. Rizo J., and T.C. Sudhof. 1998. C2-domains, structure and function of a universal Ca2+-binding domain. J Biol Chem. 273: 15879-15882.

328. Koch H., Hofmann K., and N. Brose. 2000. Definition of Munc13-homology-domains and characterization of a novel ubiquitously expressed Munc13 isoform. Biochem J. 349: 247-253.

329. Augustin I., Betz A., Herrmann C., Jo T., and N. Brose. 1999. Differential expression of two novel Munc13 proteins in rat brain. Biochem J. 337: 363-371.

330. Peng W., Premkumar A., Mossner R., Fukuda M., Lesch K.P., and R. Simantov. 2002. Synaptotagmin I and IV are differentially regulated in the brain by the recreational drug 3,4-methylenedioxymethamphetamine (MDMA). Brain Res Mol Brain Res. 108: 94-101.

331. Gerber S.H., Rizo J., and T.C Sudhof. 2002. Role of electrostatic and hydrophobic interactions in Ca(2+)-dependent phospholipid binding by the C(2)A-domain from synaptotagmin I. Diabetes. 51 Suppl 1: S12-18.

332. Sudhof TC. 2002. The synaptic vesicle cycle revisited. Neuron. 28: 317-320.

333. Sudhof TC. 1995. The synaptic vesicle cycle: a cascade of protein-protein interactions. Nature. 375: 645-653.

334. Bajjalieh S.M. 1999. Synaptic vesicle docking and fusion. Curr Opin Neurobiol. 9: 321-328.

335. Bajjalieh S.M., and R.H. Scheller. 1995. The biochemistry of neurotransmitter secretion. J Biol Chem. 270: 1971-1974.

336. Schoch S., Deak F., Konigstorfer A., Mozhayeva M., Sara Y., Sudhof T.C., and E.T. Kavalali. 2001. SNARE function analyzed in synaptobrevin/VAMP knockout mice. Science. 294: 1117-1122.

337. Brose N. 1993. Membrane fusion takes excitatory turn: syntaxin, vesicle docking protein, or glutamate receptor? Cell. 75:1043-1044.

338. Graham M.E., Washbourne P., Wilson M.C., and R.D. Burgoyne. 2002. Molecular analysis of SNAP-25 function in exocytosis. Ann N Y Acad Sci. 971: 210-21.

339. Sutton R.B., Davletov B.A., Berghuis A.M., Sudhof T.C., and S.R. Sprang. 1995. Structure of the first C2 domain of synaptotagmin I: a novel Ca2+/phospholipid-binding fold. Cell. 80: 929-938.

340. Ochoa W.F., Garcia-Garcia J., Fita I., Corbalan-Garcia S., Verdaguer N., and J.C. Gomez-Fernandez. 2001. Structure of the C2 domain from novel protein kinase Cepsilon. A membrane binding model for Ca(2+)-independent C2 domains. J Mol Biol. 311: 837-849.

341. Bittova L., Sumandea M., and W. Cho. 1999. A structure-function study of the C2 domain of cytosolic phospholipase A2. Identification of essential calcium ligands and hydrophobic membrane binding residues. J. Biol. Chem. 274: 9665-9672.

342. Shao X., Davletov B.A., Sutton R.B., Sudhof T.C., and J. Rizo. 1996. Bipartite Ca2+-binding motif in C2 domains of synaptotagmin and protein kinase C. Science. 273: 248-251.

343. Plant P.J., Yeger H., Staub O., Howard P., and D. Rotin. 1997. The C2 domain of the ubiquitin protein ligase Nedd4 mediates Ca2+-dependent plasma membrane localization. J. Biol. Chem. 272: 32329-32336.

344. Garcia R.A., Forde C.E., and H.A. Godwin. 2000. Calcium triggers an intramolecular association of the C2 domains in synaptotagmin. Proc Natl Acad Sci U S A. 97: 5883-5888.

345. Millet O., Bernado P., Garcia J., Rizo J., and M. Pons. 2002. NMR measurement of the off rate from the first calcium-binding site of the synaptotagmin I C2A domain. FEBS Lett. 516: 93-96.

346. Chae Y.K., Abildgaard F., Chapman E.R., and J.L. Markley. 1998. Lipid binding ridge on loops 2 and 3 of the C2A domain of synaptotagmin I as revealed by NMR spectroscopy. J. Biol. Chem. 273: 25659-25663.

347. Xu R.X., Pawelczyk T., Xia T.H., and S.C. Brown. 1997. NMR structure of a protein kinase C-gamma phorbol-binding domain and study of protein-lipid micelle interactions. Biochemistry. 36: 10709-10717.

348. Davletov B.A., and T.C. Sudhof. 1993. A single C2 domain from synaptotagmin I is sufficient for high affinity Ca2+/phospholipid binding. J Biol Chem. 268: 26386-26390.

349. Li C., Davletov B.A., and T.C. Sudhof. 1995. Distinct Ca2+ and Sr2+ binding properties of synaptotagmins. Definition of candidate Ca2+ sensors for the fast and slow components of neurotransmitter release. J Biol Chem. 270: 24898-24902.

350. Zhang X., Rizo J., and T.C. Sudhof. 1998. Mechanism of phospholipid binding by the C2A-domain of synaptotagmin I. Biochemistry. 37: 12395-12403.

351. Edwin R. 1998. Chapman and Anson F. Davis Direct Interaction of a Ca^{2+}-binding Loop of Synaptotagmin with Lipid Bilayers. J Biol Chem, 273: 13995-14001.

352. Zubelewicz-Szkodzinska B., and R. Braczkowski. 2000. The coexistence of breast and ovarian cancer in patient with insertion-duplication of 12bp in BRCA1 gene. Wiad Lek. 53: 227-230.

353. Risk J.M., Evans K.E., Jones J., Langan J.E., Rowbottom L., McRonald F.E., Mills H.S., Ellis A., Shaw J.M., Leigh I.M., Kelsell D.P., and J.K. Field. Characterization of a 500 kb region on 17q25 and the exclusion of candidate genes as the familial Tylosis Oesophageal Cancer (TOC) locus. Oncogene. 21: 6395-6402.

354. Iwaya T., Maesawa C., Ogasawara S., and G. Tamura. 1998. Tylosis esophageal cancer locus on chromosome 17q25.1 is commonly deleted in sporadic human esophageal cancer. Gastroenterology. 114: 1206-1210.

355. Kalikin L.M., Qu X., Frank T.S., Caduff R.F., Svoboda S.M., Law D.J., and E.M. Petty. 1996. Detailed deletion analysis of sporadic breast tumors defines an interstitial region of allelic loss on 17q25. Genes Chromosomes Cancer. 17: 64-68.

356. Dion F., Mes-Masson A.M., Seymour R.J., Provencher D., and P.N. Tonin. 2000. Allelotyping defines minimal imbalance at chromosomal region 17q25 in non-serous epithelial ovarian cancers. Oncogene. 19: 1466-1472.

357. Islam A., Kageyama H., Takada N., Kawamoto T., Takayasu H., Isogai E., Ohira M., Hashizume K., Kobayashi H., Kaneko Y., and A. Nakagawara. 2000. High expression of Survivin, mapped to 17q25, is significantly associated with poor prognostic factors and promotes cell survival in human neuroblastoma. Oncogene. 19: 617-623.

358. Martin P., and T. Papayannopoulou. 1982. HEL cells: a new human erythroleukemia cell line with spontaneous and induced globin expression. Science. 216: 1233-1235.

359. Zhang X., Rizo J., and T.C. Sudhof. 1998. Mechanism of phospholipid binding by the C2A-domain of synaptotagmin I. Biochemistry. 37: 12395-12403.

360. Brose N., Petrenko A.G., Sudhof T.C., and R. Jahn. 1992. Synaptotagmin: a calcium sensor on the synaptic vesicle surface. Science. 256: 1021-1025.

CONTRIBUTION OF COLLABORATORS

I am thankful to the following people who have contributed to the experimental work presented in this thesis: Dr. Real Lemieux generated the monoclonal antibodies for FVaH, FVaL described in chapter 2, and for p135 described in chapter 4. Dr. Jean Grundy designed and produced the ΔFV construct, described in chapter 3. Bogna Lasia assisted in the construction and production of the ΔFV construct. Erica Peterson assisted in the immunofluorescence microscopy work on p135 presented in chapter 4. Jennifer Hu assisted in the purification of the p135 monoclonal antibodies described in chapter 4.

CURRICULUM VITAE
Abed Zeibdawi

EDUCATION
1997-2003
Doctoral Program - Biochemistry
University of Ottawa
Faculty of Medicine
Supervisor: Dr. Ed Pryzdial
Expected Graduation: 2003
Thesis: Function and Structure of Anionic Phospholipid-Binding Proteins
I. Factor Va, A Coagulation Cofactor
II. P135, A Novel Protein.

1994-1997
M.Sc. Microbiology and Immunology
University of Ottawa
Faculty of Medicine
Supervisor: Dr. Francisco Diaz-Mitoma.
Conferred: May 1997
Thesis: Recombinant Human Immunodeficiency Virus Reverse Transcriptases: Activity and Fidelity

1986-1990 Carleton University
B.Sc. Honours Biology/Biotechnology
Faculty of Science (Thesis at Agriculture Canada)
Supervisor: Dr. Brian Miki and Dr. Bob Rutledge
Conferred: Feb 1992
Thesis,

Title: Amplification and Characterization of a mutant Acetohydroxyacid Synthase Gene Resistant to the Herbicide Imazapyr from Arabidopsis Thaliana Genomic DNA

Research Experience:

April 2002 – present;
Position: Senior Technologist.

Supervisor: Dr. Alex Wandeler
. Developing novel biomarkers and rabies vaccines for field applications, and developing in-house detection protocols for existing biomarkers. Improving existing rabies virus and antibodies detection methodologies.

1994-2002
Position: Research technologist
Canadian Red Cross/Canadian Blood Services
Supervisors: Dr. M.T. Aye and Dr. Antonio Giulivi
. Assisted in developing a novel patented assay for early detection of viral antibodies, and identified the structure and function of plasmin cleaved human FV and recombinant FV. Structural-functional studies on a novel human p135 protein.

1990-1994
Position: Technician
Canadian Red Cross
Supervisors: Dr. M.T. Aye
. Assisting in research on the Human Immune Deficiency Virus and haematological growth factors that induce differentiation of stem cell. Masters degree on HIV reverse transcriptase fidelity.

May-Sept 1990
Research Student
Atomic Energy of Canada (Chalk River Laboratories)
Supervisor: Dr. Paul Unrau
. Working on the "Human Genome Project" assisting in research which involved rapid mapping of human genomic DNA.

Part-time fall 1989-1990
Lab helper
Agriculture Canada
Supervisor: Dr. David Miller
Undergraduate lab assistant

PUBLICATIONS

Zeibdawi, A.R., Grundy, J.E., Lasia B., and E.L.G. Pryzdial. 2003. Coagulation factor Va Glu96-Asp111: A chelator-sensitivve site involved in function and subunit association. Biochemical J. 2003. Sep 1 (Epub ahead of print)

Zeibdawi, A.R., and E.L.G. Pryzdial. 2001. Mechanism of Factor Va Inactivation by Plasmin: Loss of A2 and A3 Domains from A CA^{2+} Dependent Complex of

Fragments Bound to Phospholipid, The Journal of Biological Chemistry, 276, 19929-19936

Zeibdawi A., and E.L.G. Pryzdial. 2001. Regulation of Clotting Factor Va, Transfusion, May 2001 Abstracts Volume

Zeibdawi A.R., and E.L.G. Pryzdial. 2000. Coagulation Factor Va-Derived Fibrinolysis Cofactor, Canadian Federation of Biological Societies, 43rd Annual Meeting, Abstracts Volume, Canadian Federation of Biological Societies, 43rd Annual Meeting, Ottawa, Ontario.

Hu Y.W., Birch P., Balaskas E., Zeibdawi A., Scalia V., 1996. Theriault-Valin S.A., Gill P., and M.T. Aye. 1996. Flow Cytometric Immunofluorescence Assay for Detection of Antibodies to Human Immunodeficiency Virus Type 1 Using Insoluble Precursor Forms of Recombinant Polyproteins as Carriers and Antigens, Journal of Clinical Microbiology. 34: 1412-1419.

Hashemi S., Aye M.T., Zeibdawi A., Cole R., and R. Goldstein. 1994. A novel HLA-DRB1*14 allele (DRB1*1417), Tissue Antigens, Vol. 44, p. 189-192

Aye M.T., Hashemi S., Leclair B., Zeibdawi A., Trudel E., Halpenny M., Fuller V., and G. Cheng. 1992. Expression of Stem Cell Factor and c-kit mRNA in Cultured Endothelial Cells, Monocytes and Cloned Human Bone Marrow Stromal Cells (CRF-RF), Experimental Hematology. 20: 523-527.

POSTERS

Zeibdawi, A.R. and Pryzdial E.L.G., (2001), Mechanism of Factor Va Inactivation by Plasmin: Loss of A2 and A3 Domains from A Ca^{2+} Dependent Complex of Fragments Bound to Phospholipid, The American Society of Hematology Conference, San Francisco, California.

Zeibdawi A.R and E.L.G. Pryzdial. 2000. Coagulation Factor Va-Derived Fibrinolysis Cofactor, Canadian Federation of Biological Societies, 43rd Annual Meeting, Ottawa, Ontario.

Hu Y.W., Balaskas E., Zeibdawi A., Smeenk C., and M.T. Aye. 1998, Terminus Deoxynucleotidyl Transferase (TDT) Activity of Retroviral Reverse Transcriptase and its association with DNA Strand Transfer, 5th Conference on Retroviruses and Opportunistic Infections, Chicago.

Hu Y.W., Balaskas E., Smeenk C., Birch P., Zeibdawi A., Scalia V., Theriault-Valin S.A., Gill P., and M.T. Aye. 1996. Appearance of Specific Immunoglobulin

D(IgD) Antibodies to Human Immunodeficiency Virus Type 1 (HIV-1) During the time of Seroconversion, 7th Canadian Flow Cytometry Consensus Meeting, Vancouver.

Hu Y.W., Birch P., Balaskas E., Zeibdawi A., Scalia V., Theriault-Valine S.A., Gill P., and M.T. Aye. 1995. Appearance of Specific Immunoglobulin D (IgD) Antibodies to Human Hepatitis B Core Antigen (Anti-HBC) Reduces False Positive Reactivity Significantly, CSTM/CRCS Joint Conference.

Hu Y.W., Birch P., Balaskas E., Zeibdawi A., Scalia V., Gill P., and M.T. Aye. 1993. Reducing the Window Period: The Use of Flow Cytometry in the Detection of Early Seronconversions. The First National Conference on Human Retroviruses and Relations Infections, Washington, D.C.

MANUSCRIPTS IN PREPARATION

Zeibdawi A., Hu J., Peterson E., Bazin R., Lemieux R., Guilivi A., and E.L.G. Pryzdial. In Preparation 2001, A Novel C2 Domain Containing Protein, P135, is Blood Cell Specific and Binds to Anionic Phospholipid. Intended for publication in Blood

CONFERENCES ATTENDED

The First National Conference on Human Retroviruses and Relations Infections, Washington, D.C., 1993

The American Society of Hematology, San Francisco, California, 2001

The International Society of Thrombosis and Haemostasis, Washington, D.C., 1999

Canadian Federation of Biological Societies, 43rd Annual Meeting, Ottawa, Ontario, 2000

The American Society of Hematology Conference, San Francisco, California, 2001

PROFESSIONAL MEMBERSHIPS

Member of the Canadian Federation of Biological Chemists
Member of the Canadian Biophysical Society